AD-A127 440 DESIGN OF A MULTIVARIABLE TRACKER CONTROL LAW FOR THE 1/2
A-7D DIGITAC II AIRCRAFT(U) AIR FORCE INST OF TECH
WRIGHT-PATTERSON AFB OH SCHOOL OF ENGI.. R N PASCHALL
UNCLASSIFIED DEC 81 AFIT/GE/EE/81D-47 F/G 1/3 NL

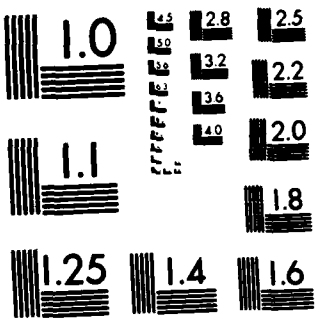

Design of a
Multivariable Tracker Control Law
for the A-7D Digitac II Aircra[illegible]

Thesis

Randall N. Paschall
AFIT/GE/EE/81D-47 2nd Lt USAF

AFIT/GE/EE/81D-47

DESIGN OF A MULTIVARIABLE TRACKER CONTROL LAW FOR THE A-7D DIGITAC II AIRCRAFT

Randall N. Paschall, B.S.E.E.
2nd Lieutenant, USAF
Graduate Electrical Engineering

School of Engineering
Air Force Institute of Technology
Wright-Patterson Air Force Base, Ohio

December, 1981

Preface

I chose this thesis topic dealing with reconfigurable control laws for two reasons. First, it is in the area of flight control which is a sequence in my graduate studies. Second, it employs a new theory which is understood by very few people, but which is extremely important. This research was a continuation of work done by Captain David Potts for the AFWAL/Flight Dynamics Laboratory (FDL).

This thesis revised the aircraft model developed by Captain Potts, and then used output feedback to design a control law for the A-7D. The technique used to design the control law was developed by Professor Brian Porter at the University of Salford, England.

I want to thank all of the people who have helped me in my research, especially Professor Porter, Professor D'Azzo, Professor Houpis, Captain Silverthorn, and Captain Potts. These men gave me the necessary guidance to understand and to complete this work.

I also wish to thank my sponsor, Mr. Duane Robertus, as well as Lieutenant Robinson, for her work in securing the needed material from Professor Porter.

Randall N. Paschall

Contents

List of Figures

List of Tables

List of Symbols

α	Angle of attack
α_r	Ratio of proportional and integral feedback
β	Sideslip angle
b	(Wing) span
γ	Flight path angle
$\bar{c}$	Mean aerodynamic (geometric) chord
C_L	Lift coefficient (airplane)
C_D	Drag coefficient (airplane)
C_m	Pitching moment coefficient (airplane, planform)
C_ℓ	Rolling moment coefficient
C_n	Yawing moment coefficient
C_y	Side force coefficient
C_{D_δ}	Variation of drag coefficient with control surface angle
$C_{L_{i_h}}$	Variation of lift coefficient with stabilizer angle
C_{L_δ}	Variation of lift coefficient with control surface angle
C_{m_α}	Variation of pitching moment coefficient with angle of attack (i.e. static longitudinal stability)
$C_{m_{i_h}}$	Variation of pitching moment coefficient with stabilizer angle (i.e. longitudinal control power)
C_{m_δ}	Variation of pitching moment coefficient with control surface angle

C_{l_δ}	Variation of rolling moment coefficeint with control surface angle
C_{y_δ}	Variation of side force coefficient with control surface angle
C_{n_δ}	Variation of yawing moment coefficient with control surface angle
d_k	Disturbance vector
δ_j	Deflection of the jth surface
$\underline{D}$	Input feed forward matrix
$\underline{e}$	Error vector
g	Acceleration of gravity
$\underline{G}(0)$	Steady state transfer function matrix
$\underline{G}(\lambda)$	Transfer function matrix
I_{xx}	Moment of inertia about X axis
I_{yy}	Moment of inertia about Y axis
I_{zz}	Moment of inertia about Z axis
I_{xz}	Product of inertia in XYZ system
i_H	Stabilizer incidence angle
$\underline{K}$	Control feedback matrix
L_β	Dimensional variation of rolling moment about X_s with sideslip angle
L_p	Dimensional variation of rolling moment about X_s with roll rate
L_r	Dimensional variation of rolling moment about X_s with yaw rate
L_δ	Dimensional variation of rolling moment about X_s with stabilizer, aileron, flap, rudder, and spoiler where $\delta = \delta_H, \delta_a, \delta_f, \delta_r, \delta_s$, angle

m	Mass (airplane)
$\underline{M}$	Transducer matrix
M_u	Dimensional variation of pitching moment with speed
M_α	Dimensional variation of pitching moment with angle of attack
$M_{\dot{\alpha}}$	Dimensional variation of pitching moment with rate of change of angle attack
M_q	Dimensional variation of pitching moment with pitch rate
M_δ	Dimensional variation of pitching moment with a stabilizer, aileron, flap, rudder, spoiler where $\delta = \delta_H, \delta_a, \delta_f, \delta_r, \delta_s$ angle
N_β	Dimensional variation of yawing moment about Z_s with sideslip angle
N_p	Dimensional variation of yawing moment about Z_s with roll rate
N_r	Dimensional variation of yawing moment about Z_s with yaw rate
N_δ	Dimensional variation of yawing moment about Z_s with stabilizer, aileron, flap, rudder, and spoiler, where $\delta = \delta_H, \delta_a, \delta_f, \delta_r, \delta_s$ angle
p	Perturbed roll rate (about x)
ϕ	Perturbed roll angle
$\bar{q}$	Dynamic pressure
q	Perturbed pitch rate (about y)
r	Perturbed yaw rate
s	Surface area, Reference (wing) area
T	Sampling period
θ	Pitch attitude angle

U_1	Forward velocity (along X_s) steady state
u	Perturbed forward velocity (along X_s)
$\underline{V}$	Command vector
w	Vertical velocity
$\underline{W}$	Controlled output quantities
X_u	Dimensional variation of X_s-force with speed
X_α	Dimensional variation of X_s-force with angle of attack
$X_{\dot{\alpha}}$	Dimensional variation of X_s-force with rate of change of angle of attack
X_δ	Dimensional variation of X_s-force with stabilizer, aileron, flap, rudder, and spoiler where $\delta = \delta_H, \delta_a, \delta_f, \delta_r, \delta_s$ angle
$\underline{x}$	State vector
Y_β	Dimensional variation of Y_s-force with sideslip angle
Y_p	Dimensional variation of Y_s-force with roll rate
Y_r	Dimensional variation of Y_s-force with yaw rate
Y_δ	Dimensional variation of Y_s-force with stabilizer, aileron, flap, rudder, and spoiler where $\delta = \delta_H, \delta_a, \delta_f, \delta_r, \delta_s$ angle
Z_u	Dimensional variation of Z_s-force with speed
Z_α	Dimensional variation of Z_s-force with angle of attack
$Z_{\dot{\alpha}}$	Dimensional variation of Z_s-force with rate of change of angle of attack

Z_q	Dimensional variation of Z_s-force with pitch rate
Z_δ	Dimensional variation of Z_s-force with stabilizer, aileron, flap, rudder, and spoiler where $\delta = \delta_H, \delta_a, \delta_f, \delta_r, \delta_s$ angle
X_s, Y_s, Z_s	Stability axes system of coordinates
z	Error integral

Abstract

This thesis uses the design procedures developed by Professor Porter at the University of Salford, England in an attempt to design a multivariable tracker control law for the A-7D Digitac II Aircraft. Some of the limitations and problems associated with this design procedure are uncovered in this study.

A six-degree-of-freedom aircraft model is developed and is then modified to a form that is required by the design procedure. The theory used for the design determines the necessary arrangement of the equations. A tracker control law is first designed for one flight condition. Then it is checked for robustness by applying the control law at a different flight condition and also by removing the rudder from the inputs. A design computer program called MULTI is developed to perform the computations and simulations.

It is found that the design techniques developed by Professor Porter are valid, but that they are not applicable to all systems. A problem occurs when the inputs, as with an aircraft, are bounded.

Problems may also be encountered when the sensor and actuator models are incorporated into the design. Therefore, for this study, the sensor and actuator models are removed and approximated as unity.

More work is needed in this research to expand knowledge about the selection of the adjustable parameters in order to develop a better design and to more effectively utilize the basic design. Further work

is also needed to prefect the useability of the program MULTI. This thesis provides a good stepping stone to a better understanding of this design technique and its applicability.

Design of a Multivariable Tracker Control Law for the A-7D Digitac II Aircraft

I. Introduction

As technology continues to advance, the use of digital flight control systems on aircraft grows. Future aircraft will have the normal set of primary control surfaces (ailerons, spoilers, flaps, and horizontal stabilizers) split into independently controlled sections. This thesis attempts to develop a tracker control law with the primary surfaces split in this fashion. In order to learn the techniques for implementing the theory, the decision was made to recombine some of the surfaces in order to arrive at a model that was more manageable. The resulting model has only one split surface (the horizontal stabliizer).

Background

It had been recently suggested that it is possible to design a direct digital flight control system that offers noninteracting control of various flight modes which allows the aircraft to maneuver in ways that are not possible using conventional techniques. Bradshaw and Porter (Ref. 3) have developed a synthesis method for this type of control which uses fast-sampling error-actuated digital control. The implementing equations necessary to perform this design have been developed by Porter under

contract to the Air Force (Ref. 12). This thesis took these equations and this theory and used them to investigate a flight control system for the A-7D aircraft.

Problem

The object of this thesis is to develop a comprehensive aircraft model for the A-7D aircraft and then to use Professor Porter's theory to design a tracker control law. The result is a review of this new design technique, and a commentary on its limitations, problem areas, and performance.

Scope

A tracker control law is designed in order to gain a complete understanding of Porter's methods. The resulting design is then checked for robustness in two ways:

1. The control law is used at a different flight condition to see how it responds over a wide range of parameter changes.
2. The rudder is made inoperative and the control law used to see how this aircraft disability is handled.

Approach

This thesis is limited to an investigation of the theory developed by Professor Porter (Ref. 4). The resulting design is not claimed to be the best possible, but rather the best the this engineer could design in

the time allowed. The design is checked for robustness, and the results are discussed. The entire design process is done using an interactive computer package called MULTI. MULTI has been developed by Captain Doug Porter, Lieutenant Joseph Smyth, and this author. The program utilizes the equations developed by Professor Porter. The steps taken in completing this thesis are:

1. Develop the necessary aircraft equations at three flight conditions.
2. Develop the interactive computer software package MULTI that performs the design and simulations.
3. Design a tracker control law using the appropriate method.
4. Check the resulting design for robustness.

Each step, by itself, could have been expanded into a separate thesis. Since there are three possible approaches to the problem (see Chapter III), step 3 proved to be very difficult. Numerous trials are attempted before an acceptable design that works is finally reached.

Assumptions

The assumptions made in this thesis deal with the aircraft model, and the aircraft operation. First, the aircraft is assumed to make only small perturbations about a trimmed straight and level flight condition. Secondly, the aircraft equations of motion developed are in the stability axis reference frame. Thirdly, the coefficients of the control derivatives

are normally for a pair of control surfaces, are halved, given the proper sign, and used whenever the control surface is split into two independent sections.

Presentation

This thesis is composed of 7 chapters. Chapter II develops the aircraft models and Appendix A provides the details and the equations used. Chapter III presents the theory used for the design of the digital control law. Three approaches are discussed, as well as when to use each one. Chapter IV discusses the development of the computer program MULTI which is needed to compute the design and simulate the results. The program handles all three design approaches. Chapter V describes several approaches taken in an attempt to find an approach that produces valid results. When more than one approach can be used, it is necessary to find out which one is better and then to use that one. Chapter VI discusses the results obtained. The results are collected in Appendix B for easy location and viewing. Chapter VII presents the conclusions and recommendations.

II. The Aircraft Models

Introduction

The model for the A-7D aircraft presented by Potts (Ref. 15) is revised and a new model is developed. Using the same six degree-of-freedom (D-O-F) aircraft model and the same approach as presented by Potts (Ref. 15), a "modified"model is derived. The model considers many control surfaces to be independent which are traditionally considered to act as one unit. For example, the horizontal stabilizer is divided into two independent control surfaces, the right and left horizontal stabilizers. A linear model is obtained by linearizing the non-linear six degree-of-freedom equations about a normal operating point. After a revised model is generated for the first flight condition at 0.6 Mach at an altitude of 15,000 feet, two additional flight conditions are considered. Models are also developed for Mach numbers of 0.18 and 0.8 at altitudes of 2,000 feet and 35,000 feet respectively. The model for 0.1 Mach is assumed to be a landing configuration. In this manner, the new control laws are checked for robustness over a wide range of flight conditions.

Aircraft Description

The A-7D is a single seat, light attack aircraft with moderately

swept wing and tail surfaces, and is powered by a single TF41-A-1 engine (Ref.17). The describing data for the aircraft as found in Reference 9 is given in Table I.

TABLE I

A-7D Descriptive Data

Item	Dimension	Unit
Fuselage Length	45.4	ft
Wing Area	375	ft^2
Wing Mean Geometric Chord	10.8	ft
Horizontal Stabilizer Area	56.2	ft^2
Horizontal Slab m.g.c.	6.1	ft
Distance from 0.25 Wing m.g.c. to 0.25 Horizontal Slab m.g.c.	16.2	ft
Weight	25,238	lbs

System Models

The models used to describe the A-7D at various flight conditions are developed using the same 6 D-O-F aircraft equations given by Potts in Reference 15. By using the same technique as Potts, control of lateral motion is made possible by using a longitudinal control surface, and control of longitudinal motion is made possible by using a lateral control surface. This is essential for reconfiguration to be possible after the loss of a primary control surface. The details of this technique are found in Appendix A. The control surfaces that are considered as input are the ailerons, the spoilers, the flaps, the rudder, and the horizontal stabilizer. The ailerons, spoilers, and the horizontal stabilizer are divided into separate individual control surfaces (right and left), while the rudder and flaps are left as single inputs. In this manner there are a total of 8 inputs considered. There are likewise 8 outputs. These include the forward velocity u, the flight path angle γ, the pitch rate q, the pitch angle θ, the roll rate p, the roll angle ϕ, and the yaw rate r. The system is square, that is, the number of inputs is equal to the number of outputs. By including the individual control surfaces, the equations of motion are not decoupled to separately describe lateral and longitudinal motion.

The stability derivatives that are needed in the equations of motion are given in Appendix A. The derivatives that are not given in either Reference 1 or Reference 9 are computed by conventional aerodynamic

techniques with the aid of a computer package called digital DATCOM (Ref. 10).

Summary

This chapter gives a description of the A-7D aircraft and identifies the control surfaces which are considered as inputs for the 6 D-O-F models developed. Models for three flight conditions are developed with 0.6, 0.18, and 0.8 Mach at altitudes of 15,000, 2,000 and 35,000 feet, respectively. With the models developed, the next step is to present the multivariable control theory by which the new control laws are designed.

III. Multivariable Digital Control Theory

Introduction

The design techniques in this thesis for development of a tracker control law use the theory developed by Professor Brian Porter (Ref. 3). The concepts involved and the describing equations are presented in this chapter. Only the digital approaches are discussed, although analog control laws based on the same concept are possible. These techniques are used to synthesize a sampled-data hybrid control system which consists of a continuous-time plant and a digital controller that produces a control input signal which is piece-wise constant for each sampling period.

Professor Porter has developed three design procedures. All three of the procedures are presented in this chapter. The procedure to use is determined by the first markov parameter. The first markov parameter is defined as the product $\underline{CB}$ and is discussed in this chapter.

Unknown Plant Design

In many cases, a state equation model is not available to describe a system. If this is the case, the steady-state transfer function matrix $\underline{G}(0)$ can be determined from off-line tests performed on the system (Ref. 13) provided that the plant is stable. If the state equations are available, then $\underline{G}(0)$ can be determined using Equation (1) for the system represented by the continuous-time state and output equations, $\dot{\underline{x}} = \underline{A}\underline{x} + \underline{B}\underline{u} + \underline{D}\underline{d}$ and $\underline{y} = \underline{C}\underline{x} + \underline{D}\underline{u}$.

$$\underline{G}(0) = -\underline{C}\,\underline{A}^{-1}\,\underline{B} \tag{1}$$

where $\underline{G}(0) \in R^{\ell x\, m}$

In either case $\underline{G}(0)$is the transfer function matrix $G(\lambda)$, as defined in Equation (2), with $\lambda = 0$, that is,

$$\underline{G}(\lambda) = \underline{C}\,(\lambda \underline{I}_n - \underline{A}\,)^{-1}\,\underline{B} \tag{2}$$

where n = number of states

In order for integral action to preserve stability, $\underline{G}(0)$ must have rank equal to the number of outputs. This condition also requires that the the number of outputs be less than or equal to the number of inputs ($\ell \leq$ m). This procedure assumes that the eigenvalues of the open loop plant matrix $\underline{A} \in R^{nxn}$ lie in the open left half-plane (Ref. 12).

Digital error-actuated controllers are described by state and output equations of the form (Ref. 13)

$$x_{k+1} = \Omega x_k + \Psi u_k \quad \Delta d_k \tag{3}$$

$$y_k = \Gamma x_k \tag{4}$$

where

$x_k = x(kT) \in R^n$ (state vector)

$u_k = u(kT) \in R^m$ (control input vector)

$y_k = y(kT) \in R^{\ell}$ (output vector)

$d_k = d(kt) \in R^p$ (disturbance vector)

$\Omega = \exp\,(\underline{A}T)$

$\Psi = \int_o^T \exp\,(\underline{A}t)\ \underline{B}\ dt$

$$\Delta = \int_0^T \exp(\underline{A}t)\ \underline{D}\ dt$$

$$\Gamma = \underline{C}$$

In these equations T is the sampling period.

When error-actuated digital control is applied to plants described by Equations (3) and (4), the proportional plus integral control law equation that results is:

$$u_k = \alpha_r T \epsilon \underline{K} \cdot e_k + \epsilon T \underline{K} \cdot z_k \qquad (5)$$

where

$e_k = e(KT) = v_k - y_k \in R^{\ell}$ (error vector)

$v_k = v_k(KT) \in R^{\ell}$ (command input vector)

$z_k = z_k(KT) \in R^{\ell}$ (integral of error)

$z_{k+1} = z_k + Te_k$

In Equation (5), α_r is a design parameter that determines the desired ratio of proportional to integral action. ϵ is a normalizing factor, and v_k is the command input vector. If α_r, T, and $\underline{K}$ are chosen so that all the closed-loop eigenvalues lie within the digital unit disc, then $\lim_{k \to \infty} e = 0$, and set-point tracking occurs (Ref. 13). According to reference 13 the parameter $\underline{K}$ is determined by the relationship

$$\underline{K} = \underline{G}^T (\underline{G}\underline{G}^T)^{-1}\ \underline{\Sigma} \qquad (6)$$

where

$$\underline{G} = \underline{G}(0)$$

$$\underline{\Sigma} = \text{diag}\left\{\sigma_1, \sigma_2, \ldots\ldots \sigma_{\ell}\right\}\ \sigma_1 > 0$$

In Equation (6), $\underline{\Sigma}$ is a matrix that is used as an additional "tuning" parameter for better results. Figure 1 is a block diagram for this control scheme.

Regular Plants

Plants that are described by state and output equations

$$\dot{\underline{x}} = \underline{A}\underline{x} + \underline{B}\underline{u} \tag{7}$$

$$\underline{y} = \underline{C}\underline{x} \tag{8}$$

can be transformed by use of a transformation matrix, if necessary, so that the new state and output equations have the form

$$\begin{bmatrix} \dot{x}_1 \\ \dot{x}_2 \end{bmatrix} = \begin{bmatrix} A_{11} & A_{12} \\ A_{21} & A_{22} \end{bmatrix} \begin{bmatrix} \dot{x}_1 \\ \dot{x}_2 \end{bmatrix} + \begin{bmatrix} 0 \\ B_2 \end{bmatrix} \underline{u} \tag{9}$$

$$\underline{y} = \begin{bmatrix} C_1 & C_2 \end{bmatrix} \begin{bmatrix} x_1 \\ x_2 \end{bmatrix} \tag{10}$$

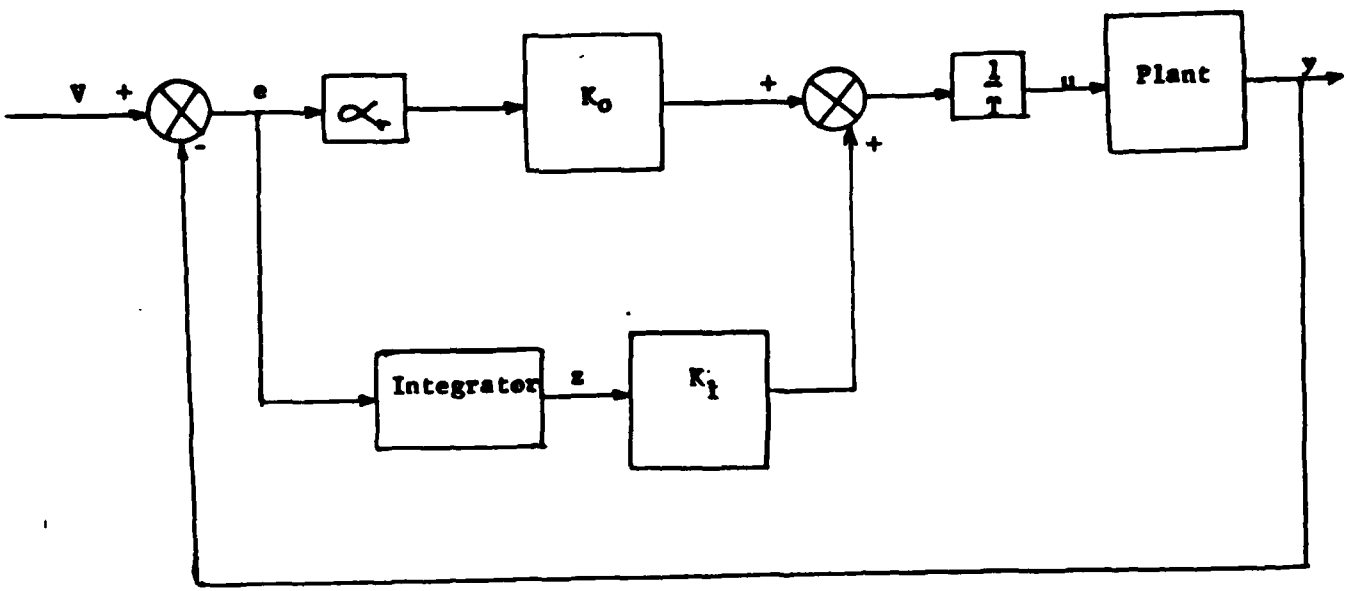

Figure 1

Unknown and Regular Plant Control Diagram (use T, not T^{-1} for unknown plants)

where

$$A_{11} \in R^{(n-\ell)\ x\ (n-\ell)}$$

$$A_{12} \in R^{(n-\ell)\ x\ \ell}$$

$$A_{21} \in R^{\ell x\ (n-\ell)}$$

$$A_{22} \in R^{\ell x \ell}$$

$$B_2 \in R^{\ell x \ell}$$

$$C_1 \in R^{\ell x\ (n-\ell)}$$

$$C_2 \in R^{\ell x \ell}$$

$$X_1 \in R^{n-\ell}$$

$$X_2 \in R^{\ell}$$

$$U \in R^{\ell}$$

$$Y \in R^{\ell}$$

The first Markov parameter is defined as $\underline{C}_2\underline{B}_2$ for equations of this form. If the rank of $\underline{C}_2\underline{B}_2 = \ell$, then the plant is referred to as "regular". For plants of this type, the governing control law equation is (Ref. 3).

$$U(kT) = \frac{1}{T}\left[\ \varepsilon \underline{K}_o e(kT) + \underline{K}_1 \varepsilon Z(kT)\ \right] \qquad (11)$$

where

$$\underline{K}_o \in R^{\ell x \ell}$$

$$\underline{K}_1 \in R^{\ell \times \ell}$$
$$e(kT) \in R^{\ell}$$
$$z(kT) \in R^{\ell}$$

For this control law, where $e(kT) = v(kT) - y(kT)$, the output vector $y(kT)$ tracks any constant command vector $v(kT)$ (Ref. 3). The relationship between $\underline{K}_o$ and $\underline{K}_1$ is

$$\underline{K}_o = \alpha_r \underline{K}_1 \tag{12}$$

where α_r is an adjustable design parameter. $\underline{K}_o$ is defined by the equation

$$\underline{K}_o = (\underline{C}_2\underline{B}_2)^{-1} \cdot \underline{\Sigma} \tag{13}$$

where

$$\underline{\Sigma} = \text{diag}\left\{ \sigma_1, \sigma_2, \ldots\ldots \sigma_\ell \right\}$$
$$-1 < (1 - \sigma_j) < 1$$
$$\sigma_j \in R$$

The closed-loop system responds faster and has less interaction as T is decreased (Ref. 3). For systems of this form, Equation (9), the transmission zeros are the set derived from the relationship

$$Z_T = \left\{ \left| \lambda I_{n-\ell} - I_{n-\ell} - TA_{11} + TA_{12}C_2^{-1}C_1 \right| = 0 \right\} \tag{14}$$

The transmission zeros must lie within the unit disc for complete stability as $T \to 0$. Transmission zeros that lie on the unit disc, or outside of it, can cause instabilities. Also, if paths to transmission zeros cross into

unstable regions, there exists a range of T that produces instability. For tracking to occur, all of the closed-loop poles must lie within the unit disc. Figure 1 is also a block diagram for this type of control scheme.

Irregular Plants

For high-performance systems described by Equation (9) and Equation (10), if the first Markov parameter $\underline{C}_2\underline{B}_2$ has rank less than ℓ, then the plant is said to be "irregular". It is assumed that $\underline{B}_2$ is full rank in such systems so that the rank deficiency is within the matrix $\underline{C}_2$. If this is the case, it is necessary to introduce a vector of extra measurements W(t) (Ref. 4) such that

$$\underline{W}(t) = [\underline{F}_1, \underline{F}_2] \begin{bmatrix} x_1 \\ x_2 \end{bmatrix} \tag{15}$$

where

$$\underline{F}_1 \in R^{\ell x (n-\ell)}$$

$$\underline{F}_2 \in R^{\ell x \ell}$$

The addition of the extra measurements changes the form of $e(t)$ so that $e(t) = v(t) - W(t)$. $\underline{F}_1$ and $\underline{F}_2$ are defined by the equations

$$\underline{F}_1 = \underline{C}_1 + \underline{M}\,\underline{A}_{11} \tag{16}$$

$$\underline{F}_2 = \underline{C}_2 + \underline{M}\,\underline{A}_{12} \tag{17}$$

In Equations (16) and (17), $\underline{M}$ is the transducer matrix of dimension

$\ell \times (n-\ell)$.

If the closed-loop system is assymptotically stable, Equation (9) implies that

$$\lim_{t\to\infty} \begin{bmatrix} A_{11}, & A_{12} \end{bmatrix} \begin{bmatrix} X_1(t) \\ X_2(t) \end{bmatrix} = 0 \tag{18}$$

for constant command inputs, so that in steady state $W(t) = y(t)$ (Ref. 4). Therefore, in the steady state

$$\lim_{k\to\infty} e(kT) = \lim_{k\to\infty} v(kT) - W(kT) = 0 \tag{19}$$

This ensures tracking of the command vector in steady state operation.

Proper choice of $\underline{M}$ "makes" the plant regular. This requires that $\underline{F}_2\underline{B}_2$ have rank ℓ. Since $\underline{B}_2$ is assumed to have rank ℓ at the start, $\underline{M}$ is chosen so that (Ref. 4).

$$\text{rank } \underline{F}_2 = \text{rank } (\underline{C}_2 + \underline{M}\,\underline{A}_{12}) = \ell \tag{20}$$

Once the plant is "made" regular by proper choice of $\underline{M}$, the governing control law is equation (11) where now

$$\underline{K}_o = (\underline{F}_2\underline{B}_2)^{-1} \cdot \underline{\Sigma} \tag{21}$$

The transmission zeros are the set derived from the relationship

$$Z_T = \left\{ \left| \lambda I_{n-\ell} - I_{n-\ell} - T A_{11} + T A_{12} F_2^{-1} F_1 \right| = 0 \right\} \tag{22}$$

The same ideas that applied to regular plants apply to irregular plants once $\underline{M}$ is chosen so as to "make" the irregular plant appear regular. Figure 2 is a block diagram for this control scheme.

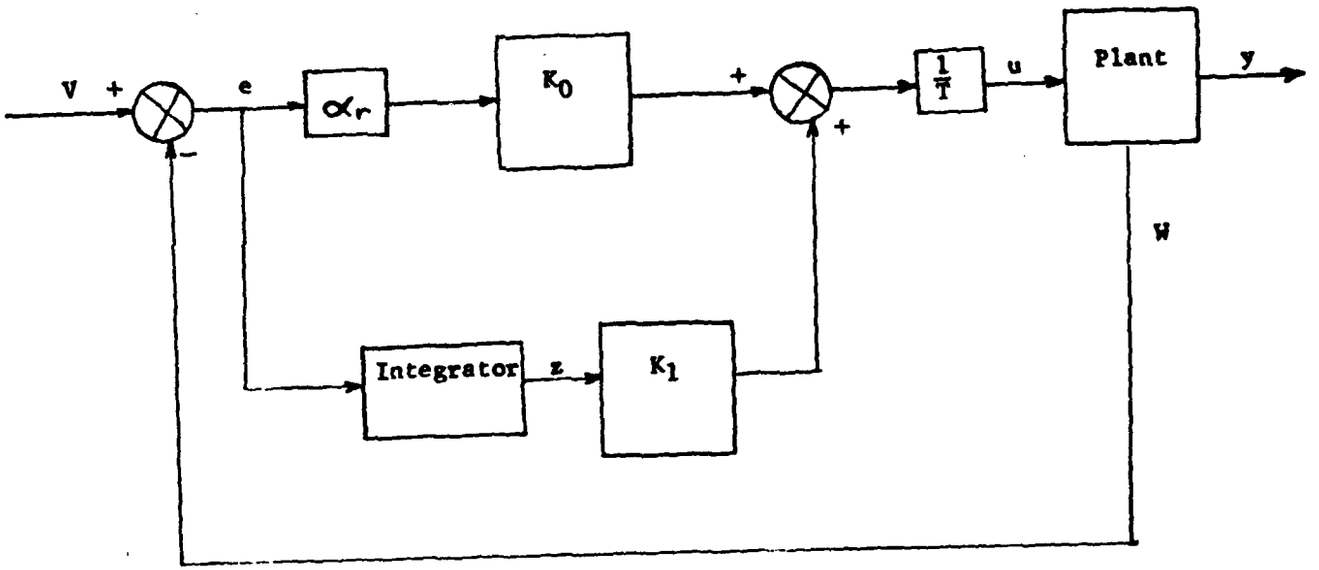

Figure 2

Irregular Plant Control Diagram

Summary

This chapter presents the three design concepts developed by Professor Porter. For further details, the reader is encouraged to see the references given in this chapter. The three catagories of plants are: unknown, regular (rank $\underline{C}_2\underline{B}_2 = \ell$), and irregular (rank $\underline{C}_2\underline{B}_2 < \ell$). The next chapter presents the computer package developed to employ these concepts. Chapter V shows how the proper design procedure is chosen and applied.

IV. Computer Program Development

Introduction

MULTI, an interactive, user-oriented computer program, is developed to design and simulate the control laws for unknown, regular, and irregular plants. The computer program is written in FORTRAN V code. It is developed along the lines of a computer package called PAK200 which was received from the University of Salford, Department of Aeronautical and Mechanical Engineering (Ref. 6). The program utilizes digital theory as opposed to continuous methods. The MULTI computer package contains approximately 40 options which give the user an interactive, iterative approach in the design and simulation of control laws for linear, multivariable plants. The control law assures that the output tracks the input and that disturbance rejection is accomplished.

This chapter relates the requirements that are set for the program, the program design emphasis, the constraints and problems faced in the development of MULTI, and the actual program structure of MULTI. A User's Manual for MULTI and a Programmer's Manual for MULTI are found in Captain Doug Porter's thesis (Ref. 14) along with a complete listing of the program.

Program Requirements

The requirements for the computer program are set so that MULTI can take full advantage of the techniques used in designing the

discrete-time tracking systems for linear multivariable plants.

These requirements include:

1. The computer package must be fully interactive, user-oriented, and allow for an interactive design process.

2. The program must allow the user to input data from the terminal keyboard or a data file and store pertinent data in local files upon normal program termination.

3. The package should include design capability for unknown, regular and irregular plants.

4. The package must be able to recognize when singular matrices are formed and direct the user to apply an alternate design technique.

5. The package must be able to form a measurement matrix from terminal input.

6. The package must include a discrete-time simulation in order to evaluate the control laws developed.

7. The package must include a plotting capability.

These requirements result in a software package that is very versatile.

Program Design Emphasis

When a computer program is divided into several modules, the content of each module and the interconnections between the modules can significantly affect the operation and complexity of the resulting program. Coupling and cohesion are two qualities that are used to check the overall design.

Coupling is the measure of the strength of the interconnections between one module and another. It is essential that coupling be kept

at a minimum so that changes in one module do not severely affect the other modules. When coupling is retained at a low level, the ease of finding and correcting program bugs is enhanced and the program's life is increased since quick modifications are made possible. Labeled common blocks are used rather than blank common blocks so that the level of coupling is reduced.

Cohesion is the degree of functional relatedness of processing elements within a single module. It also has a direct effect on the ability of a programmer to maintain and modify a program. A high level of cohesion is desirable and is kept by putting only functionally related processes within each module.

In MULTI, the major functions of the program are directed to lower-level modules. Every module is designed to use a minimum of memory core, and every labeled common block is designed to hold only those elements needed for a specific purpose. Through this type of design, MULTI is able to use minimum computer memory core, have minimum coupling and retain a high level of cohesion.

Design Constraints

There are two main design constraints when developing a computer program like MULTI. One, the computer language that is used, and two, the availability of computer core memory that is allowed when using an INTERCOM system.

FORTRAN V is chosen as the language for MULTI since it is the

latest version of FORTRAN available on the ASD CYBER computer system. Using FORTRAN V does not restrict the use of the ASD Library subroutines, even though they are coded in FORTRAN IV, since all are readily compiled into the more powerful version.

Current interactive computer users are constrained to operate in 65K words of core memory, or less. Therefore, MULTI is designed to operate within this restriction. The core memory restriction is met through the modular design of the program.

Developmental Problems

The original program design is adopted from a computer package called PAK200 which was written for controller design simulation at the University of Salford, England. It was originally conveyed that the development of a similar computer package, compatible with the ASD CYBER computer, would merely involve the substitution of certain computational subroutines from the ASD Subroutines into PAK200. The MULTI computer package is now a completely interactive design and simulation tool for all three types of plants. The main body of the code from PAK 200 is entirely contained in one option of MULTI. Two subroutines, dealing with the differential equation formation and the value of the output at the end of each time increment, are also retained to provide compatibility with the original simualtion code.

MULTI's development faced several other problems. The use of the FORTRAN V language presented a barrier which was not eliminated until

several months into MULTI's design. This problem involved the use of character statements, first available in FORTRAN V, which produced sporadic errors during MULTI's many modifications. This problem is known to FORTRAN V subscribers but not to its users.

The constant breakdown of computer operations is a big problem. Just when it seems progress is being made, the ASD CYBER system would go down. This caused the proposed time for program development to be increased by as much as a month. This is a problem that should be considered by anyone developing or modifying a program.

The final version of MULTI is the best that can be obtained by control engineer programmers within the time constraints imposed on the development, testing, and simulation of a model, controller and computer package for the newest techniques of the multivariable design of this thesis. MULTI meets all the specific requirements as outlined above.

Program Structure

Since MULTI must be able to operate in 65K words of core memory, its program structure consists of a group of various modules. Information between these modules is passed by using the data base concept of global storage. To allow MULTI to be fully interactive, the program uses a very simple Program Control Interface.

To reduce the amount of memory core required for operation, MULTI has a structure consisting of several modules, called overlays. Each overlay is an executable program and combines with all other overlays to

form a complete functioning overlay structure. There is one main overlay in MULTI. The main overlay is an Executive Program directing the actual functions of the program to 13 lower-level primary overlays.

This overlay structure is responsible for MULTI's operation within the defined 65K memory core limit. The main overlay remains in executable memory at all times. As each computational or functional requirement of the program is needed, the overlay designed to perform that procedure is loaded into executable memory behind the main overlay. When the procedure is finished, the used overlay is saved, and the overlay needed for the next procedure is loaded behind the main overlay.

Data information is passed between overlays in MULTI by the use of labeled common blocks. If a program variable in an overlay is not listed in a labeled common block, its value is not retained when the next overlay is loaded.

A complete description of overlays and how they are used in MULTI can be found in the MULTI Programmer's Manual (Ref. 14)

MULTI uses three types of data storage methods which comprises its data base. These three types of storage methods are: local storage, global storage, and mass storage. Mass storage in MULTI entails only the use of sequential-access files.

Local storage is the storage method which is used for program variables that are needed only during the execution of a particular overlay. As mentioned above, these locally stored variable values are lost when the overlay is finished executing. MULTI has several matrices which are generated during program execution whose values are destroyed when they

are no longer needed.

Global storage is used for program variables whose element values are required to be passed between overlays. All of MULTI's global storage is accomplished using labeled common blocks. The variables defined in each common block are purposely chosen to keep each overlay memory core requirement at a minimum, and still allow for the necessary data transfer between overlay loading.

Sequential-access files are used in MULTI's external data input functions and in MULTI's mass storage capability. A sequential-access, data-input file can be built by any user for use with the program. The specifics and proper formatting of these files is described in detail in the user's manual (Ref. 14). MULTI automatically creates two separate memory files when the user terminates program operation. A file called "MEMO" is generated to hold all data describing the plant of interest, and a file called "MEM10" is created to hold all design parameters.

MULTI's interface design is similar to the interface found in TOTAL (Ref. 8), but is not nearly as complex. All MULTI operations are controlled by having the user choose various option numbers which correspond to desired computational functions. Since there is minimal input data verification, the user must adhere strictly to the limitations noted in various parts of the MULTI User's Manual. Every completed option sets an internal "flag" allowing entry into other options. There is a definite pattern for successful program operation which corresponds to a normal design process. The program is designed to require the user to flow from data input, to controller design, and then to simulation. Each part of

the design can be re-accomplished interactively, but the user is not permitted to proceed in the flow until each preceeding design step is accomplished. All options are explained in the MULTI User's Manual. Data access in MULTI is accomplished by program requests and by the use of a special option number range. The user can view certain pertinent matrix combinations and other data of interest responding affirmatively when the program prints:

```
ENTER "0" TO OBTAIN DATA PRINTOUT
ENTER "1" TO SKIP DATA PRINTOUT...
```

In some cases, the data cannot be accessed again, since it is contained on a local storage device, unless the user re-enters the same option with the same plant data and design specifications.

The second method of data access is by the use of options having the value of 100 or greater. If data has been entered using OPTION #1 the same data can be accessed for verification by using OPTION #101. This method of data access is developed in the last few versions of the program. The original in-line format of displaying data takes too much time during the complete design process. The final data access method allows for easy, selective data access.

After data access the user may determine that values are not entered correctly, or for some reason need to be changed. The user can use one of the two means to change the data. The option related to the data in question can be re-entered or the user can terminate MULTI and edit the program-created data files. This last means of changing data is of

special interest when changing element values of the plant's A, B, C, and D matrices.

The error detection and recovery aspects of MULTI are limited. Since the main emphasis of the thesis was not originally perceived to entail the complete design of a computer simulation package, MULTI's design is not based upon the ability to protect the user from input errors. MULTI is designed to alert a user, and recover, when program flow is not in the proper order or when certain plant deficiencies require the use of a certain controller design.

Input errors such as character entries for numerical data, and vice versa, are all detected by the CYBER error detection capabilities. In these cases the user is allowed to re-enter the proper information and continue.

MULTI restricts the user to a 10 state, 10 input, 10 output system with 2nd order actuators and sensors. Simultaneous simulations can be run for up to two different sampling times while plots can be generated which display up to four superimposed curves. When the user's requests exceed these limitations, the entire MULTI program is aborted. It is suggested that any MULTI user become completely familiar with the user's guide for the program.

When MULTI is aborted the CYBER system relates the nature of the error which causes the abnormal termination of the program. It must be stated that MULTI is not as dynamic in its ability to receive input data as other programs with which the user may be familiar (i.e. TOTAL (Ref. 8), CESA (Ref. 7)). At present, character inputs to

display current matrix values or system design values are not available except by requesting the proper option number. Also at present, entering a "$" symbol, rather than actual data, to abort an option, is not recognized unless specifically noted in the program instructions.

Summary

This chapter discusses the development of the computer program MULTI. The program structure, requirements, and design is presented so that the reader can understand what is done, not necessarily how. The program has areas that need improvement, but these can only be identified by user involvement. The program should be modified before release so that it performs as desired by control designers. Further details of the program are contained in Captain Doug Porter's thesis (Ref.14) since he aided in developing the package. The next chapter discusses the design that is performed using MULTI.

V. Design Approaches

Introduction

This chapter discusses the several approaches that are taken to design the tracker control law. Since there are three design procedures (see Chapter III), the first thing that needs to be determined is the design procedure to be used. Then, once the proper choice is made, the design is performed using the program MULTI.

Looking at the model for Mach 0.6 at an altitude of 15,000 feet (see Appendix A) it is obvious that the $\underline{B}$ matrix does not have full rank. The first approach attempted is the use of the psuedoinverse of $\underline{B}$ in conjunction with the regular design procedure to generate a control law. The second attempt involves recombining some of the input surfaces and re-arranging the equations so that they can be put in the form of Equation (9) and Equation (10) in Chapter III. Once the equations are in the necessary form, the unknown design procedure is attempted first. However, $\underline{G}(0)$ proves to be rank deficient so the regular design procedure is used since $\underline{C}_2\underline{B}_2$ had rank $= \ell$. The first choice of outputs leads to a set of transmission zeros at the origin and an uncontrollable mode. A second choice of outputs is selected with $\underline{C}_2\underline{B}_2$ rank deficient. Using the irregular design procedure, a measurement matrix $\underline{M}$ is selected that places the transmission zeros at -3. This gives a stable response and a control law that responds to a desired input command vector. All of these attempts are explained in detail in this chapter. The results of the final attempt

are presented to show the resulting tracker control law.

Psuedoinverse Approach

The theory developed by Professor Porter considers only the case for $n > \ell$ (number of states > number of outputs). However, the model presented in Appendix A has $n = \ell$. If $n = \ell$, then the $\underline{B}$ matrix is equal to $\underline{B}_2$ since the number of zero rows above $\underline{B}_2$ (see Equation (9) Chapter III) is equal to $n - \ell$. Also since $\underline{B}_2 \in R^{\ell x \ell}$, the number of inputs must equal the number of outputs to satisfy this condition. Therefore, in order to maintain 8 inputs, 8 outputs are required. This prevented the idea of measuring less outputs to place the $\underline{B}$ matrix in the proper format. Also, if $n = \ell$, then the $\underline{C}$ matrix is equal to $\underline{C}_2$.

The first approach uses the fact that $\underline{C}_2\underline{B}_2 = \underline{C}\,\underline{B}$ and this relation is used in conjunction with the regular design procedure. Since $\underline{C}$ is chosen to have full rank, the use of a measurement matrix is not needed. However, $\underline{B}$ is rank deficient so that $\underline{K}_o$ can not be determined by the relationship

$$\underline{K}_o = (\underline{C}_2\underline{B}_2)^{-1}\underline{\Sigma} = (\underline{C}\,\underline{B})^{-1}\underline{\Sigma} = \underline{B}^{-1}\underline{C}^{-1}\underline{\Sigma} \qquad (23)$$

This makes it necessary to use a psuedoinverse for $\underline{B}^{-1}$. This inverse is noted as $\underline{B}_p^{-1}$. The psuedoinverse is not guaranteed to have a unique solution.

When the $\underline{B}$ matrix psuedoinverse is obtained, the result is a rank deficient $\underline{B}_p^{-1}$. There are two columns of zeros (fourth and eighth).

The resulting $\underline{B}_p^{-1}$ is:

$$\underline{B}_p^{-1} = \begin{bmatrix} -0.6134E-01 & -0.6699E+01 & 0.5062E-01 & 0.0 & 0.8542E+03 & 0.1020E+01 & 0.7846E+01 & 0.0 \\ 0.5106E-01 & 0.5220E+01 & -0.1508E+00 & 0.0 & -0.7837E+03 & -0.9874E+00 & -0.7208E+01 & 0.0 \\ -0.8890E-02 & -0.2823E+00 & 0.1054E-01 & 0.0 & -0.5553E+02 & -0.3387E-01 & -0.7001E+00 & 0.0 \\ -0.5145E-01 & -0.2428E+01 & 0.6748E-01 & 0.0 & 0.1163E+03 & 0.5315E-01 & 0.1051E+01 & 0.0 \\ 0.5145E-01 & 0.2428E+01 & -0.6748E-01 & 0.0 & -0.1163E+03 & -0.5315E-01 & -0.1051E+01 & 0.0 \\ -0.2916E-01 & -0.7327E+00 & 0.3057E-01 & 0.0 & -0.6437E+02 & -0.5587E-01 & -0.5897E+00 & 0.0 \\ -0.7650E+00 & -0.3081E+02 & 0.9576E+00 & 0.0 & -0.1709E+04 & -0.7543E+00 & 0.1543E+02 & 0.0 \\ 0.1508E-01 & 0.4569E+01 & -0.5126E-01 & 0.0 & 0.1605E+03 & 0.7333E-01 & 0.1450E+01 & 0.0 \end{bmatrix}$$

Using this matrix in Equation (23) along with $\alpha_r = 1$ and $\underline{\Sigma} = \underline{I}$, the resulting $\underline{K}_o$ is

$$\underline{K}_o = \begin{bmatrix} -0.6134E-01 & 0.6699E+01 & 0.5062E-01 & -0.6699E+01 & 0.8542E+03 & 0.1020E+01 & 0.7846E+01 & 0.0 \\ 0.5106E-01 & -0.5220E+01 & -0.1508E+00 & 0.5220E+01 & -0.7837E+03 & -0.9874E+00 & -0.7208E+01 & 0.0 \\ -0.8890E-02 & 0.2823E+00 & 0.1054E-01 & -0.2823E+00 & -0.5553E+02 & -0.3387E-01 & -0.7001E+00 & 0.0 \\ -0.5145E-01 & 0.2428E+01 & 0.6748E-01 & -0.2428E+01 & 0.1163E+03 & 0.5315E-01 & 0.1051E+01 & 0.0 \\ 0.5145E-01 & -0.2428E+01 & -0.6748E-01 & 0.2428E+01 & -0.1163E+03 & -0.5315E-01 & -0.1051E+01 & 0.0 \\ -0.2916E-01 & 0.7327E+00 & 0.3057E-01 & -0.7327E+00 & -0.6437E+02 & -0.5587E-01 & -0.5897E+00 & 0.0 \\ -0.7650E+00 & 0.3081E+02 & 0.9576E+00 & -0.3081E+02 & -0.1709E+04 & -0.7543E+00 & -0.1543E+02 & 0.0 \\ 0.1508E-01 & -0.4569E+01 & -0.5126E-01 & 0.4569E+01 & 0.1605E+03 & 0.7333E-01 & 0.1450E+01 & 0.0 \end{bmatrix}$$

This matrix is not acceptable due to the column of zeros. This in effect makes one error state unobservable. Also as a check on the validity of $\underline{K}_o$, Equation (23) can be re-arranged as

$$\underline{C}\,\underline{B}\,\underline{K}_o = \underline{\Sigma} \tag{24}$$

Using the value of $\underline{K}_o$ obtained from Equation (23), and using the original $\underline{C}$ and $\underline{B}$ matrices, Equation (24) can be used to see if the original $\underline{\Sigma}$ matrix can be obtained. The original $\underline{\Sigma}$ matrix used to find $\underline{K}_o$ is $\underline{\Sigma} = \underline{I}$. However, when Equation (24) is used, the resulting matrix obtained using TOTAL (Ref. 8) is

$$\underline{C}\,\underline{B}\,\underline{K}_o = \begin{bmatrix} 0.996 & 0 & 0 & 0 & 0.2893 & -0.023 & 0 & 0 \\ 0 & 1 & 0 & -1 & 0 & 0 & 0 & 0 \\ 0 & 0 & 1 & 0 & 0.2213 & -0.025 & 0 & 0 \\ 0 & 0 & 0 & 0 & 0 & 0 & 0 & 0 \\ 0 & 0 & 0 & 0 & 0.9993 & 0 & 0 & 0 \\ 0 & 0 & 0 & 0 & 0.3007 & 0.9982 & 0 & 0 \\ 0 & 0 & 0 & 0 & 0.047 & 0 & 1 & 0 \\ 0 & 0 & 0 & 0 & 0 & 0 & 0 & 0 \end{bmatrix}$$

This is not $\underline{\Sigma}$ that is used to find $\underline{K}_o$. The problem lies in the psuedoinverse of $\underline{B}$. Therefore, the psuedoinverse approach is deemed unacceptable. The next approach puts the state and output equations into the form of Equations (9) and (10).

Recombined Input Surfaces

For the model presented in Appendix A, Equations (A-39) and (A-40), $n = 8 = m = \ell$. The $\underline{B}$ matrix has two rows of zeros in it. These two rows

of zeros come from the kinematic relationships

$$\dot{\theta} = q \tag{25a}$$

$$\dot{\phi} = p \tag{25b}$$

If the state equations are put in the form of Equation (9), the number of outputs allowed is determined from the equation

$$n - \ell = \text{number of rows of zero} \tag{26}$$

Since there are two rows of zeros and eight states, the number of outputs needed is 6. Since the number of outputs must equal the number of inputs, there can only be six inputs. Since there are eight inputs in the development of the aircraft equations, some of the input surfaces must be recombined. The surfaces that are split are the horizontal tail (δ_H), the ailerons (δ_a) and the spoilers (δ_s).

The ailerons are combined so that $\underline{B}_2$ has full rank. If this surface were left divided, there would be two columns in the $\underline{B}$ matrix that are not independent. Combining the aileron input surface left the model with 7 inputs so that one other surface was recombined.

The spoilers are chosen to be the other surface to be recombined for two reasons. First, the spoilers normally act as a unit, and second, the horizontal tail is used in another study as a split surface (Ref. 14).

With only six inputs, the state equations are re-arranged so that the $\underline{B}$ matrix has the form shown in Equation (9). The resulting

state equation matrices for Mach 0.6 at an altitude of 15,000 feet are

$$\underline{A} = \begin{bmatrix} 0 & 0 & 0 & 0 & 1 & 0 & 0 & 0 \\ 0 & 0 & 0 & 0 & 0 & 0 & 1 & 0 \\ -32.2 & 0 & -0.06006 & -1.897 & 0 & 0 & 0 & 0 \\ 0 & 0 & -0.000676 & -1.006 & 1 & 0 & 0 & 0 \\ 0 & 0 & 0.001362 & -4.835 & -34.08 & 0 & 0 & 0 \\ 0 & 0.05077 & 0 & 0 & 0 & -0.01622 & 0.05106 & -0.8776 \\ 0 & 0 & 0 & 0 & 0 & -33.43 & -2.443 & 0.7382 \\ 0 & 0 & 0 & 0 & 0 & 5.326 & -8.1 & -32.1 \end{bmatrix} \quad (27)$$

$$\underline{B} = \begin{bmatrix} 0 & 0 & 0 & 0 & 0 & 0 \\ 0 & 0 & 0 & 0 & 0 & 0 \\ 0 & -7.55 & -7.55 & 0 & -2.78 & -12.04 \\ 0 & -0.0675 & -0.0675 & 0 & 0.02268 & 0.2244 \\ 0 & -8.204 & -8.204 & 0 & -0.4132 & -1.795 \\ 0.0454 & 0 & 0 & -0.01132 & 0 & 0 \\ 1.053 & 0.7866 & -0.7866 & 6.744 & 0 & 0.8808 \\ -5.08 & -0.0385 & 0.0385 & 0.4656 & 0 & -0.0054 \end{bmatrix} \quad (28)$$

$$\underline{x} = \begin{bmatrix} \theta \\ \phi \\ u \\ \alpha \\ q \\ \beta \\ p \\ r \end{bmatrix} \tag{29}$$

$$\underline{u} = \begin{bmatrix} \delta_r \\ \delta_{H_R} \\ \delta_{H_L} \\ \delta_a \\ \delta_s \\ \delta_f \end{bmatrix} \tag{30}$$

The $\underline{B}_2$ matrix has full rank (rank = ℓ) and a choice of outputs is made so that $\underline{C}_2$ has rank = ℓ. The output vector chosen is

$$\underline{y} = \begin{bmatrix} \gamma \\ u \\ q \\ \beta \\ r \\ p \end{bmatrix} \tag{31}$$

This choice of outputs (where γ is the flight path angle) yields a $\underline{C}$ matrix

$$\underline{C} = \begin{bmatrix} 1 & 0 & 0 & -1 & 0 & 0 & 0 & 0 \\ 0 & 0 & 1 & 0 & 0 & 0 & 0 & 0 \\ 0 & 0 & 0 & 0 & 1 & 0 & 0 & 0 \\ 0 & 0 & 0 & 0 & 0 & 1 & 0 & 0 \\ 0 & 0 & 0 & 0 & 0 & 0 & 0 & 1 \\ 0 & 0 & 0 & 0 & 0 & 0 & 1 & 0 \end{bmatrix} \tag{32}$$

The $\underline{C}_2$ matrix has full rank (rank $= \ell$) so the first procedure used with this new model is the unknown design procedure.

Unknown Design

In trying to use the unknown procedure, the primary criterion is

that rank $G(0) = \ell$. When the new model is entered into the computer program, the resulting $\underline{G}(0)$ matrix is

$$\underline{G}(0) = \begin{bmatrix} 0 & 2.002 & 2.002 & 0 & -0.3332 & 22.48 \\ 0 & 5422.0 & 5422.0 & 0 & 436.5 & -1685.0 \\ 0 & 0 & 0 & 0 & 0 & 0 \\ 0.2781 & 0.1524 & -0.1524 & 1.98 & 0 & 0.2203 \\ -0.4829 & 0.01181 & -0.01181 & 0.3447 & 0 & 0.02059 \\ 0 & 0 & 0 & 0 & 0 & 0 \end{bmatrix} \quad (33)$$

Clearly, the rank of $\underline{G}(0)$ is not equal to ℓ. Therefore, the unknown plant approach cannot be used. The next approach is to use the regular design since rank $\underline{C}_2\underline{B}_2 = \ell$.

Regular Design

The regular design produces a $\underline{K}_o$ matrix according to Equation (13). The necessary criteria is that both $\underline{C}_2$ and $\underline{B}_2$ have rank $= \ell$. This is the case for the outputs given in Equation (31). Also, it is necessary that the transmission zeros of the plant be in the unit disc (or in the left half s-plane). The location of the transmission zeros is given by Equation (14). Using this equation, it is determined that the transmission zeros lie on the unit disc; not inside of it. This corresponds to being

at the origin in the s-plane. The result of this is that an uncontrollable mode (namely the forward perturbation velocity u) is present. The reason the transmission zeros are on the unit disc is that the kinematic parameters p and q are included in the outputs. Therefore, to obtain a stable response, these outputs cannot be controlled. Removing them makes $\underline{C}_2$ rank deficient so the necessary approach is to use the irregular design.

Irregular Design

A new output vector is chosen so that p and q are not included. The resulting vector is

$$y = \begin{bmatrix} \gamma \\ u \\ \theta \\ \beta \\ r \\ \phi \end{bmatrix} \tag{34}$$

Using this output vector produces a $\underline{C}$ matrix that is

$$\underline{C} = \begin{bmatrix} 1 & 0 & 0 & -1 & 0 & 0 & 0 & 0 \\ 0 & 0 & 1 & 0 & 0 & 0 & 0 & 0 \\ 1 & 0 & 0 & 0 & 0 & 0 & 0 & 0 \\ 0 & 0 & 0 & 0 & 0 & 1 & 0 & 0 \\ 0 & 0 & 0 & 0 & 0 & 0 & 0 & 1 \\ 0 & 1 & 0 & 0 & 0 & 0 & 0 & 0 \end{bmatrix} \tag{35}$$

The $\underline{C}_2$ matrix in this case is rank deficient. Since the $\underline{B}$ matrix is not changed, $\underline{B}_2$ has full rank. This fits the form for the irregular design.

The main objective of the irregular design is to choose a measurement matrix $\underline{M}$ that makes the matrix $\underline{C}_2$ have full rank. The measurement matrix $\underline{M}$ also determines the location of the transmission zeros. It is necessary to place them within the unit disc (or equivalently in the left half s-plane). The measurement matrix must have the same number of rows as $\underline{C}_2$, and the number of columns in $\underline{M}$ is equal to the number of rows in $\underline{A}_{12}$. For the case at hand, $\underline{M}$ must have dimension 6 x 2. The matrix $\underline{C}_2$ can be made to have full rank by placing elements in the (3,3) position and the (6,5) position. Since the matrix $\underline{A}_{12}$ cannot be changed, the $\underline{M}$ matrix must have elements in the (3,1) and (6,2) locations in order to make $\underline{C}_2$ full rank. The chosen $\underline{M}$ matrix is

$$\underline{M} = \begin{bmatrix} 0 & 0 \\ 0 & 0 \\ 0.25 & 0 \\ 0 & 0 \\ 0 & 0 \\ 0 & 0.25 \end{bmatrix} \tag{36}$$

The matrices $\underline{F}_1$ and $\underline{F}_2$ are determined by using Equation (16) and (17). Since $\underline{A}_{11} = \underline{0}$, $\underline{F}_1$ is equal to $\underline{C}_1$ for any choice of $\underline{M}$. For the $\underline{M}$ chosen, $\underline{F}_2$ is

$$\underline{F}_2 = \begin{bmatrix} 0 & -1 & 0 & 0 & 0 & 0 \\ 1 & 0 & 0 & 0 & 0 & 0 \\ 0 & 0 & 0.25 & 0 & 0 & 0 \\ 0 & 0 & 0 & 1 & 0 & 0 \\ 0 & 0 & 0 & 0 & 0 & 1 \\ 0 & 0 & 0 & 0 & 0.25 & 0 \end{bmatrix} \tag{37}$$

The location of the transmission zeros can be determined by applying Equation (22). For a sampling period of 0.01 and for the $\underline{M}$ chosen, the two transmission zeros are located at 0.96 (or -3 in the s-plane). This location is accepted for this design. A different location might be

better, and this needs to be investigated in future work.

A problem that has been observed by designers using high gain techniques is that large inputs are required for "good" responses. For aircraft applications, the inputs have physical limits that cannot be exceeded. For instance, the spoilers cannot go negative, the flaps cannot go positive, and the surface deflections cannot exceed a set angle limit. Tracking simulations are used to adjust design parameters until a design is achieved that does not exceed the aircraft's physical limits. The limits assumed for this study are shown in Table II.

TABLE II

Aircraft Surface Limits

SURFACE	- LIMIT
Rudder	$\pm$ 30°
Horizontal Tail	$\pm$ 30°
Aileron	$\pm$ 45°
Spoiler	+ 60°
Flap	- 60°

The design is initiated with $T = 0.01$, $\alpha_r = 2$, $\epsilon = 1$, and $\underline{\Sigma} = \underline{I}$. It is determined that $\alpha_r = 1$ is better than $\alpha_r = 2$, and that ϵ must be 0.1. The sampling period is satisfactory. The main parameter that has to be adjusted is the $\underline{\Sigma}$ matrix. Tracking γ produces inputs that are too large by a factor of 10. Therefore, the first element of the $\underline{\Sigma}$ matrix is reduced by a factor of 10 from 1 to 0.1. Likewise, tracking β, r, and ϕ causes input problems so the corresponding $\underline{\Sigma}$ matrix elements have to be reduced. Figures 3 and 4 show input values obtained tracking β before and after adjusting the $\underline{\Sigma}$ matrix element. Likewise, Figures 5 and 6 show the adjustment needed for tracking r while Figures 7 and 8 show the adjustment needed when tracking ϕ.

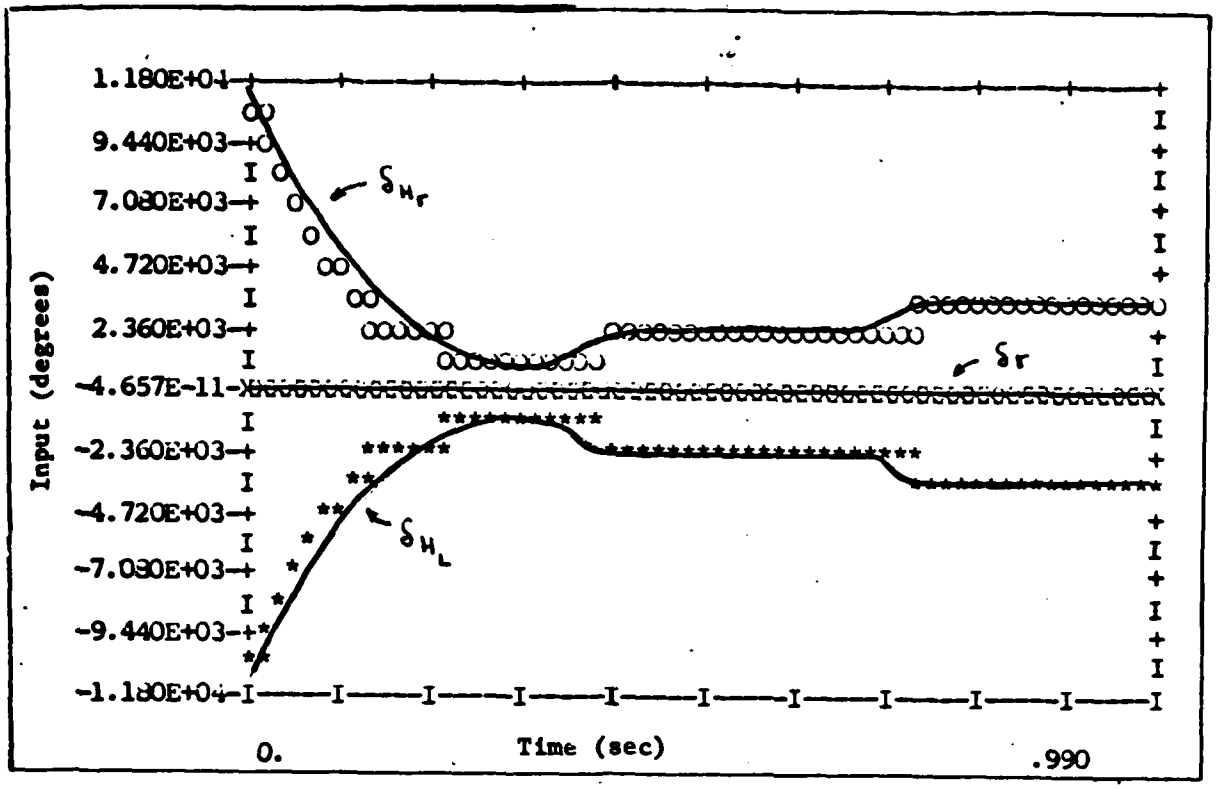

Figure 3 Input Responses Tracking β with 4th Element of Σ Equal to 1

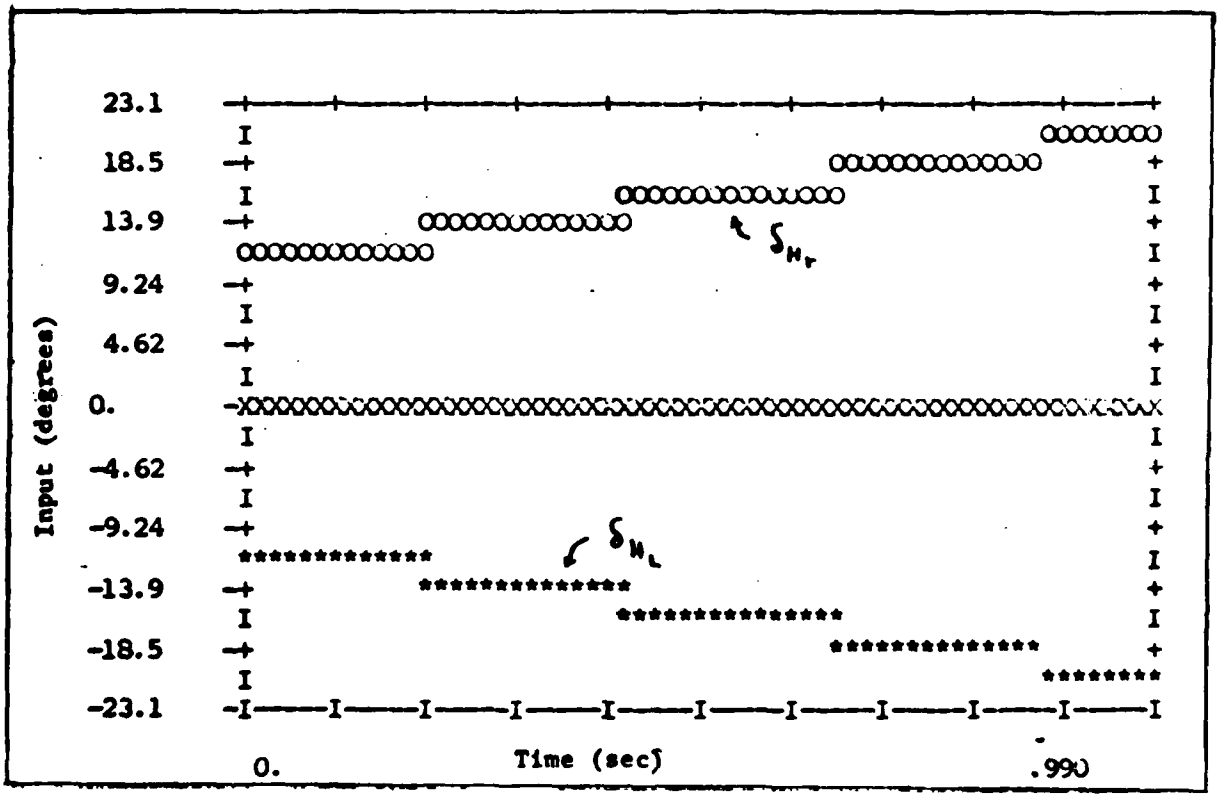

Figure 4 Input Responses Tracking β with 4th Element of Σ Equal to 0.001

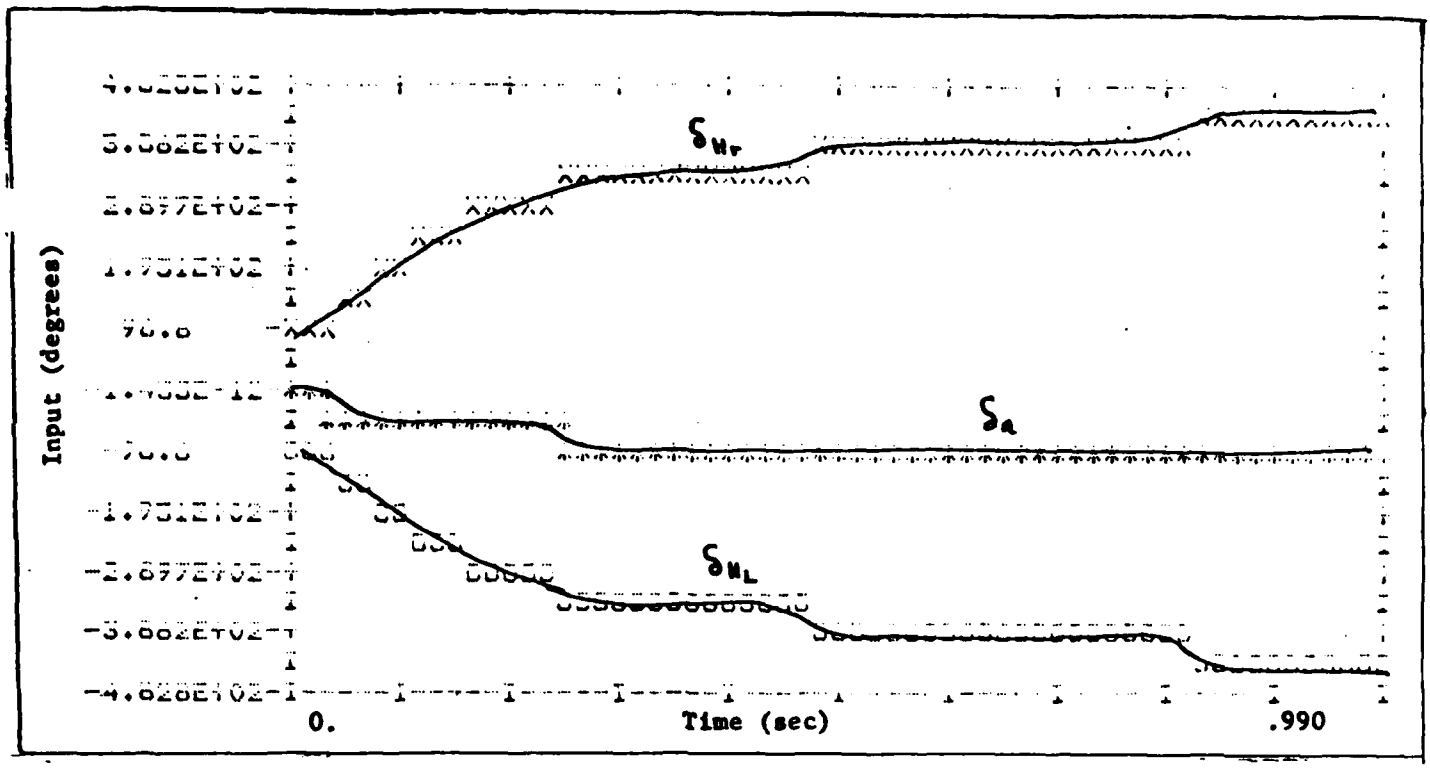

Figure 5 Input Responses Tracking r with 5th Element of Σ Equal to 1

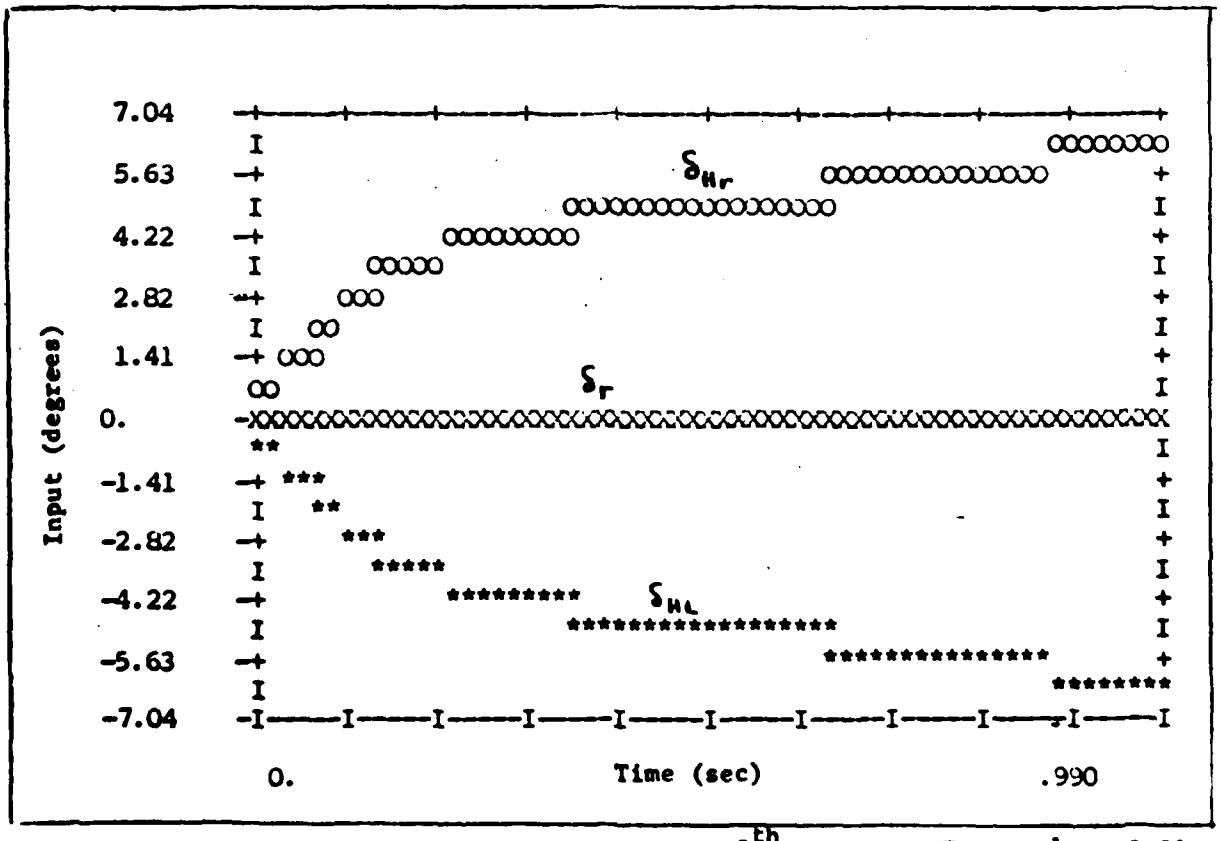

Figure 6 Input Responses Tracking r with 5th Element Σ Equal to 0.01

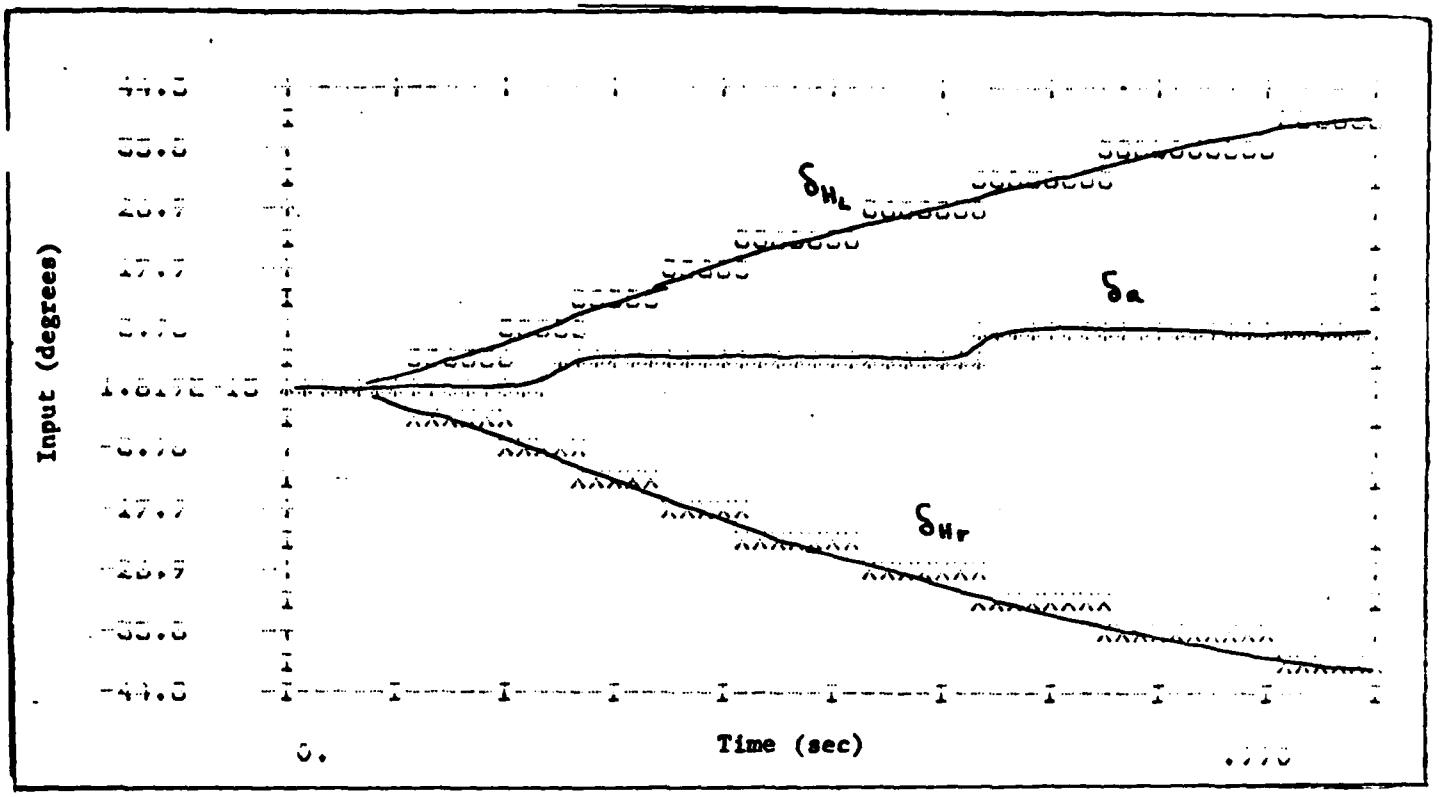

Figure 7 Input Responses Tracking ϕ with 6th Element of $\underline{\Sigma}$ Equal to 0.01

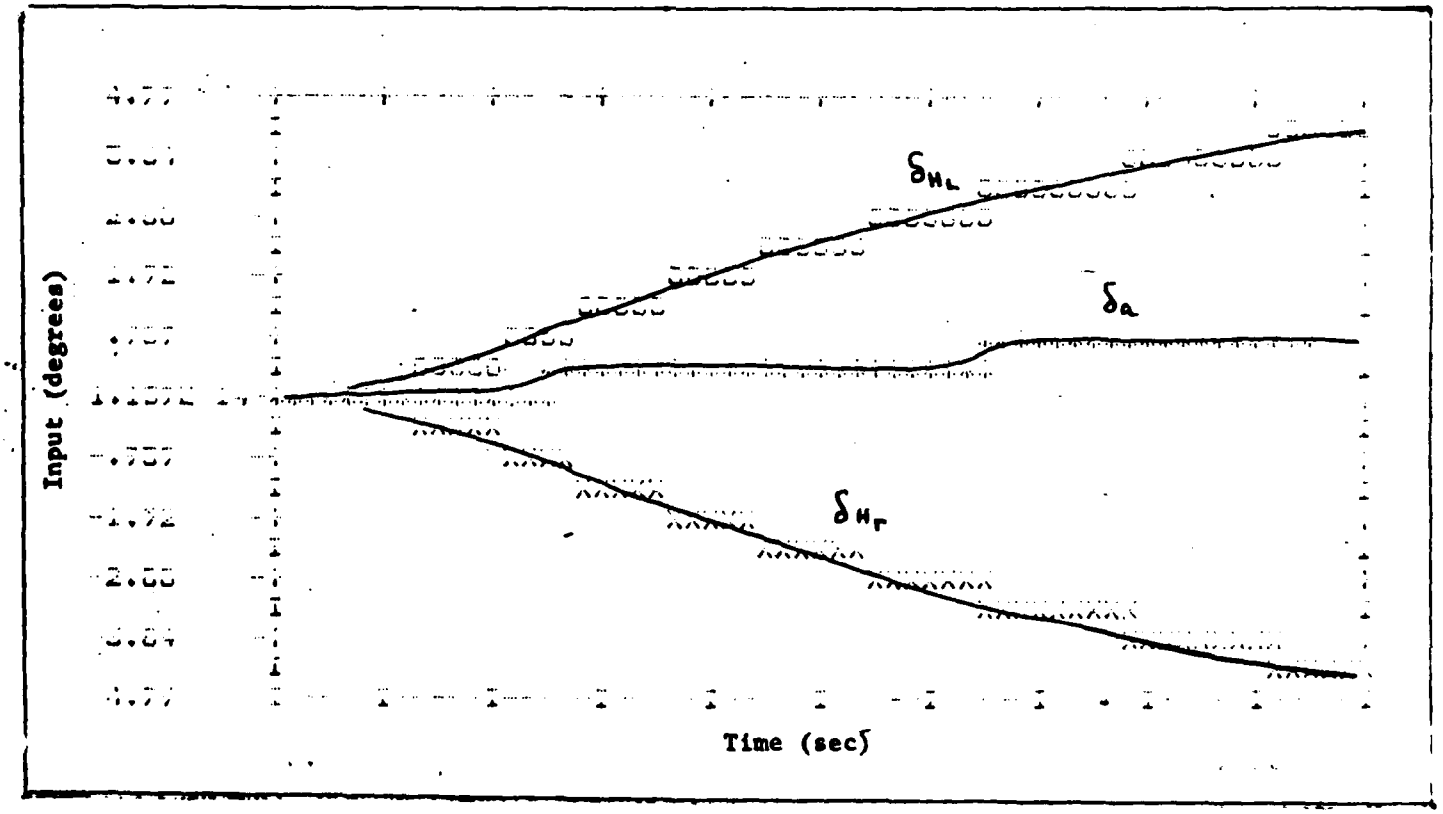

Figure 8 Input Responses Tracking ϕ with 6th Element of $\underline{\Sigma}$ Equal to 0.001

After adjusting the design parameter so that the inputs are not bounded, the final set of design parameters are

$$T = 0.01$$

$$\alpha_r = 1$$

$$\epsilon = 0.1$$

and

$$\underline{\Sigma} = \begin{bmatrix} 0.1 & 0 & 0 & 0 & 0 & 0 \\ 0 & 1 & 0 & 0 & 0 & 0 \\ 0 & 0 & 1 & 0 & 0 & 0 \\ 0 & 0 & 0 & 0.001 & 0 & 0 \\ 0 & 0 & 0 & 0 & 0.01 & 0 \\ 0 & 0 & 0 & 0 & 0 & 0.001 \end{bmatrix} \tag{38}$$

The matrix $\underline{K}_o$ is computed using Equation (21). The $\underline{K}_o$ for this design is

$$\underline{K}_o = \begin{bmatrix} -0.1625E-02 & 0.1767E-03 & -0.1185E-02 & -0.3826E-02 & -0.5443E-03 & -0.1066E-04 \\ 0.7340E-01 & -0.6928E-02 & 0.2528E-01 & 0.1062E+00 & 0.9722E-02 & 0.4446E-03 \\ -0.7334E-01 & 0.9020E-02 & -0.8172E-01 & -0.1062E+00 & -0.9722E-02 & -0.4446E-03 \\ -0.6519E-02 & 0.7085E-03 & -0.4753E-02 & -0.2418E-01 & -0.2183E-02 & -0.4274E-04 \\ 0.3428E+00 & -0.7893E-01 & 0.4034E+00 & 0.3999E-14 & 0.3661E-15 & 0.1674E-16 \\ -0.7919E-01 & 0.8606E-02 & -0.5774E-01 & -0.6333E-15 & -0.5797E-16 & -0.2651E-17 \end{bmatrix}$$

As a check on the validity of this $\underline{K}_o$, Equation (21) is re-arranged to solve for $\underline{\Sigma}$. The resulting equation is

$$\underline{F}_2\underline{B}_2\underline{K}_o = \underline{\Sigma} \tag{39}$$

The result of using Equation (39) is the $\underline{\Sigma}$ matrix of Equation (38). This is a necessary condition, but not a sufficient one to guarantee a good design. The final tracker control law designed is

$$U(kT) = \tilde{T}\epsilon\,\underline{K}_o\, e(kT) + \tilde{T}\epsilon\,\underline{K}_1\, z(kT) \tag{40}$$

where

$$T = 0.01$$

$$\epsilon = 0.1$$

$$\underline{K}_o = \underline{K}_1$$

$$\alpha_r = 1$$

The tracking responses and robustness of this control law is demonstrated in Appendix B, and a discussion of these results is found in Chapter VI.

Summary

This chapter presents the different design approaches taken to develop a tracker control law for the A-7D aircraft. The design is for the flight condition of Mach 0.6 at an altitude of 15,000 feet. All design procedures are used, but the irregular approach proves to be

the only one that gives reasonable design. The sensors and actuators are not used in the simulation, and this is discussed in greater detail in Chapter VI. Responses obtained for the final control law are in Appendix B. All the designs are accomplished using the computer package discussed in Chapter IV.

VI. Results

Introduction

This chapter discusses the results of the tracker control law designed in Chapter V. The simulation results obtained using this design are in Appendix B. Each output variable is tracked by itself for a total of six different tracking commands. In each case, the other five outputs are commanded to zero. For example, when the flight path angle is commanded, the command vector is

$$\underline{V} = \begin{bmatrix} 1 \\ 0 \\ 0 \\ 0 \\ 0 \\ 0 \end{bmatrix} \tag{41}$$

In Equation (41), the tracked output is commanded to one unit, and the other outputs are commanded to zero.

After showing the tracking responses of the control law, Appendix B presents the robustness results. First, the control law is applied without a rudder in the plant. Second, the control law is applied at another

flight condition (Mach 0.18 at 2,000 feet). The robustness is discussed in this chapter.

To conclude this chapter, the effect of changing design parameters (α_r, T, $\mathcal{E}$, $\underline{\Sigma}$) is mentioned.

Tracking Responses

The final design presented in Chapter V does not track lateral flight modes very well; if at all. The reason for this is the fact that the last three elements of the $\underline{\Sigma}$ matrix are small. These values had to be made small so that inputs do not exceed their physical limits. The end result is that the control law designed in this thesis is a good longitudinal tracker.

Looking at Figures B-7, B-20, and B-33 it can be seen that "good" tracking is obtained for the longitudinal outputs. What is considered "good" is determined solely by the designer. In all cases the inputs do not exceed their assumed limits. However, some inputs appear to still be growing at the end of the simulation. These inputs will stop increasing when final steady state tracking is achieved. In one case the spoiler is shown going negative and the flap positive. This can not be physically done, but a relation between the surface can be derived that gives the same effect with opposite deflections. Therefore, this is not considered a problem. The interaction achieved is reasonable. Interaction of 5% is obtained when tracking γ (see Figures B-8 thru B-12).

The amount of interaction can be easily seen looking at Table 5 where the peak magnitudes of all the outputs are shown. By having essentially no interaction, the system responds as if it is decoupled. The unit for the inputs is degrees. The units for the outputs are:

1. For angles, the unit is degrees.
2. For rates, the unit is degrees per second.
3. For forward velocity, the unit is miles per hour.

TABLE 3

Figures of Merit for γ Tracking

Figure of Merit	Desired Value	Achieved Value
t_p	3 sec	2.7
t_s	3 sec	2.7
M_p	1.0	1.0

TABLE 4

Peak Inputs for γ Tracking (in 3 sec)

Input	Max Value	Assumed Limit
δ_r	-0.142	$\pm 30^o$
δ_{H_r}	7.4	$\pm 30^o$
δ_{H_L}	-7.4	$\pm 30^o$
δ_a	-0.658	$\pm 45^o$
δ_s	34.5	$+ 60^o$
δ_f	-8.0	$- 60^o$

TABLE 5

Peak Output Values for γ Tracking

Output	Peak Value
γ	1.0
u	0.036
θ	0.045
β	0.0
r	0.0
ϕ	0.0

u Tracking Responses

For the case when the forward perturbation velocity is tracked, the command vector is

$$v = \begin{bmatrix} 0 \\ 1 \\ 0 \\ 0 \\ 0 \\ 0 \end{bmatrix}$$

Looking at Figures B-13 thru B-24, it is seen that good tracking is again possible. Table 6 shows the desired figures of merits and the achieved values for the case of u tracking. Note that the desired values are different for this tracking case because faster response is possible. Table 7 gives the maximum input values needed for u tracking. Notice that none of the inputs exceed their limits.

For this case the spoiler is shown going negative and the flap positive. This can not be physically done, but a relationship between the surfaces can be derived that gives the same effect with deflections in the opposite directions. Therefore, this is not considered a big problem. Table 8 gives the maximum values of the outputs. By looking at this data, it is seen that interaction of less than 1% is obtained when tracking u.

TABLE 6

Figures of Merit for u Tracking

Figure of Merit	Desired Value	Achieved Value
t_p	0.75	0.5
t_s	1.5	1.3
M_p	1.15	1.07

TABLE 7

Peak Inputs for u Tracking (in 2 sec)

Input	Max Value	Assumed Limit
δ_r	0.02	$\pm$ 30°
δ_{H_r}	-0.735	$\pm$ 30°
δ_{H_L}	0.956	$\pm$ 30°
δ_a	0.075	$\pm$ 45°
δ_s	-8.4	+ 60°
δ_f	0.913	- 60°

TABLE 8

Peak Output Values for u Tracking

Output	Peak Value
γ	2.8 E-4
u	1.07
θ	3.2 E-5
β	0.0
r	0.0
ϕ	0.0

<u>θ Tracking Responses</u>

For tracking the pitch angle; the command vector is

$$v = \begin{bmatrix} 0 \\ 0 \\ 1 \\ 0 \\ 0 \\ 0 \end{bmatrix}$$

Looking at Figures B-25 thru B-36 it is seen that the tracking for θ is acceptable although not as good as for the other longitudinal modes. Table 9 gives the desired figures of merit for θ tracking along with the achieved values. The figures of merit were achieved very well. Table 10 shows the maximum input values needed for θ tracking. As in the other cases, none of the assumed limits are exceeded, but the spoiler and flap

try to go negative and positive respectively. However, they both cross the zero point at the same time so that this problem could be avoided in the same way it is for u tracking. The peak values of the outputs are given in Table 11. Extreme interaction is obtained when tracking θ. This is due to the physical relationship of output variables γ and u to θ. When pitch angle θ is commanded, there must be a slow down, and the aircraft must have a small flight path angle. The only way to overcome this is to introduce control surfaces like jet flaps, and possibly canards. Physical reality causes the interaction; not bad designing.

When interpreting the meaning of the aileron input (δ_a), it must be remembered that positive δ_a is when the right aileron is up and left aileron is down. Just the opposite is true for negative δ_a. This is the case when the ailerons are considered as one input.

TABLE 9

Figures fo Merit for θ Tracking

Figure of Merit	Desired Value	Achieved Value
t_p	2	1.9
t_s	2	1.9
M_p	1.15	1.10

TABLE 10

Peak Inputs for θ Tracking (in 2 sec)

Input	Max Value	Assumed Limit
δ_r	0.17	$\pm$ 30°
δ_{H_r}	-7.9	$\pm$ 30°
δ_{H_L}	-8.0	$\pm$ 30°
δ_a	0.69	$\pm$ 45°
δ_s	-50	+ 60°
δ_f	7.7	- 60°

TABLE 11

Peak Output Values for θ Tracking

Output	Peak Value
γ	0.37
u	-1.6
θ	1.10
β	0.0
r	0.0
ϕ	0.0

Lateral Mode Tracking

The lateral modes do not track the command values because the last three $\underline{\Sigma}$ matrix elements are so small. However, these cannot be increased without exceeding the input physical limits (see Chapter V).

Table 12 gives the peak values of the outputs being tracked. None of the lateral modes even come near the desired value of 1.

TABLE 12

Peak Lateral Mode Tracking Values

Output being Tracked	Peak Value
β	7.2 E-3
r	3.5 E-3
ϕ	1.2 E-2

No Rudder Responses

The longitudinal tracking is maintained when the rudder is removed as shown by looking at Figures B-73 thru B-89. However, this does not say a lot for the design since the rudder has little input to longitudinal modes anyway. Figures B-1 and B-13 demonstrate this fact. A better look at the

capability of this design to handle a lost input as a disability is presented in Reference 14. In Captain Porter's thesis, a horizontal stabilizer unit is removed. This has a significant effect on the longitudinal modes. Table 13 gives the achieved figures of merit without a rudder. Table 14 gives the maximum input values obtained, and Table 15 shows the interaction when the rudder is removed. All the results were very good with the rudder disabled. The only real noticeable difference is that the lateral modes are not zeroed out as well without the rudder when tracking u. However, interaction is maintained at less than 1% for this case.

TABLE 13

Figure of Merit without a Rudder

Figure of Merit	Achieved Value Tracking γ	Achieved Value Tracking u
t_p	3 sec	0.5
t_s	3 sec	1.3
M_p	1.0	1.07

TABLE 14

Input Peak Values when Tracking without a Rudder

Input	Max Value Tracking	Max Value Tracking u
δ_{H_r}	7.4	-0.735
δ_{H_L}	-7.4	0.956
δ_a	-6.6	7.5 E-2
δ_s	34.6	-8.35
δ_f	-8.0	0.91

TABLE 15

Peak Output Values Obtained without a Rudder Input

Output	Peak Value Tracking γ	Peak Value Tracking u
γ	1.0	2.8 E-4
u	3.4 E-2	1.07
θ	4.25 E-2	3.2 E-5
β	0.0	-4.3 E-4
r	0.0	2.0 E-3
ϕ	0.0	1.5 E-3

New Flight Condition

The tracker control law designed at the flight condition of Mach 0.6 and 15,000 feet is applied at a different flight condition; i.e. Mach 0.18 and 2,000 feet. In this way the control law is checked for robustness when faced with changing parameters. The control law did not respond well at all. In fact, all of the inputs exceeded their limits after about 1.5 seconds, and the commanded output grew unstable also. This trend is seen in Figures B-90 thru B-96. This does not mean that the control theory does not work, but rather that this is either a case the theory does not handle or this is a poor design. A more robust design can probably result if the design is done at the flight condition of Mach 0.18. The theory has been shown effective on several other plants.

Parameter Effects

In doing the design, the effect of changing design parameters (α_r, T, ε, and $\underline{\Sigma}$) is noticed. T acts like a gain parameter since the control law is proportioned to 1/T or frequency. Fast sampling corresponds to a small T and this acts like high gain. So the result is that decreasing T speeds up the response. Likewise, increasing T slows down the system performance. The parameter α_r is merely a direct change in the damping ratio of the system. Increasing α_r produces less damping, and decreasing α_r gives more. The parameter ε is a normalizing factor used to scale the outputs down to the commanded value. For instance, with ε = 1, the

outputs for this thesis are on the order of 10. Therefore, ϵ is set equal to 0.1 so the outputs can track to a value of 1 and not 10. The parameter $\underline{\Sigma}$ has diagonal elements that can be changed to change the magnitude of inputs. Supposedly, if the fifth input exceeds a desired magnitude, then the fifth $\underline{\Sigma}$ element can be adjusted to reduce the magnitude. However, it is found in this thesis that if problems arise with input magnitude with the fifth output; then the fifth element of the $\underline{\Sigma}$ matrix is adjusted to compensate. This is shown clearly in Chapter V. This is the reason that this matrix is referred to as an output weighting matrix (Ref. 12).

Summary

The sensor and actuators are not used in the simulations because acceptable responses can bot be achieved. The units are instead taken out of the design process by approximating their transfer functions as unity. This may be a reason that the program had difficulty with simulations of more than four seconds. A good study on how to include the sensor and actuator models is found in Joseph Smyth's thesis (Ref. 18).

This chapter discusses the tracking capability of the control law designed in this thesis. The result is that longitudinal tracking is possible, but not lateral. The robustness of the design is discussed. The design is not robust when applied at another flight condition. Further robustness checking of this type is found in Reference 14. The ability of the design to handle a surface disability is discussed also. The dis-

ability considered is the removal of the rudder. Since the rudder has little effect on longitudinal motion, this disability is handled easily by the longitudinal tracker. The final area presented in this chapter is the effect of design parameters. That section may prove to be the most valuable to future designers using this technique. The final chapter presents the recommendation of the author for future work.

VII. Conclusions and Recommendations

Conclusions

Although a control law that can track any of the six outputs is not designed, a fairly good longitudinal tracker design is achieved. The methods developed by Professor Porter are good in many cases, and have been proven so on many examples. However, the irregular design technique is actually a high gain approach to the problem. It has been noted by several designers that often high gain control causes inputs to be too large to be useful in aircraft applications. This is the problem encountered in this thesis. When the design is adjusted so that inputs do not exceed physical limits, the result is poor performance for lateral tracking. Perhaps someone more experienced in this type of design can develop a control law that performs better. As some engineers may describe it, this requires more fine tuning. This thesis should provide a good starting point for a better design.

It should also be kept in mind that the choice of outputs affects the design. One choice of outputs places the transmission zeros on the digital unit disc, and a measurement matrix can not be used to move them due to uncontrollability. A second choice of outputs provides the capability to choose a measurement matrix that can move the transmission zeros within the unit disc. This is the choice used in this thesis design. A different choice of outputs may prove even better.

The theory does not appear to allow for the case where the number of states equals the number of inputs. This is the case when all primary control surfaces are split into separate independent control surfaces. Because of this, it is concluded that this is not a good approach to reconfigurable control when the plant is like that found in Appendix A. Also, the theory does not allow for rank deficiencies in the $\underline{B}$ matrix. This prohibits the operation of the ailerons independently.

The best part of the technique developed by Professor Porter is that there is no discretization process required. As Professor Porter puts it, the plant does not change just because digital control is being used. Digital concepts are inherent in the design equations, but the plants used are continuous. This makes the design process much easier to apply than other techniques.

Recommendations

There are several areas that need to be investigated in the future. The design should be performed at the flight condition of Mach 0.18 at an altitude of 2,000 feet. Work has been done and it appears that a robust tracker can be designed at this condition (Ref. 14). It may be possible to design a more robust tracker around this condition. Also, a different choice of outputs may prove to be better. A look at how different output choices affect the design should be studied.

Since a longitudinal tracker is designed in this thesis, future

research can concentrate on designing a lateral tracker. Then once a good lateral tracker is designed, the two control laws can be combined into one or stored separately in a digital computer. The latter would probably prove to be easier to achieve.

Since the computer program is essential to design work, improvement of MULTI should be performed. At present the program is not capable of producing calcomp plots. This option needs to be corrected. Also, it is desirable in many cases to slow down a system response by ramping or shaping the inputs until they reach the step value. MULTI does not have the ability to use ramped inputs. Only step inputs which are piecewise constant are available. Software needs to be developed so that the designer has the ability to use either ramped or step inputs.

The simulation package developed and used by Professor Porter uses a Runge-Kutta solution of the differential equations. MULTI uses a library routine called ODE (Ref. 11). It should be determined in future work if using a Runge-Kutta routine can give better simulation results than ODE, and if so, why. A final area of needed improvement in MULTI is to increase the total time for a simulation. The simulation can not be run for more than 4 seconds without running out of CP time. Whether, this is due to ill conditioned equations, or whether it is a problem inherent in the program could not be determined. Research in this area needs to be done so that the simulation time can be increased.

While there is much work still to be done, the most important recommendation is that this thesis be continued to gain a better understanding of the problems associated with high-gain control theory and the program MULTI.

Bibliography

1. Bender, M.A., Wolf. Flight Test Evaluation of a Digital Flight Control System for the A-7D Aircraft Simulation Test Plan. Contract F33615-73-C-3098. Aeronautical Systems Division, Wright-Patterson AFB, OH, 15 February 1974.

2. Blakelock, John H. Automatic Control of Aircraft and Missiles. New York: John Wiley and Sons, Inc., 1965.

3. Bradshaw, A., B. Porter. Singular Perturbation Methods in the Design of Tracking Systems Incorporating Fast-Sampling Error-Actuated Controllers. IJSS, Vol. 12, pp 1181-1192, 1981.

4. Bradshaw, A., B. Porter. Singular Perturbation Methods in the Design of Tracking Systems Incorporating Inner-Loop Compensators and Fast-Sampling Error-Actuated Controllers. IJSS, Vol. 12, pp 1207-1220, 1981.

5. Broxmeyer, Charles. Inertial Navigation Systems. New York: M^{c}Graw-Hill, 1964.

6. Hemami, A. PACK200- Program for Computing the Transient Behavior of Tracking Systems Incorporating Unknown Plants, Actuator and Sensor Dynamics and Digital Controllers. University of Salford, 1981.

7. Kennedy, Tom A. CESA-An Interactive Computer for Complete Eigenstructure Assignement to Aid in Designing State-Space Control Law for MIMO Systems. Master Thesis. Air Force Institute of Technology, Wright-Patterson AFB, OH, March 1979.

8. Larimer, S.J. TOTAL-An Interactive Computer Aided Design Program for Digital and Continuous Control System Analysis and Synthesis. Master Thesis. Air Force Institute of Technology, Wright-Patterson AFB, OH, March 1978

9. LTV Vought Aeronautics Division; A-7 Aero-Dynamic Data Report. Report No. 2-53310/5R-1981, 21 May 1965.

10. McDonnell Douglas Corporation; The USAF Stability and Control Digital DATCOM. Volume I User's Manual, AFFDL-TR-76-45, Air Force Flight Dynamics Laboratory, Wright-Patterson AFB, OH, 1976.

11. Nikolai, Paul J., D.S. Clemm. Solution of Ordinary Differential Equations on the CDC 6600/CYBER 74 Processors. User's Manual, AFFDL-TR-76-130-FBR, Air Force Flight Dynamics Laboratory, Wright-Patterson AFB, OH, January 1977.

12. Porter, B. Distributed Multivariable Digital Control. Report USAME/DC/101/81. University of Salford, England, 1981

13. Porter, B. Design of Error-Actuated Controllers for Unknown Multivariable Plants. Report USAME/DC/108/80, University of Salford, 1980.

14. Porter, D. Reconfigurable Multivariable Tracker Control Law Design and Analysis. Masters thesis. AFIT/GE/EE/81D-48, Air Force Institute of Technology, Wright-Patterson AFB, OH, December 1981.

15. Potts, D. Direct Digital Design Method for Reconfigurable Multivaribale Control Laws for the A-7D Digital II Aircraft. Masters Thesis. Air Force Institute of Technology, Wright-Patterson, AFB, OH, December 1980.

16. Roskam, Jan. Airplane Flight Dynamics and Automatic Flight Controls. Lawerence, KS: Roskam Aviation and Engineering Corporation, 1976.

17. Seth, W.A. A-7D Estimated Flying Qualities. Report No. 2-53300/8R-8089. Dallas, TX: Vought Aeronautics Division, LTV Aerospace Company, 19 February 1969.

18. Smyth, J. Digital Fligh Control System Design Using Singular Perturbation Methods. Masters Thesis. AFIT/GE/EE/81D-55, Air Force Institute of Technology, Wright-Patterson, AFB, OH, December 1981.

Appendix A

Introduction

This appendix presents three models of the A-7D using linearized equations of motion. The linearized equations are used to derive the continuous state space models needed in the design of the tracker control law.

Equations of Motion

The lateral and longitudinal equations are developed with coupling between axes accomplished by non-traditional control inputs. Control derivatives not normally associated with either lateral or longitudinal axes are derived as described in Reference 15. For example, Equation (A-1) is a longitudinal dimensional control derivative produced by the lateral rudder displacement and is proportional to the coupling coefficient $C_{D_{\delta_r}}$:

$$X_{\delta_r} = \frac{S\bar{q}C_{D_{\delta_r}}}{m} \qquad \text{(A-1)}$$

The linear equations assume:

1. The mass of the aircraft is constant.
2. The aircraft body is rigid.
3. Perturbations from equilibrium are small.
4. The X, Y, and Z axes lie in the plane of symmetry, and the origin of the axes is at the aircraft center of gravity.
5. Flow is quasi-steady.

6. The earth is an inertial reference

7. Stability axes are used.

8. The aircraft flies in a straight and level trimmed flight condition.

The equations of motion are developed using the inputs for the horizontal tail (δ_H), the rudder (δ_r), the ailerons (δ_a), the flaps (δ_f), and the spoilers (δ_s). The linearized longitudinal equations of motion are as follows:

$$\dot{u} = -g\,\theta\cos\theta_1 + X_u u + X_\alpha \alpha + X_{\dot{\alpha}}\dot{\alpha} + X_{\delta_H}\delta_H + X_{\delta_r}\delta_r + X_{\delta_a}\delta_a + X_{\delta_s}\delta_s + X_{\delta_f}\delta_f \quad \text{(A-2)}$$

$$\dot{w} = U_1 q - g\,\theta\sin\theta_1 + Z_u u + Z_\alpha \alpha + Z_{\dot{\alpha}}\dot{\alpha} + Z_q q + Z_{\delta_H}\delta_H + Z_{\delta_r}\delta_r + Z_{\delta_a}\delta_a + Z_{\delta_s}\delta_s + Z_{\delta_f}\delta_f \quad \text{(A-3)}$$

$$\dot{q} = M_u u + M_{\dot{\alpha}}\dot{\alpha} + M_q q + M_{\delta_H}\delta_H + M_{\delta_r}\delta_r + M_{\delta_a}\delta_a + M_{\delta_s}\delta_s + M_{\delta_f}\delta_f \quad \text{(A-4)}$$

$$\dot{\theta} = q$$

The lateral equation of motion are:

$$\dot{v} = -U_1 r + g\,\phi\cos\theta_1 + Y_\beta \beta + Y_p p + Y_r r + Y_{\delta_H}\delta_H + Y_{\delta_r}\delta_r + Y_{\delta_a}\delta_a + Y_{\delta_s}\delta_s + Y_{\delta_f}\delta_f \quad \text{(A-6)}$$

$$\dot{p} = \frac{I_{xz}}{I_{xx}} f + L_\beta \beta + L_p p + L_r r + L_{\delta_H}\delta_H + L_{\delta_r}\delta_r + L_{\delta_a}\delta_a + L_{\delta_s}\delta_s + L_{\delta_f}\delta_f \quad \text{(A-7)}$$

$$\dot{r} = \frac{I_{xz}}{I_{xx}}\dot{p} + N_{\beta}\beta + N_p\, p + N_r\, r + N_{\delta_H}\delta_H + N_{\delta_r}\delta_r + N_{\delta_a}\delta_a + N_{\delta_s}\delta_s + N_{\delta_f}\delta_f \qquad \text{(A-8)}$$

$$\dot{\phi} = p + r\tan\theta_1 \qquad \text{(A-9)}$$

Notice that by using separate control of the segments of the lateral control surfaces (δ_r, δ_a) it is possible to excite longitudinal motion. This is developed later in this appendix. Also, note that the longitudinal control surfaces (δ_H, δ_s, δ_f) can excite lateral motion.

Dimensional Control Derivative Equations

The equations for the longitudinal dimensional control derivatives as given in Reference 16 are as follows:

$$X_{\delta} = -XC_{D_{\delta}} \qquad \text{(A-10)}$$

$$X_u = \frac{-X\,(C_{D_u} + 2C_{D_1})}{U_1} \qquad \text{(A-11)}$$

$$X_{\alpha} = -X\,(C_{D_{\alpha}} - C_{L_1}) \qquad \text{(A-12)}$$

where $X = \bar{q}s/m$

For the Z force inputs the equations are:

$$Z_{\delta} = -ZC_{L_{\delta}} \qquad \text{(A-13)}$$

$$Z_u = \frac{-2\,(C_{L_u} + 2C_{L_1})}{U_1} \qquad \text{(A-14)}$$

$$Z_{\alpha} = -Z \left(C_{L_{\alpha}} + C_{D_1} \right) \tag{A-15}$$

where $Z = \bar{q}s/m$

For the moment inputs around the y axis, the equations are:

$$M_{\delta} = MC_{m_{\delta}} \tag{A-16}$$

$$M_u = \frac{M \left(C_{m_u} + 2C_{m_1} \right)}{U_1} \tag{A-17}$$

$$M_{\alpha} = MC_{m_{\alpha}} \tag{A-18}$$

$$M_{\dot{\alpha}} = \frac{M \bar{c} C_{m_{\dot{\alpha}}}}{2U_1} \tag{A-19}$$

$$M_q = \frac{M \bar{c} C_{mq}}{2U_1} \tag{A-20}$$

where $M = \bar{q}s\bar{c} / I_{yy}$

The equations for the lateral control derivatives are:

$$Y_{\delta} = YC_{y_{\delta}} \tag{A-21}$$

$$Y_{\beta} = YC_{y_{\beta}} \tag{A-22}$$

$$Y_p = \frac{Y b Cy_p}{2U_1} \tag{A-23}$$

$$Y_r = \frac{Y b Cy_r}{2U_1} \tag{A-24}$$

where $Y = \bar{q}s / m$

For the L and N moment inputs around the x and z axes, respectively, the equations are as follows:

$$L_{\zeta} = LC_{\ell_{\delta}} \tag{A-25}$$

$$L_{\beta} = LC_{\ell_{\beta}} \tag{A-26}$$

$$L_{p} = \frac{LbC_{\ell_{p}}}{2U_{1}} \tag{A-27}$$

$$L_{r} = \frac{LbC_{\ell_{r}}}{2U_{1}} \tag{A-28}$$

$$N_{\delta} = NC_{n_{\zeta}} \tag{A-29}$$

$$N_{\beta} = NC_{n_{\beta}} \tag{A-30}$$

$$N_{p} = \frac{NbC_{n_{p}}}{2U_{1}} \tag{A-31}$$

$$N_{r} = \frac{NbC_{n_{r}}}{2U_{1}} \tag{A-32}$$

where $N = \bar{q}sb / I_{zz}$ and $L = \bar{q}sb / I_{xx}$

In all of these equations, $\delta = \delta_{H}$, δ_{a} , δ_{r} , δ_{s} , δ_{f} .
The data for use in these equations is given in Table A-1 (Ref. 1).

TABLE A-1

Aircraft Data at Different Mach Numbers

Mach	0.18	0.6	0.8	Units
Altitude	2,000	15,000	35,000	ft
Weight	25,338	25,338	25,338	lbs
Center of gravity	28.71 %	28.71 %	28.71 %	% of m.g.c.
$\bar{q}$	44.67	300.88	435.99	lbs / ft^2
s	375	375	375	ft^2
b	38.73	38.73	38.73	ft
$\bar{c}$	10.84	10.84	10.84	ft
I_{xx}	15,475	15,365	13,323	slug·ft^2
I_{zz}	73,697	79,005	79,005	slug·ft^2
I_{yy}	66,566	69,528	69,528	slug·ft^2
I_{xz}	-3870	-1664	-2046	slug·ft^2

AD-A127 440 DESIGN OF A MULTIVARIABLE TRACKER CONTROL LAW FOR THE A-7D DIGITAC II AIRCRAFT(U) AIR FORCE INST OF TECH WRIGHT-PATTERSON AFB OH SCHOOL OF ENGI.. R N PASCHALL 2/2

UNCLASSIFIED DEC 81 AFIT/GE/EE/81D-47 F/G 1/3 NL

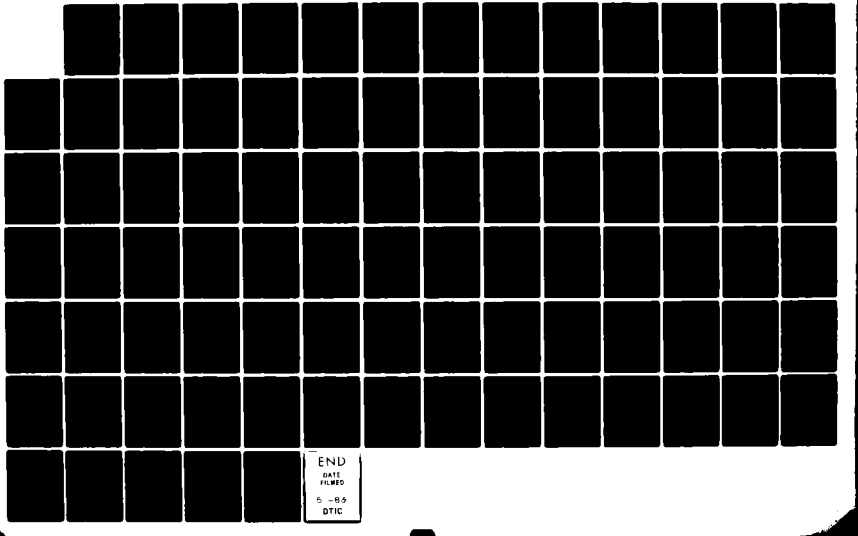

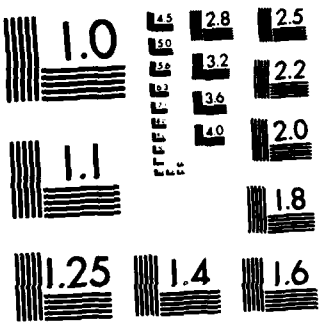

Derivation of Non-Dimensional Control Derivatives

The control derivatives are found by using the following three references: digital DATCOM (Ref. 10), A-7 Aerodynamic Data (Ref. 9), and from Reference 1. The DATCOM program is used to find the non-dimensional derivatives which are not available from other sources. At 0.8 Mach, some derivatives are interpolated from other flight condition data with the assumption that a linear relationship with Mach numbers exists. This is done only in cases where values can not be derived exactly. Table A-II gives the derivatives for 0.18 Mach at an altitude of 2,000 feet assuming a landing configuration. Table A-III gives the derivatives for 0.6 Mach at an altitude of 15,000 feet for a cruise configuration. Table A-IV gives the derivatives for 0.8 Mach at an altitude of 35,000 feet for a cruise configuration. To find the needed control derivatives using digital DATCOM (Ref. 10), the same equations and methods developed by Potts (Ref. 15) are employed. Therefore, the reader is instructed to see Appendix B of Reference 15. As a summary, Table A-V summarizes all the equations needed when using DATCOM.

After finding the needed non-dimensional derivatives, the dimensional control derivatives are found by using the equations of the previous section. The dimensional control derivatives for the three flight conditions are given in Tables A-VI, A-VII, and A-VIII.

TABLE A-II

Non-dimensional Stability and Control Derivatives* for Mach 0.18

$C_{D_{\delta_H}}$	0.06876	$C_{L_{\delta_s}}$	-0.0783	C_{m_α}	0.0	$C_{\ell_{\delta_r}}$	0.02704	$C_{n_{\delta_f}}$	0.0007904
$C_{L_{\delta_H}}$	0.31515	$C_{m_{\delta_s}}$	-0.00358	C_{D_1}	0.016	$C_{n_{\delta_r}}$	-0.11346	C_{y_β}	-0.7163
$C_{m_{\delta_H}}$	-0.41543	$C_{D_{\delta_f}}$	0.0237	C_{L_1}	0.1	$C_{y_{\delta_a}}$	0.07334	C_{ℓ_β}	-0.0708
$C_{D_{\delta_r}}$	0.0	$C_{L_{\delta_f}}$	0.9187	C_{m_1}	0.018	$C_{\ell_{\delta_a}}$	-0.08681	C_{n_β}	0.0808
$C_{L_{\delta_r}}$	0.0	$C_{m_{\delta_f}}$	-0.1285	C_{m_q}	-111.735	$C_{n_{\delta_a}}$	-0.02152	C_{y_p}	5.099
$C_{m_{\delta_r}}$	0.0	C_{D_u}	0.0	$C_{m_{\dot{\alpha}}}$	-21.459	$C_{y_{\delta_s}}$	-0.003152	C_{ℓ_p}	-10.113
$C_{D_{\delta_a}}$	0.0	C_{L_u}	0.0	$C_{y_{\delta_H}}$	0.0	$C_{\ell_{\delta_s}}$	0.00334	C_{n_p}	-3.58
$C_{L_{\delta_a}}$	0.2292	C_{m_u}	0.0	$C_{\ell_{\delta_H}}$	-0.01344	$C_{n_{\delta_s}}$	0.001206	C_{y_r}	13.093
$C_{m_{\delta_a}}$	-0.1528	C_{D_α}	0.1097	$C_{n_{\delta_H}}$	0.0	$C_{y_{\delta_f}}$	0.0	C_{ℓ_r}	4.126
$C_{D_{\delta_s}}$	0.00556	C_{L_α}	1.948	$C_{y_{\delta_r}}$	0.25786	$C_{\ell_{\delta_f}}$	0.01941	C_{n_r}	-10.113

* units are rad^{-1} ; only right control surface values are listed except for rudder and flaps.

TABLE A-III

Non-dimensional Stability and Control Derivatives* for Mach 0.6

$C_{D_{\delta_H}}$	0.0525	$C_{L_{\delta_s}}$	-0.05	C_{m_α}	-0.2318	$C_{\ell_{\delta_r}}$	0.019	$C_{n_{\delta_f}}$	0.0007232
$C_{L_{\delta_H}}$	0.29796	$C_{m_{\delta_s}}$	-0.0096	C_{D_1}	0.0155	$C_{n_{\delta_r}}$	-0.09168	C_{y_β}	-0.3581
$C_{m_{\delta_H}}$	-0.45276	$C_{D_{\delta_f}}$	0.0838	C_{L_1}	0.1	$C_{y_{\delta_a}}$	0.02504	C_{ℓ_β}	-0.0453
$C_{D_{\delta_r}}$	0.0	$C_{L_{\delta_f}}$	0.991	C_{m_1}	0.01	$C_{\ell_{\delta_a}}$	-0.06045	C_{n_β}	0.0361
$C_{L_{\delta_r}}$	0.0	$C_{m_{\delta_f}}$	-0.1446	C_{m_q}	-113.167	$C_{n_{\delta_a}}$	-0.007105	C_{y_p}	3.6959
$C_{m_{\delta_r}}$	0.0	C_{D_u}	0.1017	$C_{m_{\dot{\alpha}}}$	-22.06	$C_{y_{\delta_s}}$	-0.00591	C_{ℓ_p}	-9.913
$C_{D_{\delta_a}}$	0.0	C_{L_u}	0.7478	$C_{y_{\delta_H}}$	0.0	$C_{\ell_{\delta_s}}$	-0.00645	C_{n_p}	-0.1137
$C_{L_{\delta_a}}$	0.212	C_{m_u}	0.1848	$C_{\ell_{\delta_H}}$	-0.01402	$C_{n_{\delta_s}}$	0.0021	C_{y_r}	8.853
$C_{m_{\delta_a}}$	-0.1309	C_{D_α}	0.0934	$C_{n_{\delta_H}}$	0.0	$C_{y_{\delta_f}}$	0.0	C_{ℓ_r}	2.979
$C_{D_{\delta_s}}$	0.00968	C_{L_α}	2.206	$C_{y_{\delta_r}}$	0.20056	$C_{\ell_{\delta_f}}$	0.0167	C_{n_r}	-8.652

* units are rad^{-1} ; only right control surface values are listed except for rudder and flaps.

TABLE A-IV

Non-dimensional Stability and Control Derivatives* for Mach 0.8

#$C_{D_{\delta_H}}$	0.0486	$C_{L_{\delta_s}}$	-0.0751	C_{m_α}	-0.3409	#$C_{\ell_{\delta_r}}$	0.01532	$C_{n_{\delta_f}}$	0.001021
$C_{L_{\delta_H}}$	0.31802	$C_{m_{\delta_s}}$	0.00238	C_{D_1}	0.015	#$C_{n_{\delta_r}}$	-0.10314	C_{y_β}	-0.3882
$C_{m_{\delta_H}}$	-0.4928	#$C_{D_{\delta_f}}$	0.047	C_{L_1}	0.13	$C_{y_{\delta_a}}$	0.02865	C_{ℓ_β}	-0.0489
$C_{D_{\delta_r}}$	0.0	$C_{L_{\delta_f}}$	0.5505	C_{m_1}	0.016	$C_{\ell_{\delta_a}}$	-0.05157	C_{n_β}	0.0524
$C_{L_{\delta_r}}$	0.0	#$C_{m_{\delta_f}}$	-0.0811	C_{m_q}	-123.625	$C_{n_{\delta_a}}$	-0.00537	C_{y_p}	4.16
$C_{m_{\delta_r}}$	0.0	C_{D_u}	0.5254	$C_{m_{\dot{\alpha}}}$	-29.08	$C_{y_{\delta_s}}$	-0.0135	C_{ℓ_p}	-11.517
$C_{D_{\delta_a}}$	0.0	C_{L_u}	-1.076	$C_{y_{\delta_H}}$	0.0	$C_{\ell_{\delta_s}}$	0.00549	C_{n_p}	-0.0401
$C_{L_{\delta_a}}$	0.2244	C_{m_u}	0.3381	$C_{\ell_{\delta_H}}$	0.01577	$C_{n_{\delta_s}}$	0.0047	C_{y_r}	9.154
$C_{m_{\delta_a}}$	-0.14043	C_{D_α}	0.2417	$C_{n_{\delta_H}}$	0.0	$C_{y_{\delta_f}}$	0.0	C_{ℓ_r}	3.925
$C_{D_{\delta_s}}$	0.02167	C_{L_α}	2.521	#$C_{y_{\delta_H}}$	0.20914	$C_{\ell_{\delta_f}}$	0.01826	C_{n_r}	-10.013

* units are rad^{-1}; only right control surface values are listed except for rudder and flaps.
\# indicates an interpolated value

TABLE A-V

Equations to use with DATCOM

$$C_{D\delta_H} = \frac{\left[C_{D/(i_H - i_{H/x} + i_{H_T})} - C_{D/i_H}\right]}{\Delta x}$$

$$C_{D\delta_r} = \frac{C_{D_{min}} + C_{D_i}}{\Delta\delta_r}$$

(same for δ_f)

$$C_{L\delta_f} = \frac{\Delta C_L}{\Delta\delta_f}$$

$$C_{m\delta_f} = \frac{\Delta C_m}{\Delta\delta_f}$$

$$C_{l\delta_H} = \frac{\Delta C_l}{\Delta\delta_H}$$

$$C_{n\delta_f} = \frac{\Delta C_n}{\Delta\delta_f}$$

$$C_{Y\delta_f} = \frac{\Delta C_l}{\Delta\delta_f}$$

TABLE A-VI

Dimensional Stability and Control Derivatives for Mach 0.18

X_{δ_H}	-14.287	Z_{δ_e}	16.269	M_{α}	-0.7346	L_{δ_H}	-5.129	N_{δ_a}	-1.7245
X_{δ_r}	0.0	Z_{δ_f}	-190.88	M_q	-8.276	L_{δ_r}	10.325	N_{δ_e}	0.0967
X_{δ_a}	0.0	Z_u	-0.0213	Y_{δ_H}	0.0	L_{δ_a}	-33.136	N_{δ_f}	0.0634
X_{δ_e}	-1.161	Z_{α}	-41.809	Y_{δ_r}	53.578	L_{δ_e}	1.276	N_{β}	0.7113
X_{δ_f}	-4.926	M_{δ_H}	-10.589	Y_{δ_a}	15.238	L_{δ_f}	7.14	N_p	-3.057
X_u	-0.0034	M_{δ_r}	0.0	Y_{δ_e}	-0.6549	L_{β}	-7.117	N_r	-8.637
X_{α}	-0.2065	M_{δ_a}	-3.895	Y_{δ_f}	0.0	L_p	-1.977	$M_{\dot{\alpha}}$	-1.5809
Z_{δ_H}	-65.48	M_{δ_e}	-0.0913	Y_{β}	-15.248	L_r	0.8115		
Z_{δ_r}	0.0	M_{δ_f}	-3.276	Y_p	10.53	N_{δ_H}	0.0		
Z_{δ_a}	-47.623	M_u	0.00049	Y_r	27.039	N_{δ_r}	-9.094		

TABLE A-VII

Dimensional Stability and Control Derivatives for Mach 0.6

X_{δ_H}	-7.55	Z_{δ_s}	7.19	M_{α}	-4.0877	Y_r	38.819	N_{δ_r}	-5.08
X_{δ_r}	0.0	Z_{δ_f}	-142.44	$M_{\dot{\alpha}}$	-3.32	L_{δ_H}	-3.995	N_{δ_a}	-0.394
X_{δ_a}	0.0	Z_u	-0.2146	M_q	-17.039	L_{δ_r}	5.416	N_{δ_s}	0.116
X_{δ_s}	-1.39	Z_{α}	-319.316	Y_{δ_H}	0.0	L_{δ_a}	-17.225	N_{δ_f}	0.04
X_{δ_f}	-12.04	M_{δ_H}	-7.98	Y_{δ_r}	-28.82	L_{δ_s}	1.841	N_{β}	2.002
X_u	-0.03003	M_{δ_r}	0.0	Y_{δ_a}	3.59	L_{δ_f}	4.7614	N_p	-0.1923
X_{α}	-0.9487	M_{δ_a}	-2.31	Y_{δ_s}	-0.849	L_{β}	-32.967	N_r	-14.635
Z_{δ_H}	-42.83	M_{δ_s}	-0.169	Y_{δ_f}	0.0	L_p	-2.4232		
Z_{δ_r}	0.0	M_{δ_f}	-2.54	Y_{β}	-51.473	L_r	0.7252		
Z_{δ_a}	-30.47	M_u	0.0057	Y_p	16.206	N_{δ_H}	0.0		

TABLE A-VIII

Dimensional Stability and Control Derivatives for Mach 0.8

X_{δ_H}	-1.034	Z_{δ_s}	1.599	M_{α}	-8.689	Y_r	44.398	N_{δ_r}	-0.8468
X_{δ_r}	0.0	Z_{δ_f}	23.438	$M_{\dot{\alpha}}$	-4.843	L_{δ_H}	0.7679	N_{δ_a}	-0.0441
X_{δ_a}	0.0	Z_u	-0.2044	M_q	-20.588	L_{δ_r}	0.7458	N_{δ_s}	0.0386
X_{δ_s}	-0.461	Z_{α}	-502.759	Y_{δ_H}	0.0	L_{δ_a}	-2.5107	N_{δ_f}	0.00838
X_{δ_f}	-2.0	M_{δ_H}	-1.286	Y_{δ_r}	4.452	L_{δ_s}	0.2674	N_{β}	4.199
X_u	-0.1391	M_{δ_r}	0.0	Y_{δ_a}	0.6099	L_{δ_f}	0.8884	N_p	-0.075
X_{α}	-23.209	M_{δ_a}	-0.366	Y_{δ_s}	-0.2873	L_{β}	-68.912	N_r	-18.734
Z_{δ_H}	-6.77	M_{δ_s}	0.0062	Y_{δ_f}	0.0	L_p	-1.8267		
Z_{δ_r}	0.0	M_{δ_f}	-0.424	Y_{β}	-80.659	L_r	0.6225		
Z_{δ_a}	-4.777	M_u	0.0114	Y_p	20.176	N_{δ_H}	0.0		

Continous State Space Model

The aircraft model has eight state variables and is normally considered to have five control inputs. These are described in Table A-IX.

TABLE A-IX

State Variables and Inputs

STATES	u	perturbation forward velocity
	α	perturbation angle of attack
	β	perturbation sideslip
	q	perturbation pitch rate
	θ	perturbation pitch angle
	p	perturbation roll rate
	r	perturbation yaw rate
	ϕ	perturbation roll angle
INPUTS	δ_H	horizontal stabilizer deflection
	δ_r	rudder deflection
	δ_a	aileron deflection
	δ_s	spoiler deflection
	δ_f	flap deflection

The controls surfaces are split into left and right control surfaces (with the exception of the rudder and flaps). In this manner a model can be

developed with 8 inputs. With each state considered to be an output, there exist 8 outputs and thus a square transfer function matrix is possible.

In order to derive a state space model, eight equations involving the time derivatives of $u, \alpha, q, \theta, \beta, p, r$, and ϕ are required. They can be obtained by using Equations (A-2) through (A-9) along with the assumptions that:

1. $X_{\dot{\alpha}}$, $Z_{\dot{\alpha}}$, and Z_q are zero
2. U_1 = constant and $V_1 = 0 = W_1$
3. Stability axes are used
4. $\theta_1 = 0 = \phi_1$
5. $P_1 = Q_1 = R_1 = 0$
6. $w = U_1\alpha$ and $\dot{w} = U_1\dot{\alpha}$

Using this procedure as outlined in Reference 15, the equations for $\dot{u}$, $\dot{\alpha}$, $\dot{q}$, $\dot{\theta}$, $\dot{\beta}$, $\dot{p}$, $\dot{r}$, and $\dot{\phi}$ can be put in the matrix form

$$\dot{\underline{x}} = \underline{\underline{A}}\underline{x} + \underline{\underline{B}}\underline{u} \qquad \text{(A-33)}$$

where

$$\dot{\underline{x}} = \begin{bmatrix} \dot{u} \\ \dot{\alpha} \\ \dot{q} \\ \dot{\theta} \\ \dot{\beta} \\ \dot{p} \\ \dot{r} \\ \dot{\phi} \end{bmatrix} \qquad \underline{x} = \begin{bmatrix} u \\ \alpha \\ q \\ \theta \\ \beta \\ p \\ r \\ \phi \end{bmatrix} \qquad \underline{u} = \begin{bmatrix} \delta_H \\ \delta_r \\ \delta_a \\ \delta_s \\ \delta_f \end{bmatrix}.$$

$$\underline{A} = \begin{bmatrix} X_u & X_\alpha & 0 & -g & 0 & 0 & 0 & 0 \\ Z_u/U_1 & Z_\alpha/U_1 & 1 & 0 & 0 & 0 & 0 & 0 \\ (M_u + \frac{M_\alpha Z_u}{U_1}) & (M_\alpha + \frac{M_\dot{\alpha} Z_\alpha}{U_1}) & M_q & 0 & 0 & 0 & 0 & 0 \\ 0 & 0 & 1 & 0 & 0 & 0 & 0 & 0 \\ 0 & 0 & 0 & 0 & Y_\beta/U_1 & Y_p/U_1 & \left[\frac{Y_r}{U_1} - 1\right] & \frac{g}{U_1} \\ 0 & 0 & 0 & 0 & L'_\beta & L'_p & L'_r & 0 \\ 0 & 0 & 0 & 0 & N'_\beta & N'_p & N'_r & 0 \\ 0 & 0 & 0 & 0 & 0 & 1 & 0 & 0 \end{bmatrix}$$

$$\underline{B} = \begin{bmatrix} X_{\delta_H} & X_{\delta_r} & X_{\delta_a} & X_{\delta_s} & X_{\delta_f} \\ Z_{\delta_H}/U_1 & Z_{\delta_r}/U_1 & Z_{\delta_a}/U_1 & Z_{\delta_s}/U_1 & Z_{\delta_f}/U_1 \\ \frac{M_\alpha Z_{\delta_H} + M_{\delta_H}}{U_1} & \frac{M_\alpha Z_{\delta_r} + M_{\delta_r}}{U_1} & \frac{M_\alpha Z_{\delta_a} + M_{\delta_a}}{U_1} & \frac{M_\alpha Z_{\delta_s} + M_{\delta_s}}{U_1} & \frac{M_\alpha Z_{\delta_f} + M_{\delta_f}}{U_1} \\ 0 & 0 & 0 & 0 & 0 \\ Y_{\delta_H}/U_1 & Y_{\delta_r}/U_1 & Y_{\delta_a}/U_1 & Y_{\delta_s}/U_1 & Y_{\delta_f}/U_1 \\ L'_{\delta_H} & L'_{\delta_r} & L'_{\delta_a} & L'_{\delta_s} & L'_{\delta_f} \\ N'_{\delta_H} & N'_{\delta_r} & N'_{\delta_a} & N'_{\delta_s} & N'_{\delta_f} \\ 0 & 0 & 0 & 0 & 0 \end{bmatrix}$$

where

$$L_i' = \frac{L_i + \frac{I_{xz}}{I_{xx}} N_i}{1 - \frac{I_{xz}^2}{I_{xx}(I_{zz})}}$$

$$N_i' = \frac{N_i + \frac{I_{xz}}{I_{zz}} L_i}{1 - \frac{I_{xz}^2}{I_{xx}(I_{zz})}}$$

and i represents β, p, r, δ_H, δ_r, δ_a, δ_s, and δ_f. The values of L_i' and N_i' are given in Table A-X and Table A-XI.

TABLE A-X

B Matrix Roll Coefficients

	0.18 Mach	0.6 Mach	0.8 Mach
L_β'	-7.1425	-33.425	-69.24
L_p'	-1.98	-2.443	-1.834
L_r'	0.8104	0.7382	0.6262
L_{δ_H}'	-5.1416	-4.0445	0.7709
L_{δ_r}'	10.556	5.735	0.7708
L_{δ_a}'	-33.178	-17.419	-2.5196
L_{δ_s}'	1.2769	1.858	0.2675
L_{δ_f}'	7.427	4.8184	0.89172

TABLE A-XI

$\underline{B}$ Matrix Yaw Coefficients

	0.18 Mach	0.6 Mach	0.8 Mach
N'_{β}	1.5614	5.326	9.6398
N'_{p}	-4.2536	8.10	6.492
N'_{r}	-18.082	-32.184	-39.882
N'_{δ_H}	0.0244	0.0385	-0.0034
N'_{δ_r}	-9.166	-5.1952	-0.8534
N'_{δ_a}	-1.5712	-0.2328	-0.0333
N'_{δ_s}	0.0908	0.0997	0.0376
N'_{δ_f}	0.0284	-0.0054	0.00452

Note that the values for N'_{δ_H}, N'_{δ_a}, N'_{δ_s}, L'_{δ_H}, L'_{δ_a}, and L'_{δ_s} are for the right side control surfaces only.

If the control inputs are divided as mentioned previously, the input $\underline{U}$ vector becomes:

$$\underline{U}^* = \begin{bmatrix} \delta_{H_R} \\ \delta_{H_L} \\ \delta_r \\ \delta_{a_R} \\ \delta_{a_L} \\ \delta_{s_R} \\ \delta_{s_L} \\ \delta_f \end{bmatrix} \qquad \text{(A-34)}$$

where δ_{H_R} refers to the right horizontal stabilizer input and δ_{H_L} refers to the left unit. The $\underline{B}$ matrix must also be changed and the split surface $\underline{B}$ matrix is :

$$
\underline{B}^{*} = \begin{bmatrix}
X_{\delta_{H_R}} & X_{\delta_{H_L}} & X_{\delta_r} & X_{\delta_{a_R}} & X_{\delta_{a_L}} & X_{\delta_{s_R}} & X_{\delta_{s_L}} & X_{\delta_f} \\
Z_{\delta_{H_R}}/U_1 & Z_{\delta_{H_L}}/U_1 & Z_{\delta_{r_R}}/U_1 & Z_{\delta_{a_R}}/U_1 & Z_{\delta_{a_L}}/U_1 & Z_{\delta_{s_R}}/U_1 & Z_{\delta_{s_L}}/U_1 & Z_{\delta_f}/U_1 \\
\dfrac{(M_{\dot{\alpha}} Z_{\delta_H} + M_{\delta_H})_R}{U_1} & (\ )_L & \dfrac{(M_{\dot{\alpha}} Z_{\delta_r} + M_{\delta_r})}{U_1} & (M_{\dot{\alpha}} Z_{\delta_a} + M_{\delta_a})_R & (\ )_L & \dfrac{(M_{\dot{\alpha}} Z_{\delta_{s_R}} + M_{\delta_s})_R}{U_1} & (\ )_L & \dfrac{(M_{\dot{\alpha}} Z_{\delta_f} + M_{\delta_f})}{U_1} \\
0 & 0 & 0 & 0 & 0 & 0 & 0 & 0 \\
Y_{\delta_{H_R}}/U_1 & Y_{\delta_{H_L}}/U_1 & Y_{\delta_r}/U_1 & Y_{\delta_{a_R}}/U_1 & Y_{\delta_{a_L}}/U_1 & Y_{\delta_{s_R}}/U_1 & Y_{\delta_{s_L}}/U_1 & Y_{\delta_f}/U_1 \\
L'_{\delta_{H_R}} & L'_{\delta_{H_L}} & L'_{\delta_r} & L'_{\delta_{a_R}} & L'_{\delta_{a_L}} & L'_{\delta_{s_R}} & L'_{\delta_{s_L}} & L'_{\delta_f} \\
N'_{\delta_{H_R}} & N'_{\delta_{H_L}} & N'_{\delta_r} & N'_{\delta_{a_R}} & N'_{\delta_{a_L}} & N'_{\delta_{s_R}} & N'_{\delta_{s_L}} & N'_{\delta_f} \\
0 & 0 & 0 & 0 & 0 & 0 & 0 & 0
\end{bmatrix}
$$

where $(\ )_L$ indicates quantity for right surface repeated for left surface

(A-35)

Using the state equations in the form

$$\dot{\underline{x}} = \underline{A}\underline{X} + \underline{B}^*\underline{U}^* \qquad \text{(A-36)}$$

and substituting the values given in this Appendix, the desired aircraft models are constructed at the three flight conditions.

For the flight condition of 0.18 Mach at an altitude of 2,000 feet (assuming a landing configuration) the A matrix is as follows:

$$A = \begin{bmatrix} -0.0068 & -0.413 & 0 & -32.2 & 0 & 0 & 0 & 0 \\ -0.0002134 & -0.4189 & 1 & 0 & 0 & 0 & 0 & 0 \\ 0.0008291 & -0.0689 & -16.552 & 0 & 0 & 0 & 0 & 0 \\ 0 & 0 & 1 & 0 & 0 & 0 & 0 & 0 \\ 0 & 0 & 0 & 0 & -0.1528 & 0.1055 & -0.7291 & 0.1613 \\ 0 & 0 & 0 & 0 & -7.1425 & -1.98 & 0.8104 & 0 \\ 0 & 0 & 0 & 0 & 1.5614 & -4.2536 & -18.082 & 0 \\ 0 & 0 & 0 & 0 & 0 & 1 & 0 & 0 \end{bmatrix}$$

$$\text{where } x = \begin{bmatrix} U \\ \alpha \\ q \\ \theta \\ \beta \\ p \\ r \\ \phi \end{bmatrix} \qquad \text{(A-37)}$$

The $\underline{B}$ matrix for this condition is:

$$\underline{B} = \begin{bmatrix} -14.287 & -14.287 & 0 & 0 & 0 & -1.161 & -1.161 & -4.926 \\ -0.328 & -0.328 & 0 & 0.2386 & -0.2386 & 0.0815 & 0.0815 & -0.9573 \\ -4.774 & -4.774 & 0 & 1.5685 & -1.5685 & -0.1752 & -0.1752 & -0.1186 \\ 0 & 0 & 0 & 0 & 0 & 0 & 0 & 0 \\ 0 & 0 & 0.2684 & 0.07634 & -0.07634 & 0.003281 & -0.003281 & 0 \\ 1.0796 & -1.0796 & 2.3792 & 6.936 & 6.936 & -0.2664 & 0.2664 & 1.558 \\ -0.0244 & 0.0244 & -9.166 & 1.5712 & 1.5712 & -0.0909 & 0.0909 & 0.0284 \\ 0 & 0 & 0 & 0 & 0 & 0 & 0 & 0 \end{bmatrix}$$

where $\underline{U}^* = \begin{bmatrix} \delta_{H_R} \\ \delta_{H_L} \\ \delta_r \\ \delta_{a_R} \\ \delta_{a_L} \\ \delta_{s_R} \\ \delta_{s_L} \\ \delta_f \end{bmatrix}$ (A-38)

The sign convention employed is: positive δ_H, δ_{a_L}, and δ_f is trailing edge down; positive δ_r is trailing edge left; positive δ_s is spoiler up; positive δ_{a_R} is trailing edge up.

For the flight condition of 0.6 Mach at an altitude of 15,000 feet (cruise configuration), the $\underline{A}$ matrix is as follows:

$$\underline{A} = \begin{bmatrix} -0.06006 & -1.8974 & 0 & -32.2 & 0 & 0 & 0 & 0 \\ -0.000676 & -1.006 & 1 & 0 & 0 & 0 & 0 & 0 \\ 0.001362 & -4.835 & -34.078 & 0 & 0 & 0 & 0 & 0 \\ 0 & 0 & 1 & 0 & 0 & 0 & 0 & 0 \\ 0 & 0 & 0 & 0 & -0.01622 & 0.05106 & -0.8776 & 0.05077 \\ 0 & 0 & 0 & 0 & -33.426 & -2.443 & 0.7382 & 0 \\ 0 & 0 & 0 & 0 & 5.326 & -8.10 & -32.184 & 0 \\ 0 & 0 & 0 & 0 & 0 & 1 & 0 & 0 \end{bmatrix}$$

where $x = \begin{bmatrix} u \\ \alpha \\ q \\ \theta \\ \beta \\ p \\ r \\ \phi \end{bmatrix}$ (A-39)

The $\underline{B}$ matrix is as follows:

$$\underline{B} = \begin{bmatrix} -7.55 & -7.55 & 0 & 0 & 0 & -1.39 & -1.39 & -12.04 \\ -0.0675 & -0.0675 & 0 & 0.0479 & -0.0479 & 0.01134 & 0.01134 & 0.2244 \\ -8.204 & -8.204 & 0 & 2.151 & -2.151 & -0.2066 & -0.2066 & -1.795 \\ 0 & 0 & 0 & 0 & 0 & 0 & 0 & 0 \\ 0 & 0 & 0.0454 & 0.00566 & 0.00566 & 0.00134 & -0.00134 & 0 \\ 0.7866 & -0.7866 & 1.0534 & -3.372 & -3.372 & -0.3567 & 0.3567 & 0.8808 \\ -0.0385 & 0.0385 & -5.08 & -0.2328 & -0.2328 & -0.0997 & 0.0997 & -0.0054 \\ 0 & 0 & 0 & 0 & 0 & 0 & 0 & 0 \end{bmatrix} \quad \text{(A-40)}$$

The final model is for a flight condition of 0.8 Mach at an altitude of 35,000 feet (cruise configuration). The $\underline{A}$ matrix for this condition is as follows:

$$\underline{A} = \begin{bmatrix} -0.2872 & -46.418 & 0 & -32.2 & 0 & 0 & 0 & 0 \\ -0.0004927 & -1.212 & 1 & 0 & 0 & 0 & 0 & 0 \\ 0.01378 & -2.8197 & -41.176 & 0 & 0 & 0 & 0 & 0 \\ 0 & 0 & 0 & 0 & 0 & 0 & 0 & 0 \\ 0 & 0 & 0 & 0 & -0.1945 & 0.04864 & -0.893 & 0.0388 \\ 0 & 0 & 0 & 0 & -69.24 & -1,834 & 0.6262 & 0 \\ 0 & 0 & 0 & 0 & 9.6398 & -6.492 & -39.882 & 0 \\ 0 & 0 & 0 & 0 & 0 & 1 & 0 & 0 \end{bmatrix} \quad \text{(A-41)}$$

The $\underline{B}$ matrix for this flight condition is:

$$\underline{B} = \begin{bmatrix} -1.034 & -1.034 & 0 & 0 & 0 & -0.461 & -0.461 & -2.0 \\ -0.00816 & -0.00816 & 0 & 0.00576 & -0.00576 & 0.001927 & 0.001927 & 0.02825 \\ -0.6034 & -0.6034 & 0 & 0.15511 & -0.15511 & -0.00624 & -0.00624 & -0.34883 \\ 0 & 0 & 0 & 0 & 0 & 0 & 0 & 0 \\ 0 & 0 & 0.00537 & 0.00074 & -0.00074 & 0.000346 & -0.000346 & 0 \\ 0.13002 & 0.13002 & 0.1484 & -0.4239 & 0.4239 & -0.0443 & 0.0443 & 0.15018 \\ -0.0034 & 0.0034 & -0.8534 & -0.0333 & 0.0333 & -0.0376 & 0.0376 & 0.00452 \\ 0 & 0 & 0 & 0 & 0 & 0 & 0 & 0 \end{bmatrix} \quad \text{(A-42)}$$

To design a tracker control law, the output equation has the form

$$\underline{y} = \underline{Cx} \quad \text{(A-43)}$$

For this study the desired command input is:

$$\underline{v}(t) = \begin{bmatrix} 0 \\ 1 \\ 0 \\ 0 \\ 0 \\ 0 \\ 0 \\ 0 \end{bmatrix} \begin{matrix} = u \\ = \theta - \alpha = \gamma \\ = q \\ = \theta \\ = \beta \\ = p \\ = r \\ = \phi \end{matrix} \quad \text{(A-44)}$$

where γ is the flight path angle. The $\underline{C}$ matrix for Equation (A-42) is:

$$\underline{C} = \begin{bmatrix} 1 & 0 & 0 & 0 & 0 & 0 & 0 & 0 \\ 0 & -1 & 0 & 1 & 0 & 0 & 0 & 0 \\ 0 & 0 & 1 & 0 & 0 & 0 & 0 & 0 \\ 0 & 0 & 0 & 1 & 0 & 0 & 0 & 0 \\ 0 & 0 & 0 & 0 & 1 & 0 & 0 & 0 \\ 0 & 0 & 0 & 0 & 0 & 1 & 0 & 0 \\ 0 & 0 & 0 & 0 & 0 & 0 & 1 & 0 \\ 0 & 0 & 0 & 0 & 0 & 0 & 0 & 1 \end{bmatrix} \quad \text{(A-45)}$$

In this way there are eight outputs.

Sensors and Actuators

A physical plant must have some means of sensing outputs and a means to move, or actuate, control surfaces. For the A-7D the actuators are servos that can be approximated by a first order lag as given in Reference 1. The transfer function of this servo is:

$$\frac{\delta}{e_\delta} = \frac{20}{S+20} \quad \text{(A-46)}$$

where δ is the deflection of the control surface (output), and e_δ is the voltage to the servo (input); see Figure A-I.

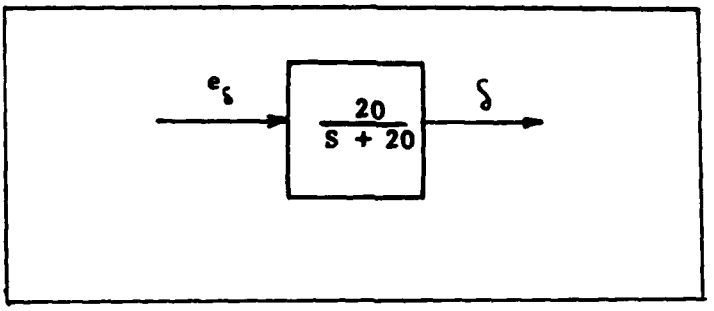

Figure A-I A-7D Servo Block Diagram

If the transfer function is written in state space form, the actuator equation becomes

$$\dot{\delta} = -20\,\delta + 20\,e_\delta \qquad \text{(A-47)}$$

$$Y = \delta \qquad \text{(A-48)}$$

Comparing this to the standard state space format it is evident that for the actuators:

$$A = -20$$

$$B = 20$$

$$C = 1$$

$$D = 0$$

To measure the output vector y, three types of sensors are assumed. An accelerometer can be used to measure perturbation forward velocity (u). The describing equation for this case, found in Reference 5 is:

$$\dot{V}_i = -W_i V_i + R_i \qquad \text{(A-49)}$$

where R_i is the inertial acceleration, V_i is the inertial velocity and W_i is the rotation of the body with respect to inertial space (earth). If straight and level flight is assumed, then $W_i = 0$ and Equation (A-48) becomes simply:

$$\dot{V}_i = R_i \qquad \text{(A-50)}$$

Since velocity is the desired output, the output equation can be written as:

$$y = V_i \tag{A-51}$$

From Equation (A-49) and (A-50) it can be seen that for the accelerometer that

$$A = 0$$

$$B = 1$$

$$C = 1$$

$$D = 0$$

To measure angles, an integrating gyro can be used. The transfer function is:

$$\frac{A_g}{W_i} = \frac{H/K}{\frac{S^2}{W_n} + \frac{2\zeta S}{W_n} + 1} \tag{A-52}$$

The integrating gyro can be used to measure β, θ, α, ϕ, and/or γ. Typical values of H, K, w_n, and ζ as given in Reference 2 are:

$$H = 10^4 \text{ gm} \cdot \text{cm}^2/\text{sec}$$

$$K = 3.03 \times 10^5 \text{ gm} \cdot \text{cm}^2/\text{sec}$$

$$w_n = 94.25 \text{ rad}/\text{sec}$$

$$\zeta = 0.78$$

Using these values, the transfer function can be written in state variable form as:

$$\ddot{A}_g + 147.015\,\dot{A}_g + 8883.063\,A_g = 293.141\,W_i \tag{A-54}$$

Letting $A_g = X_1$ and $\dot{A}_g = X_2$, Equation (A-52) can be written as:

$$\begin{bmatrix} \dot{X}_1 \\ \dot{X}_2 \end{bmatrix} = \begin{bmatrix} 0 & 1 \\ -8883.063 & -147.015 \end{bmatrix} \begin{bmatrix} X_1 \\ X_2 \end{bmatrix} + \begin{bmatrix} 0 \\ 293.141 \end{bmatrix} \begin{bmatrix} W_i \\ W_i \end{bmatrix} \tag{A-54}$$

Since A_g is the desired angle output, the output equation can be written as:

$$\underline{Y} = \begin{bmatrix} 1 & 0 \end{bmatrix} \begin{bmatrix} X_1 \\ X_2 \end{bmatrix} \tag{A-55}$$

From Equations (A-53) and (A-54) it can be seen that for the integrating gyro:

$$\underline{A} = \begin{bmatrix} 0 & 1 \\ -8883.063 & -147.015 \end{bmatrix}$$

$$\underline{B} = \begin{bmatrix} 0 \\ 293.141 \end{bmatrix}$$

$$\underline{C} = \begin{bmatrix} 1 & 0 \end{bmatrix}$$

$$\underline{D} = \underline{0}$$

Rate gyro can be used to measure the rate output. The rate gyro can measure q, p, and r. The transfer function of the rate gyro is given in Reference 2 as:

$$\frac{A_g}{W_i} = \frac{H/C_D}{S\left(\frac{I_{D_A}}{C_D} S + 1\right)}$$

(A-56)

Typcial values of H, C_D, and I_{D_A} as given in Reference 2 are:

$$H = 10^4 \text{ gm} \cdot \text{cm}^2/\text{sec}$$

$$C_D = 5 \times 10^3 \text{ gm} \cdot \text{cm}^2/\text{sec}$$

$$I_{D_A} = 34 \text{ gm} \cdot \text{cm}^2$$

With these values, the transfer function can be written as:

$$\frac{A_g}{W_i} = \frac{294.118}{S^2 + 147.059\, S}$$

(A-57)

This can be written in phase variable form as:

$$\begin{bmatrix} \dot{X}_1 \\ \dot{X}_2 \end{bmatrix} = \begin{bmatrix} 0 & 1 \\ 0 & -147.059 \end{bmatrix} \begin{bmatrix} X_1 \\ X_2 \end{bmatrix} + \begin{bmatrix} 0 \\ 294.188 \end{bmatrix} W_i$$

(A-58)

where

$$A_g = X_1$$

$$\dot{A}_g = X_2$$

Since A_g is the desired output, the output equation is the same as Equation (A-54). From Equations (A-57) and (A-54) it is evident that for the rate gyro:

$$\underline{A} = \begin{bmatrix} 0 & 1 \\ 0 & -147.059 \end{bmatrix}$$

$$\underline{B} = \begin{bmatrix} 0 \\ 294.118 \end{bmatrix}$$

$$\underline{C} = \begin{bmatrix} 1 & 0 \end{bmatrix}$$

$$\underline{D} = \underline{0}$$

Appendix B

Simulation Results

Tracking

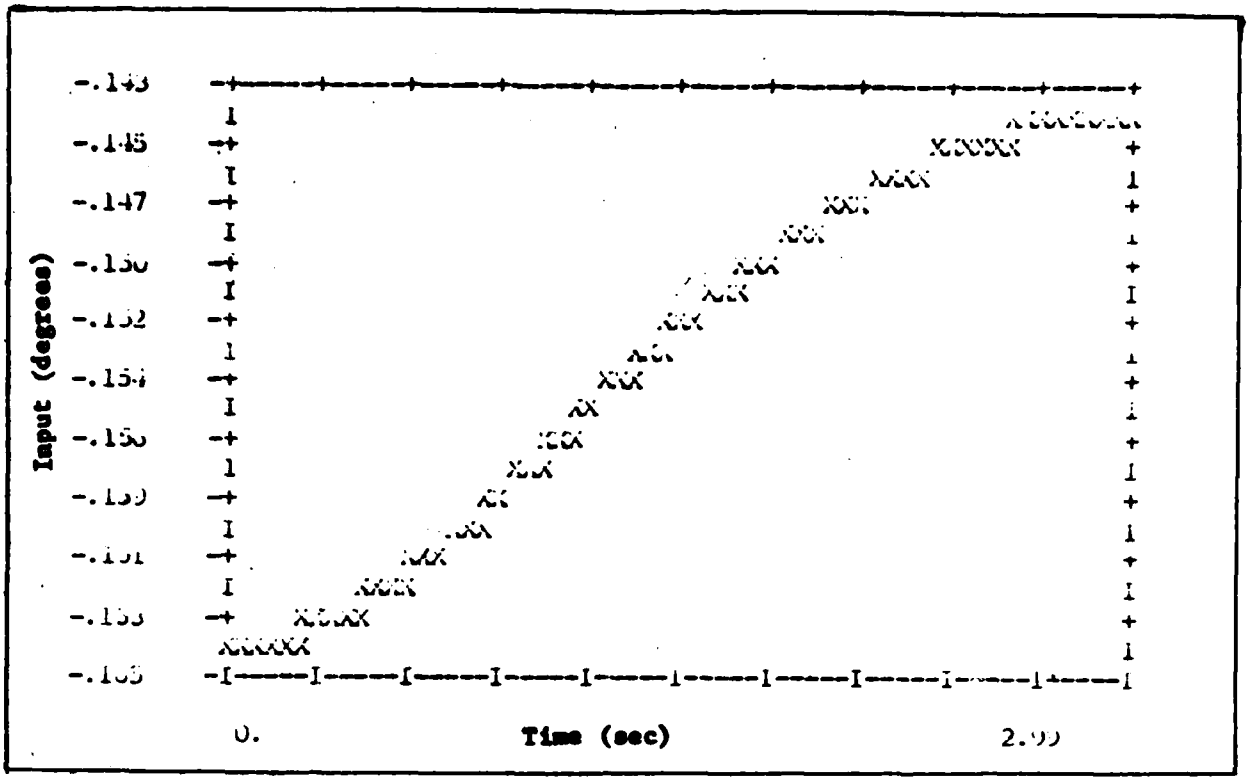

Figure B-1 Rudder Input for γ Tracking

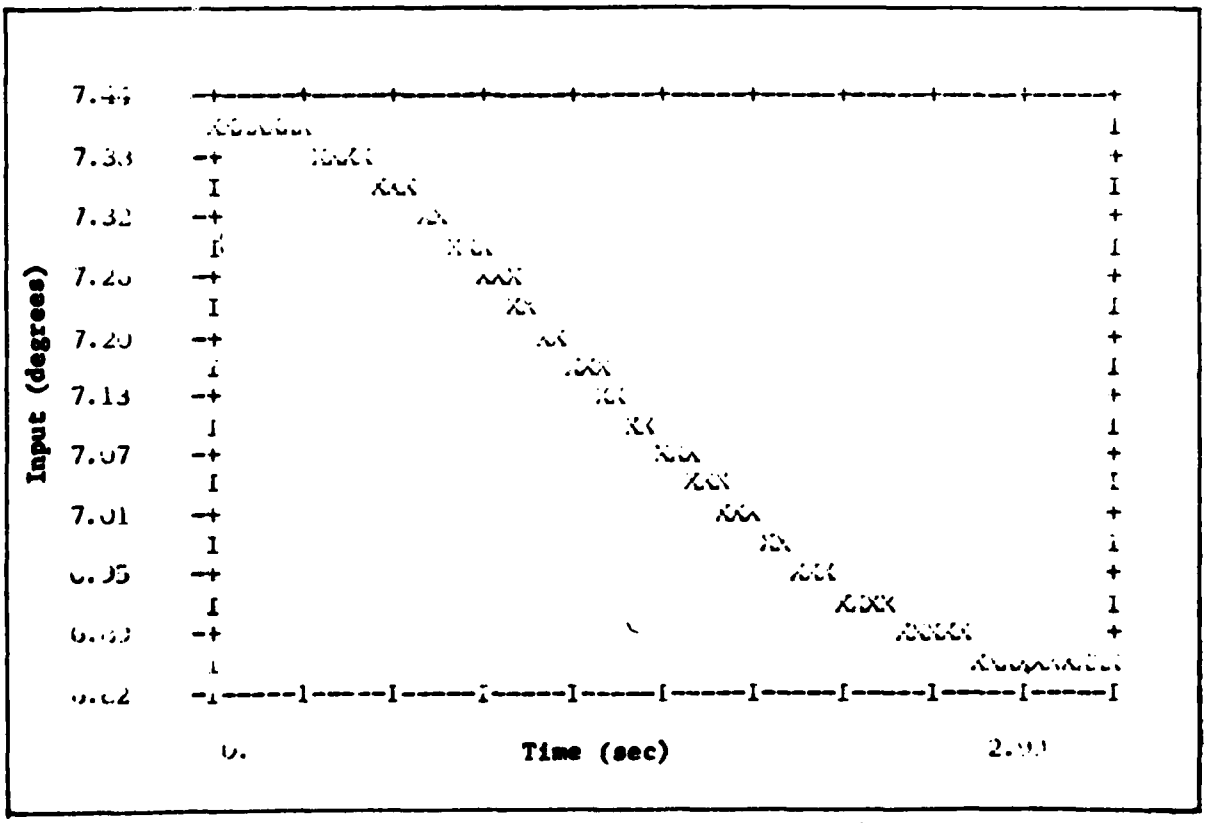

Figure B-2 Right Horizontal Tail Input For γ Tracking

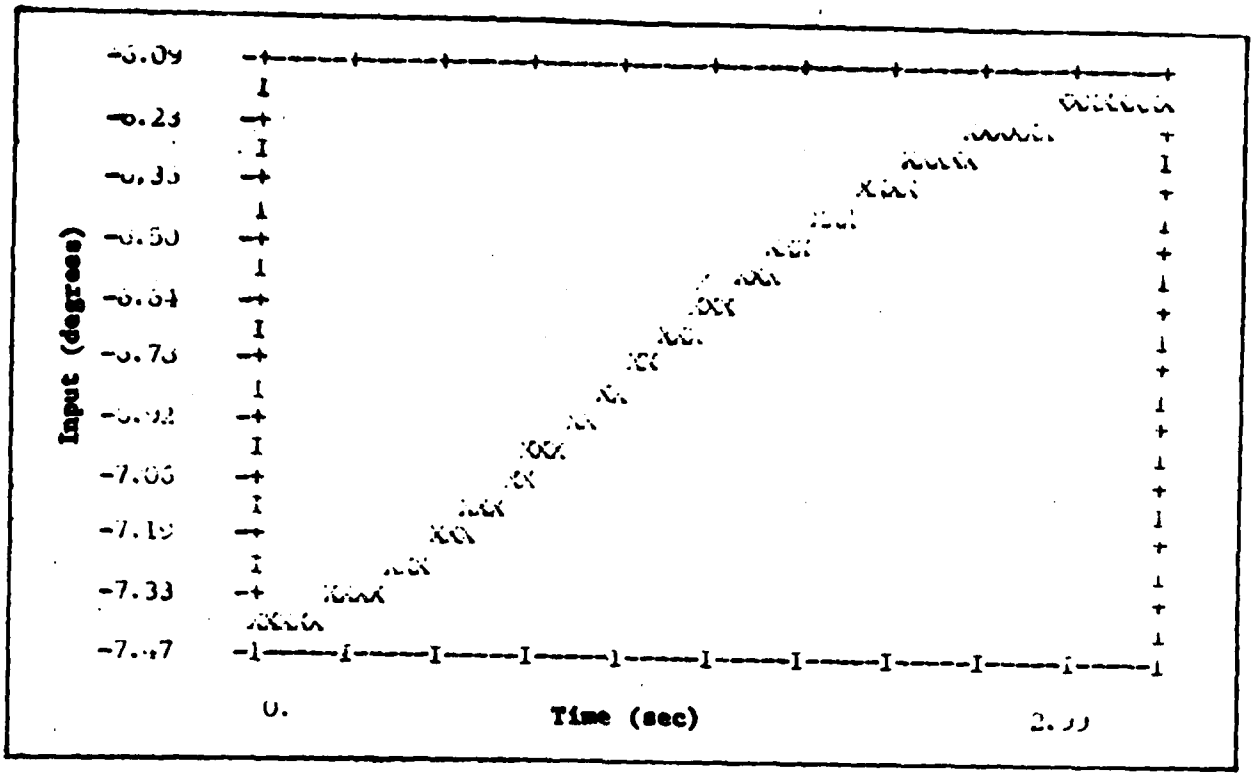

Figure B-3 Left Horizontal Tail Input for γ Tracking

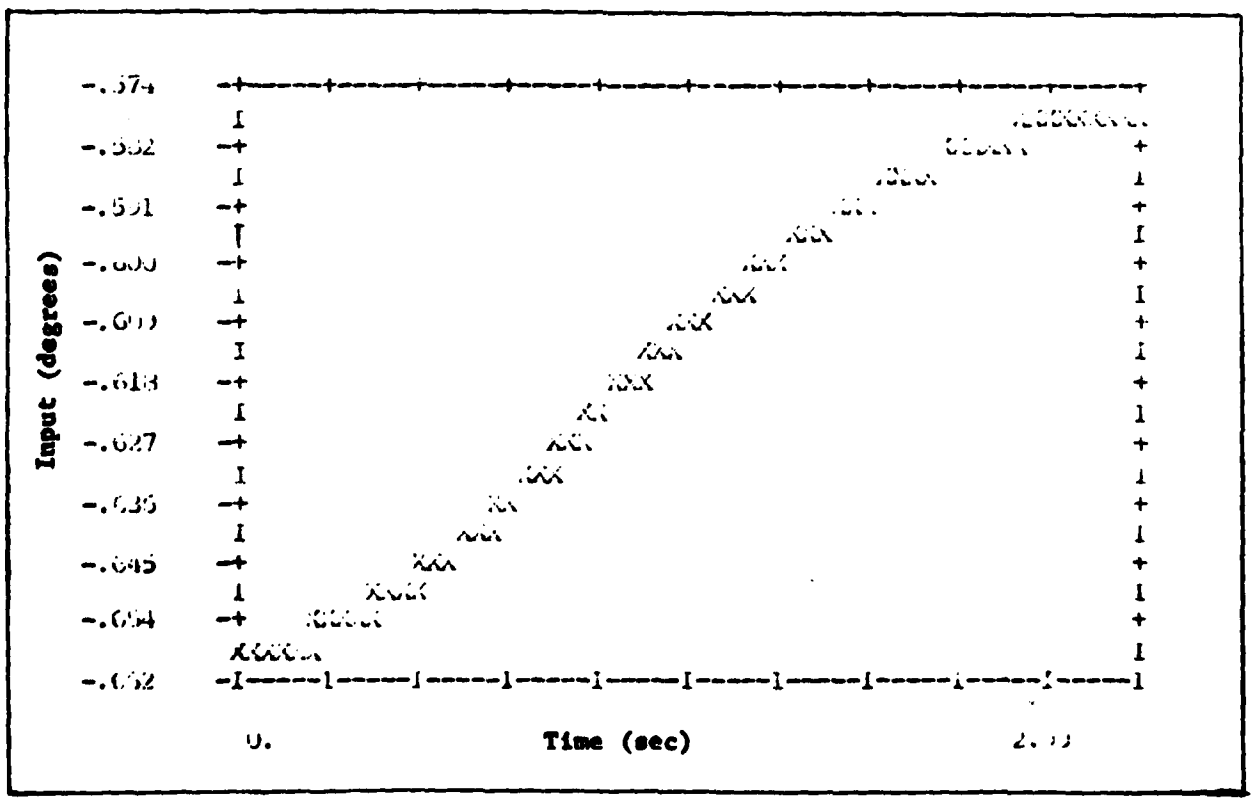

Figure B-4 Aileron Input for γ Tracking

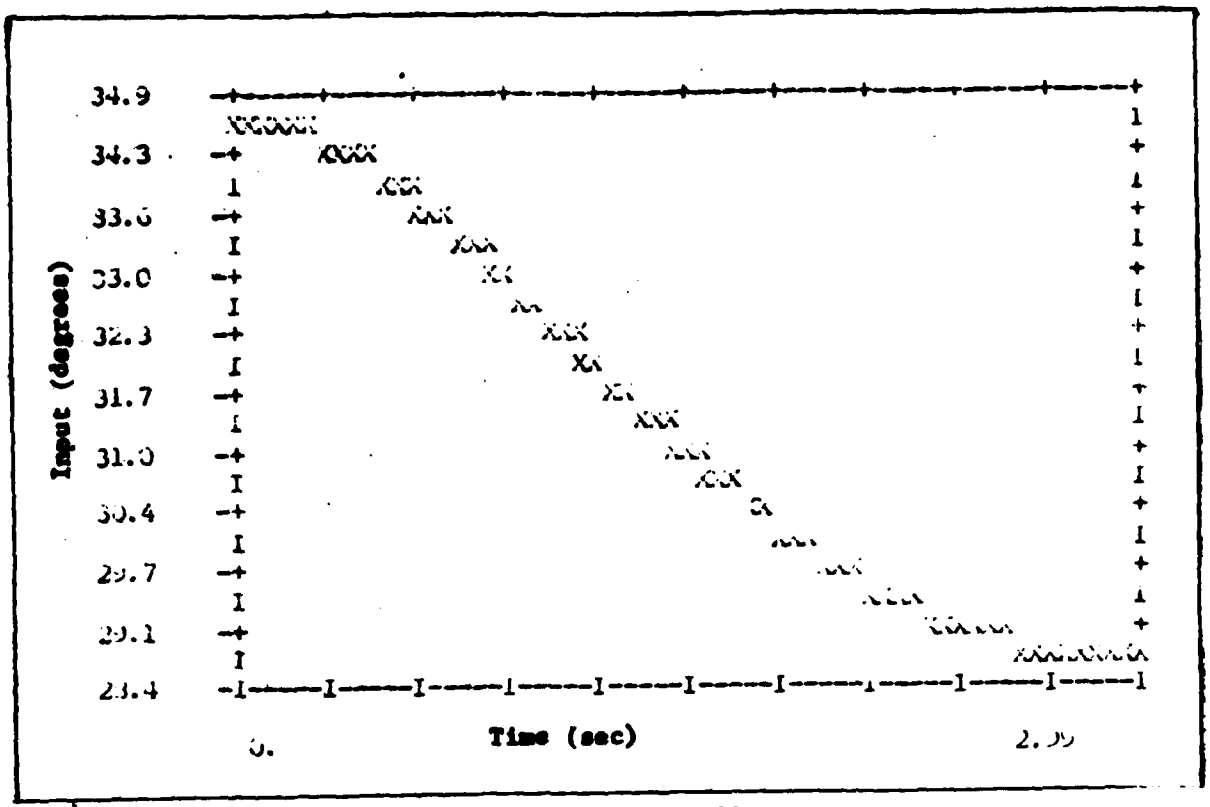

Figure B-5 Spoiler Input for γ Tracking

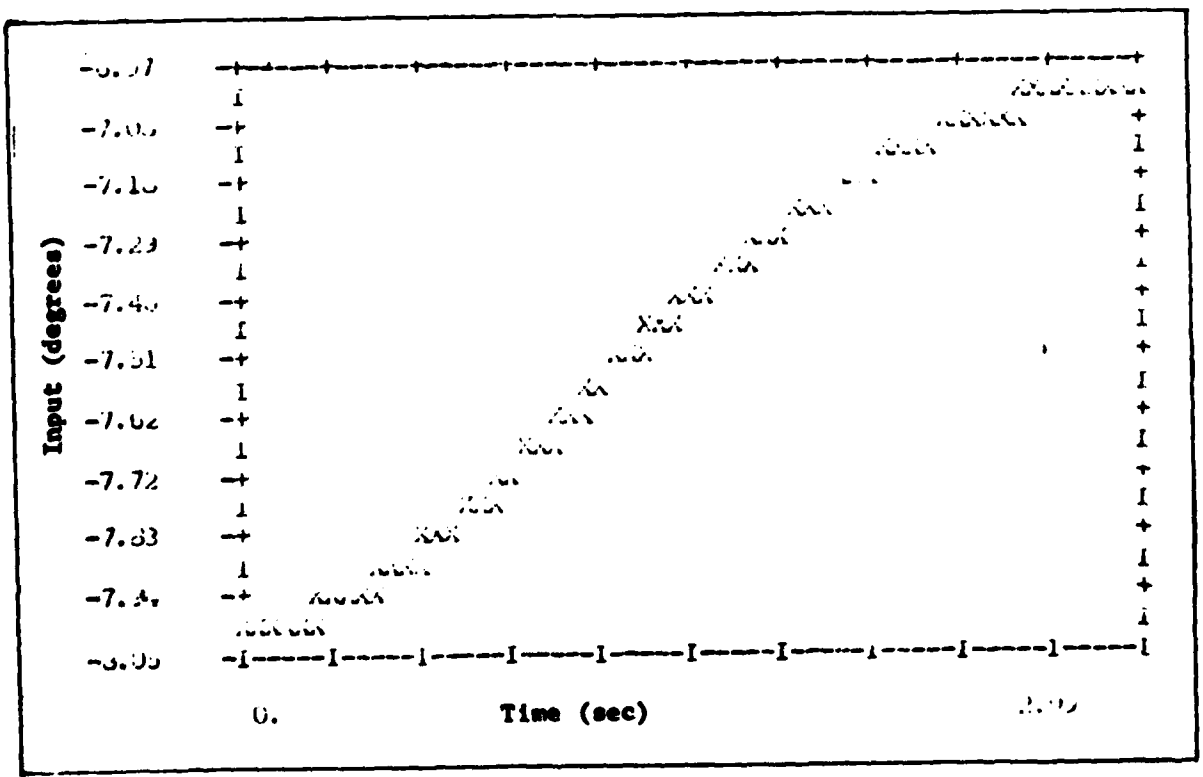

Figure B-6 Flap Input for γ Tracking

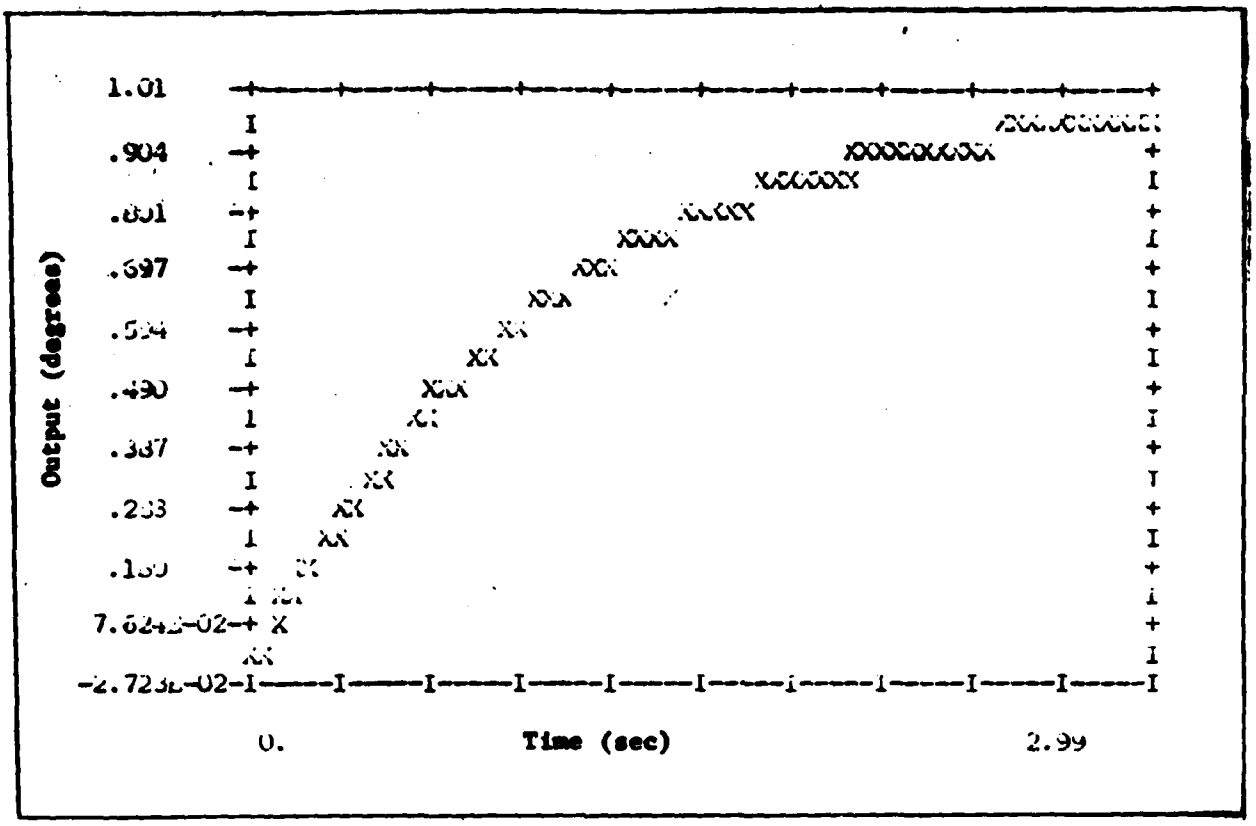

Figure B-7 Flight Path Angle (γ) Tracking Response

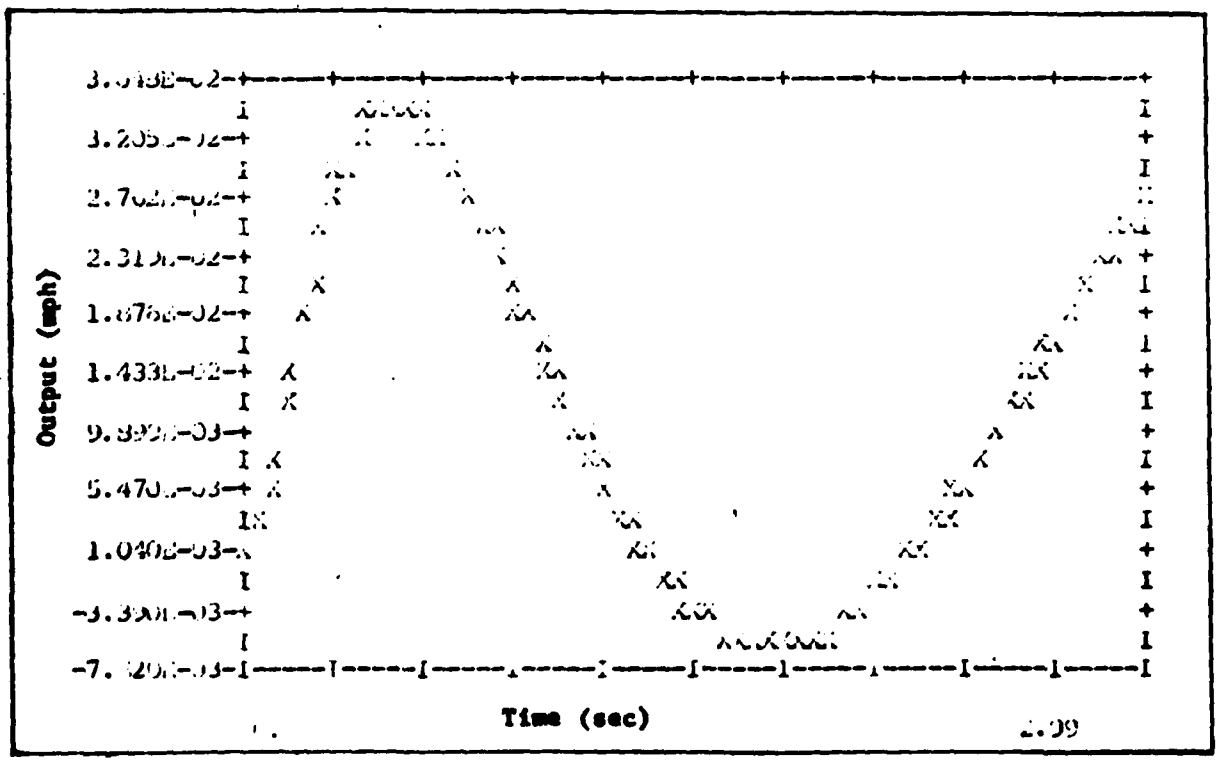

Figure B-8 u Response for Tracking

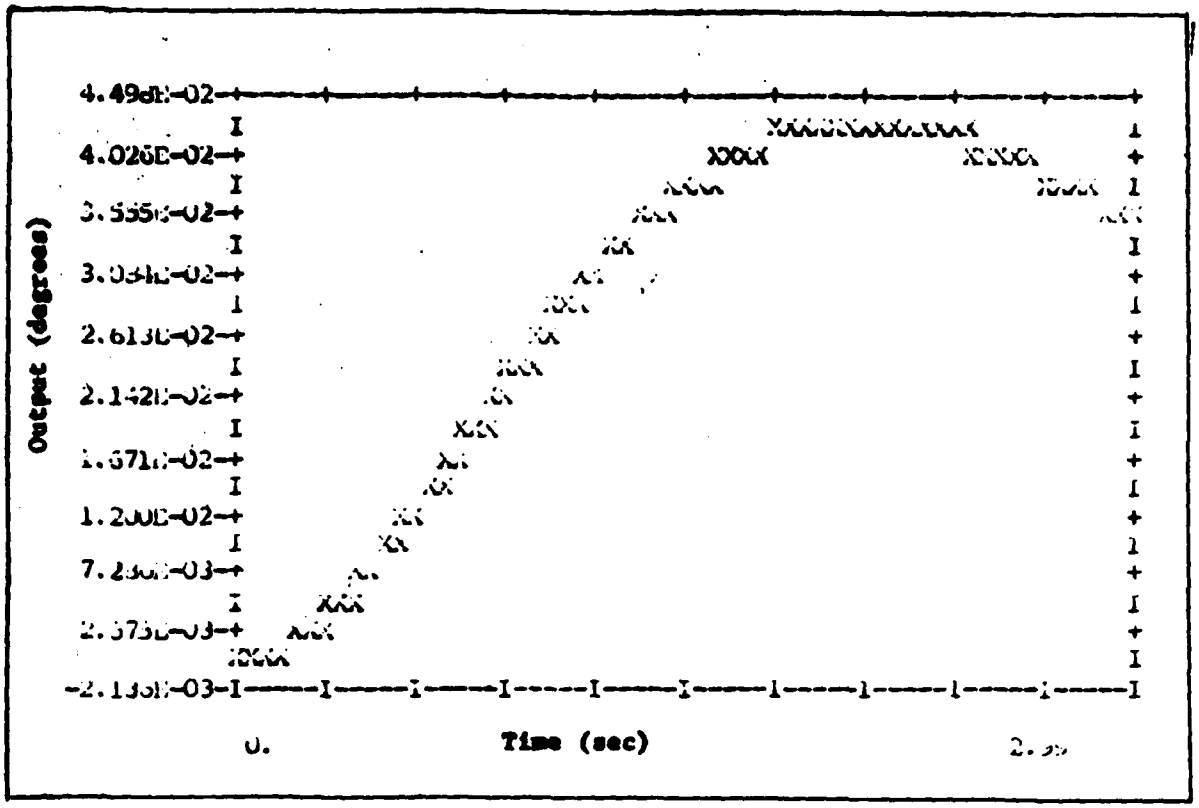

Figure B-9 θ Response for γ Tracking

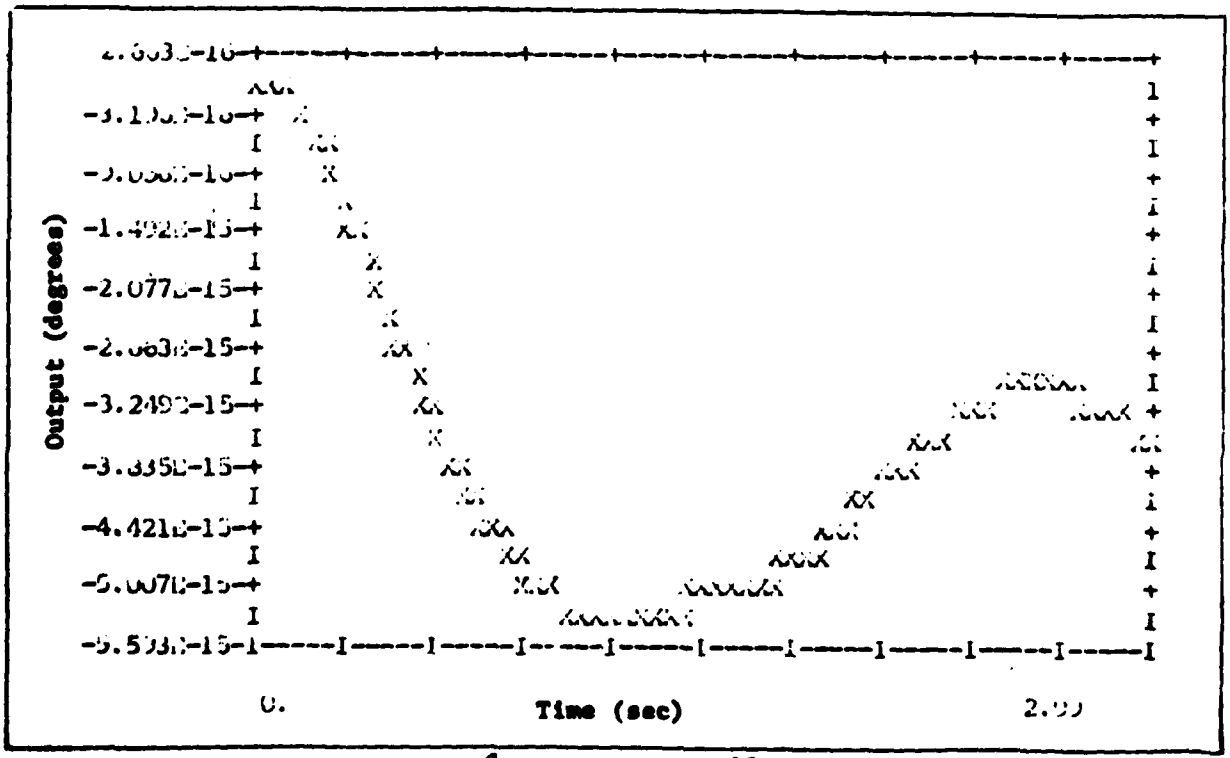

Figure B-10 β Response for γ Tracking

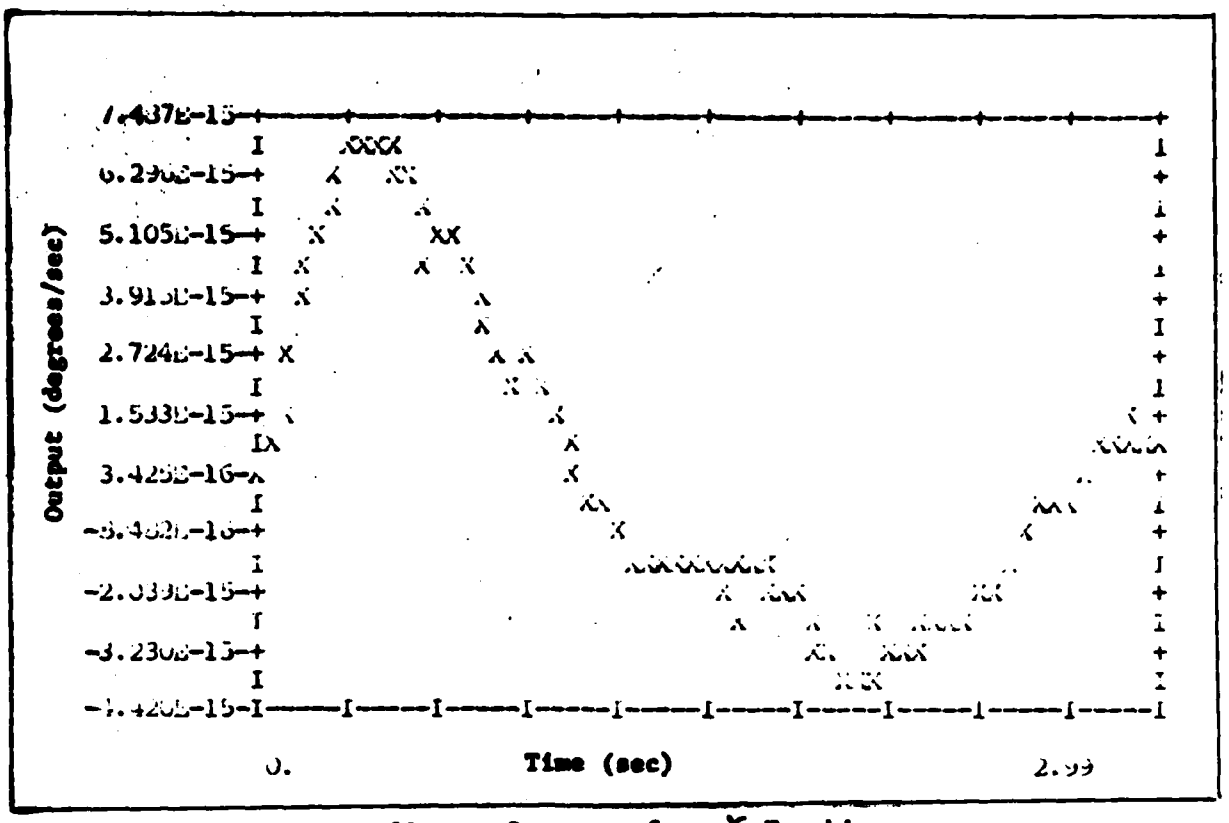

Figure B-11 r Response for γ Tracking

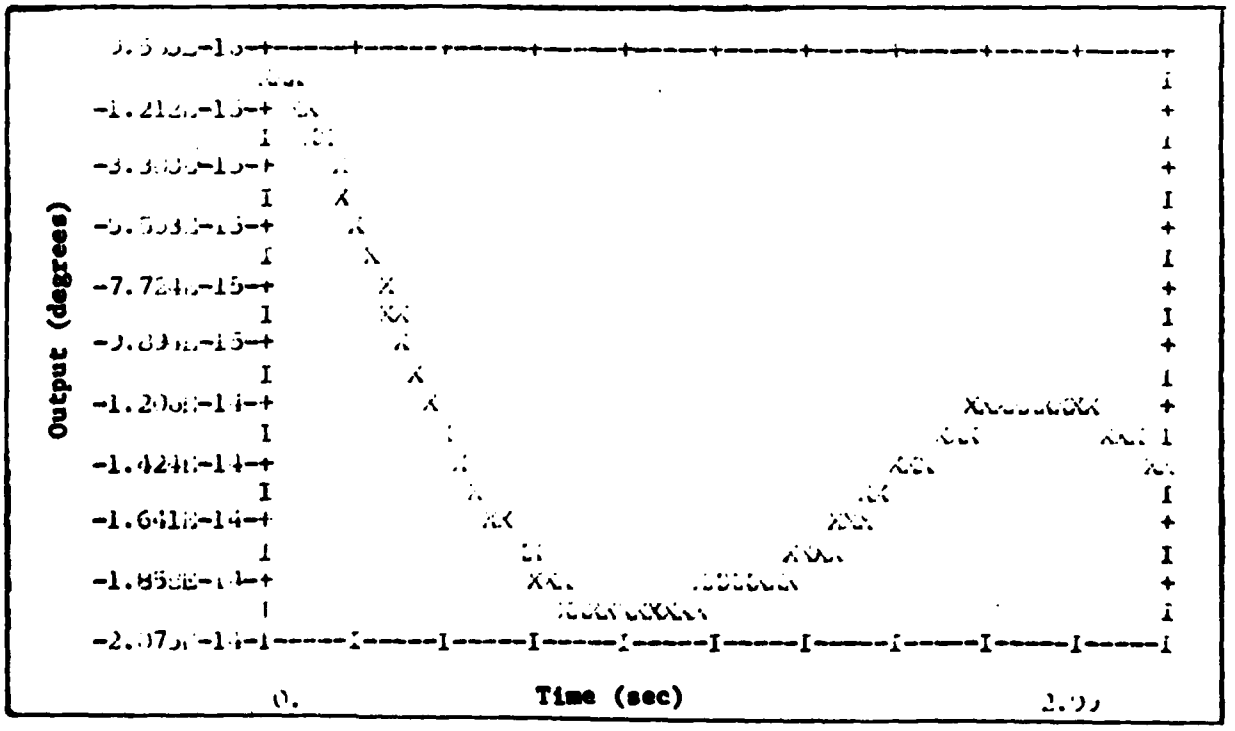

Figure B-12 ϕ Response for γ Tracking

u Tracking

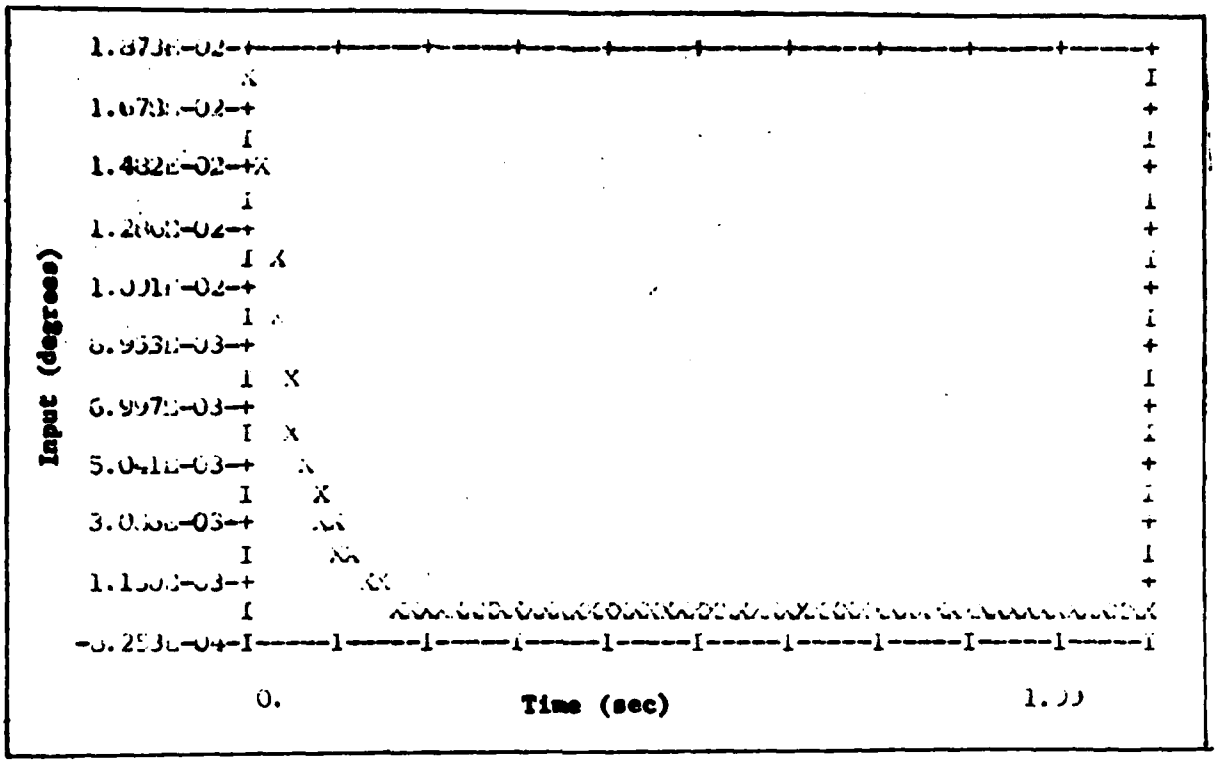

Figure B-13 δ_r Input for u Tracking

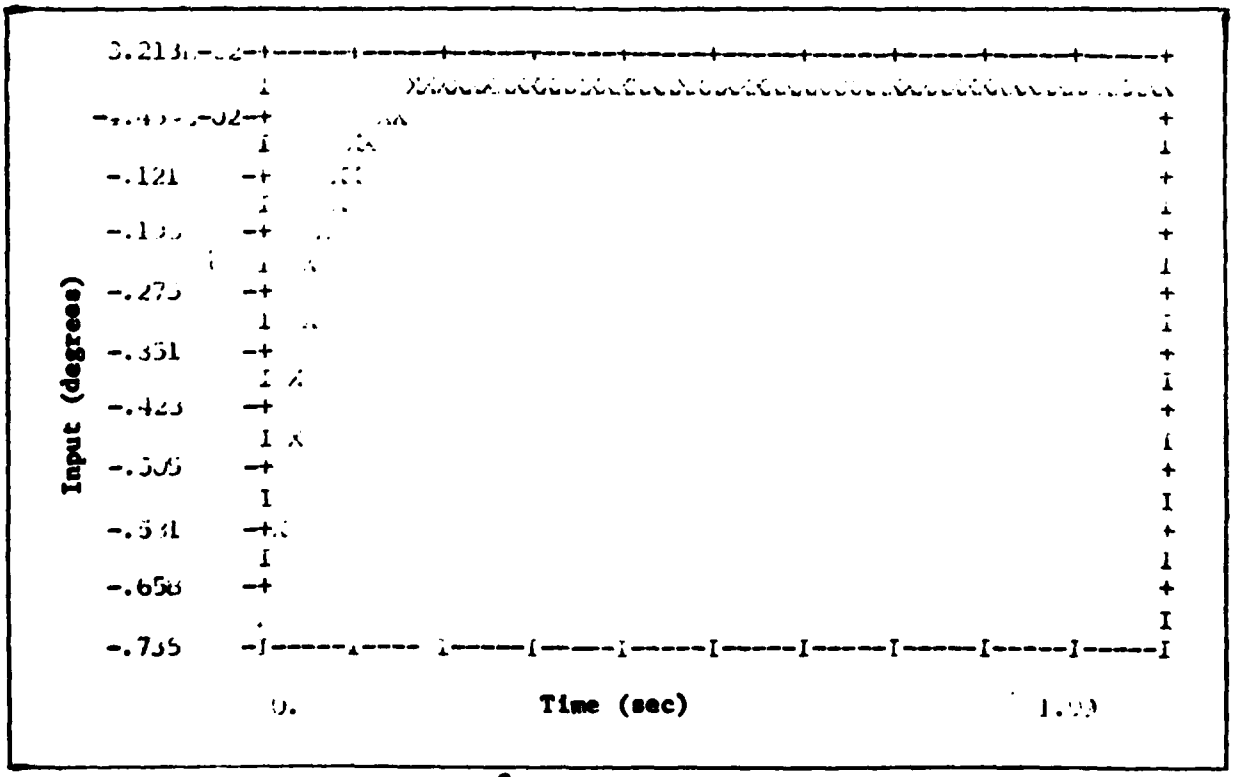

Figure B-14 δ_{H_r} Input for u Tracking

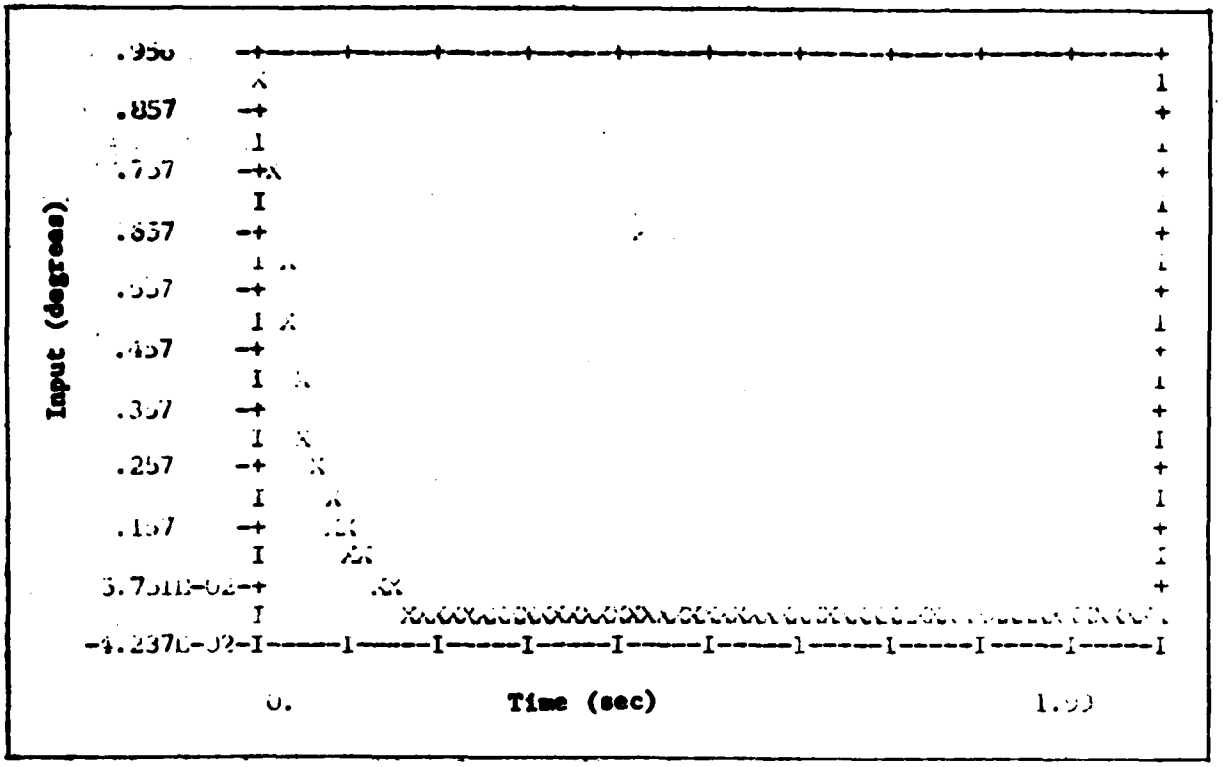

Figure B-15 δ_{H_L} Input for u Tracking

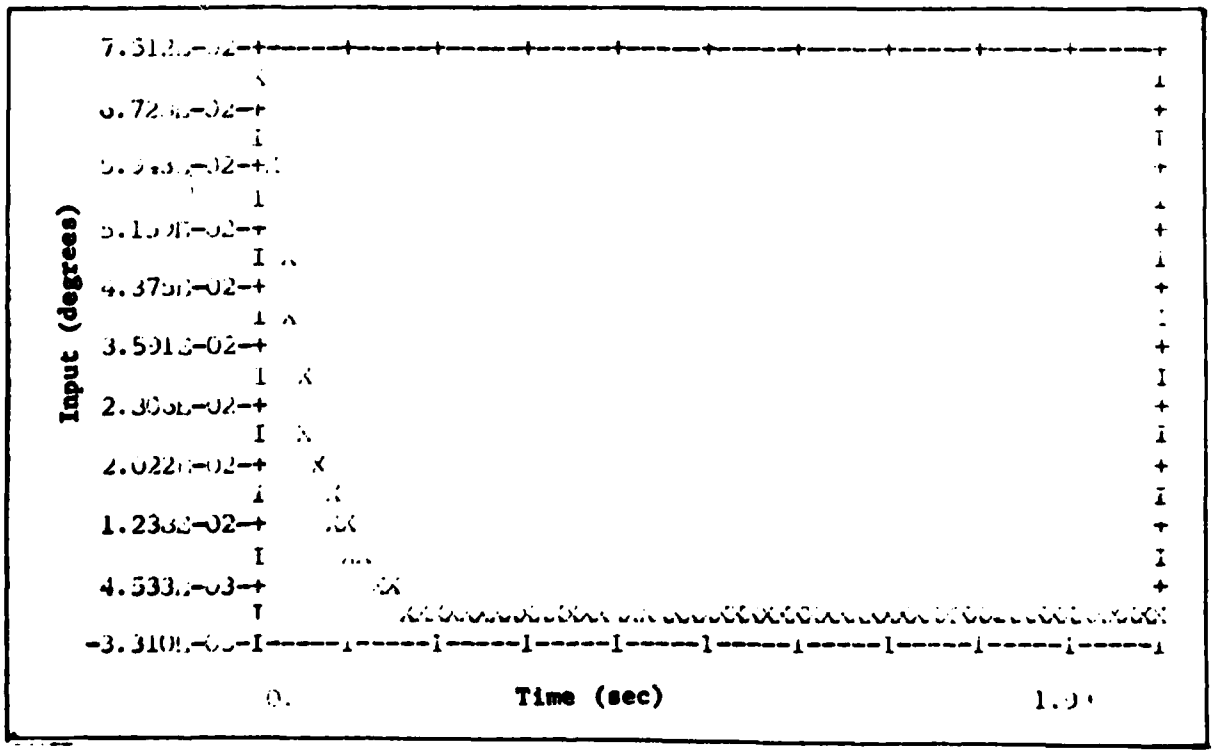

Figure B-16 δ_a Input for u Tracking

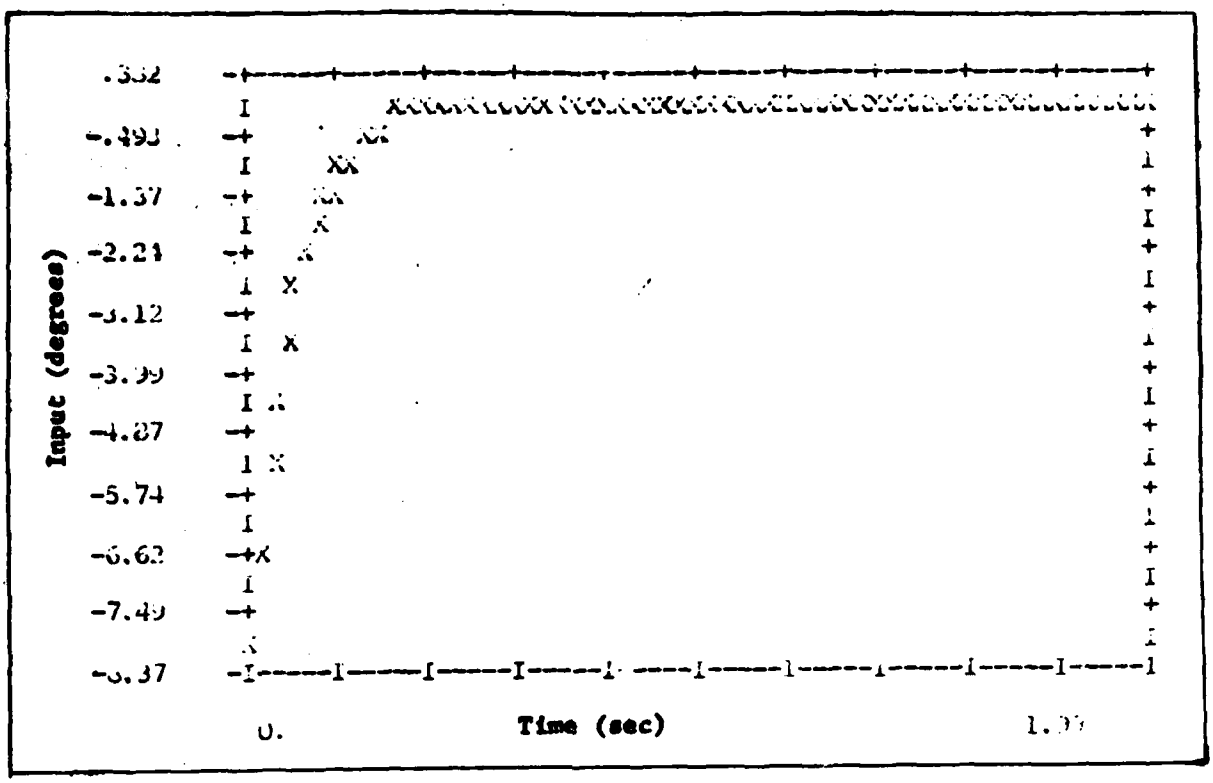

Figure B-17 δ_s Input for u Tracking

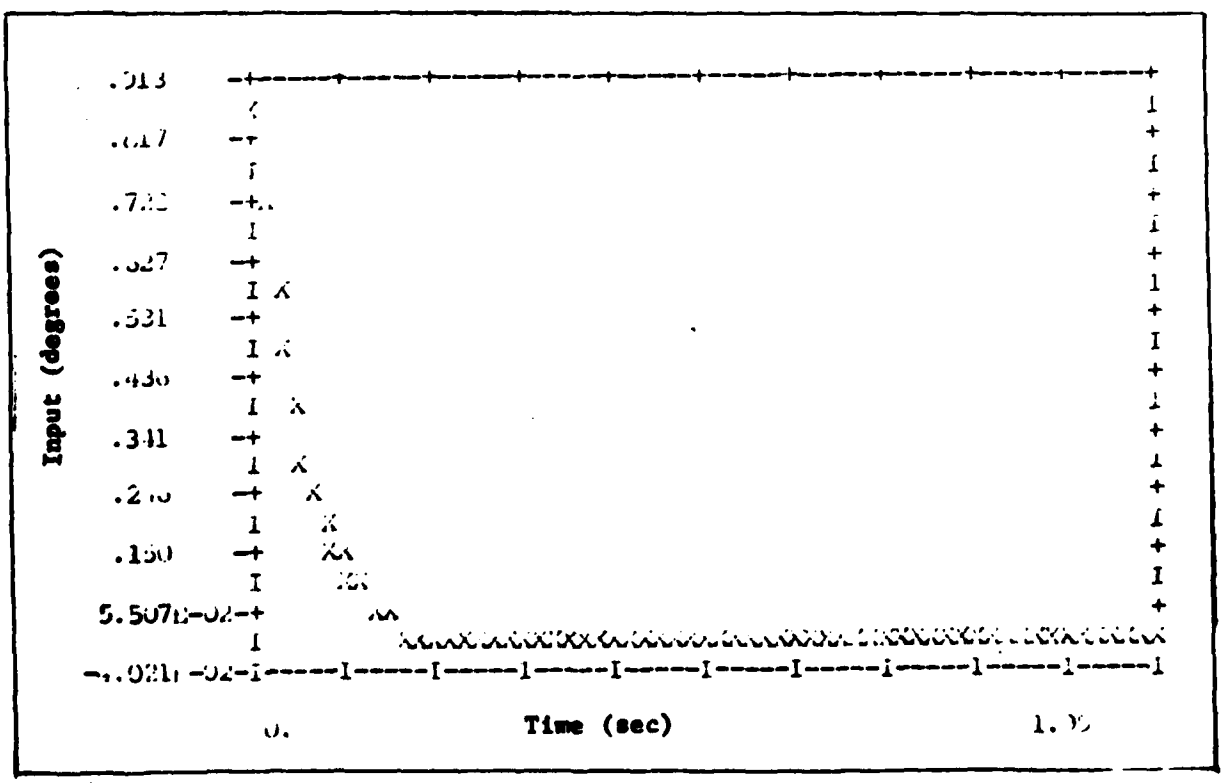

Figure B-18 δ_f Input for u Tracking

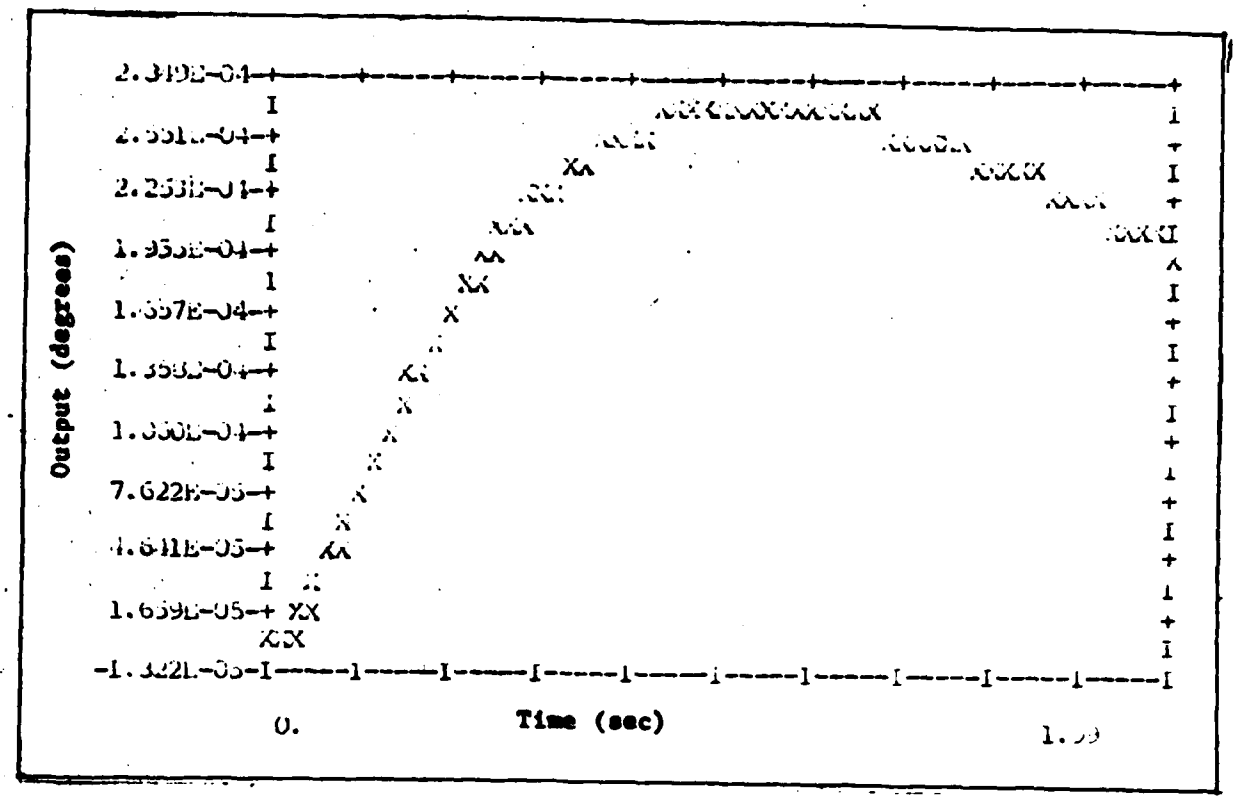

Figure B-19 γ **Response for u Tracking**

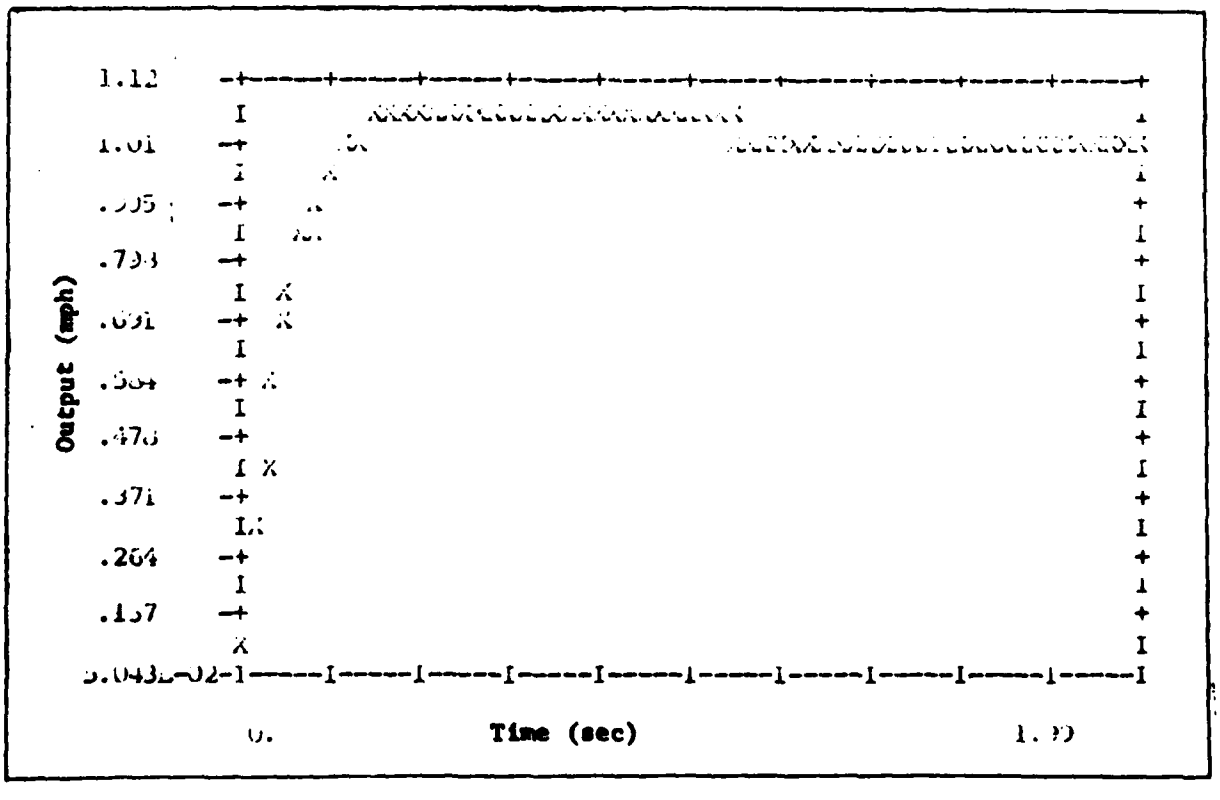

Figure B-20 **u Tracking Response**

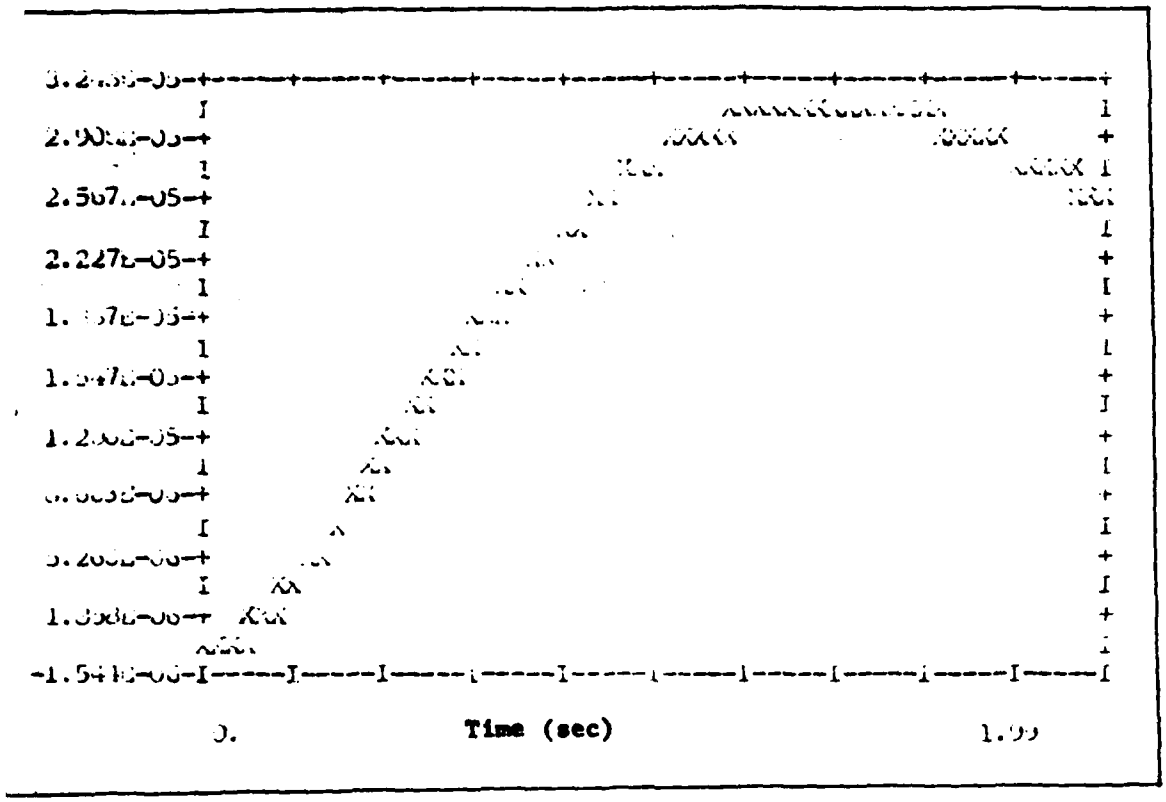

Figure B-21 θ Response for u Tracking

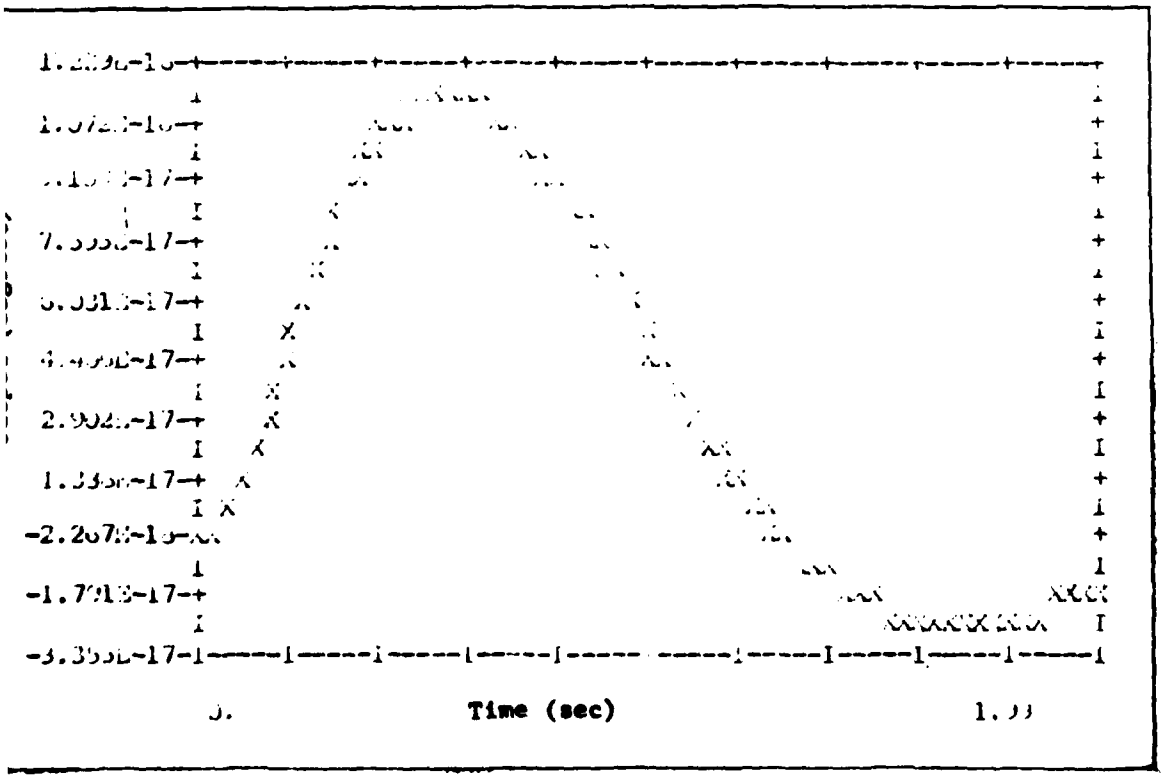

Figure B-22 β Response for u Tracking

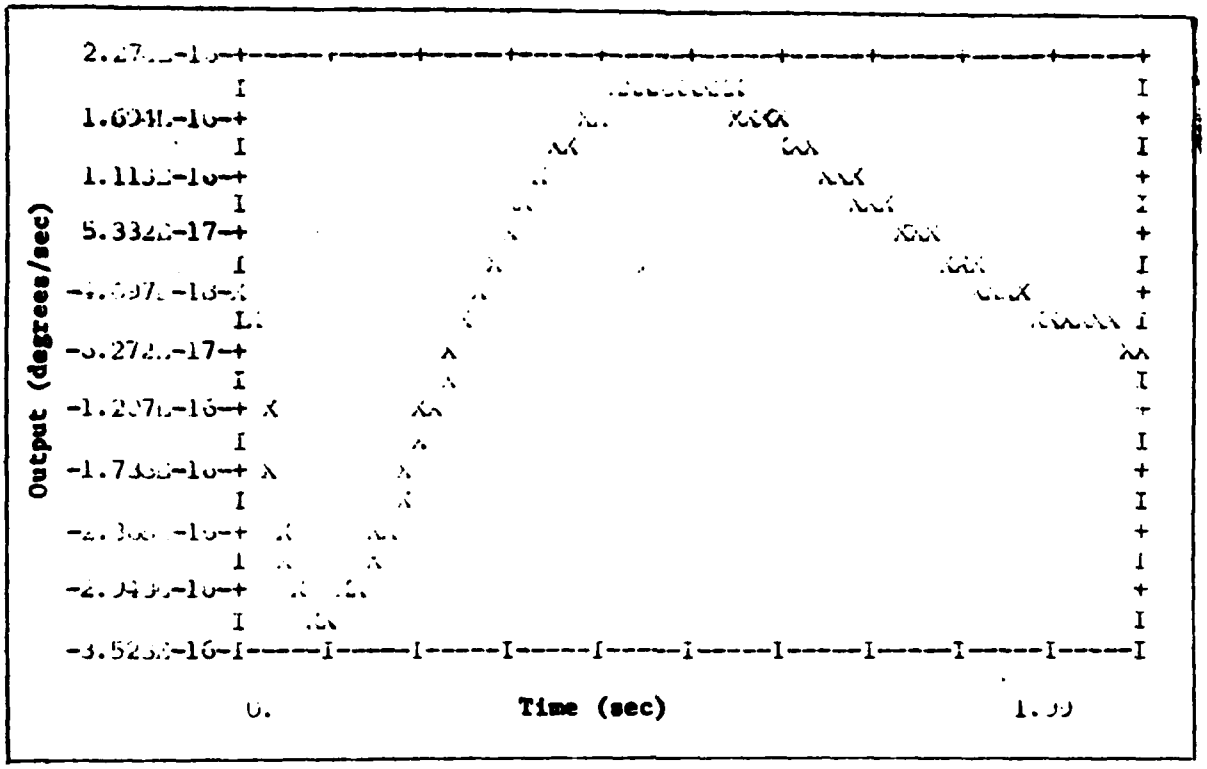

Figure B-23 r Response for u Tracking

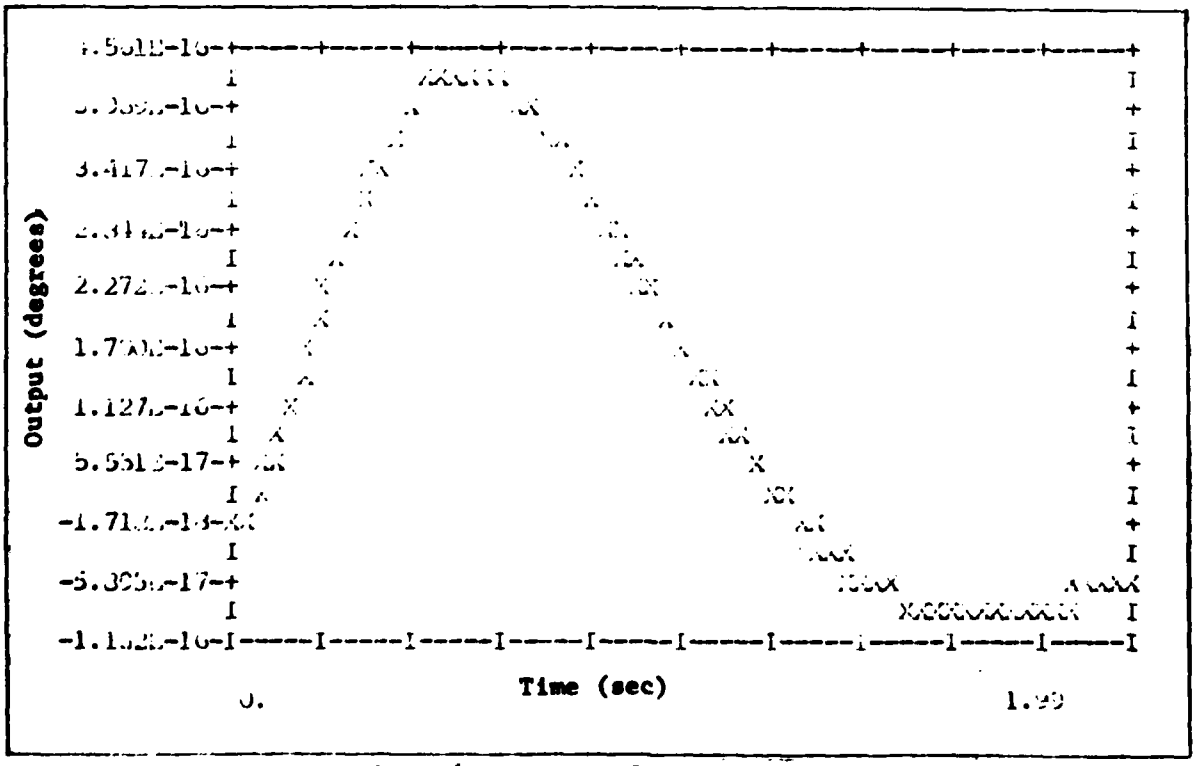

Figure B-24 ϕ Response for u Tracking

θ Tracking

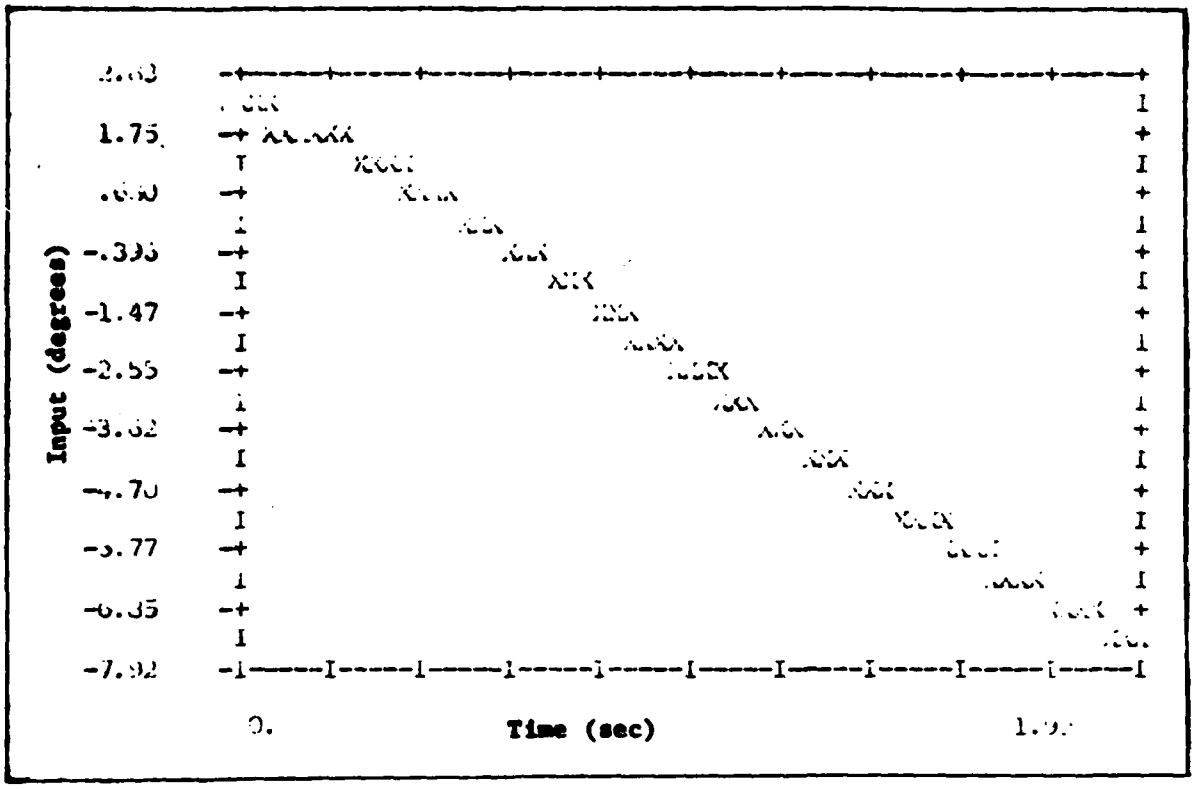

Figure B-25 δ_{H_r} Input for θ Tracking

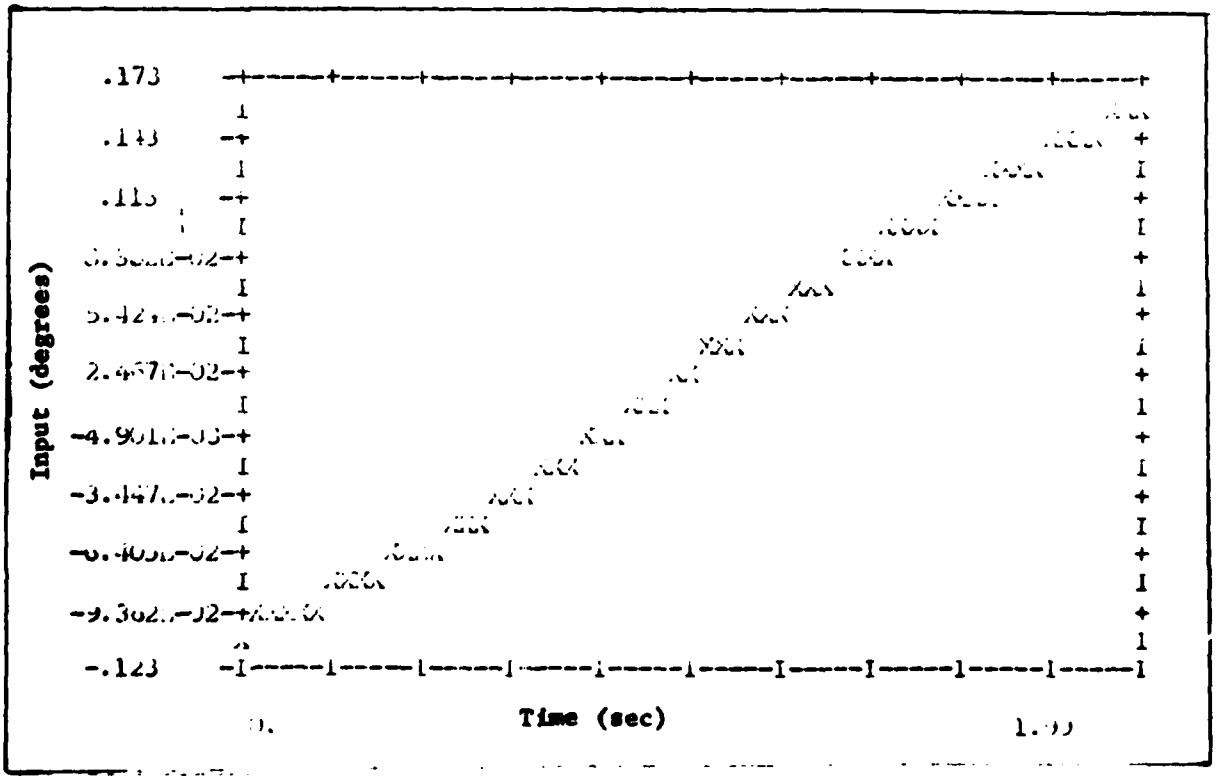

Figure B-26 δ_r Input for θ Tracking

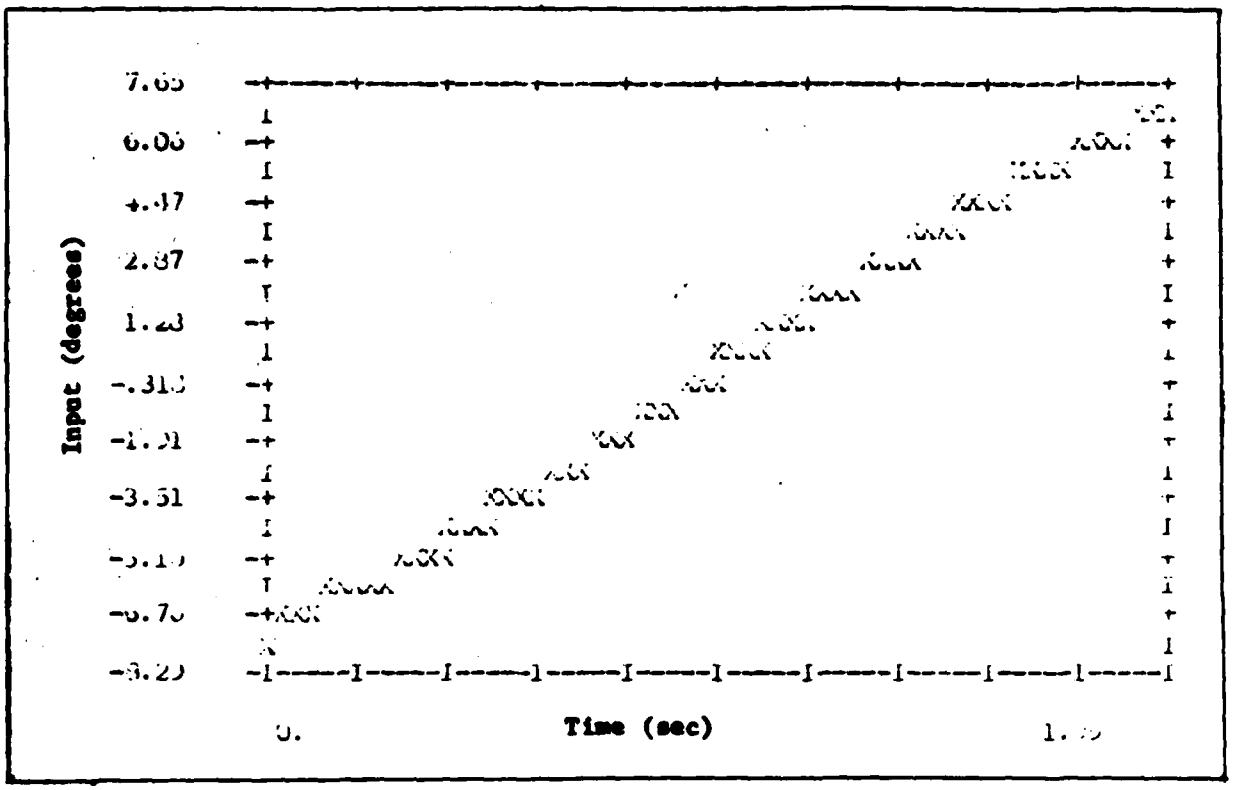

Figure B-27 δ_{H_L} Input for θ Tracking

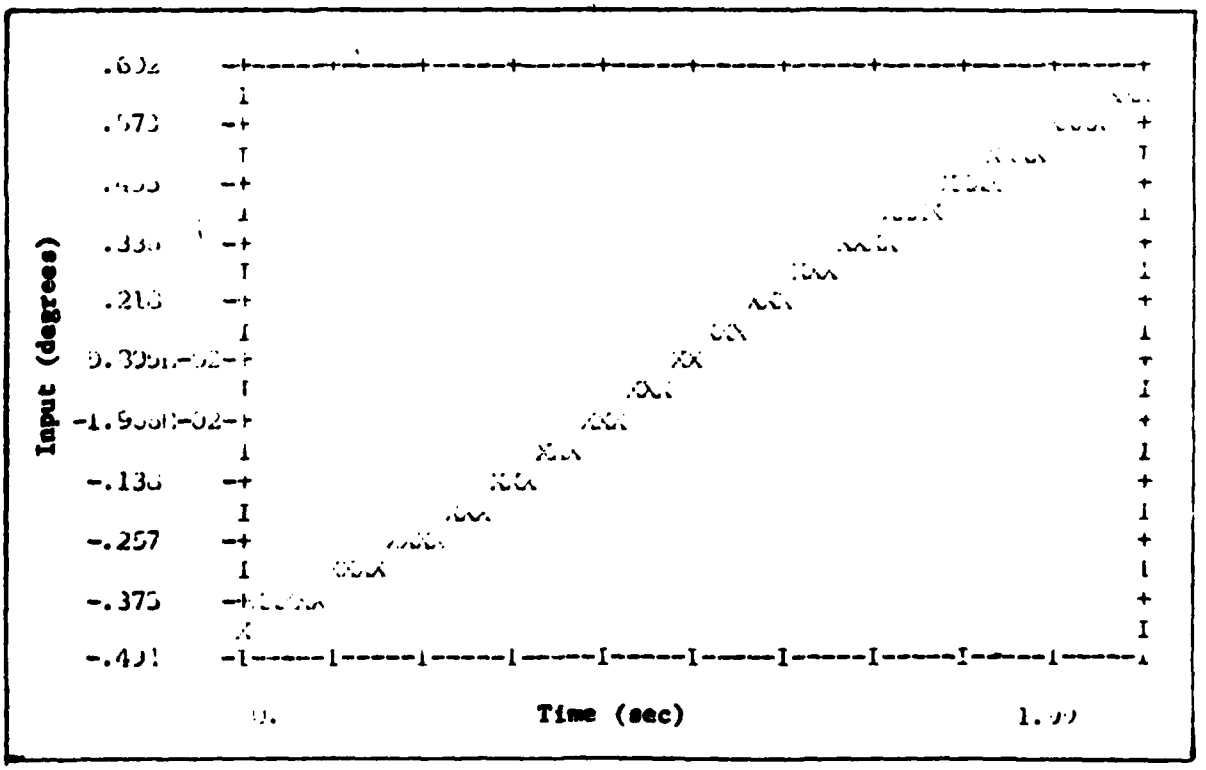

Figure B-28 δ_a Input for θ Tracking

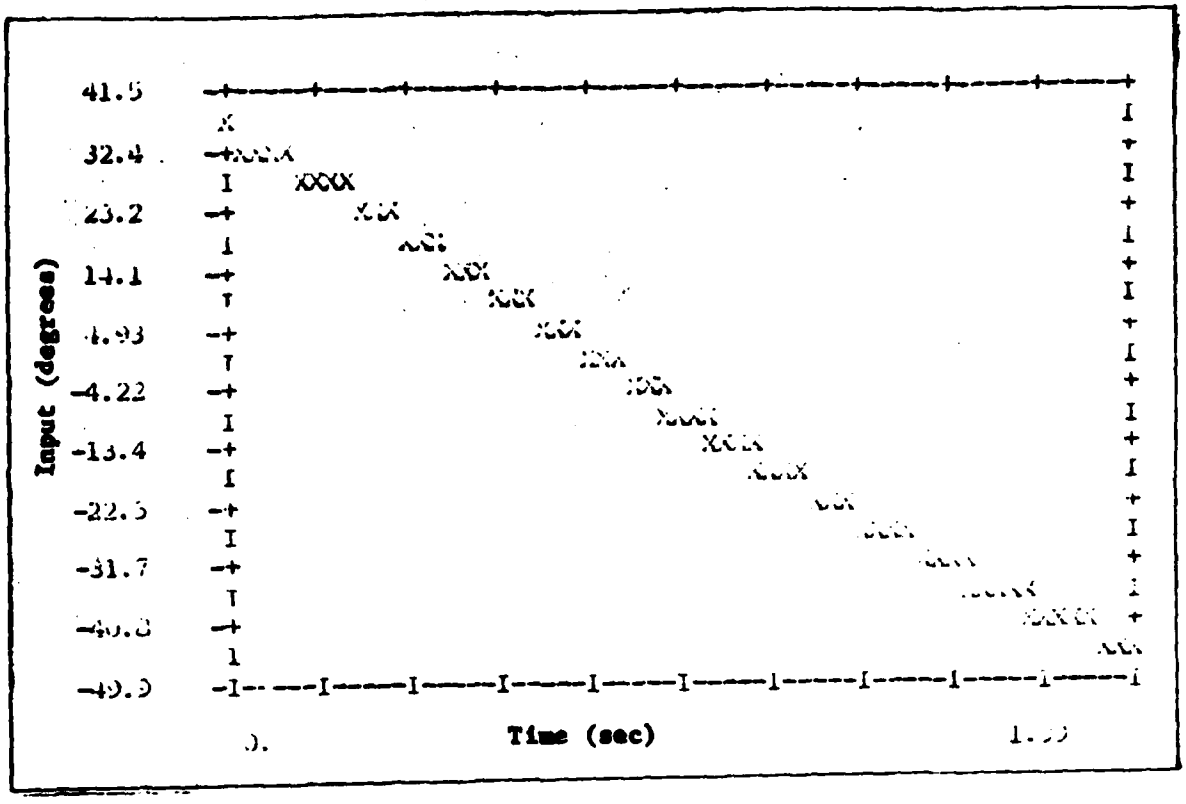

Figure B-29 δ_s Input for 0 Tracking

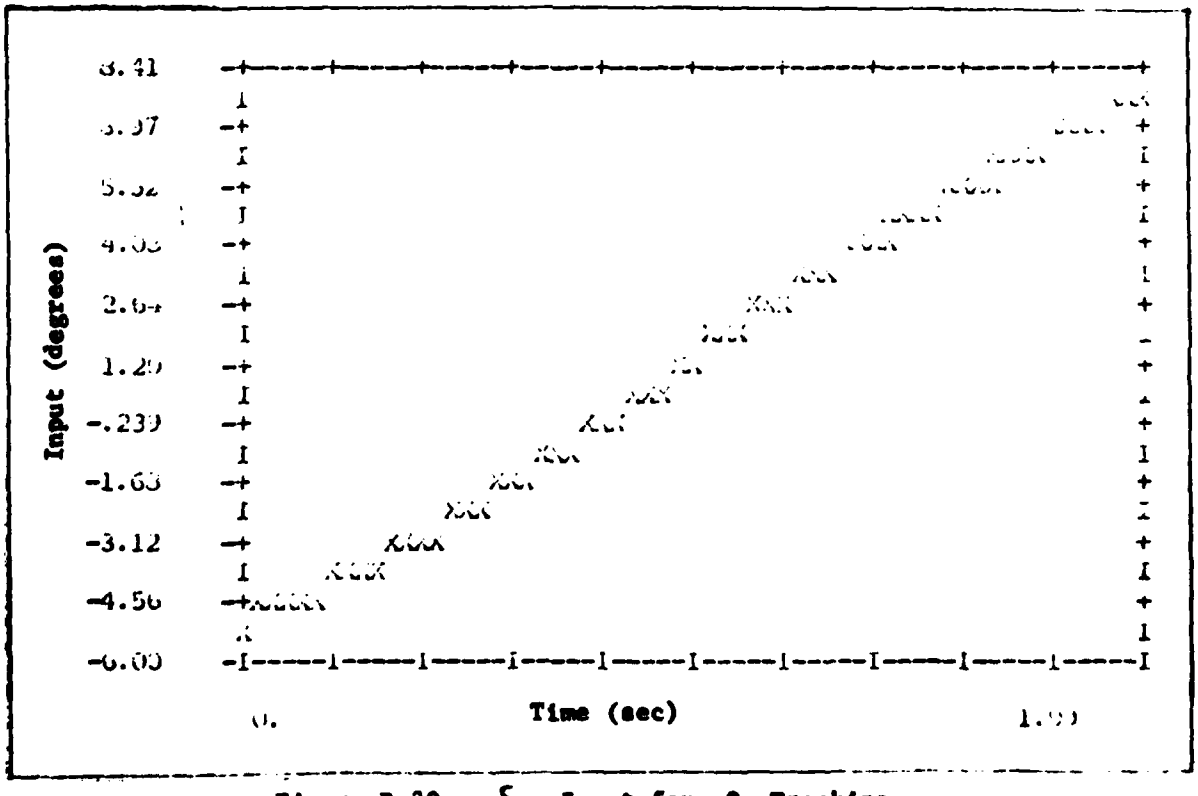

Figure B-30 δ_f Input for 0 Tracking

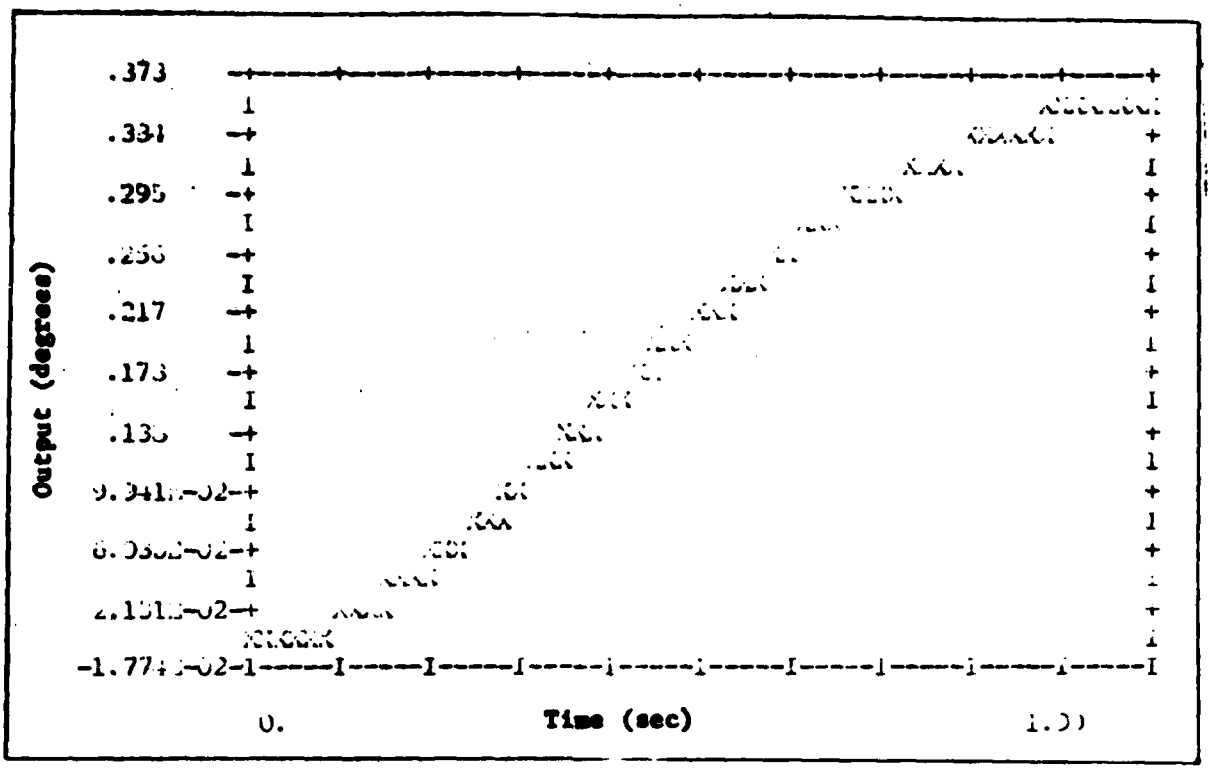

Figure B-31 γ Response for θ Tracking

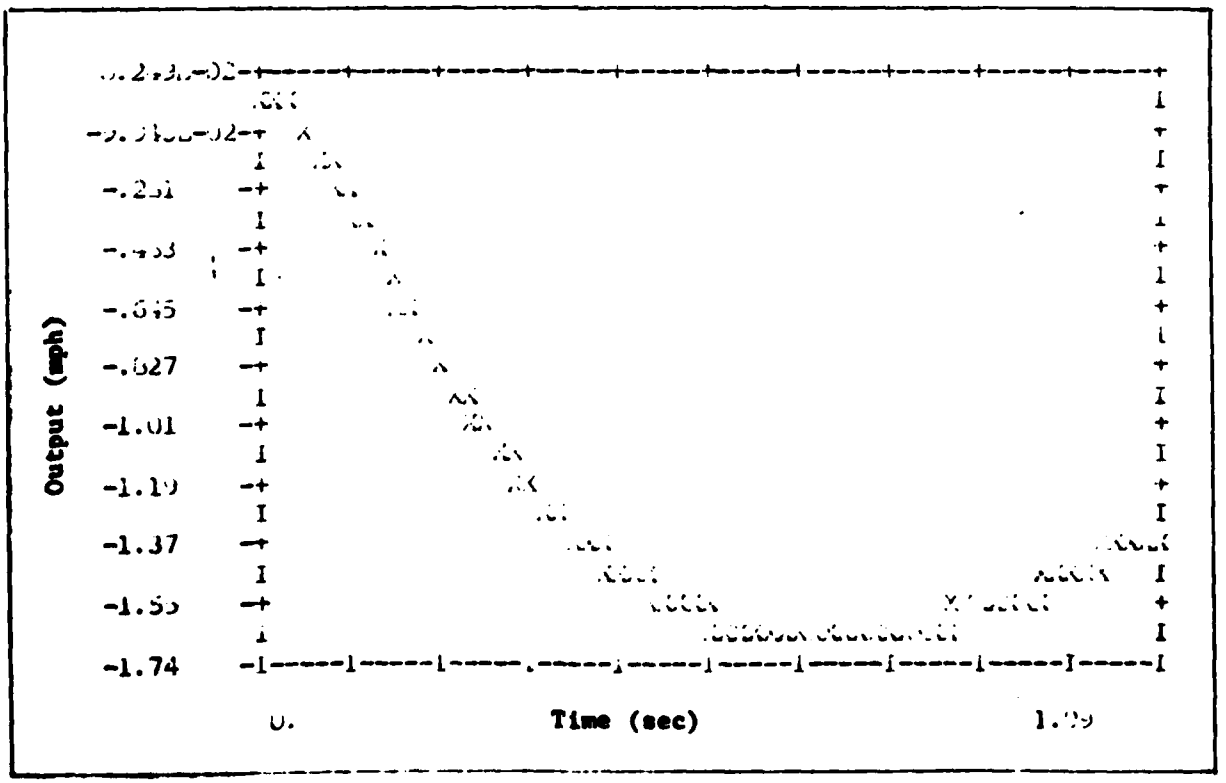

Figure B-32 u Response for θ Tracking

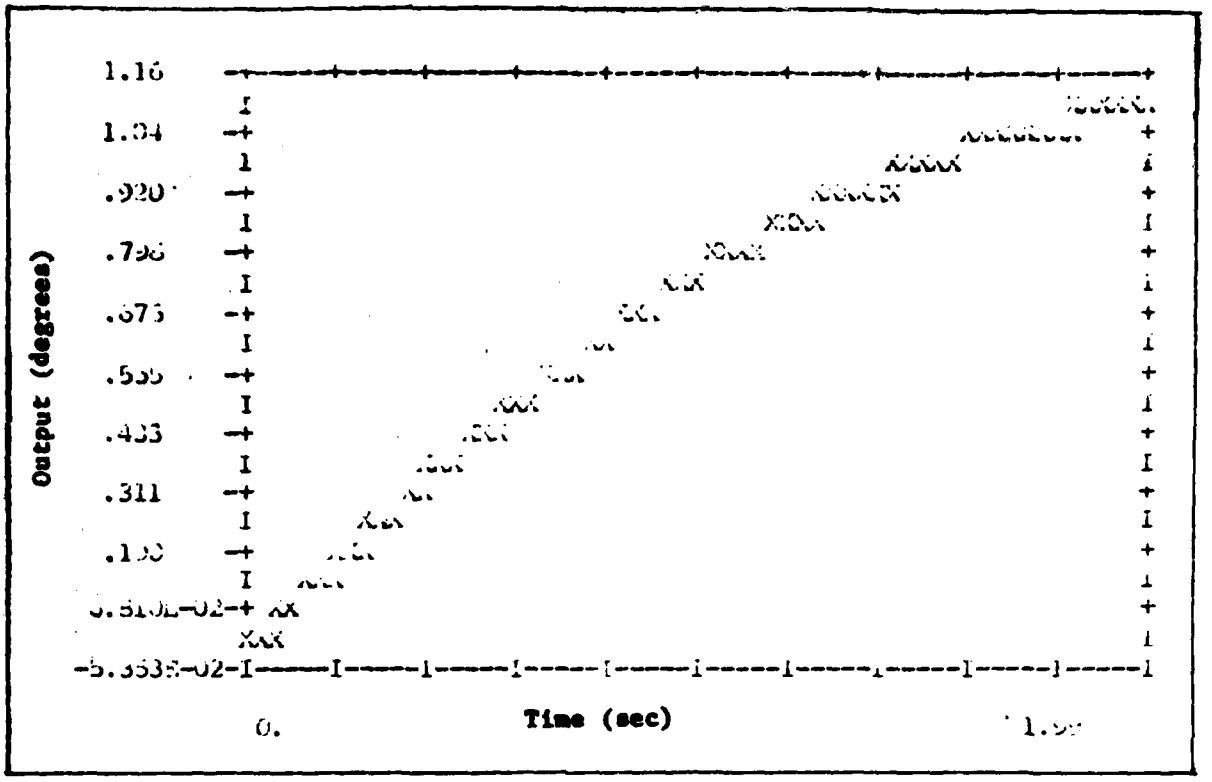

Figure B-33 θ Tracking Response

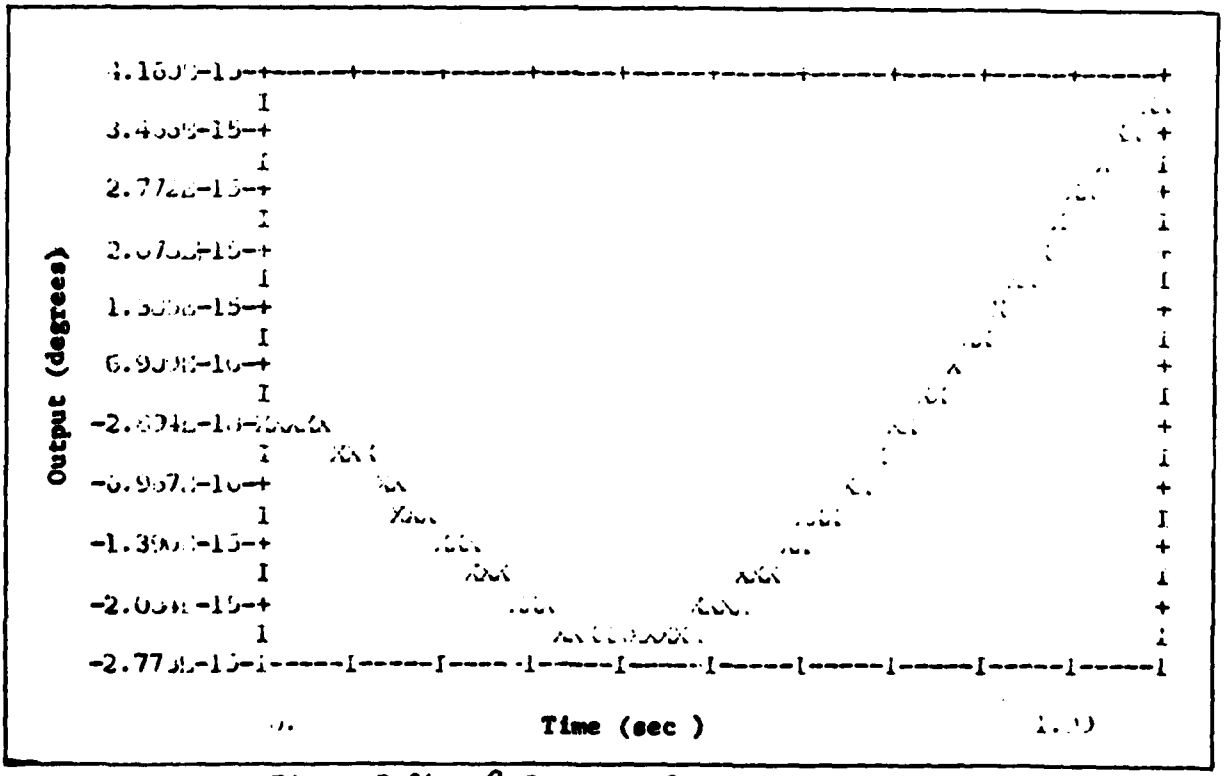

Figure B-34 β Response for θ Tracking

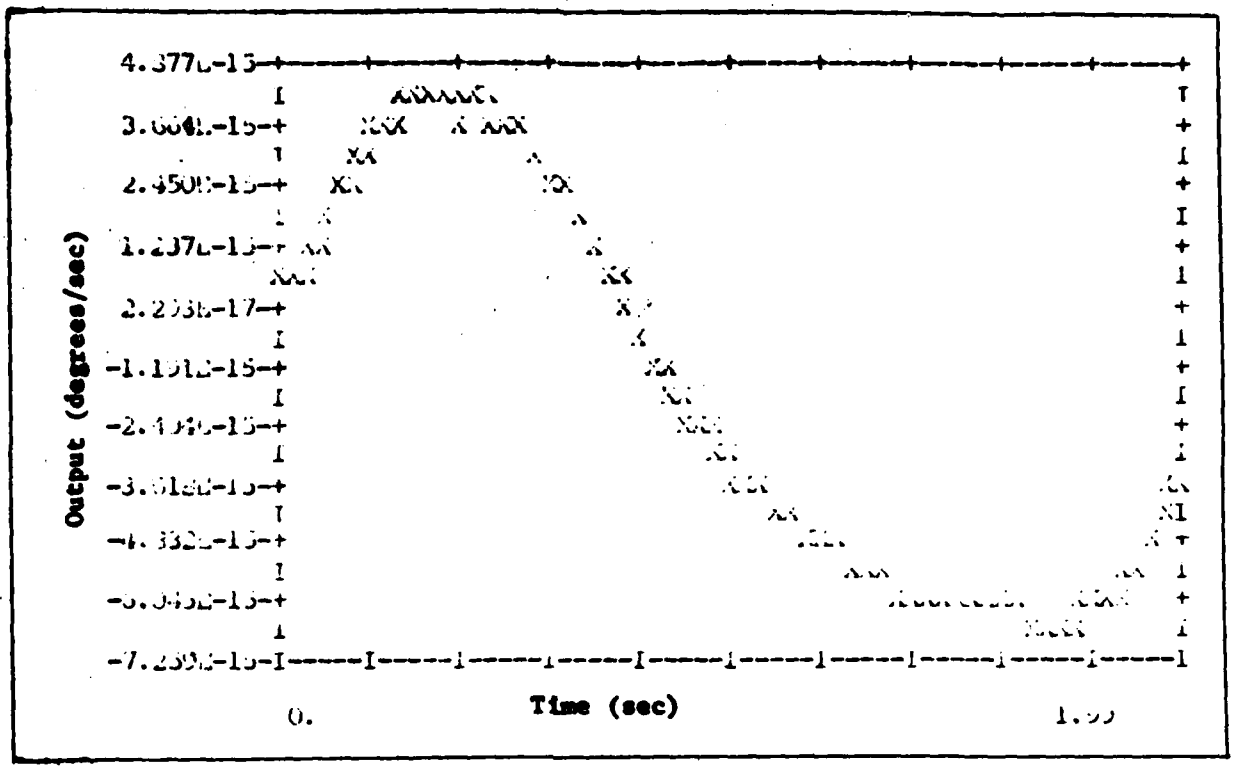

Figure B-35 r Response for θ Tracking

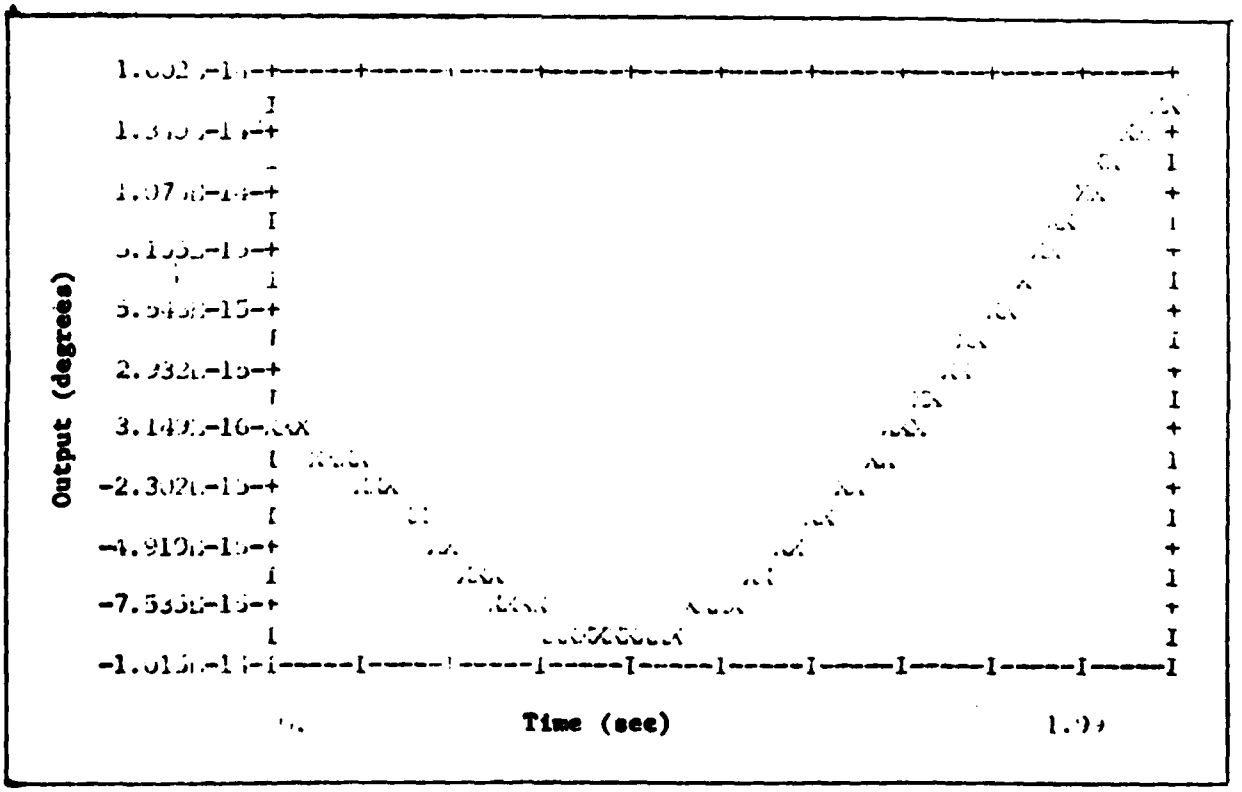

Figure B-36 ϕ Response for θ Tracking

β Tracking

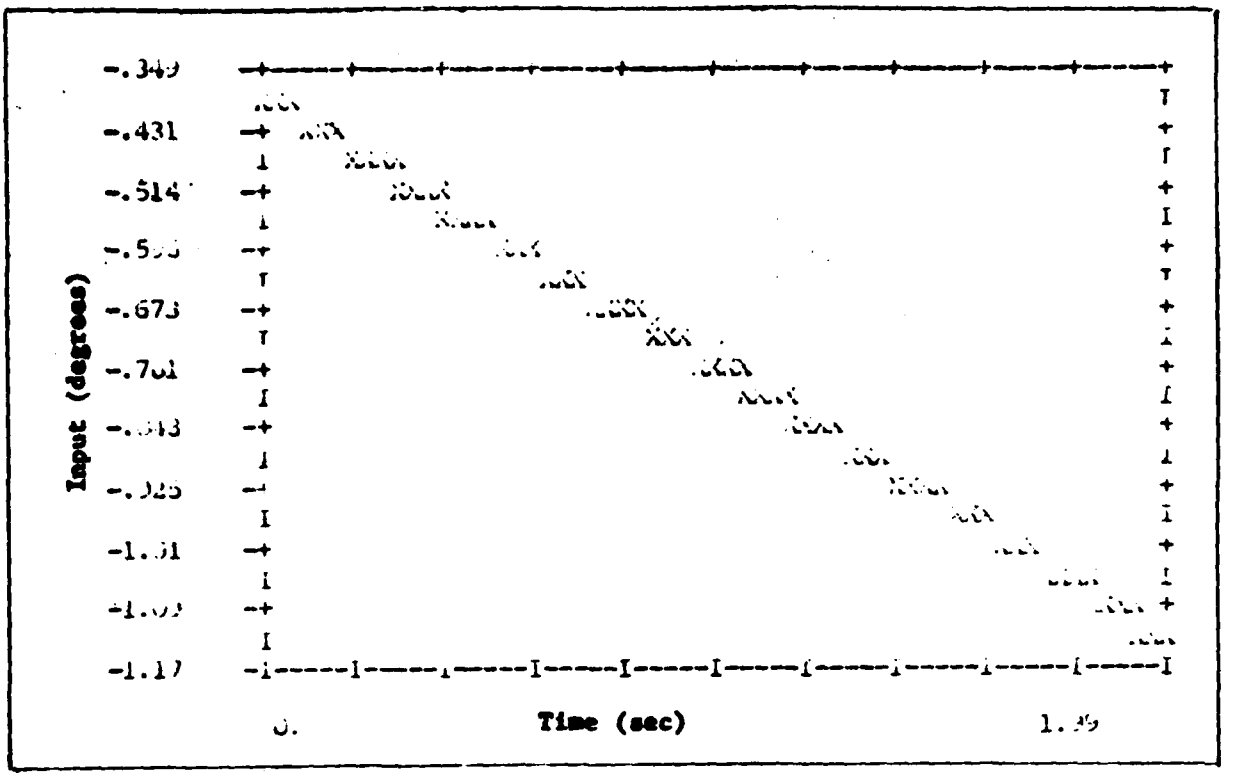

Figure B-37 δ_r Input for β Tracking

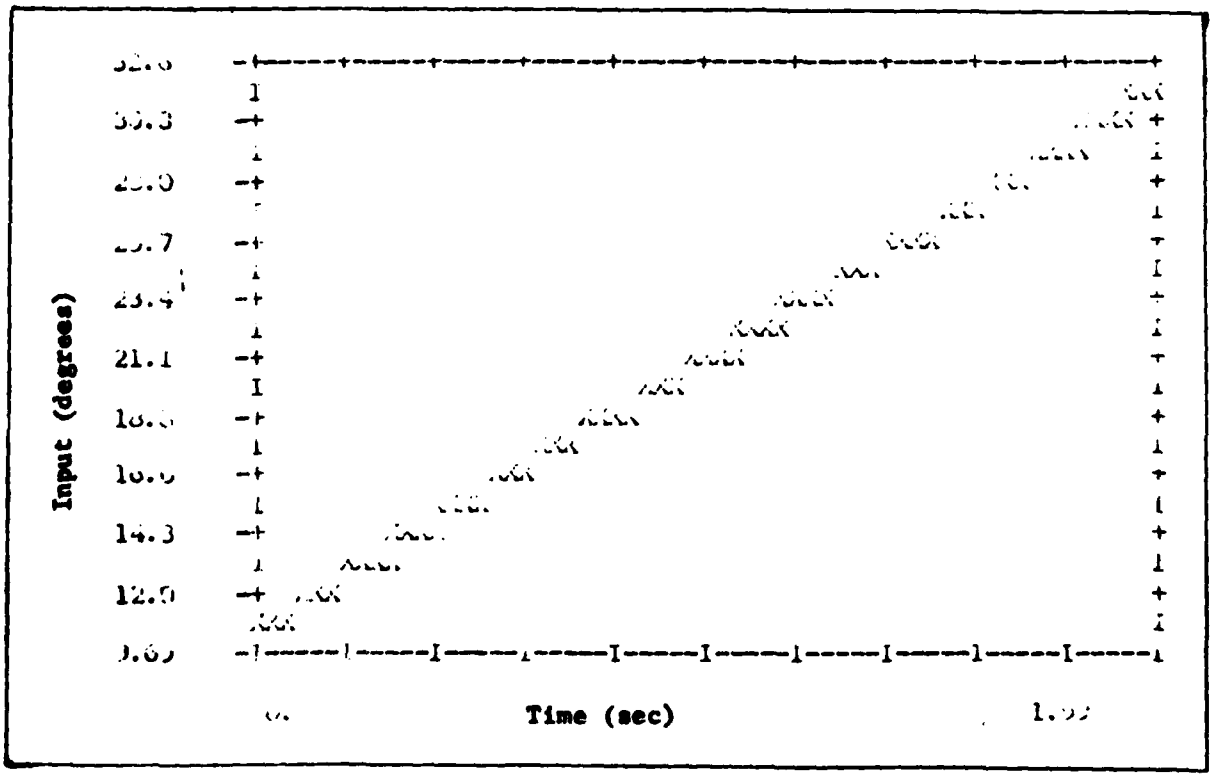

Figure B-38 δ_{H_r} Input for β Tracking

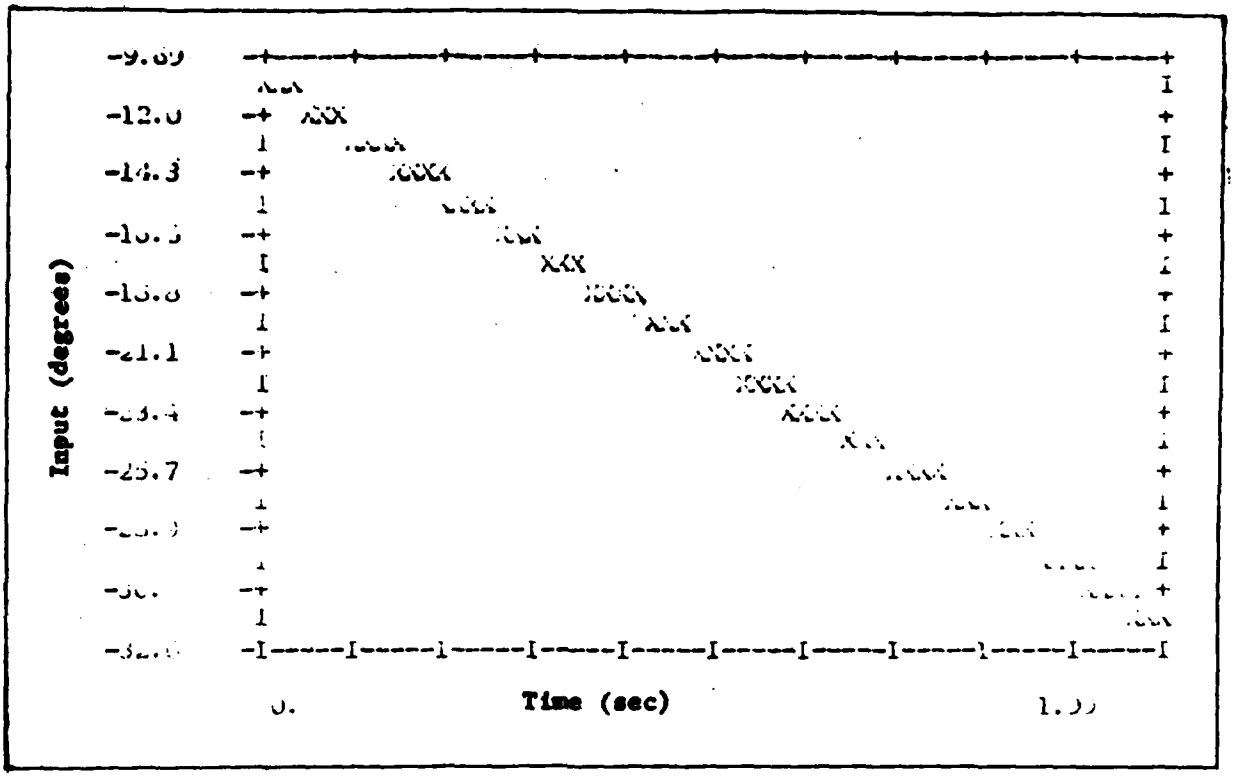

Figure B-39 δ_{H_L} Input for β Tracking

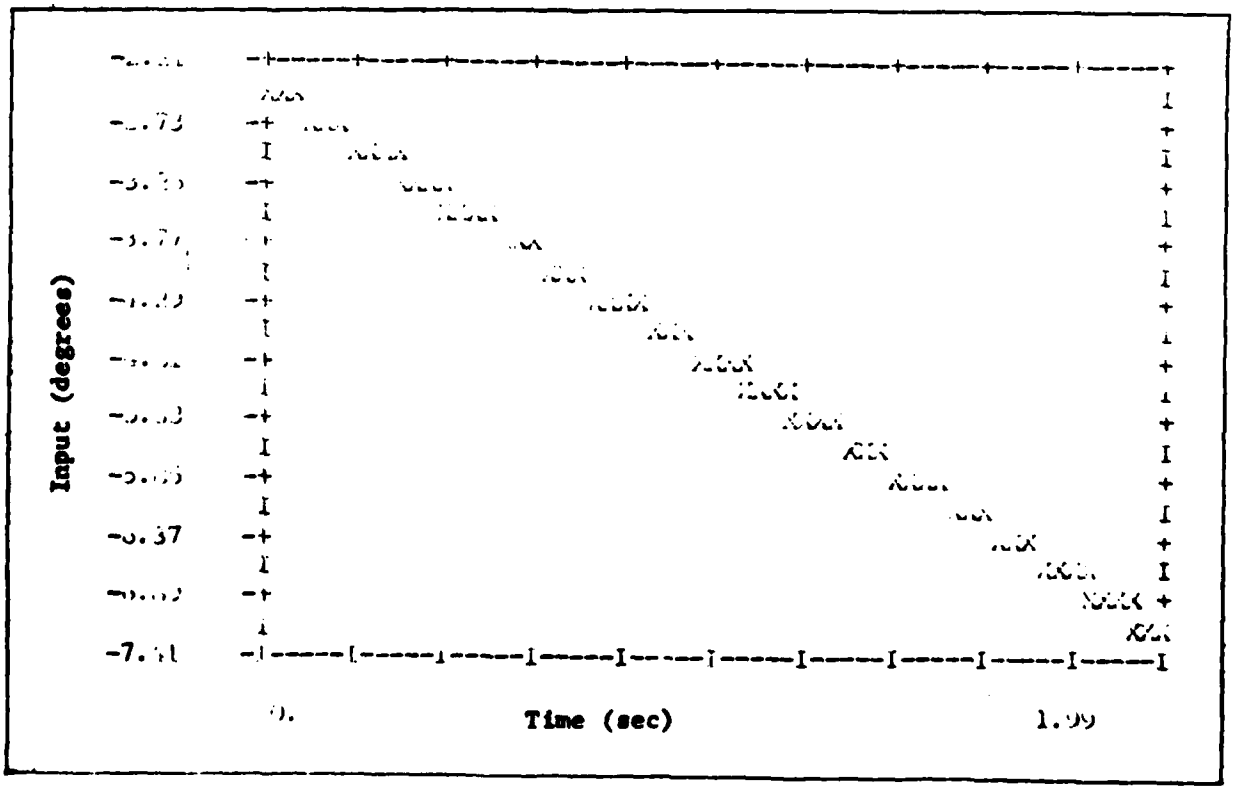

Figure B-40 δ_a Input for β Tracking

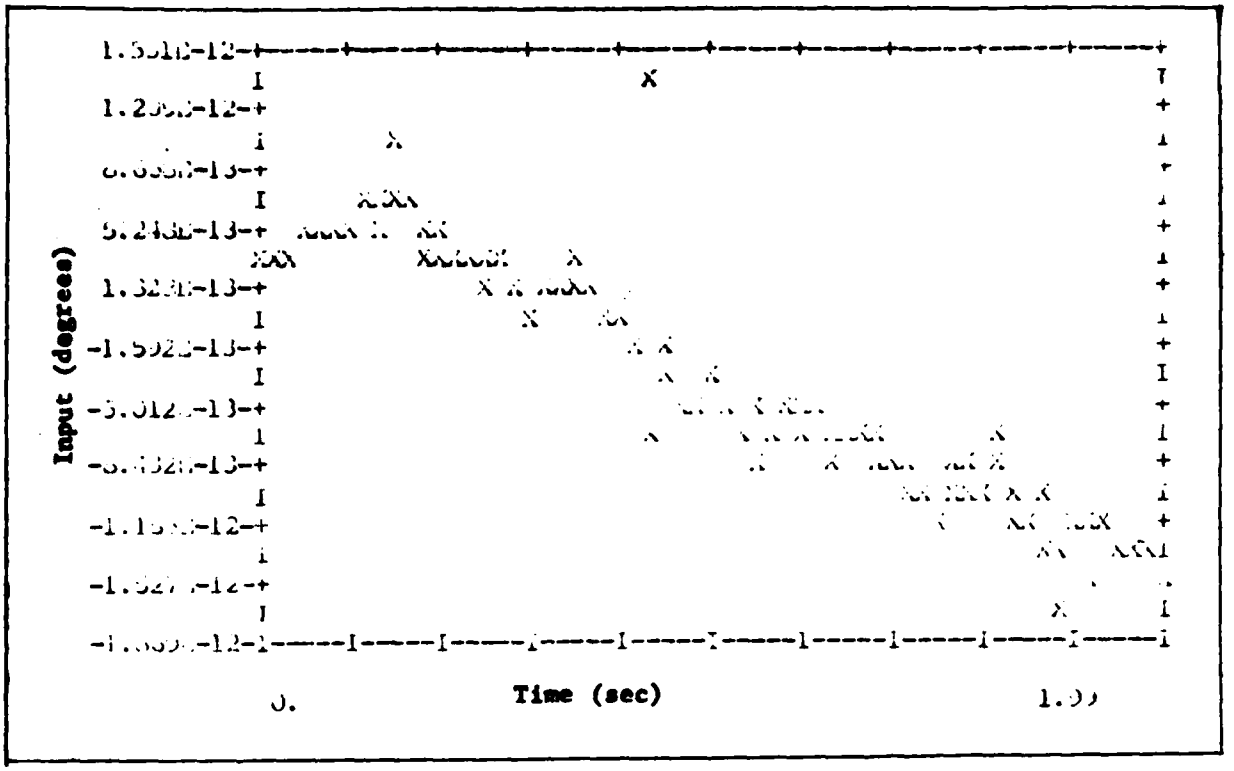

Figure B-41 δ_a **Input for** β **Tracking**

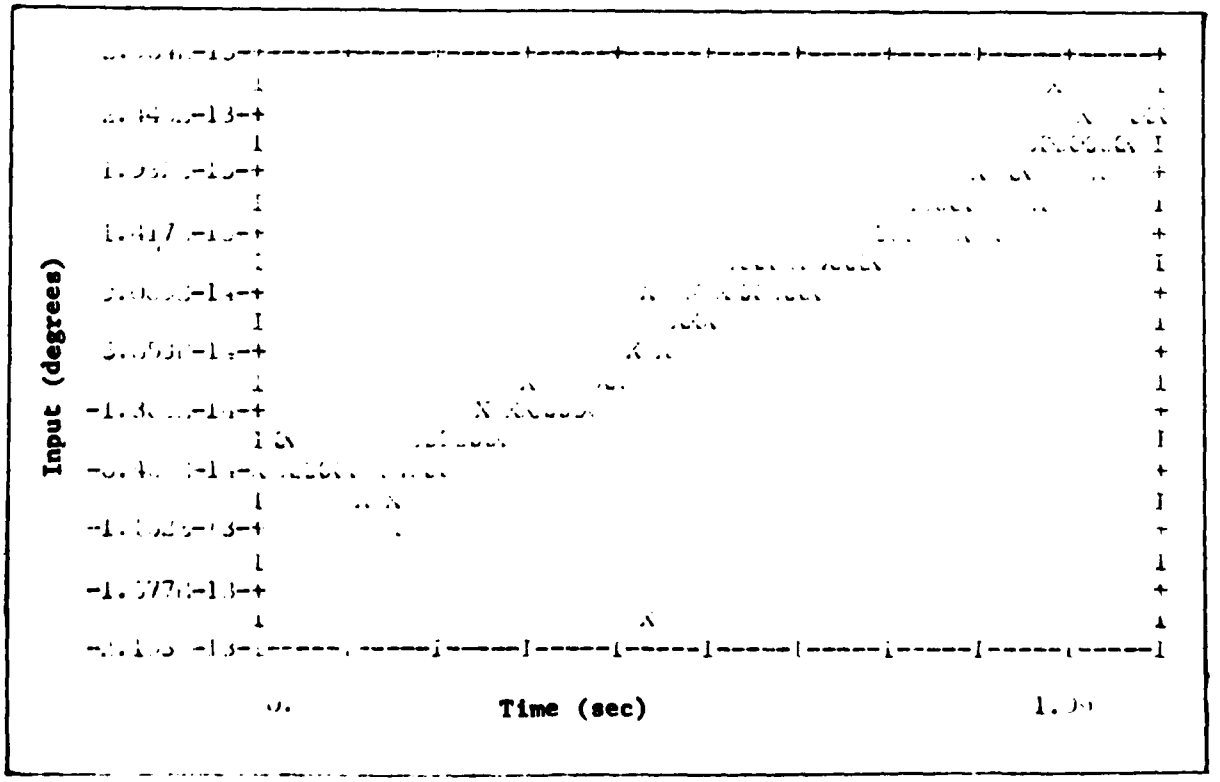

Figure B-42 δ_f **Input for** β **Tracking**

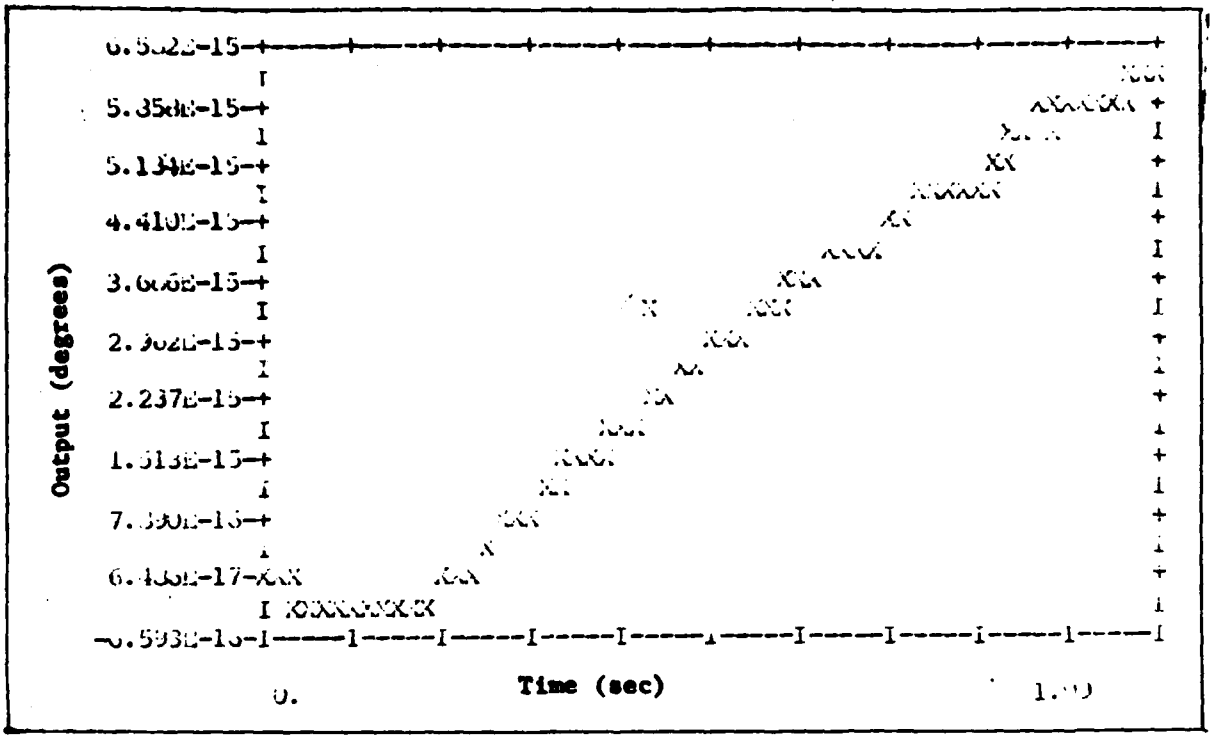

Figure B-43 γ Response for β Tracking

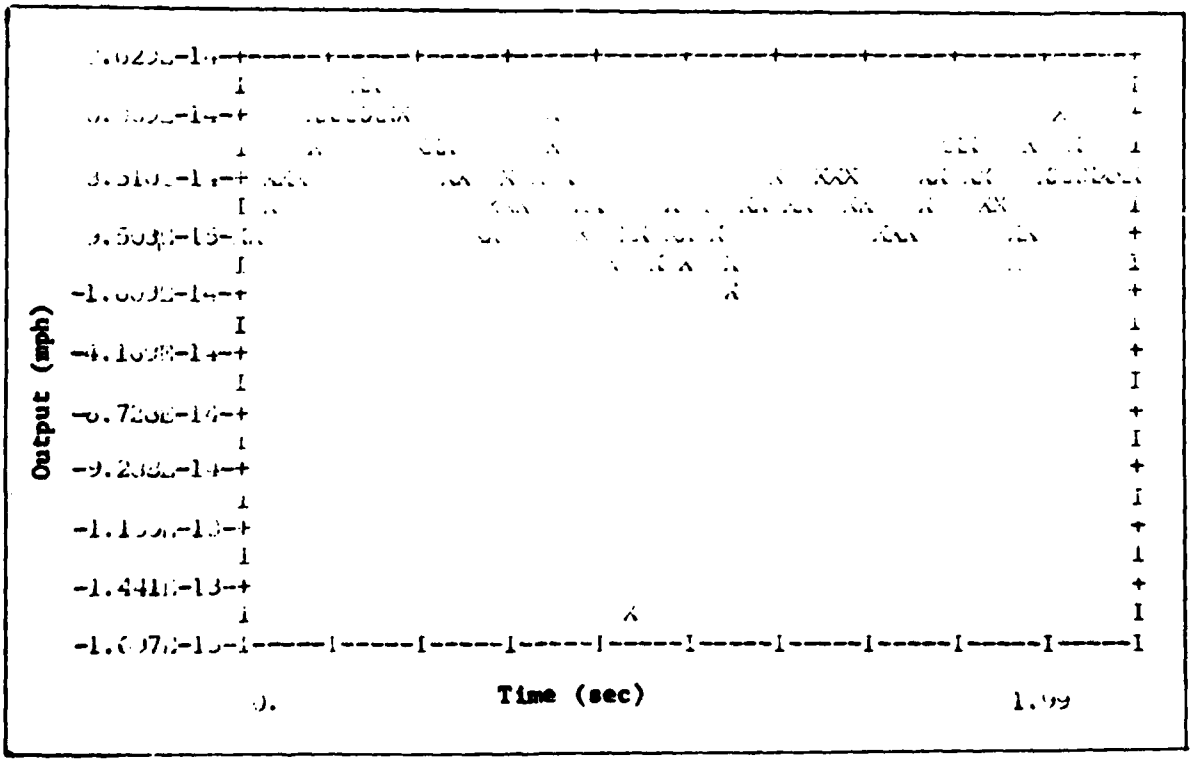

Figure B-44 u Response for β Tracking

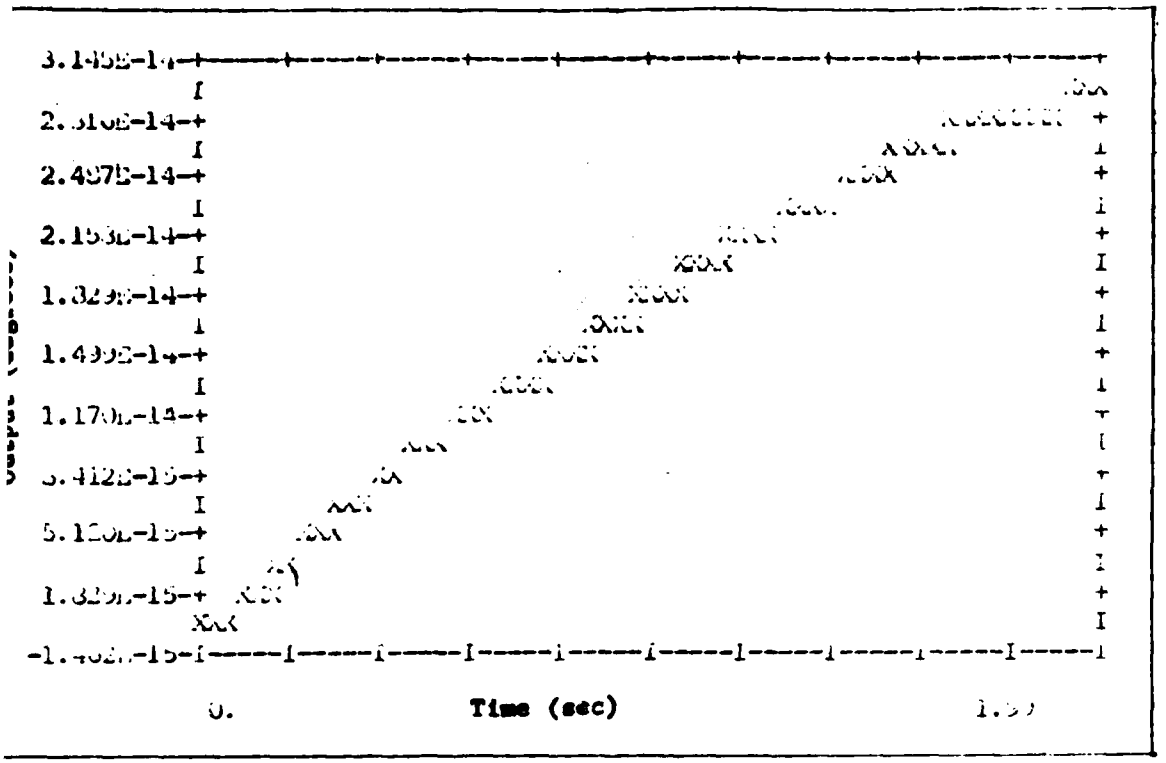

Figure B-45 θ Response for ϕ Tracking

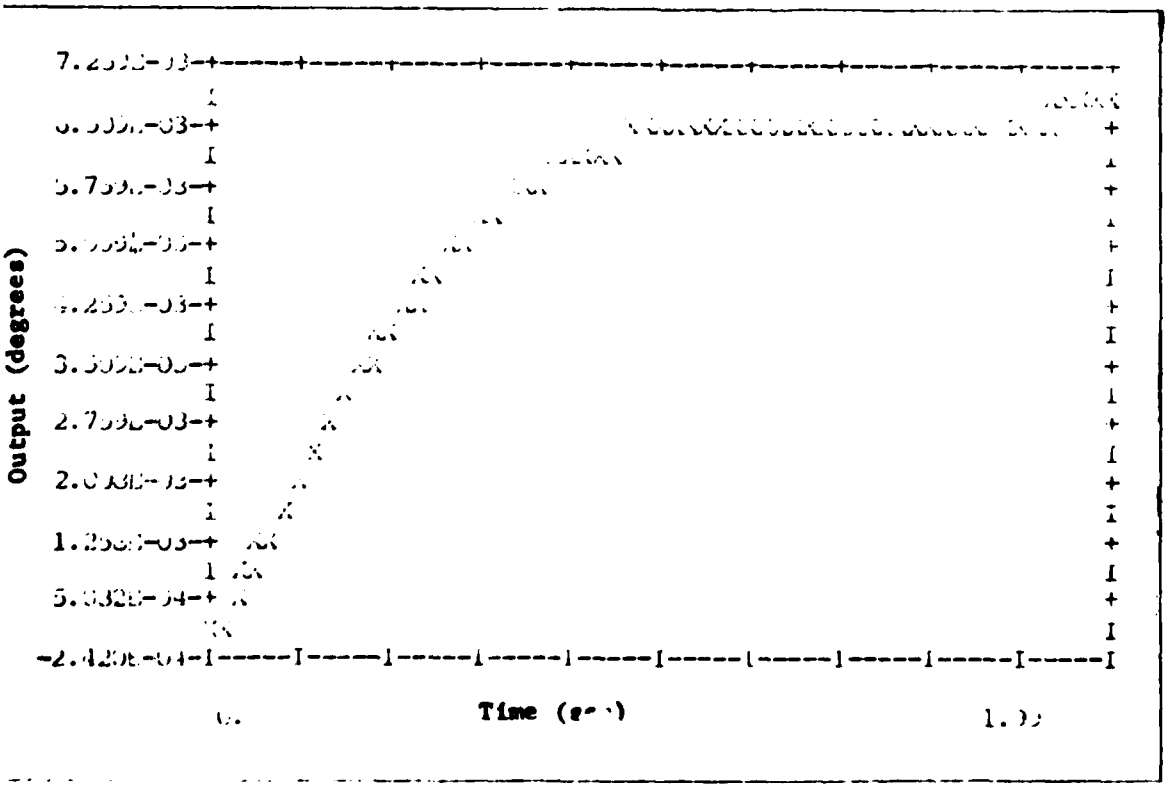

Figure B-46 β Tracking Response

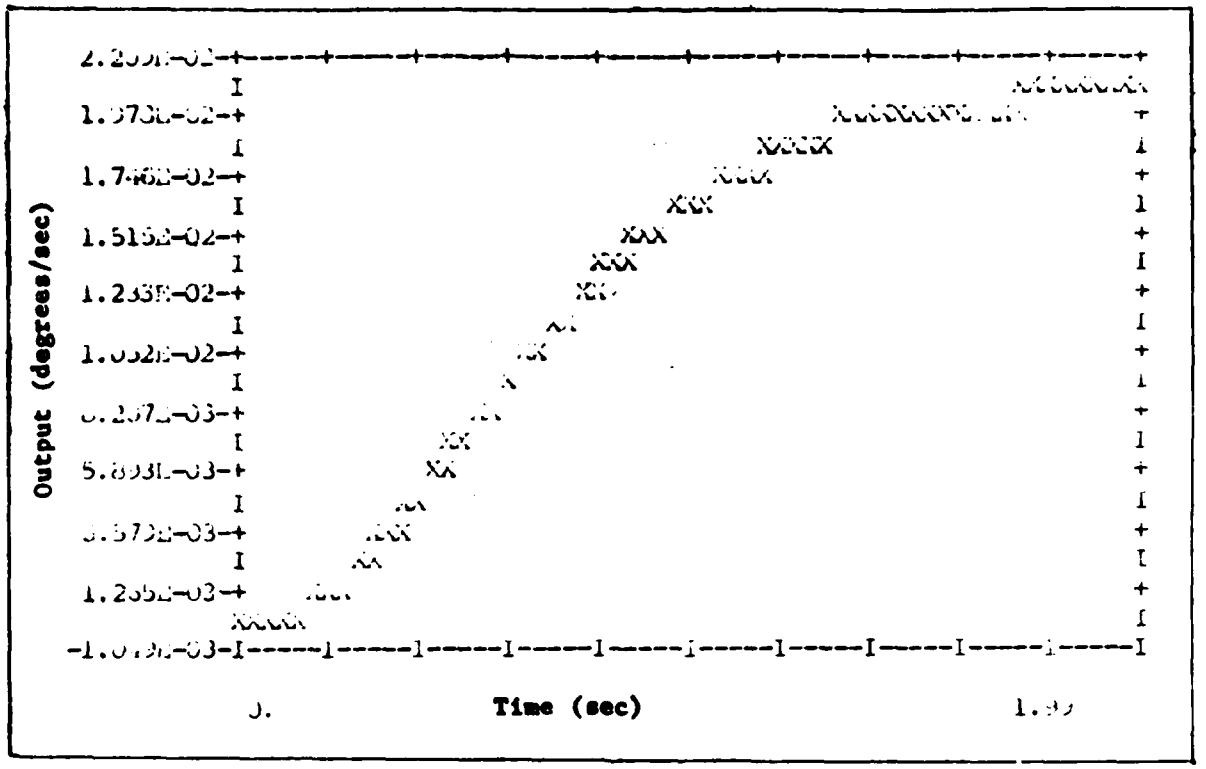

Figure B-47 r Response for β Tracking

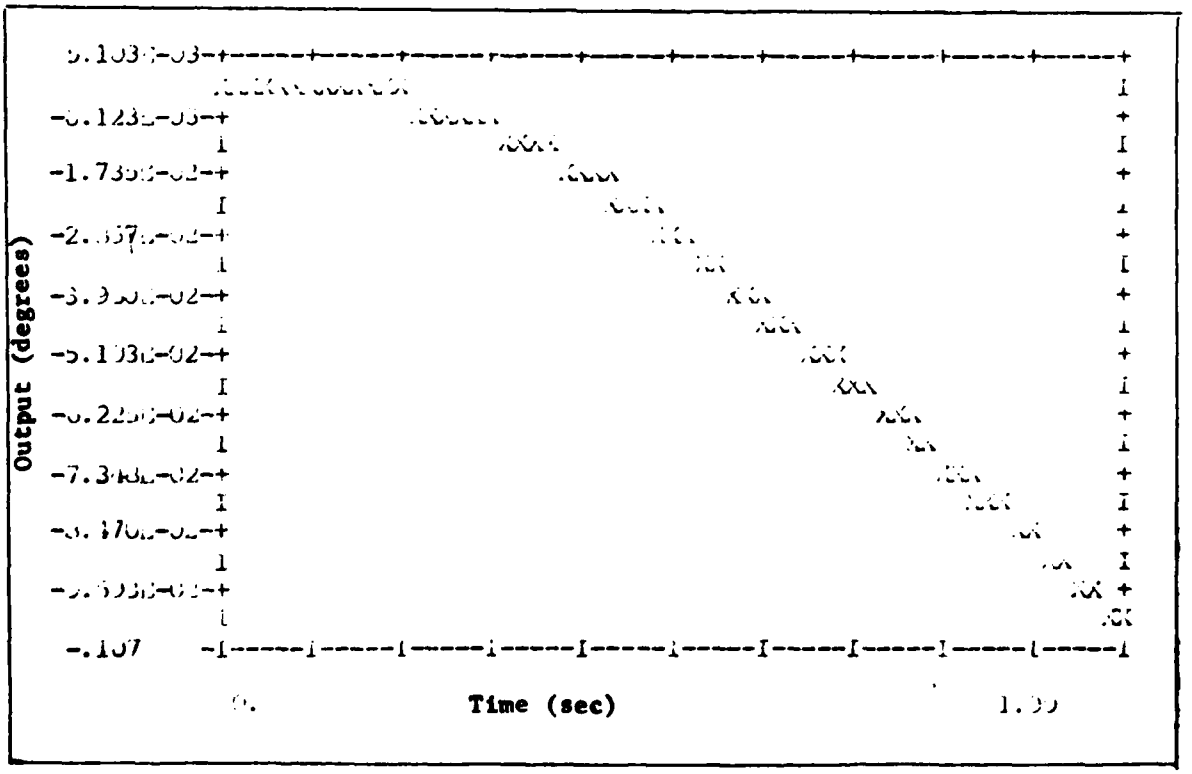

Figure B-48 ϕ Response for β Tracking

r Tracking

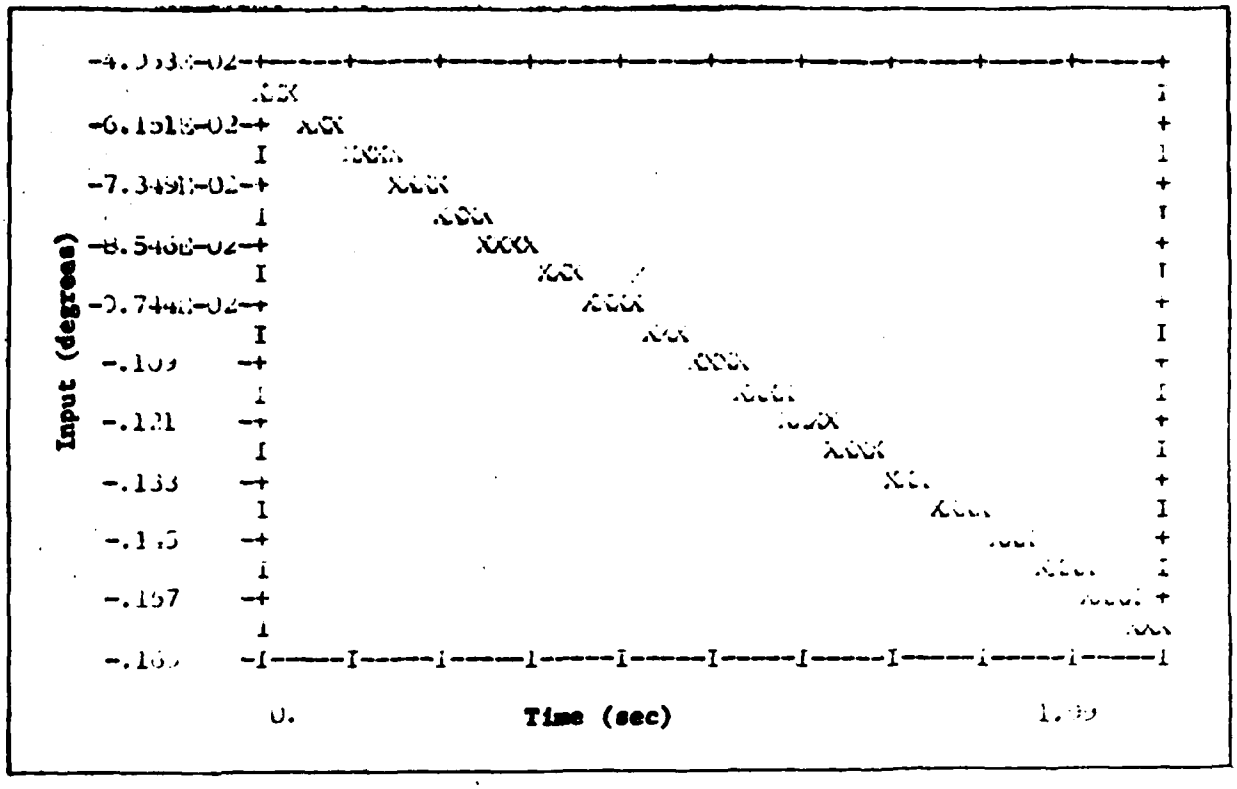

Figure B-49 δ_r Input for r Tracking

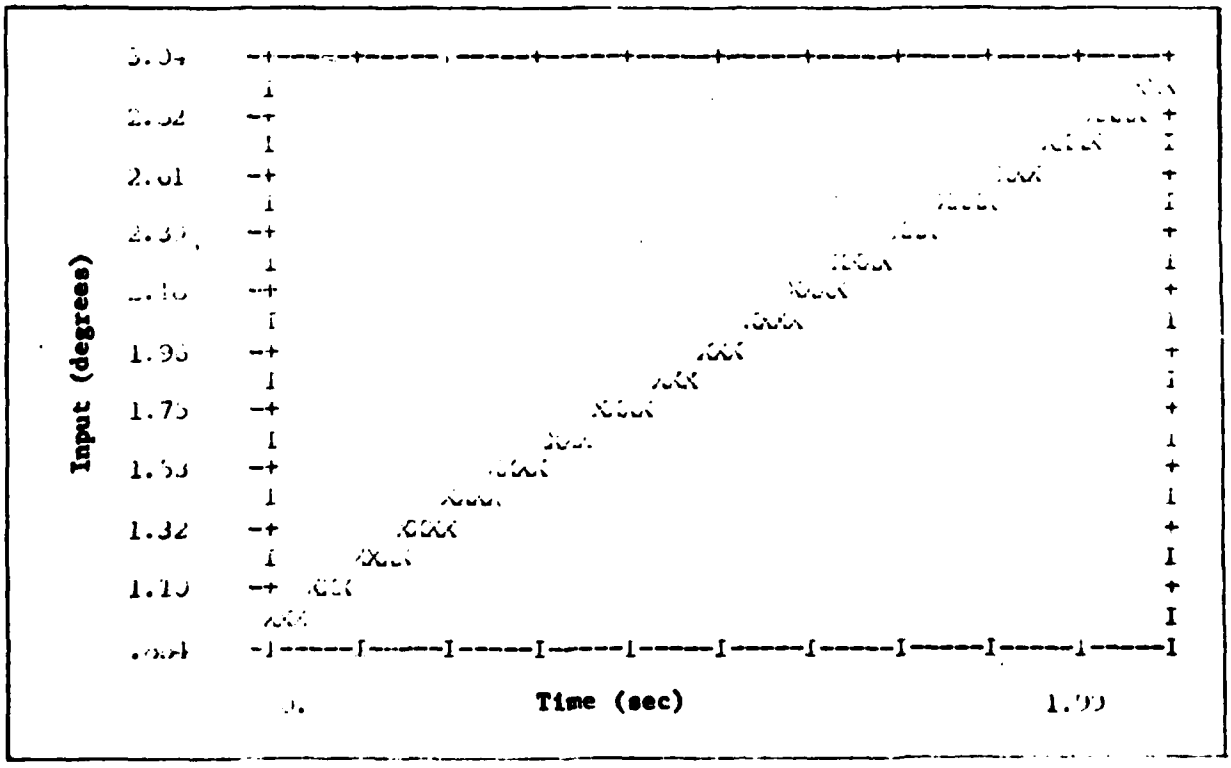

Figure B-50 δ_{H_r} Input for r Tracking

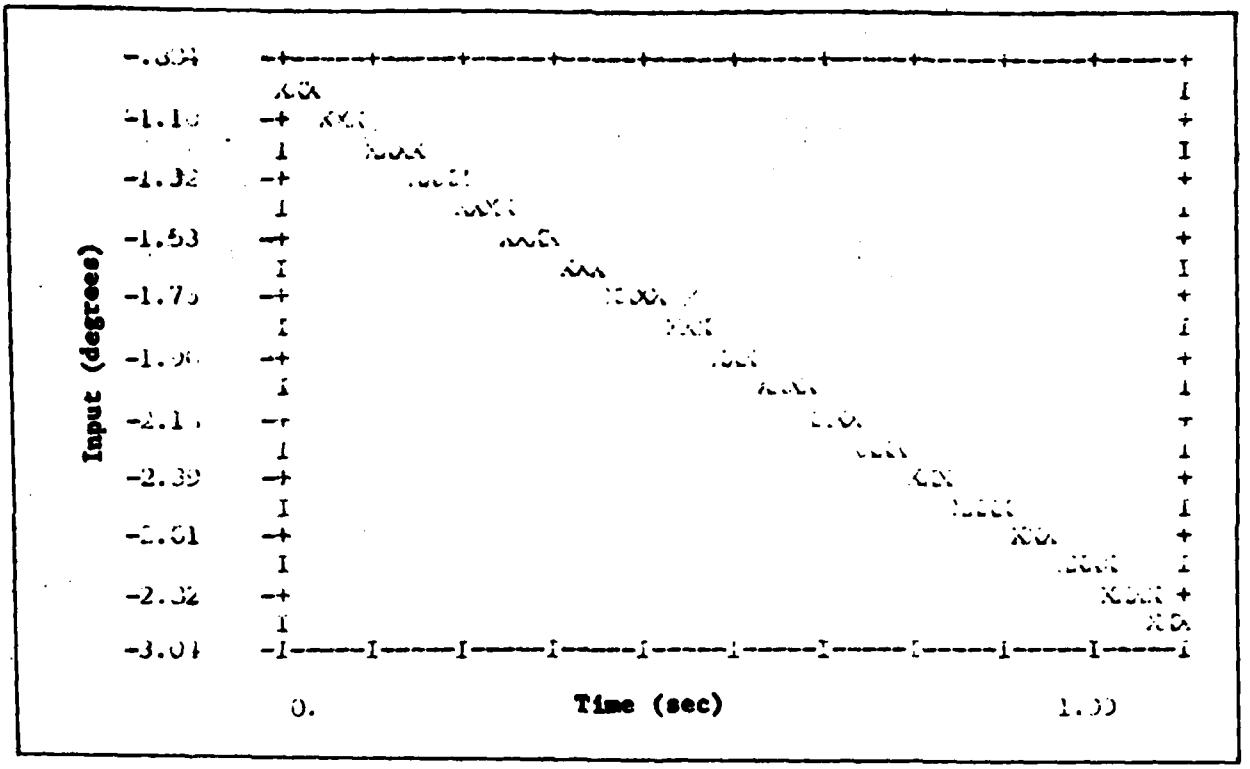

Figure B-51 δ_{H_L} Input for r Tracking

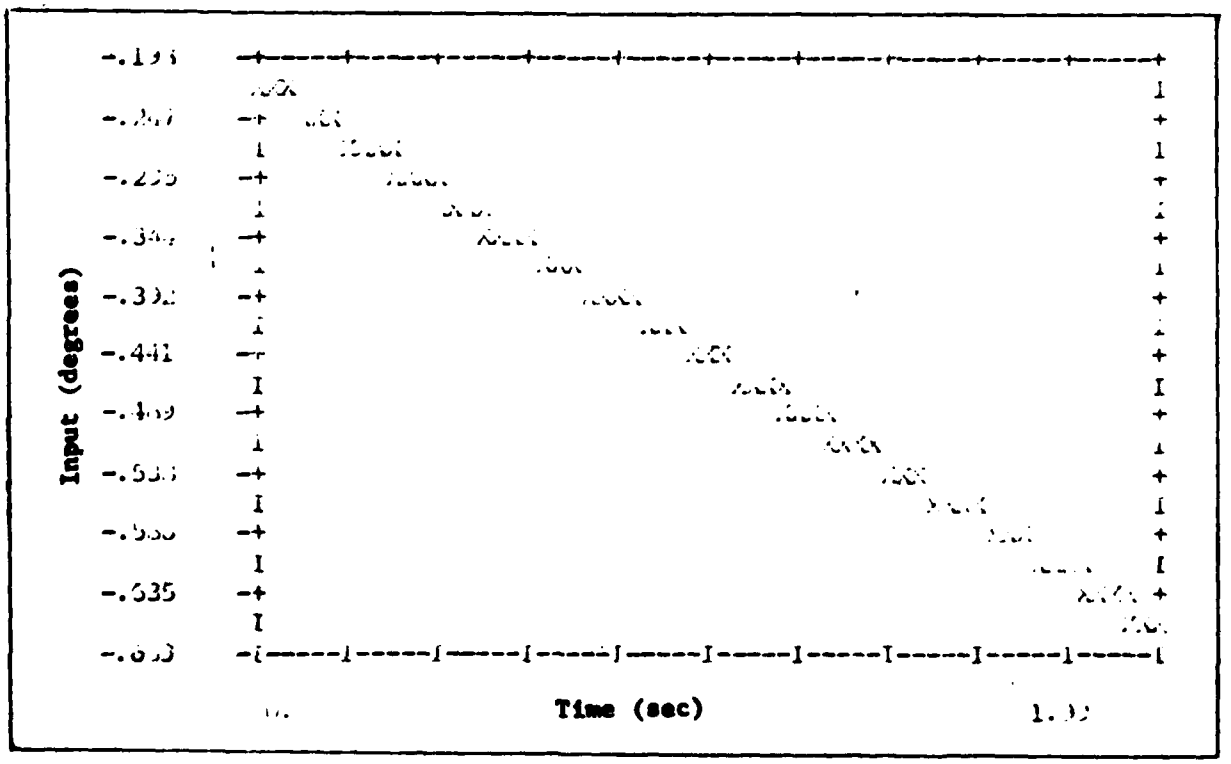

Figure B-52 δ_a Input for r Tracking

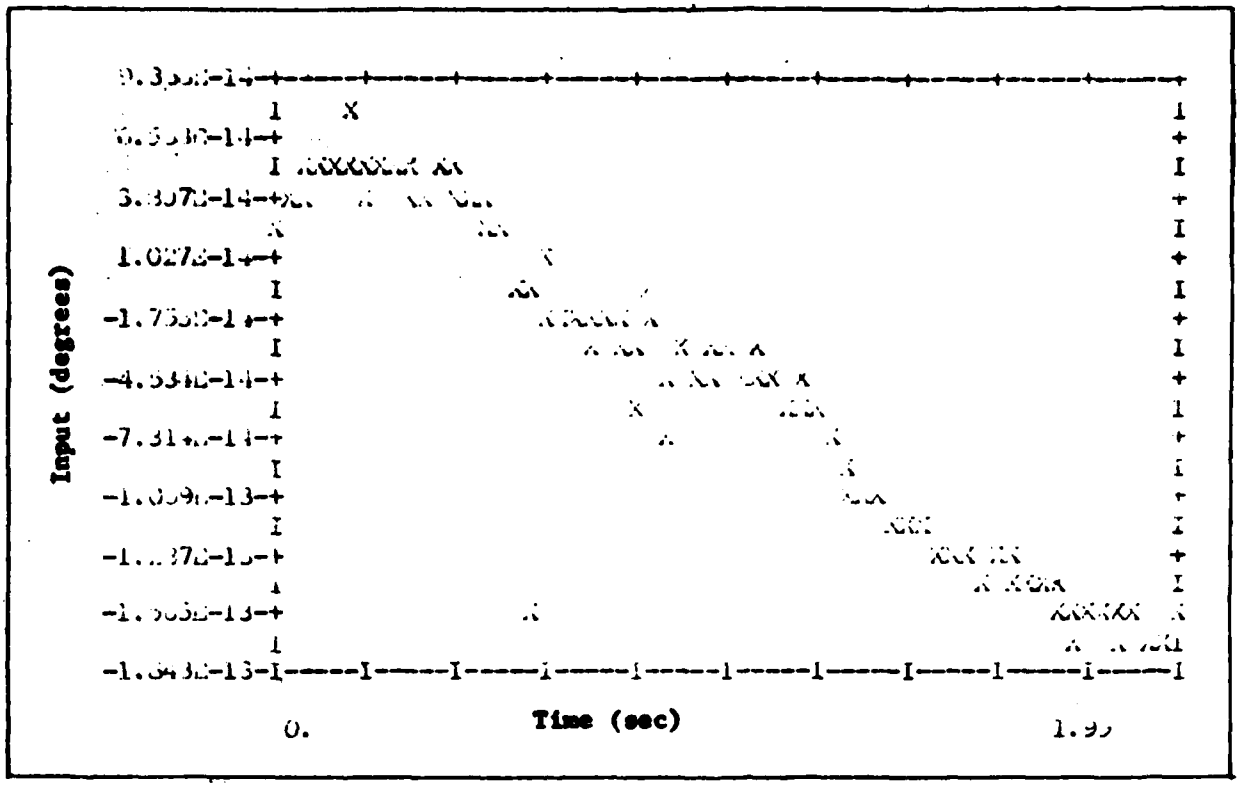

Figure B-53 δ_s **Input for r Tracking**

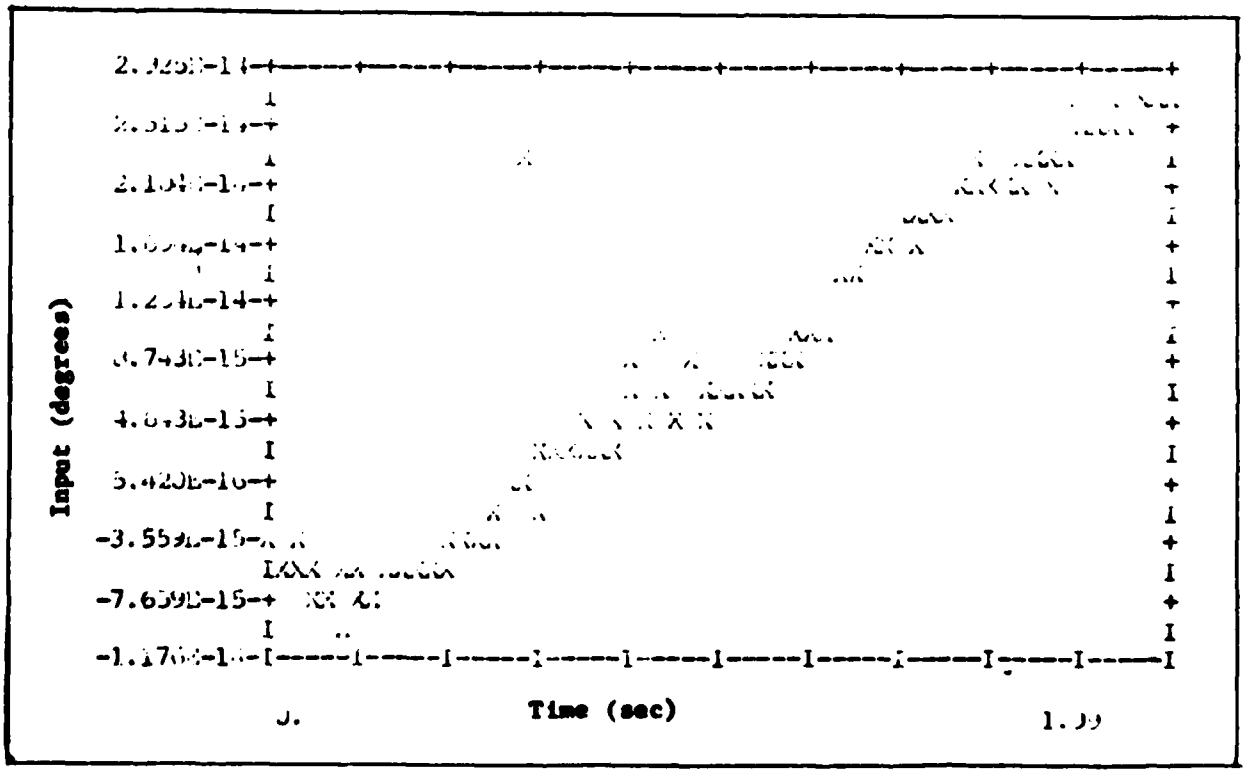

Figure B-54 δ_f **Input for r Tracking**

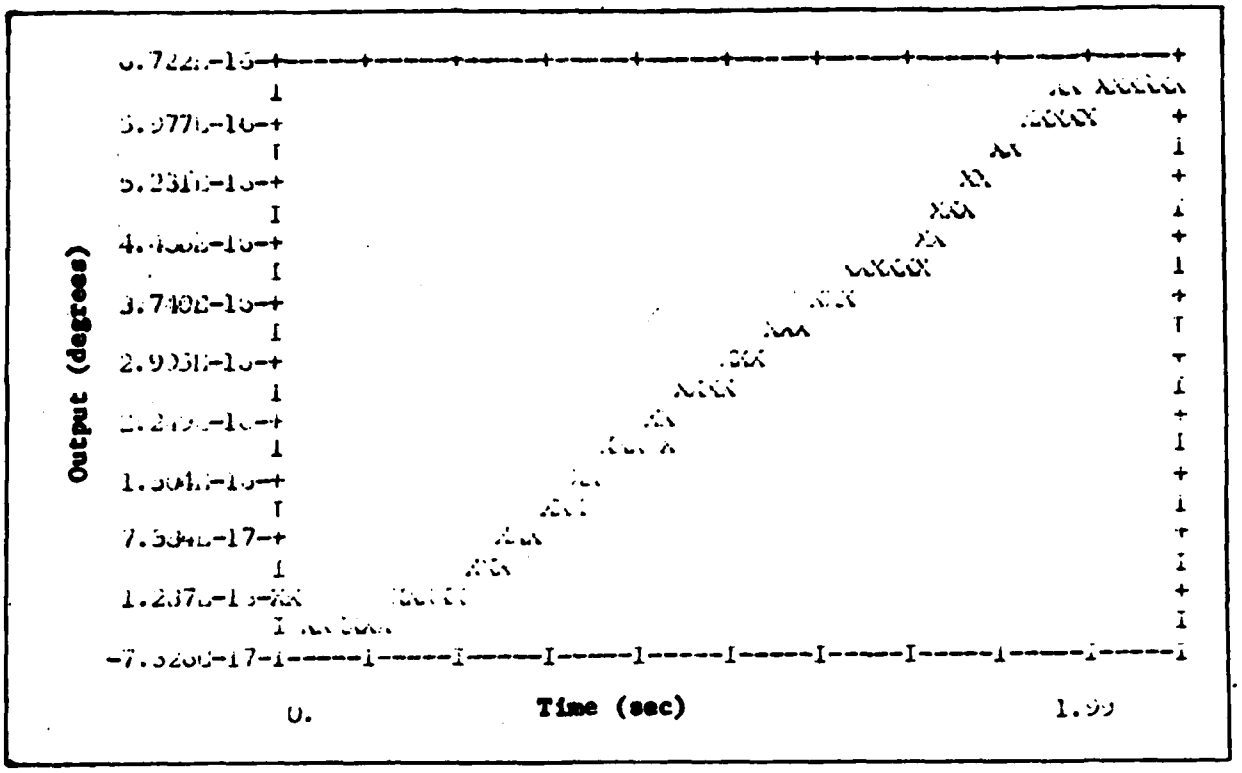

Figure B-55 γ Response for r Tracking

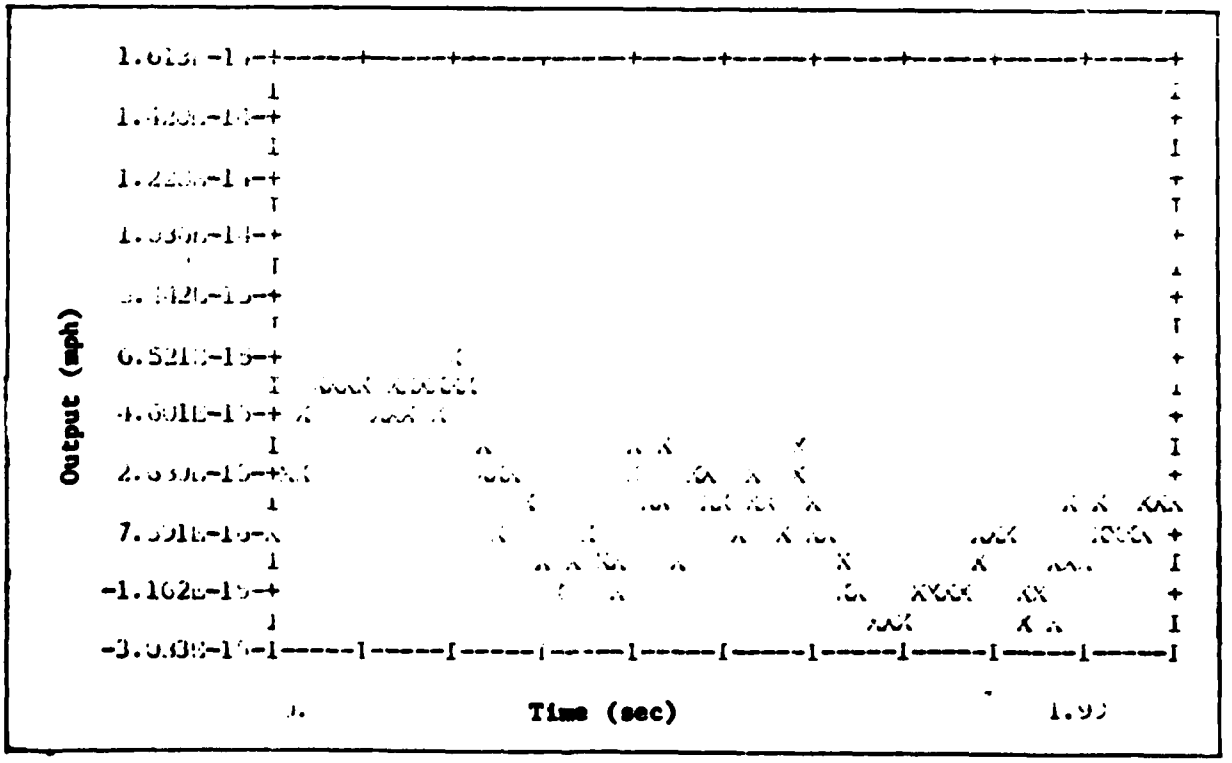

Figure B-56 u Response for r Tracking

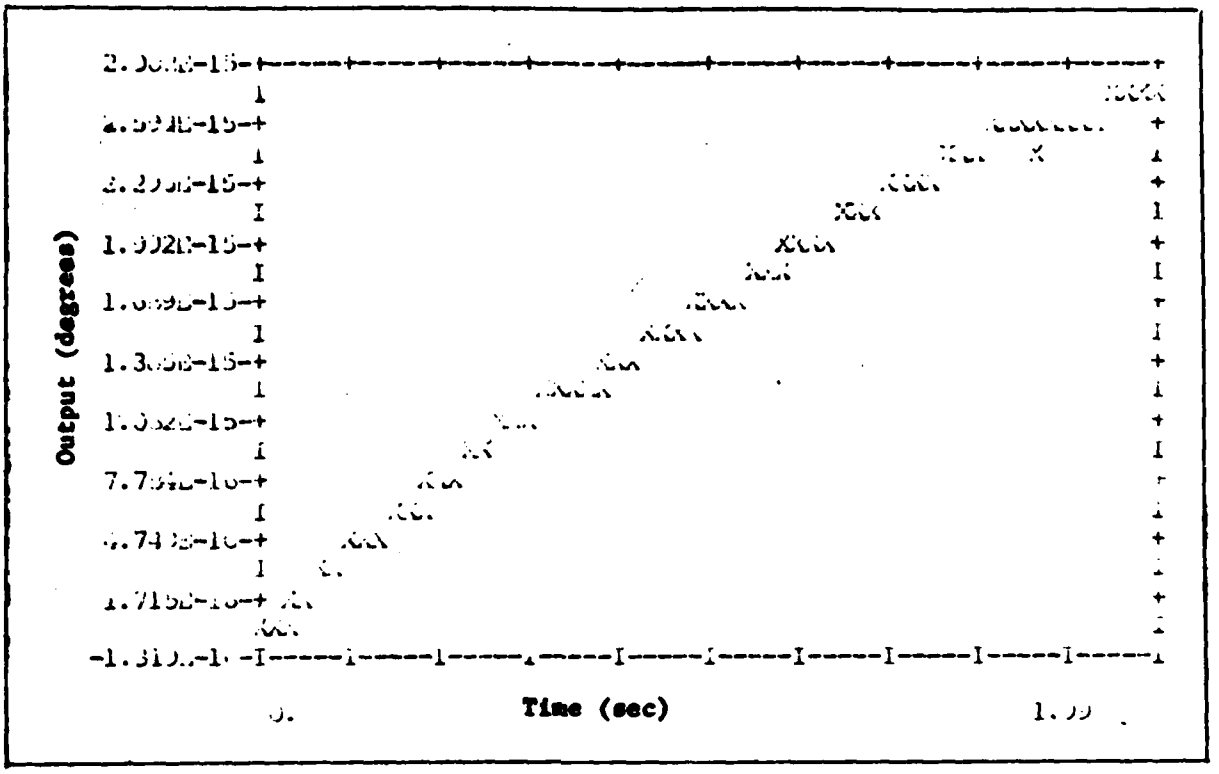

Figure B-57 θ Response for r Tracking

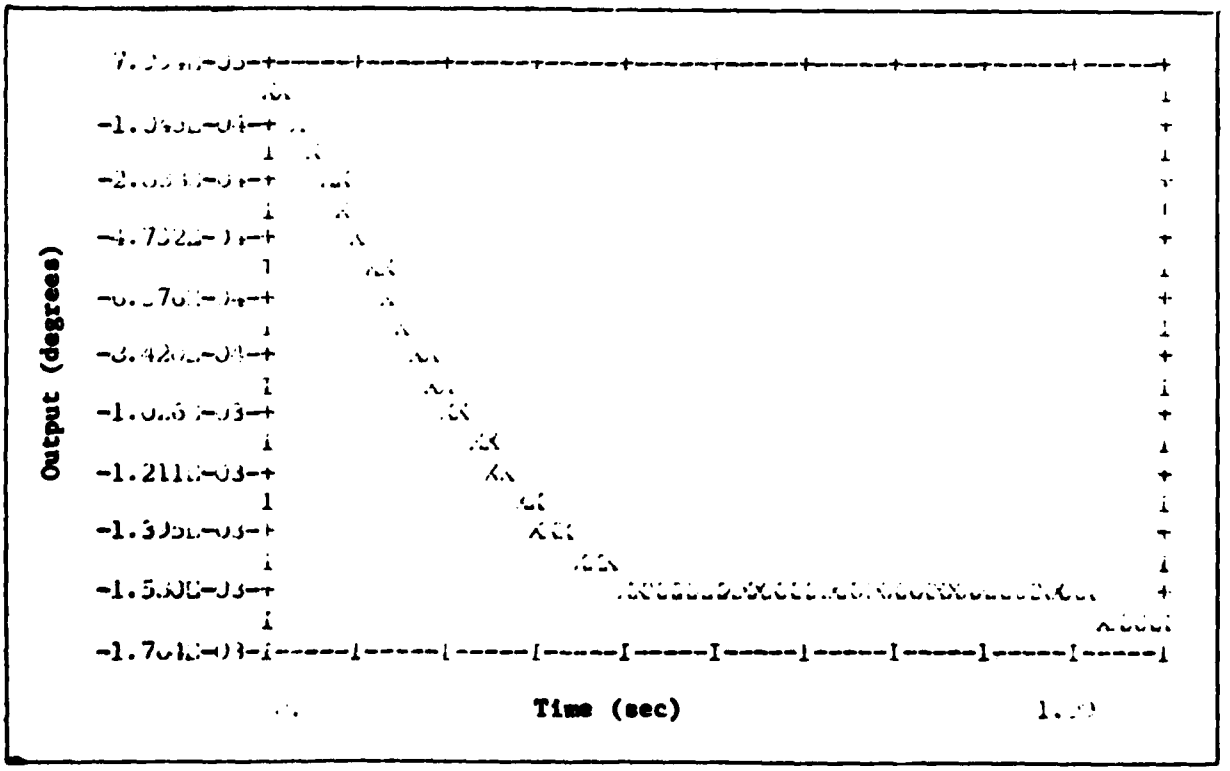

Figure B-58 β Response for r Tracking

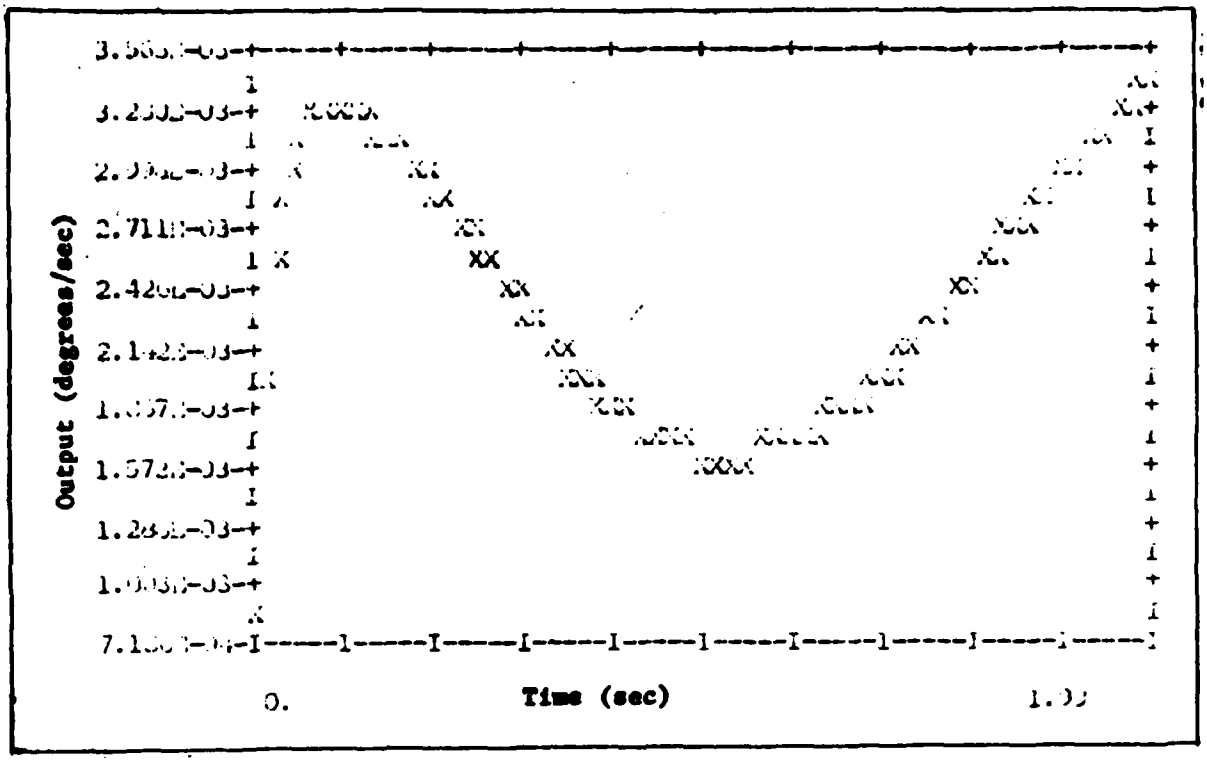

Figure B-59 r Tracking Response

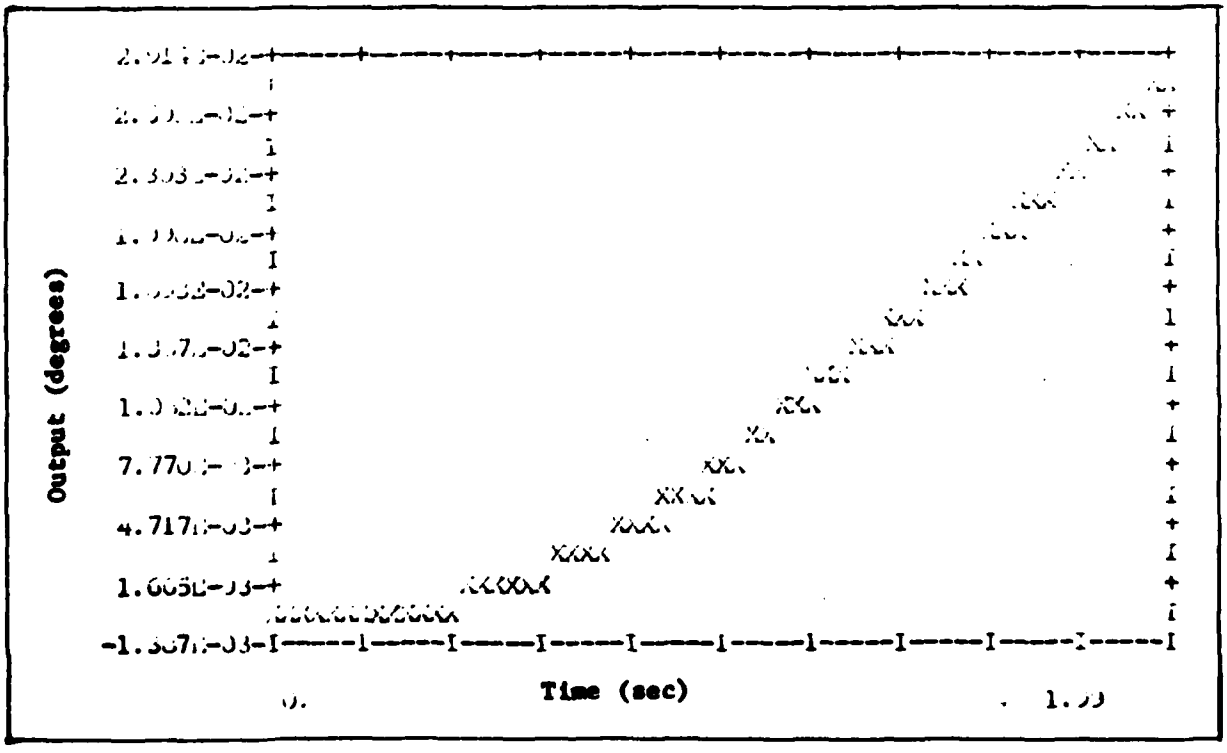

Figure B-60 ϕ Response for r Tracking

8 Tracking

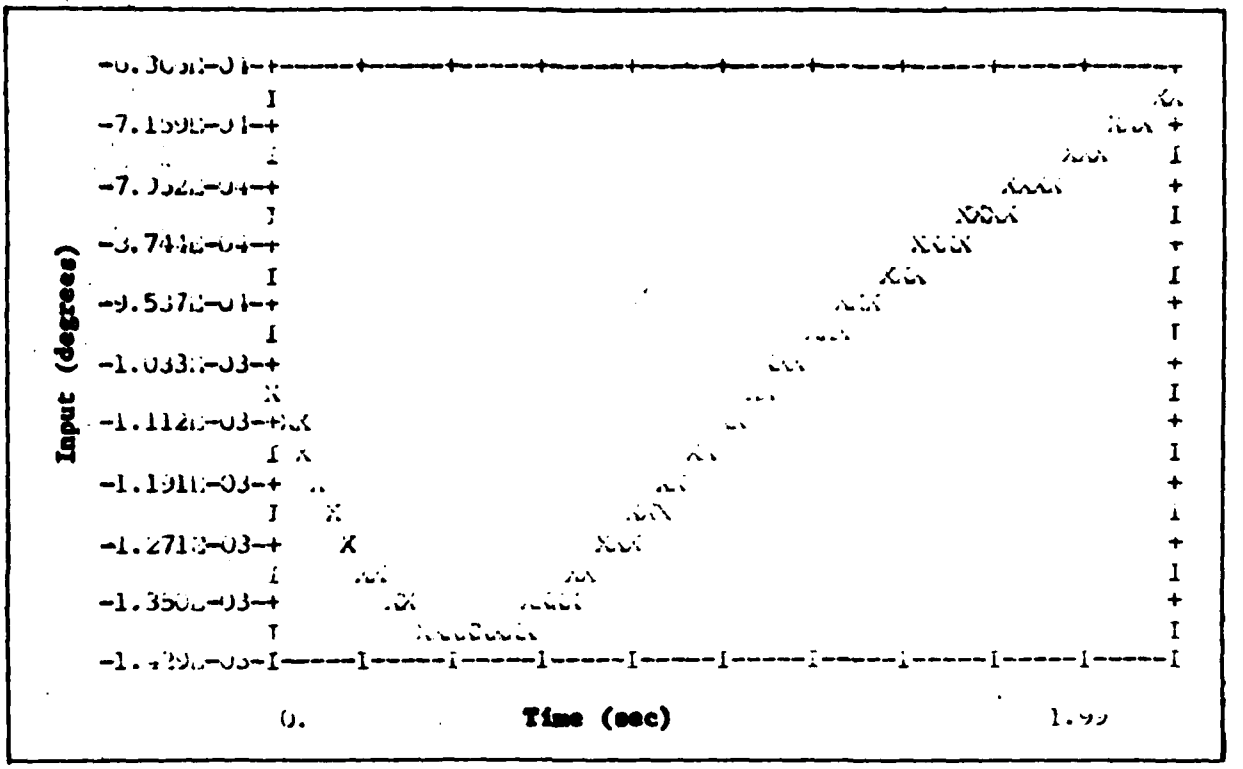

Figure B-61 δ_r **Input for** ϕ **Tracking**

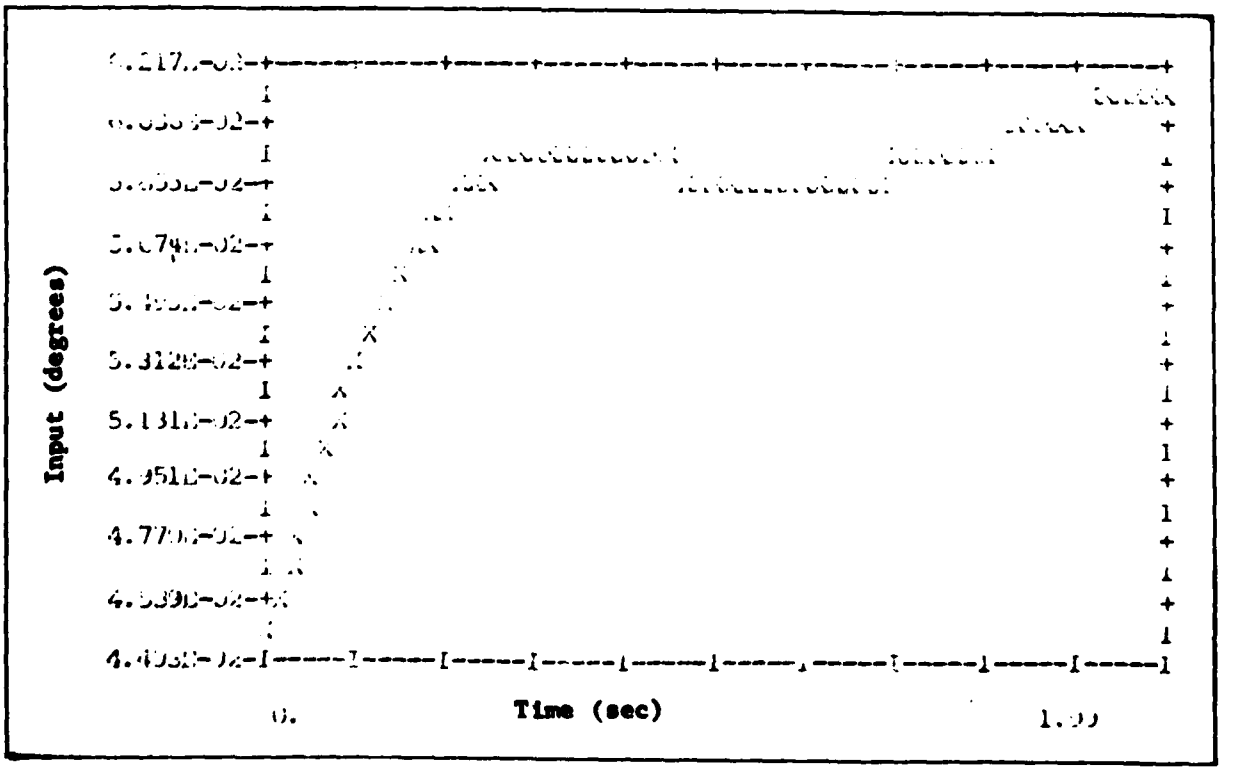

Figure B-62 δ_{H_r} **Input for** ϕ **Tracking**

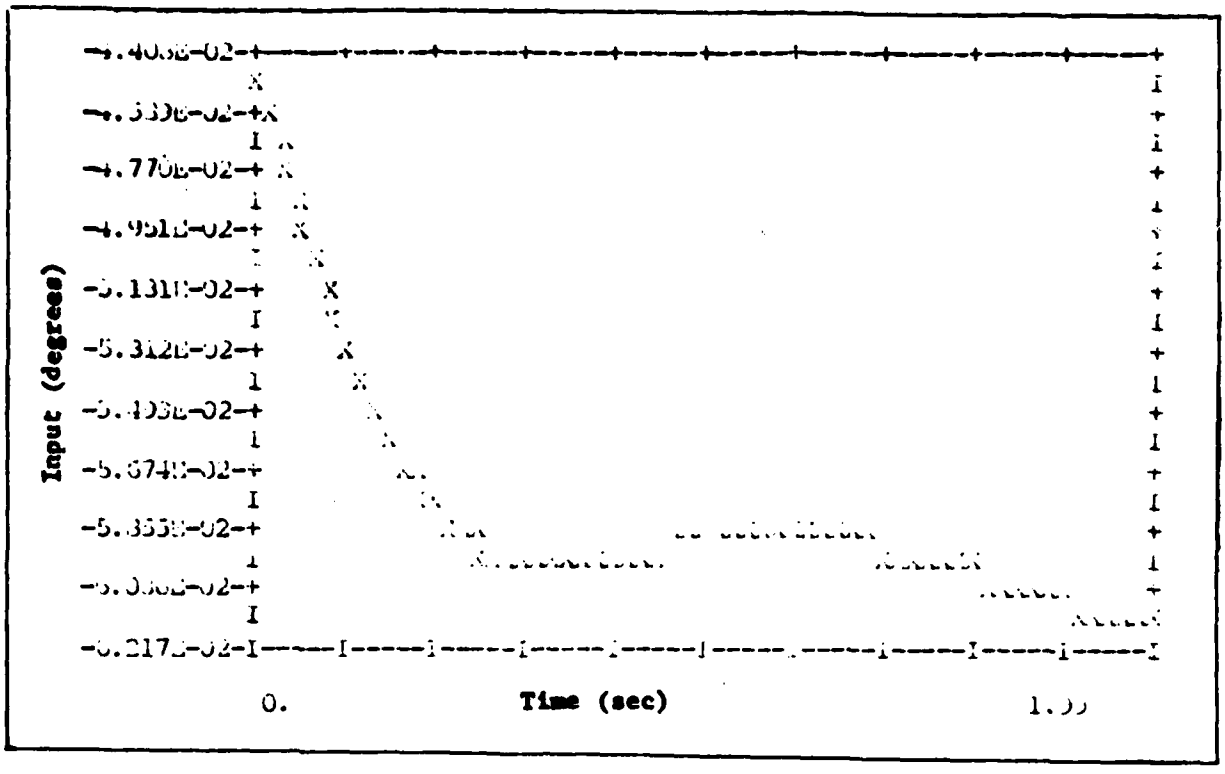

Figure B-63 δ_{H_L} Input for ϕ Tracking

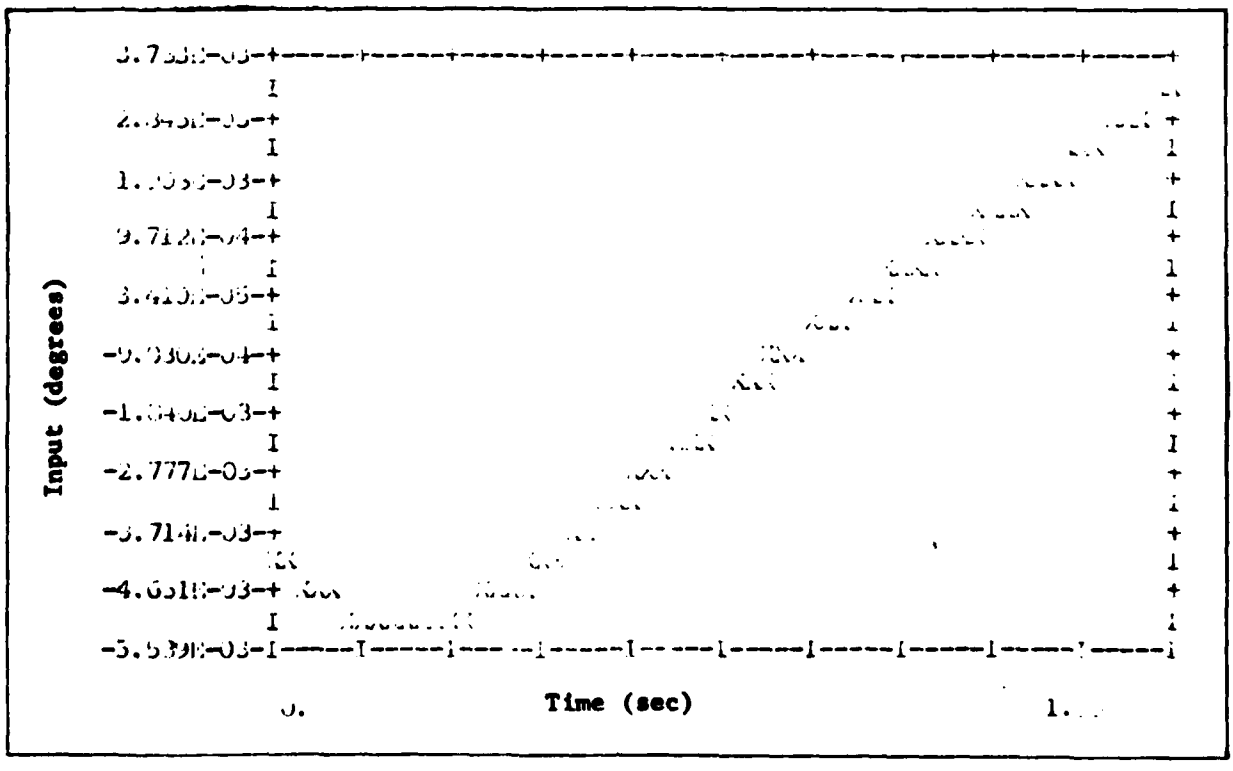

Figure B-64 δ_a Input for ϕ Tracking

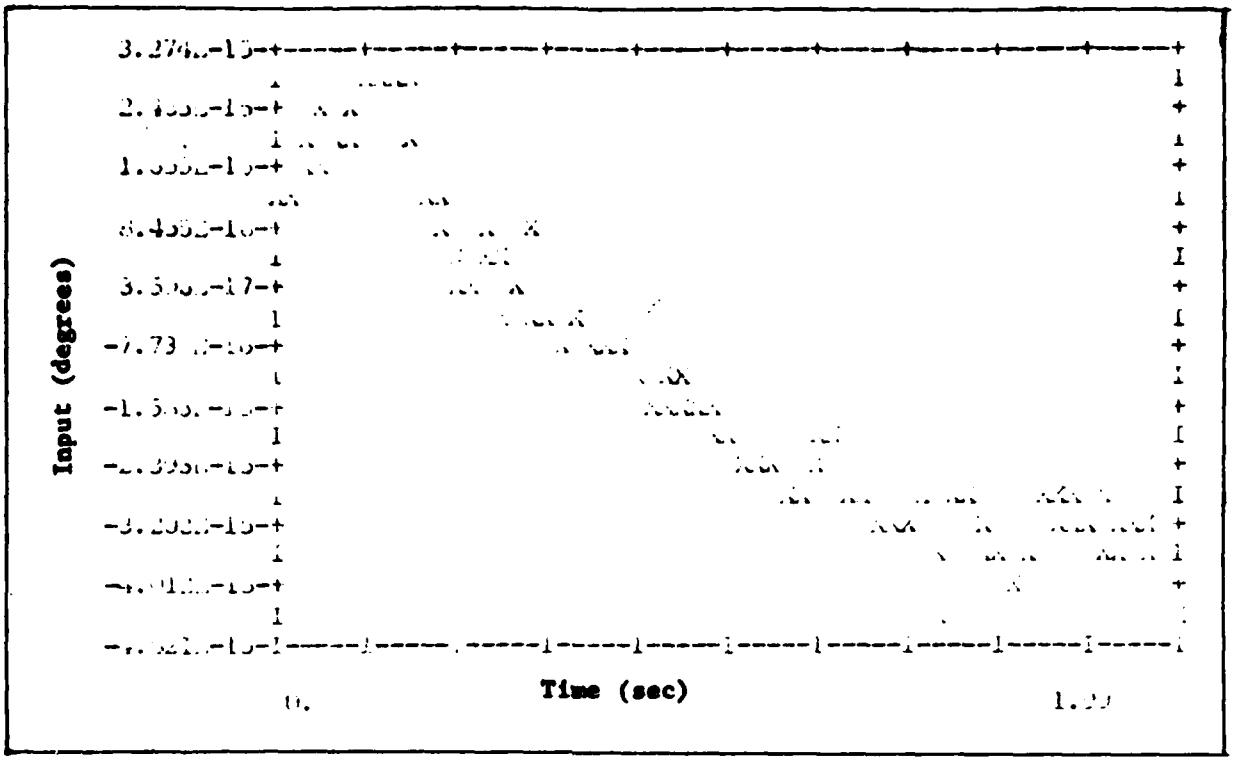

Figure B-65 δ_s Input for ϕ Tracking

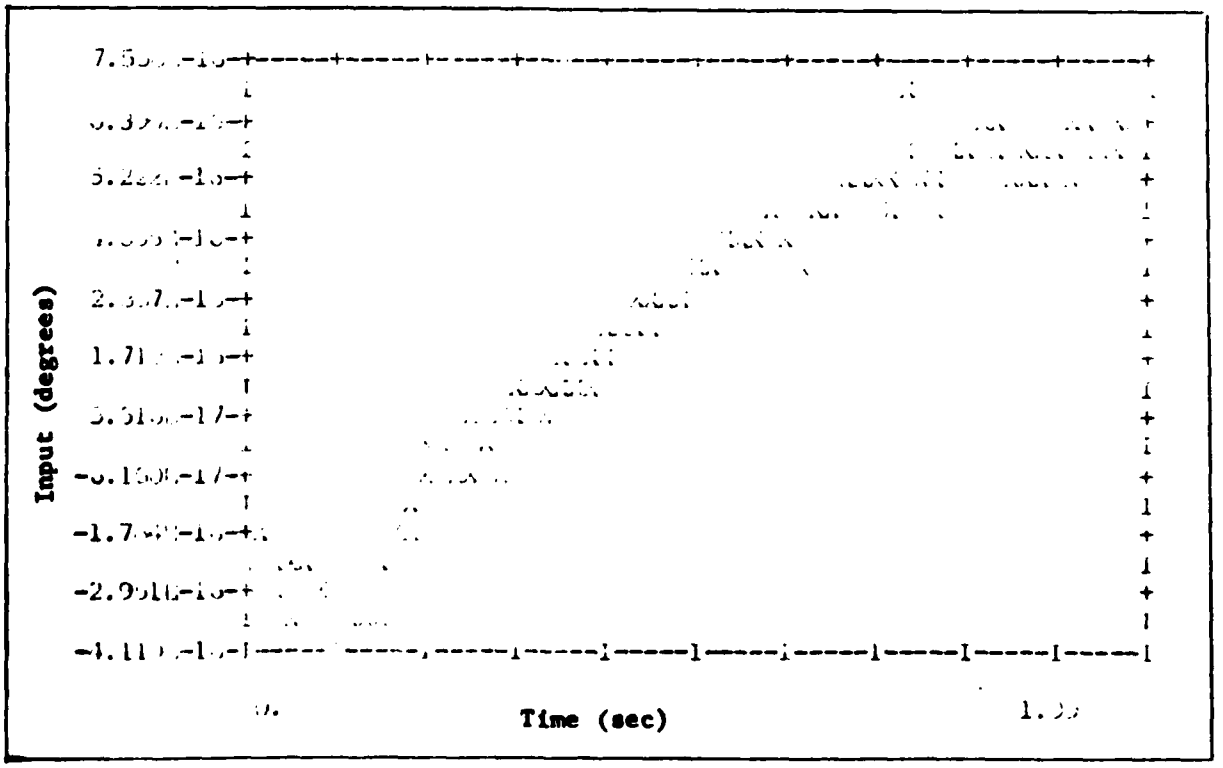

Figure B-66 δ_f Input for ϕ Tracking

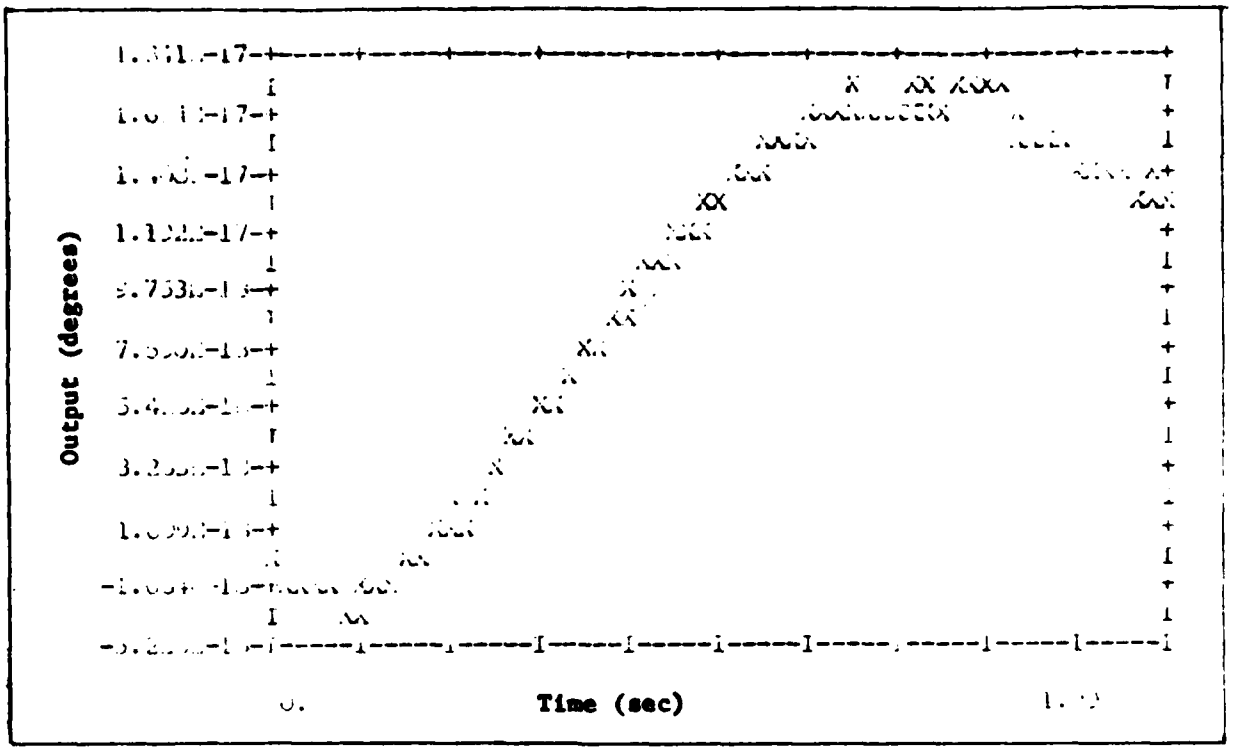

Figure B-67 γ **Response for** ϕ **Tracking**

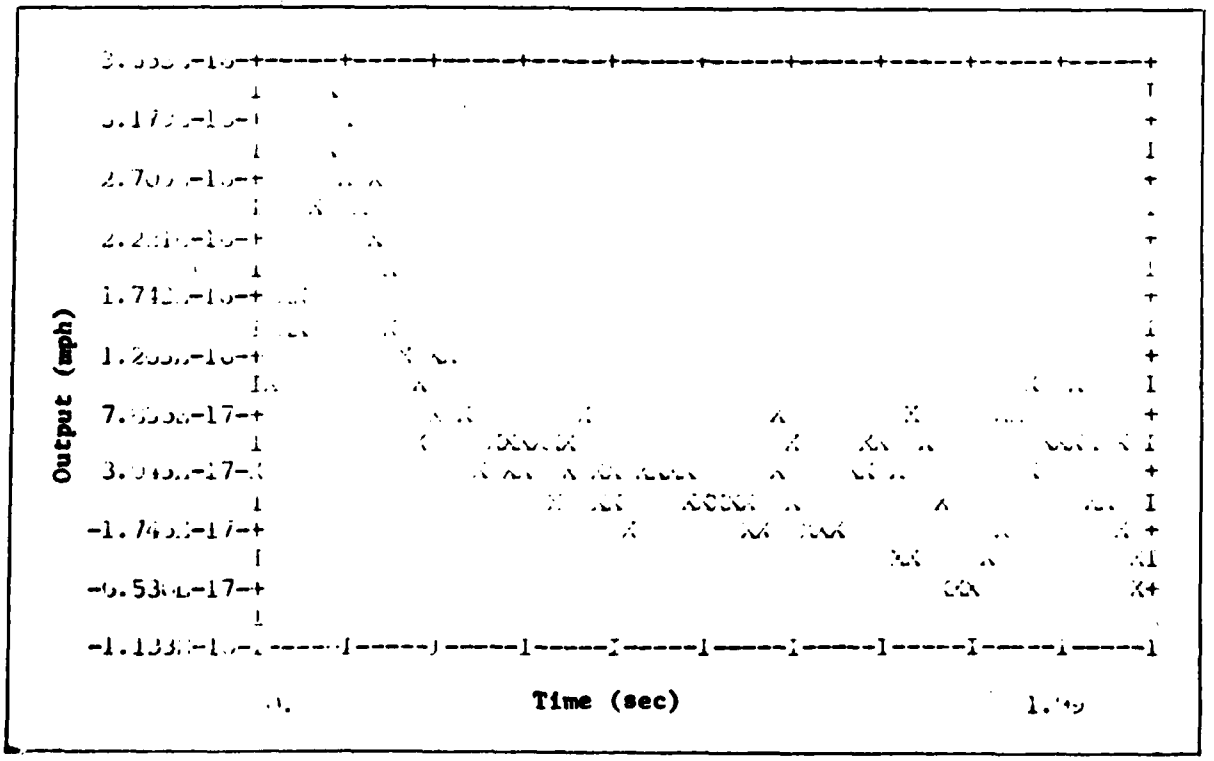

Figure B-68 u **Response for** ϕ **Tracking**

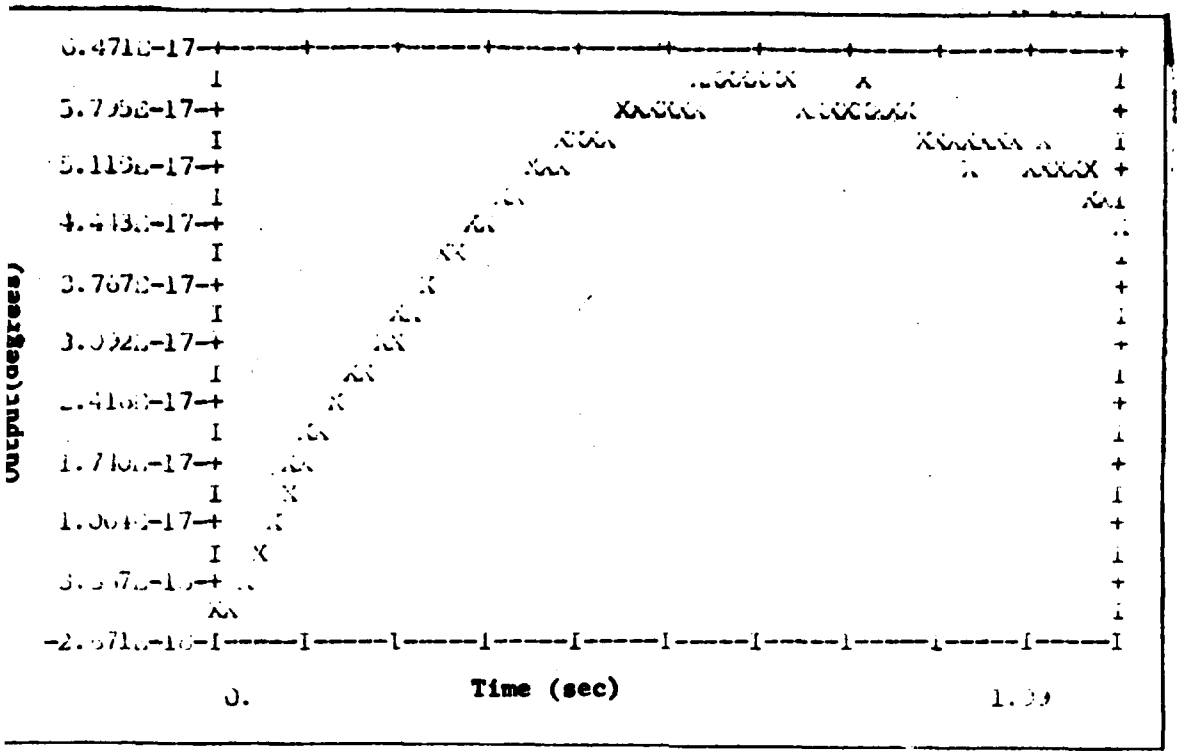

Figure B-69 θ Response for ϕ Tracking

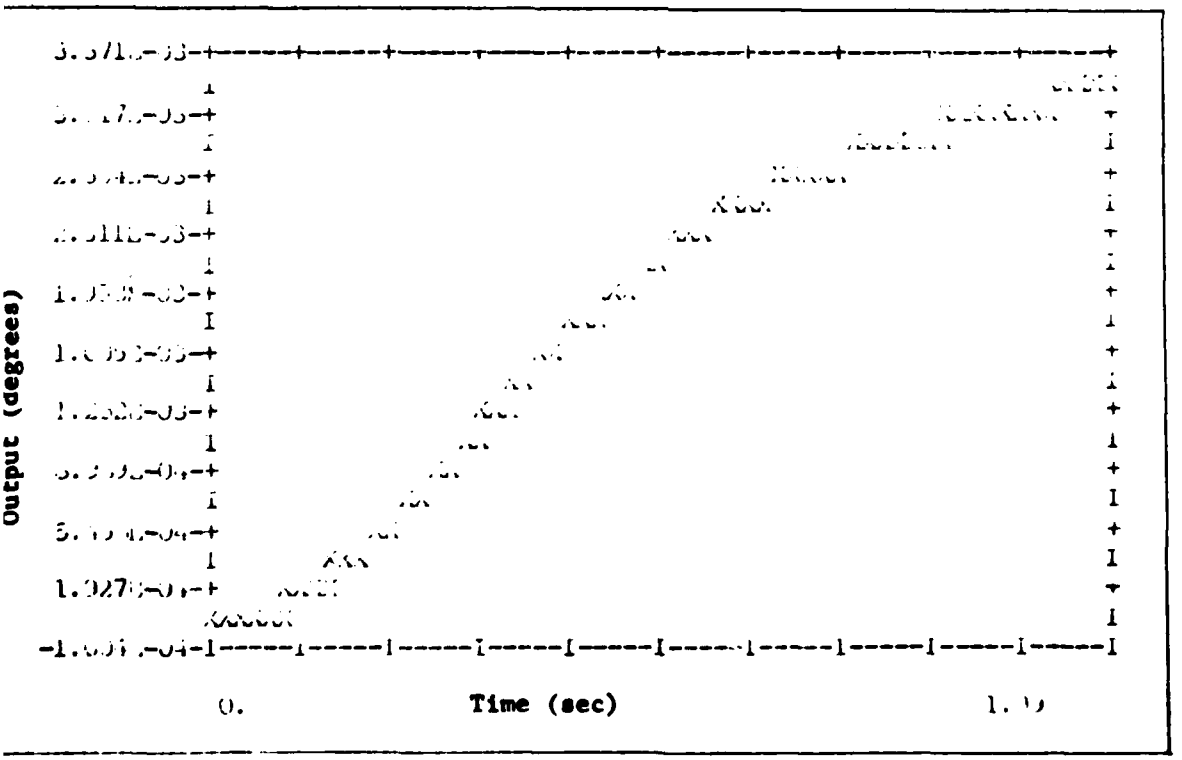

Figure B-70 β Response for ϕ Tracking

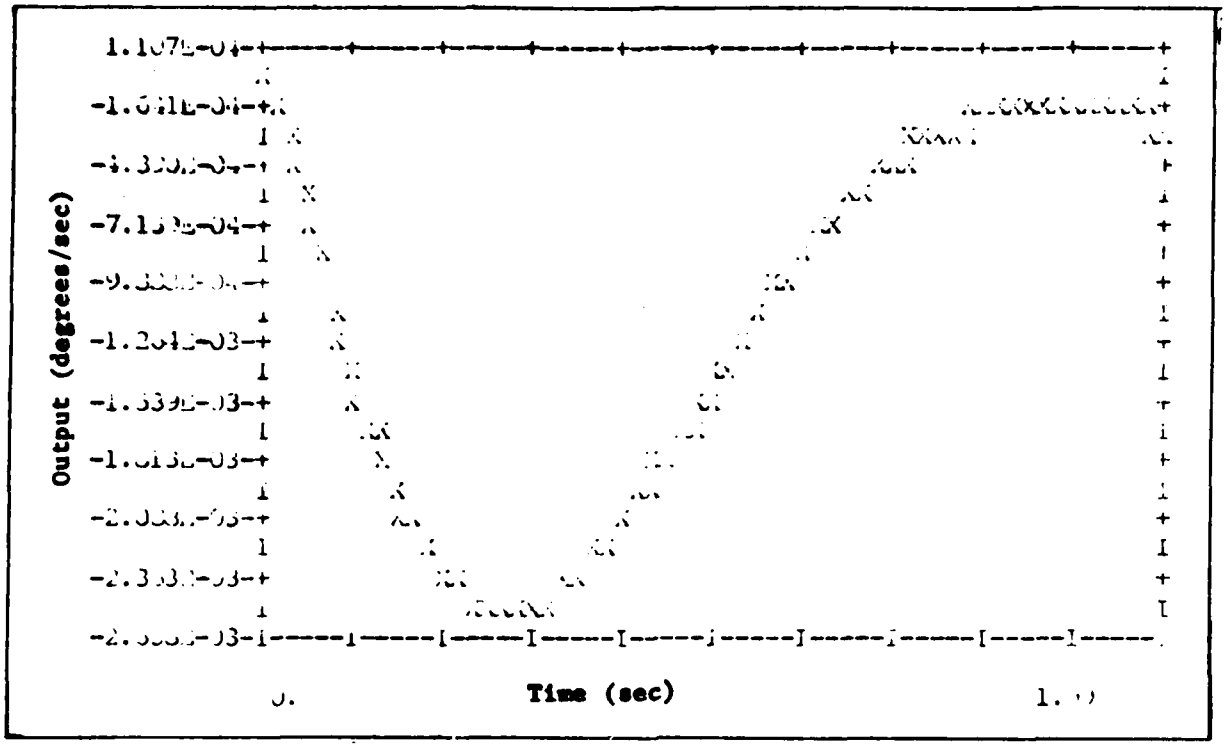

Figure B-71 r Response for ∅ Tracking

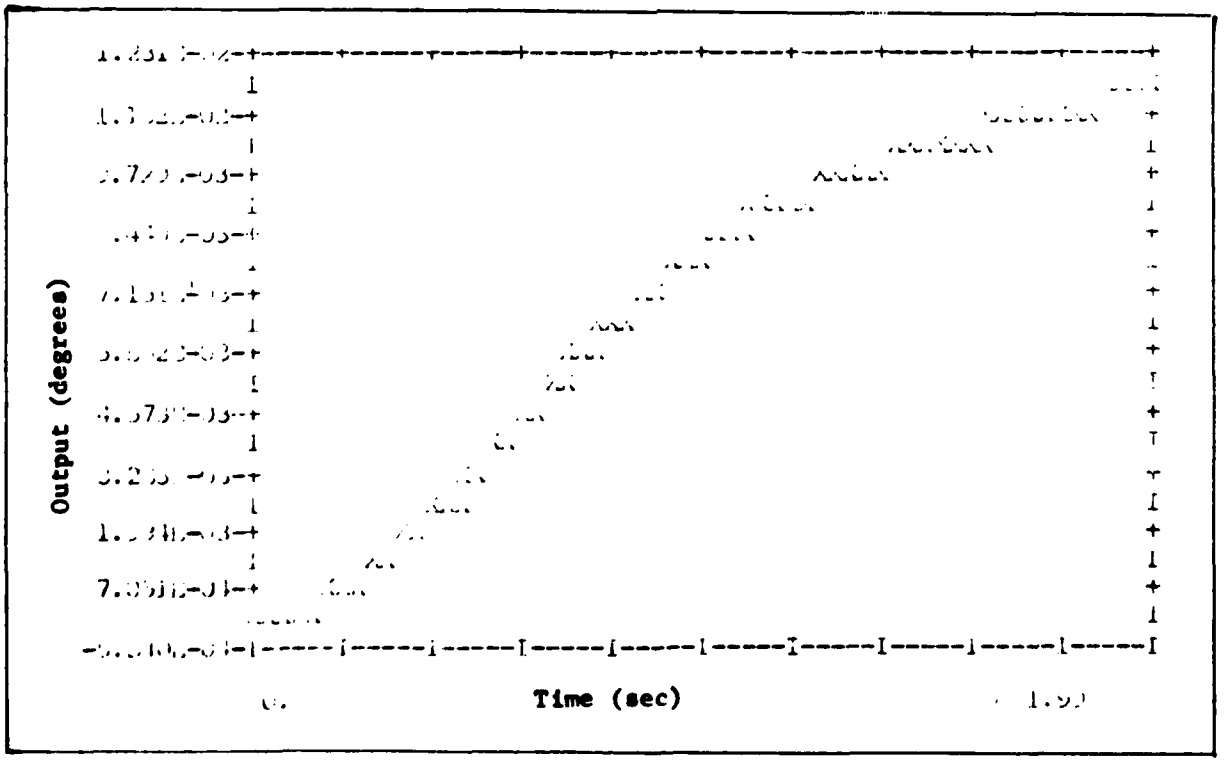

Figure B-72 ∅ Tracking Response

No Rudder Responses

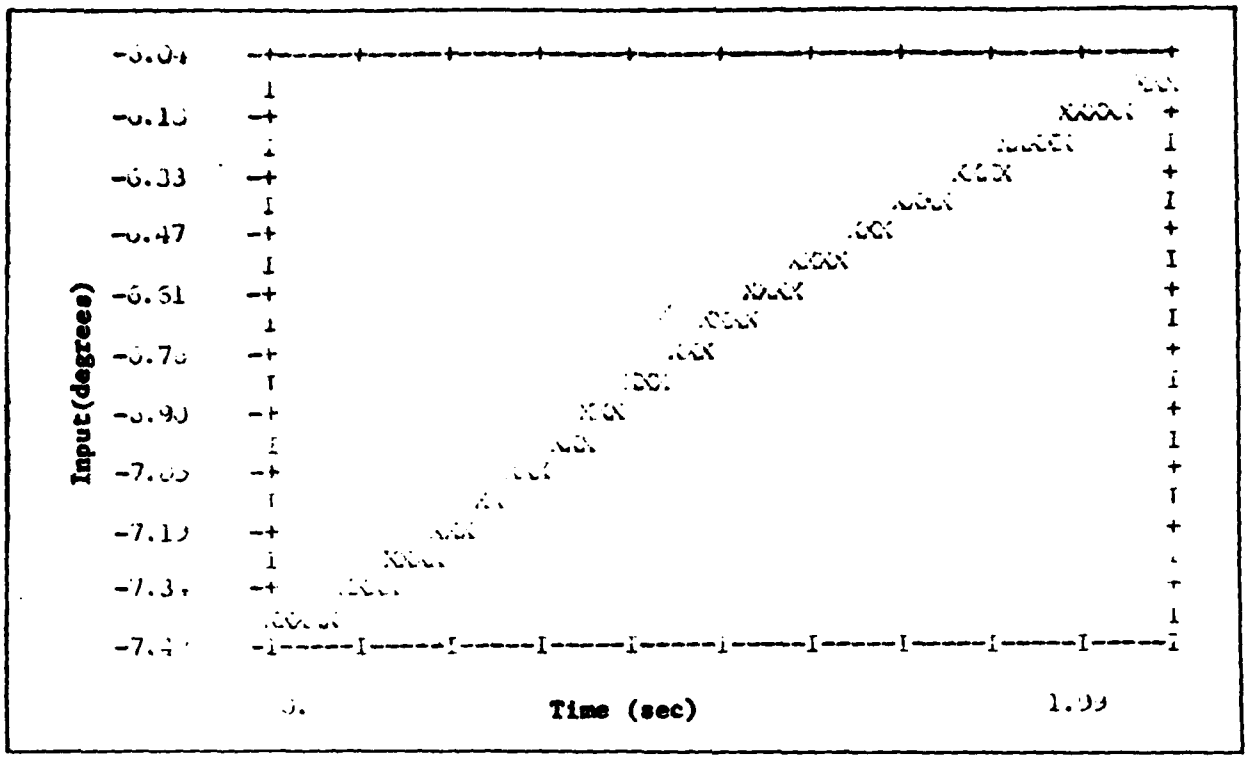

Figure B-73 δ_{H_L} Input for γ Tracking without a Rudder

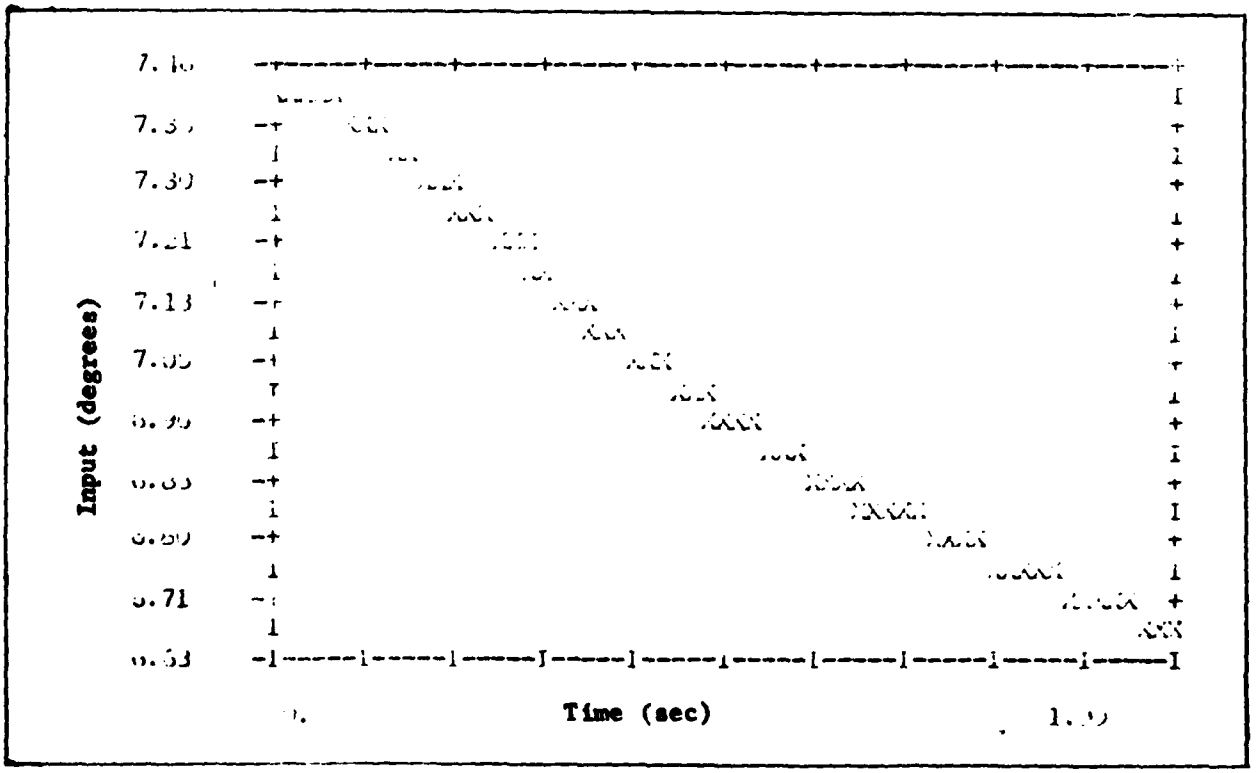

Figure B-74 δ_{H_r} Input for γ Tracking without a Rudder

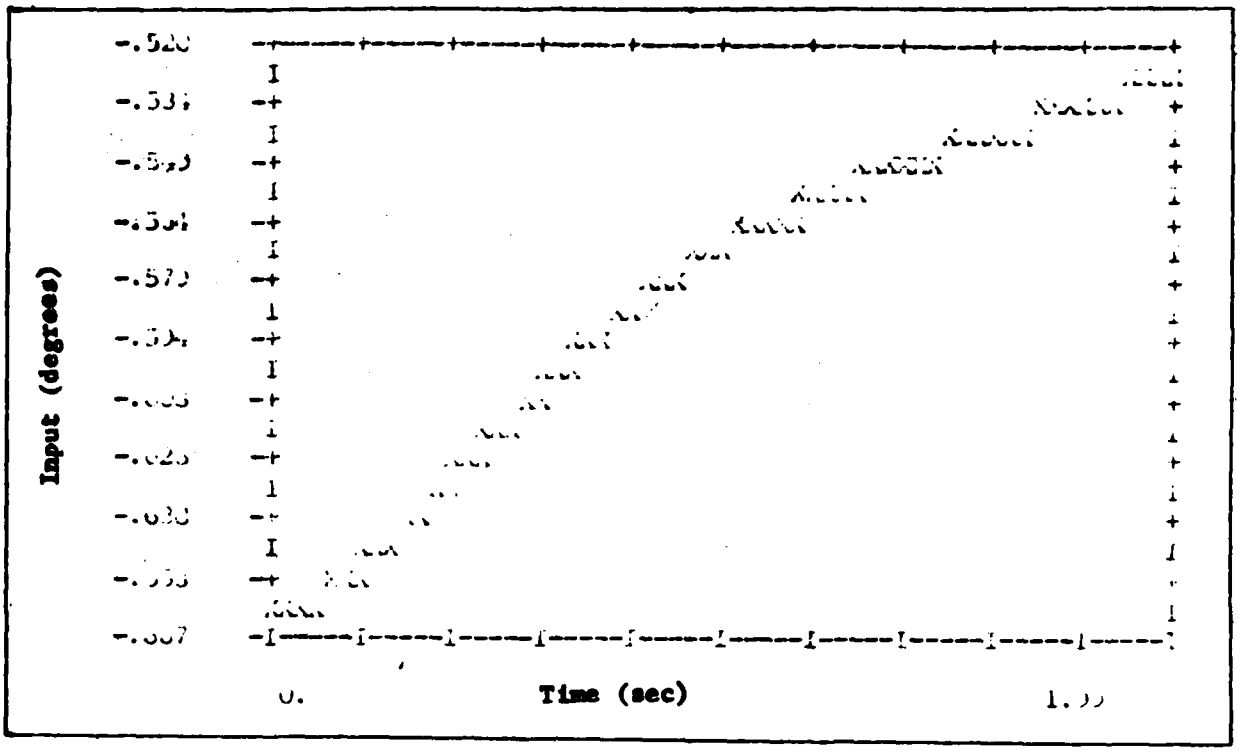

Figure B-75 δ_a Input for γ Tracking without a Rudder

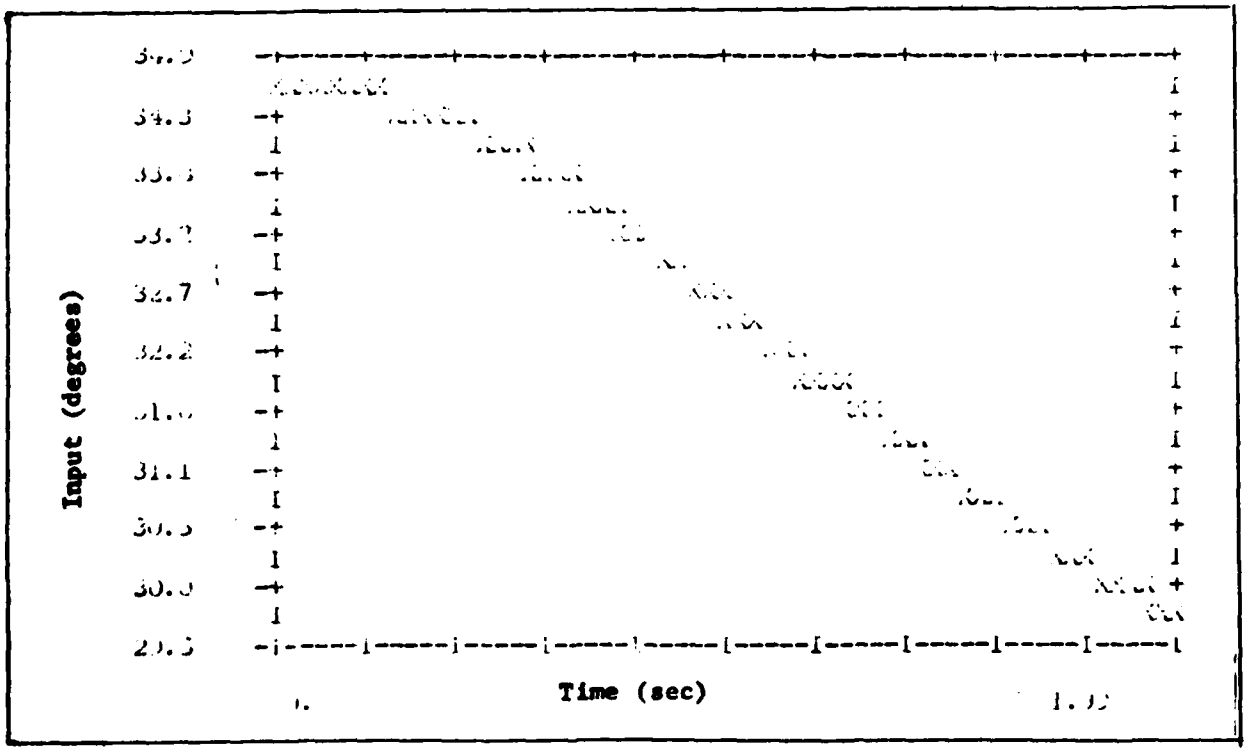

Figure B-76 δ_a Input for γ Tracking without a Rudder

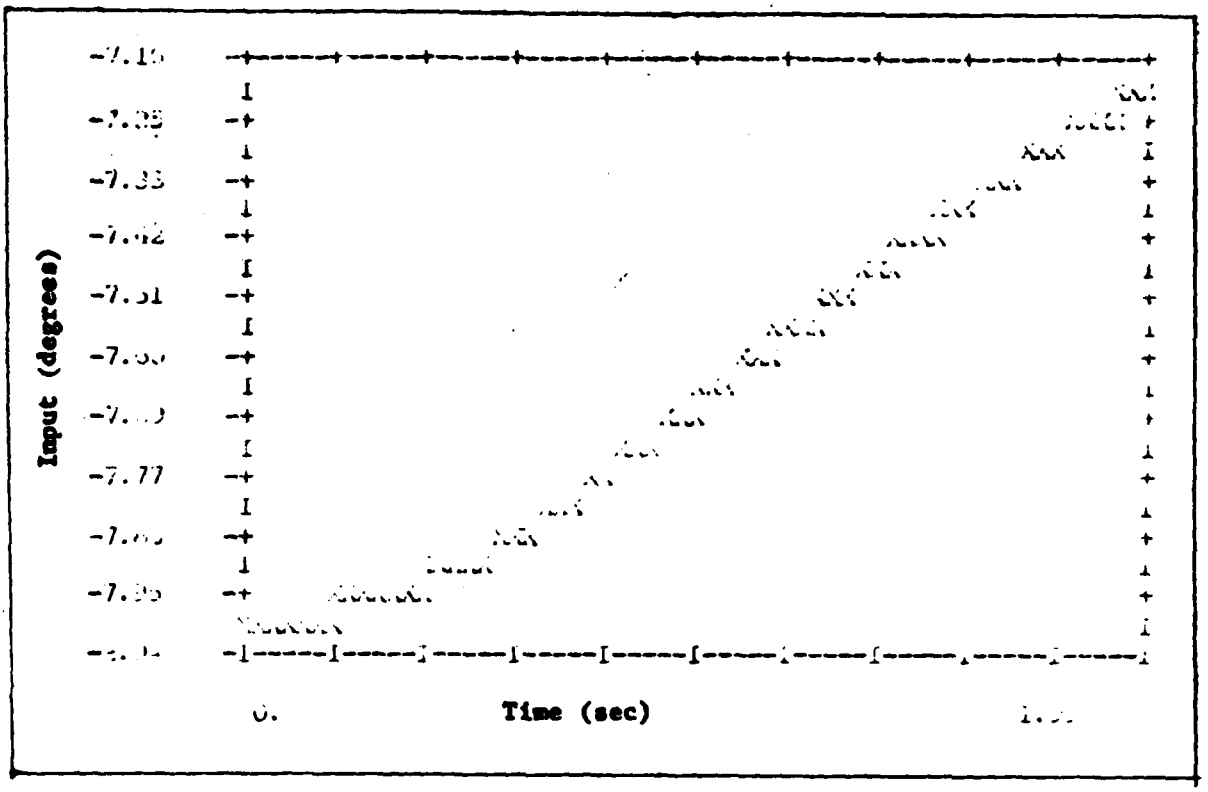

Figure B-77 δ_f Input for γ Tracking without a Rudder

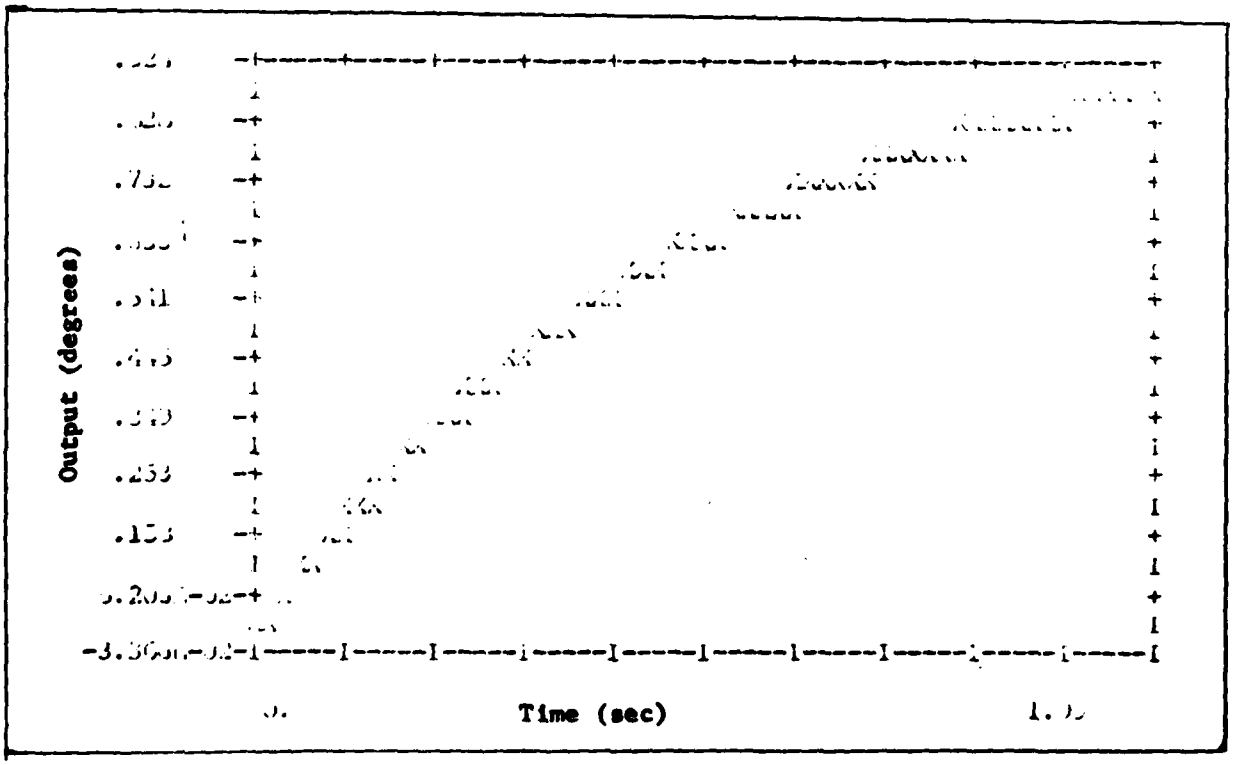

Figure B-78 γ Tracking without a Rudder

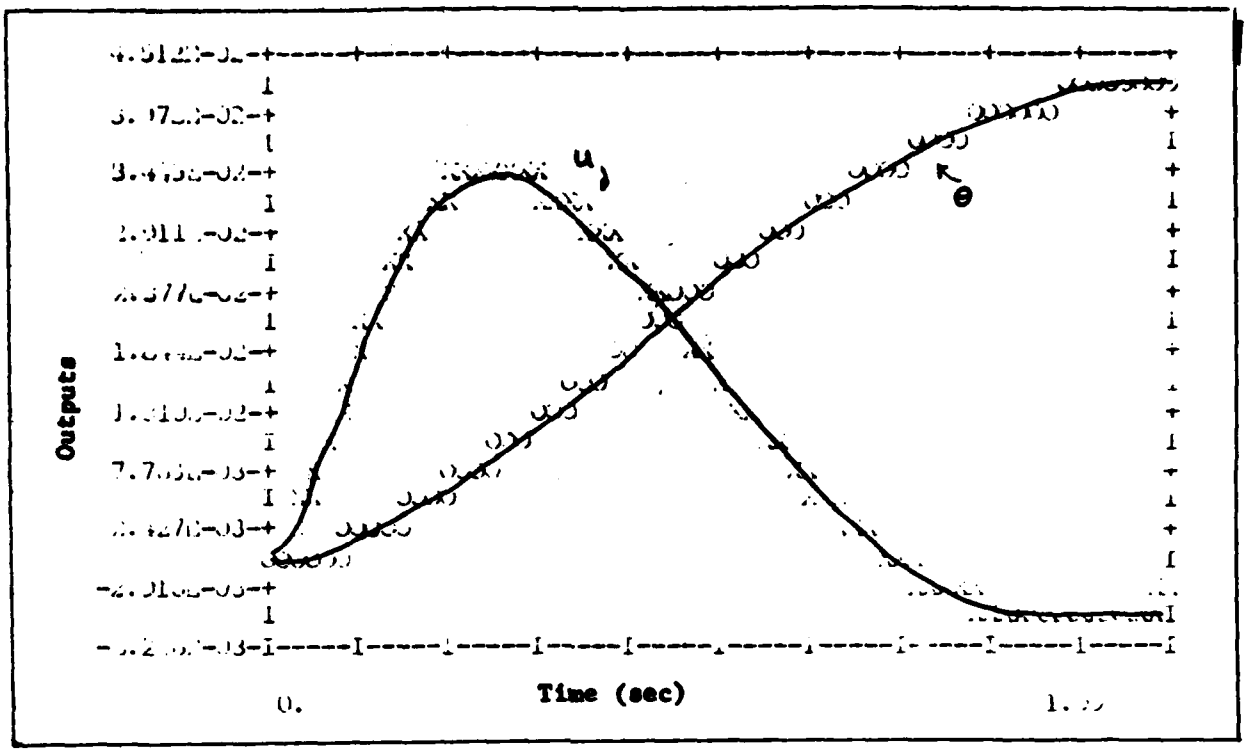

Figure B-79 u and θ Responses for γ Tracking without a Rudder

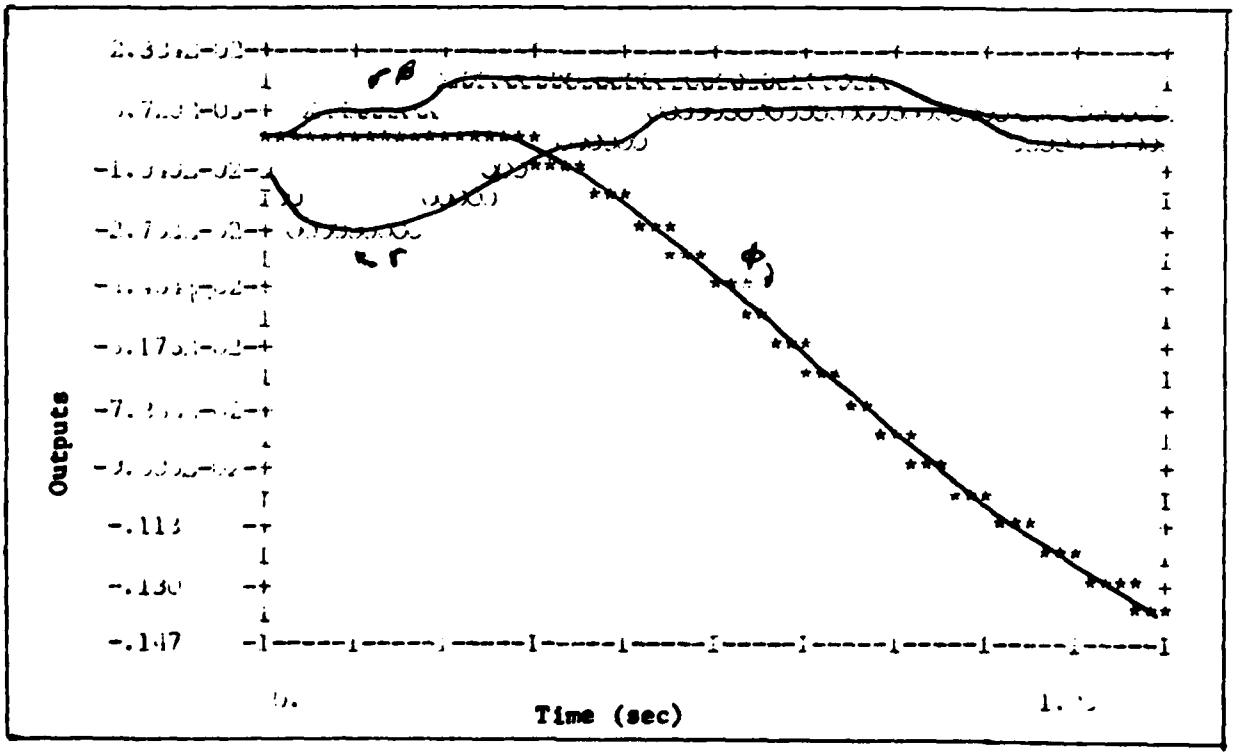

Figure B-80 Lateral Mode Responses for γ Tracking without a Rudder

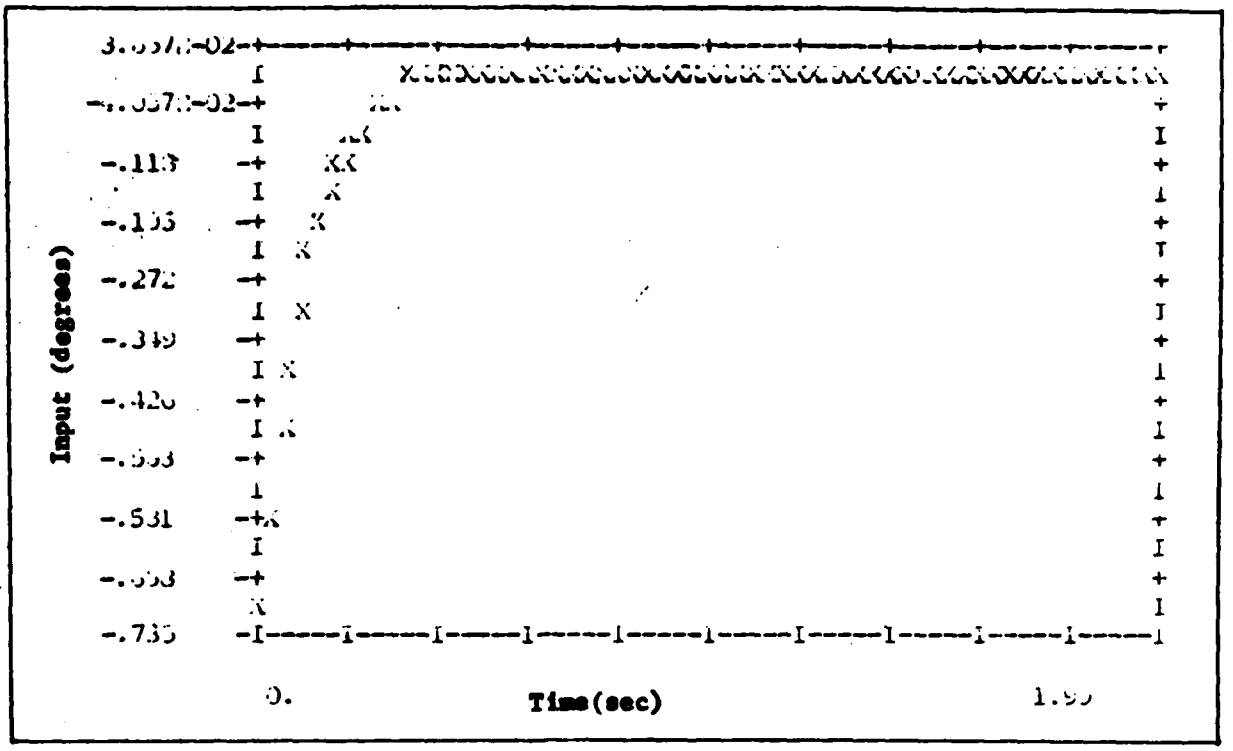

Figure B-81 δ_{H_r} Input for u Tracking without a Rudder

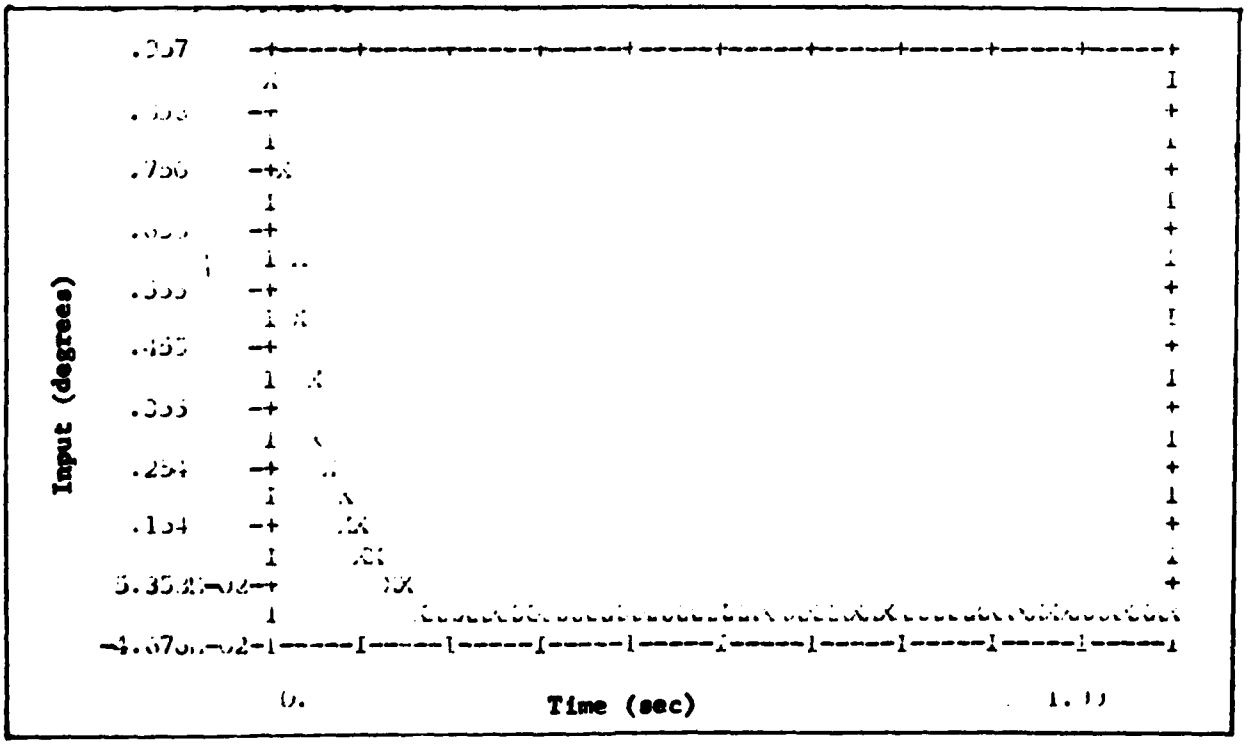

Figure B-82 δ_{H_L} Input for u Tracking without a Rudder

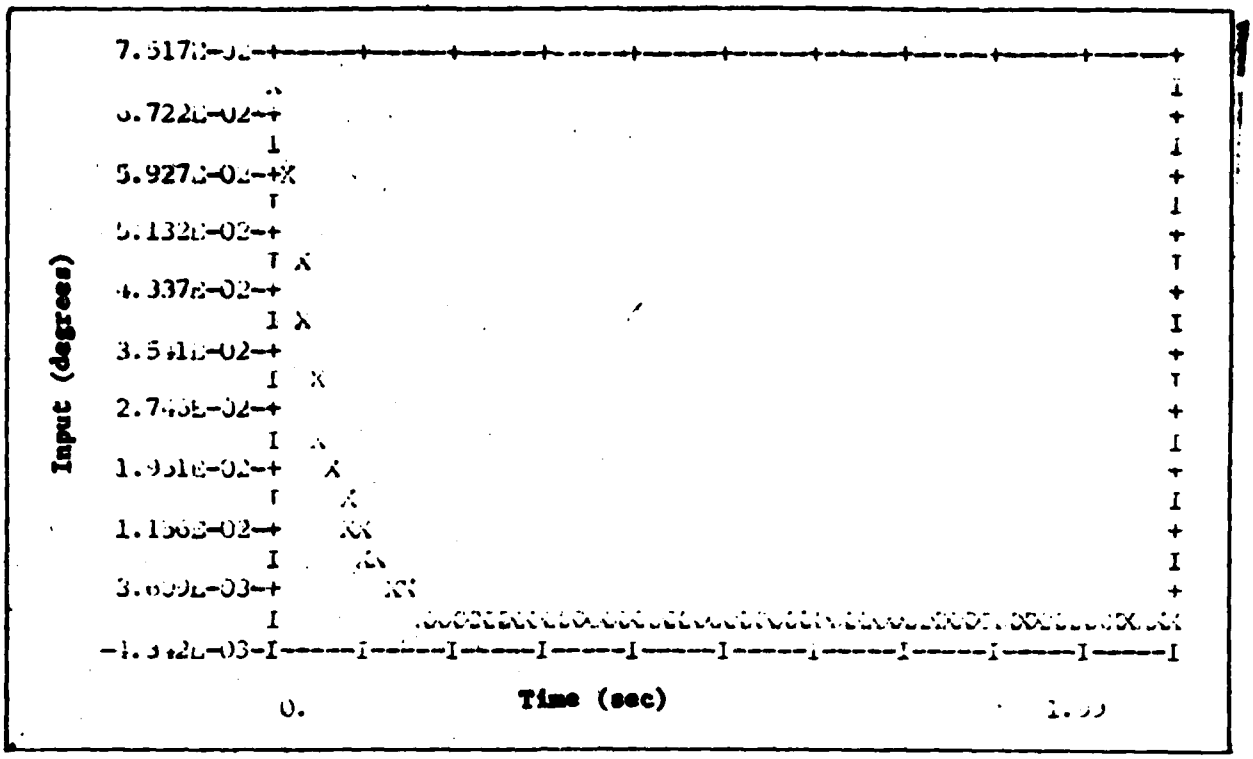

Figure B-83 δ_a Input for u Tracking without a Rudder

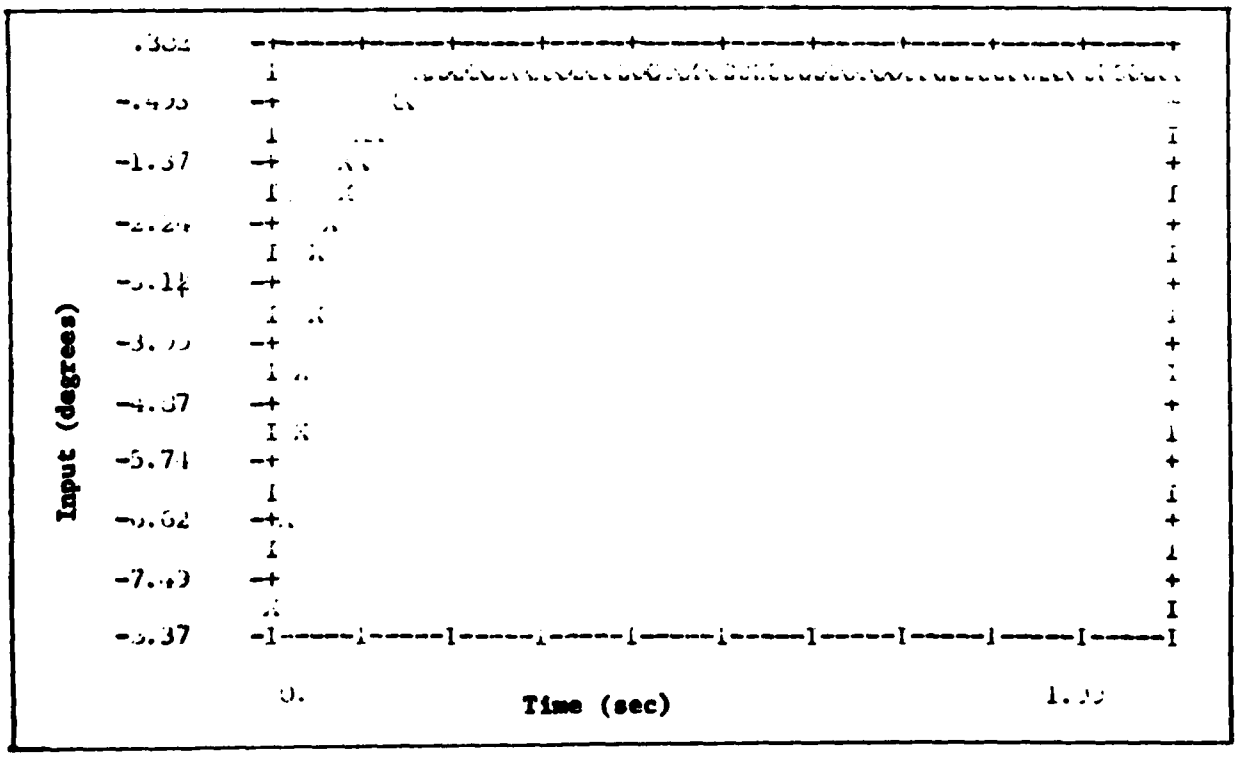

Figure B-84 δ_a Input for u Tracking without a Rudder

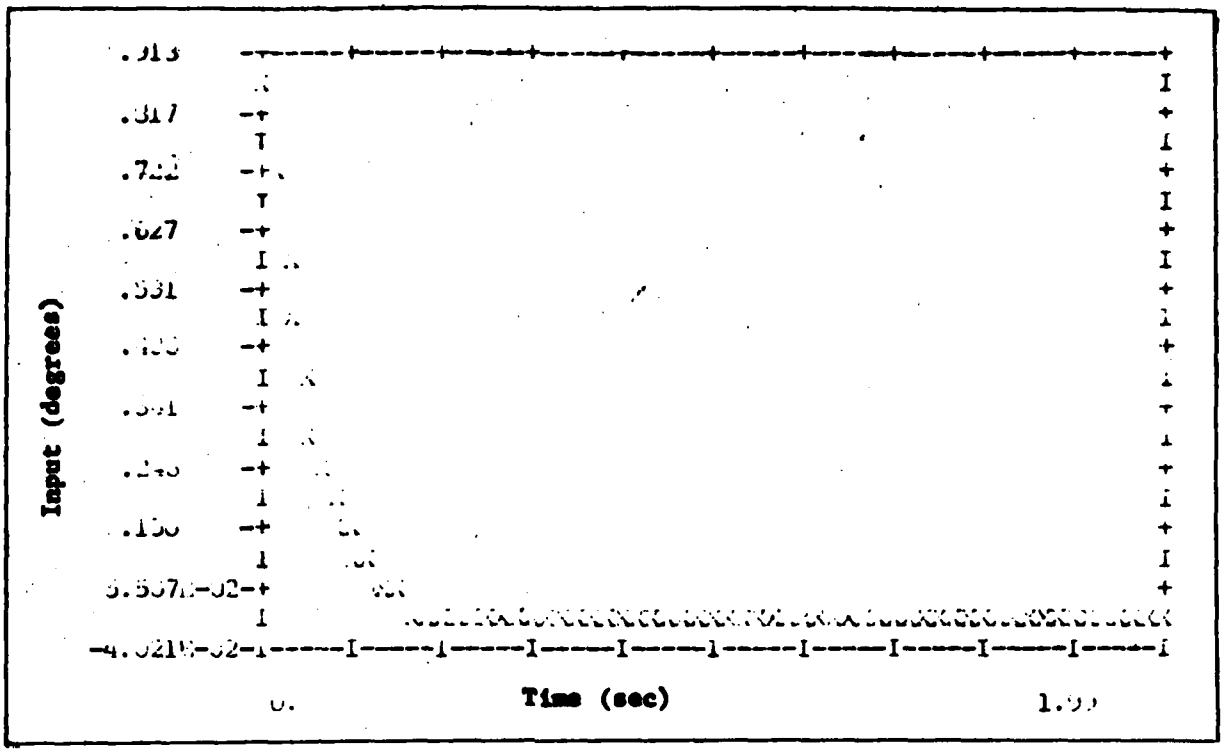

Figure B-85 δ_f Input for u Tracking without a Rudder

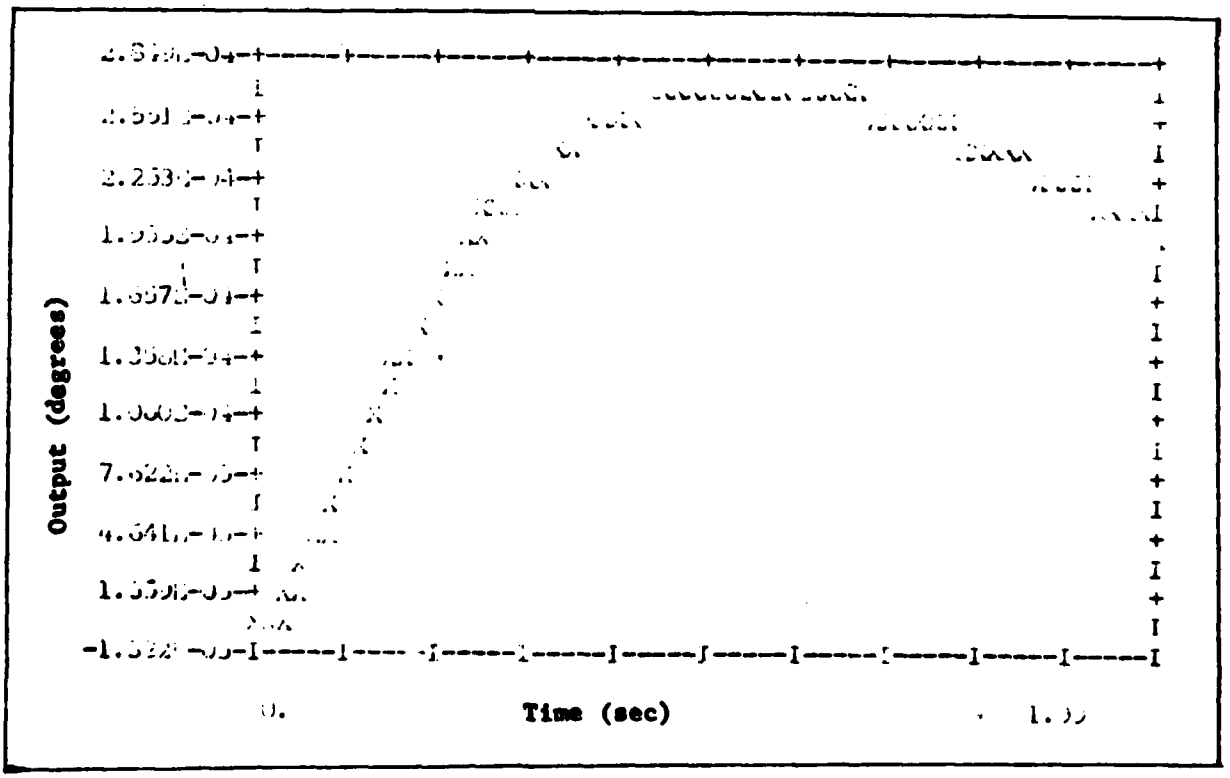

Figure B-86 γ Response for u Tracking without a Rudder

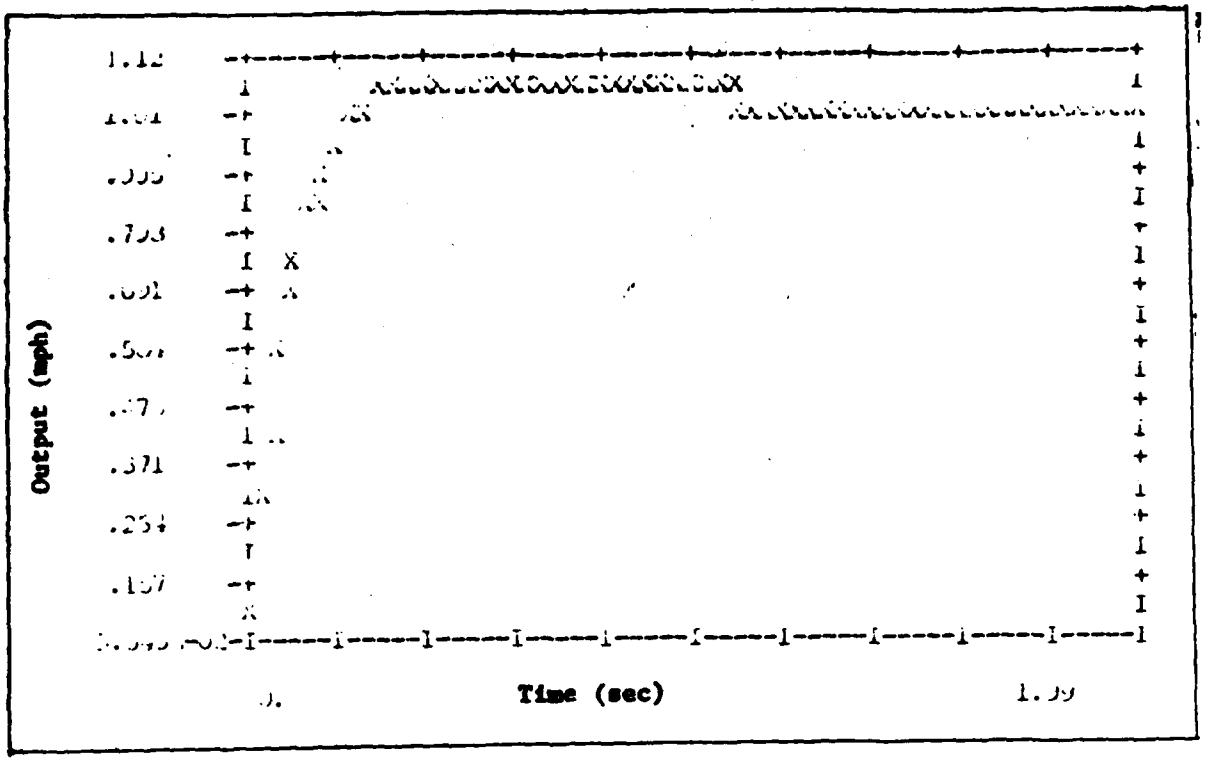

Figure B-87 u Tracking Response without a Rudder

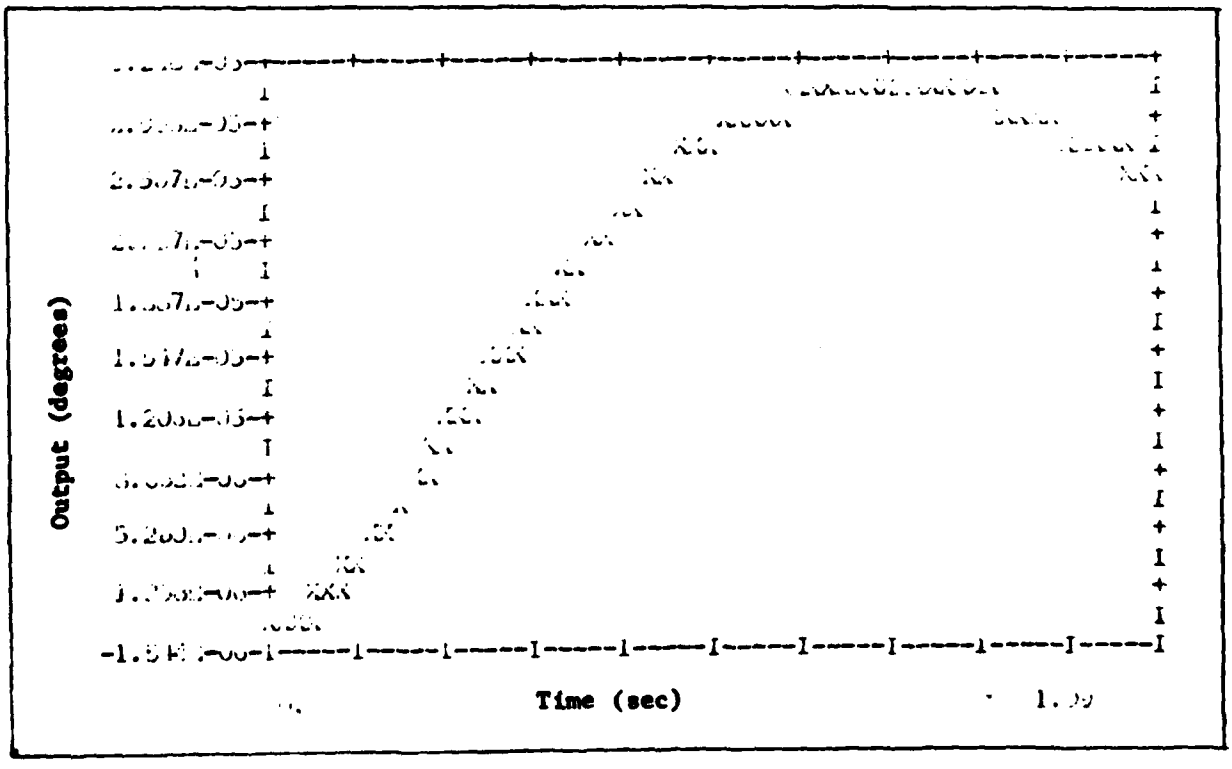

Figure B-88 θ Response for u Tracking without a Rudder

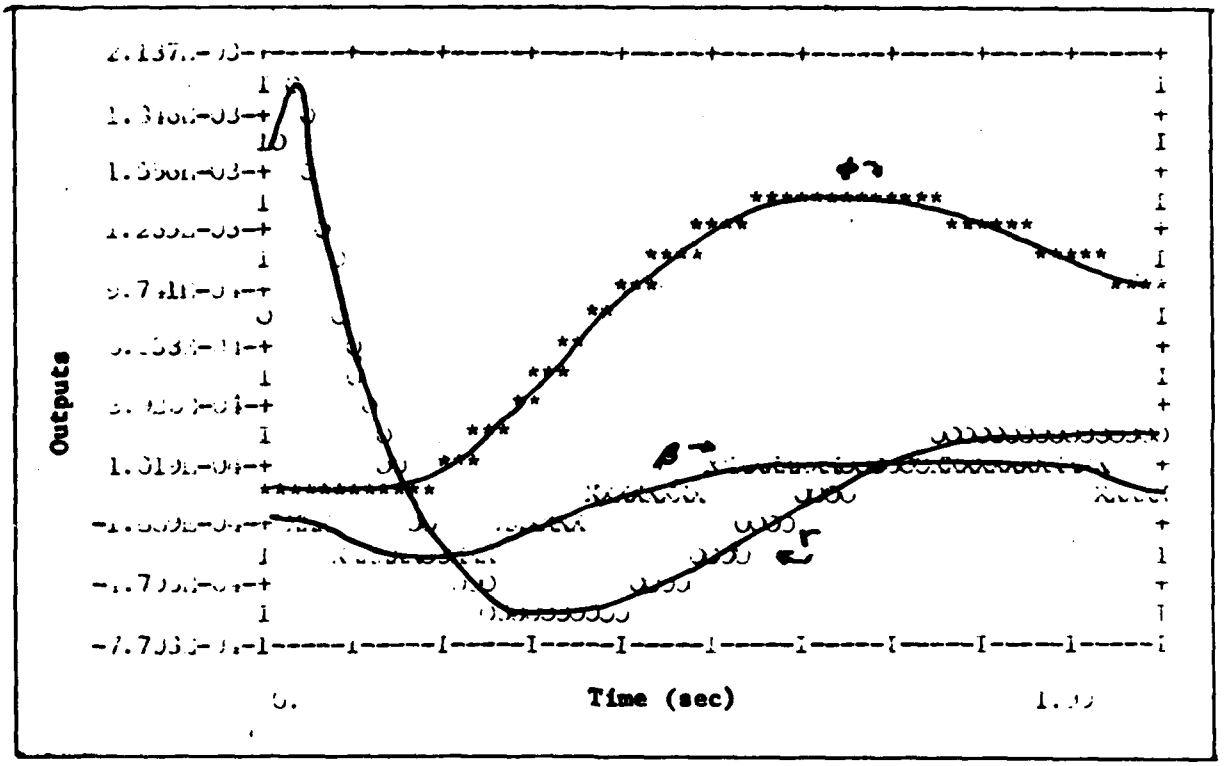

Figure B-89 Lateral Responses for u Tracking without a Rudder

Mach 0.18 Robustness Check

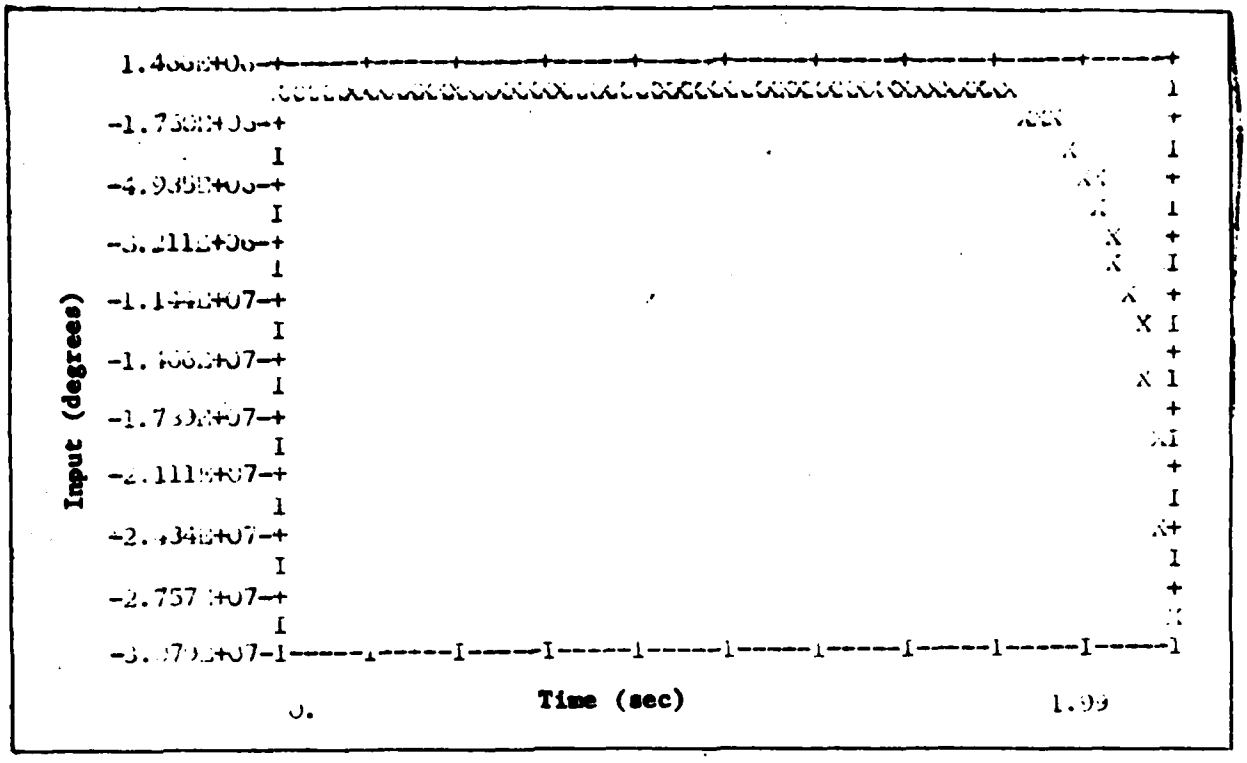

Figure B-90 δ_r Input for γ Tracking using Mach 0.6 Control Law at Mach 0.18

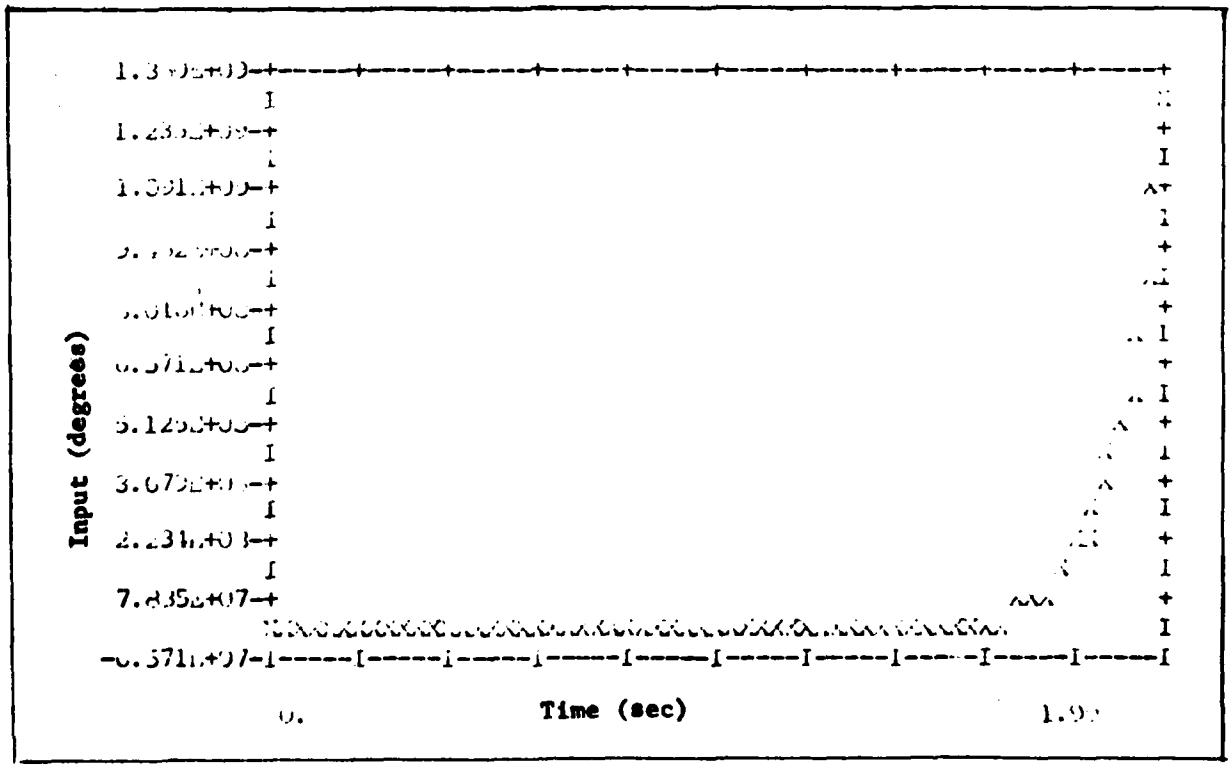

Figure B-91 δ_{H_r} Input for γ Tracking using Mach 0.6 Control Law at Mach 0.18

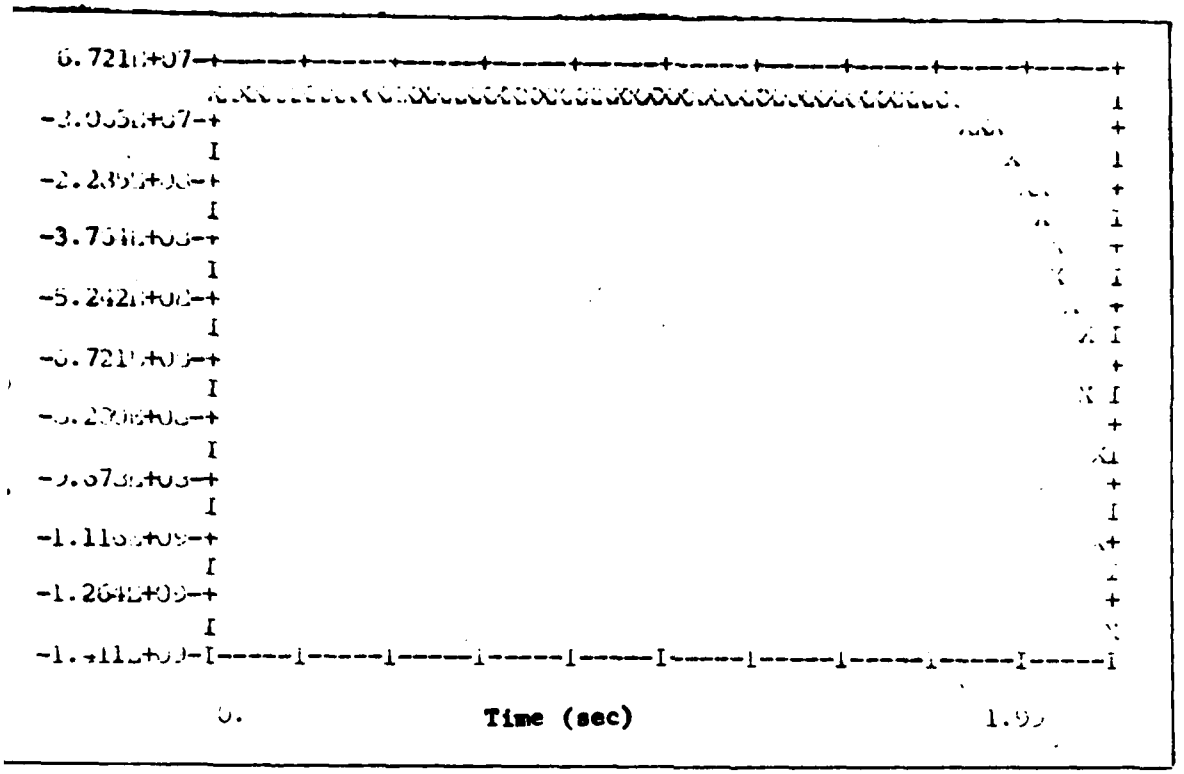

re B-92 δ_{H_L} Input for γ Tracking Using Mach 0.6 Control Law at Mach 0.18

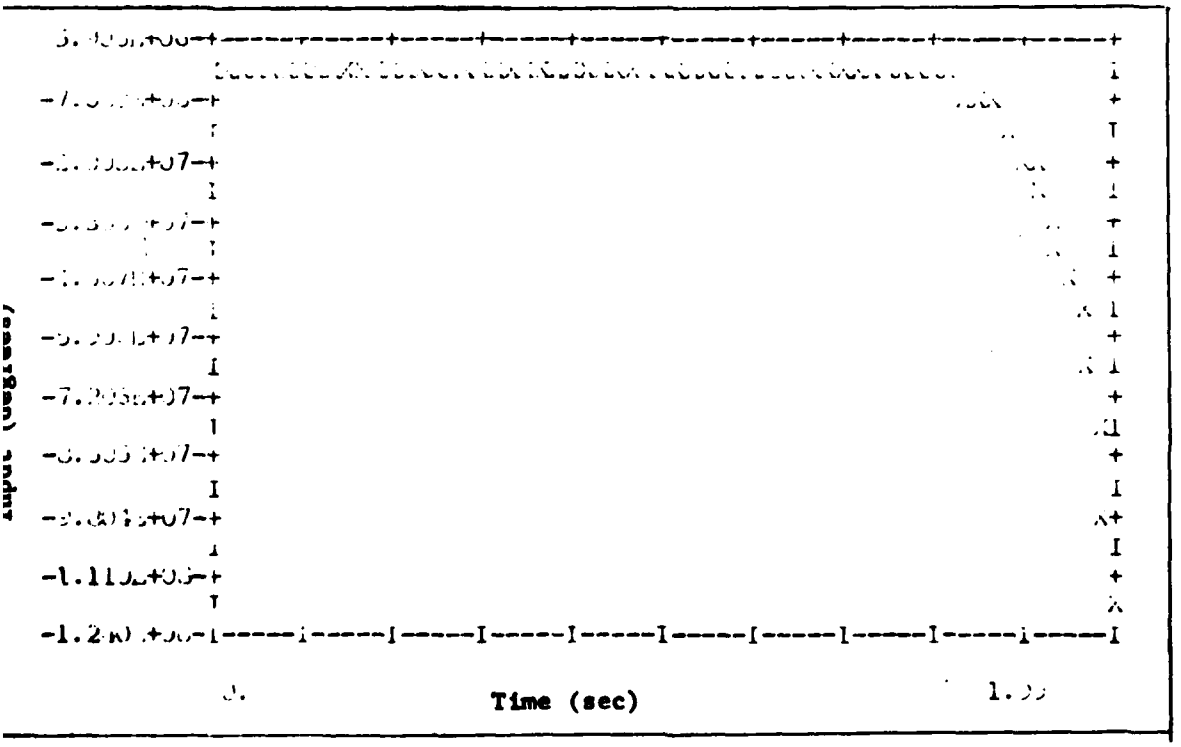

re B-93 δ_a Input for γ Tracking Using Mach 0.6 Control Law at Mach 0.18

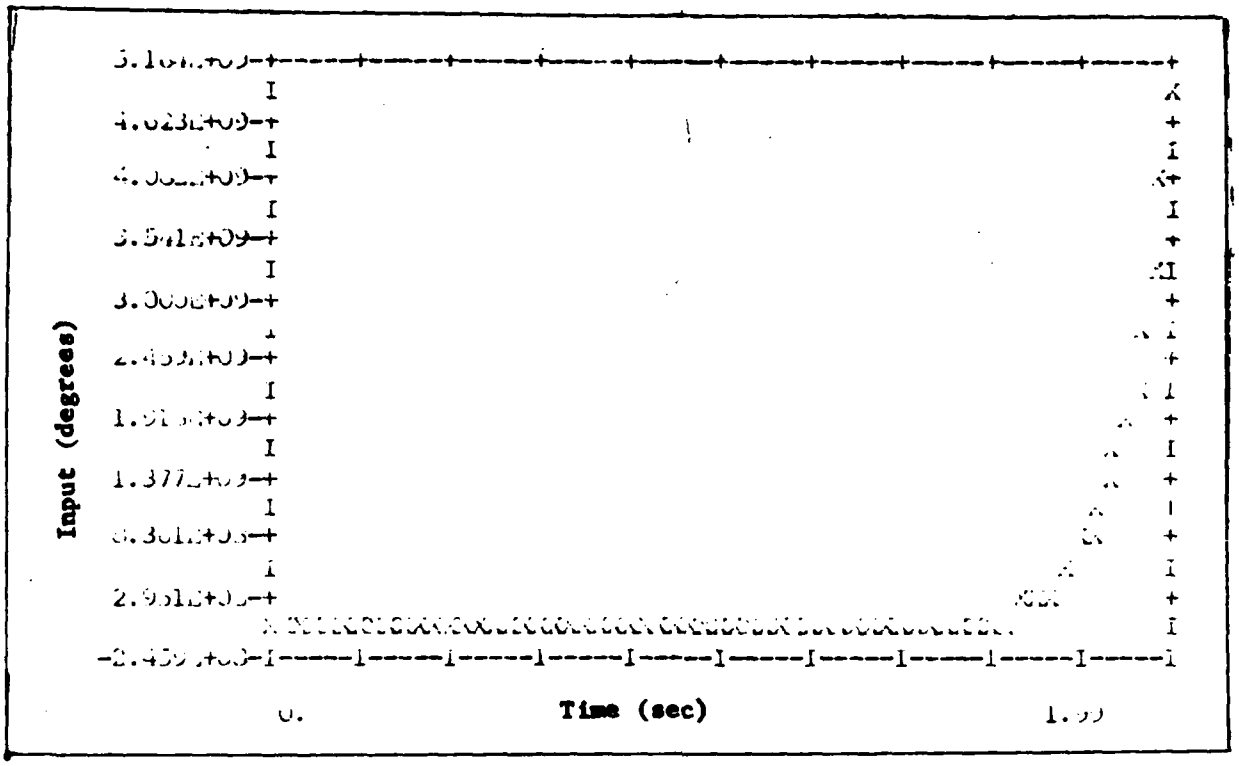

Figure B-94 δ_s **Input for** γ **Tracking Using Mach 0.6 Control Law at Mach 0.18**

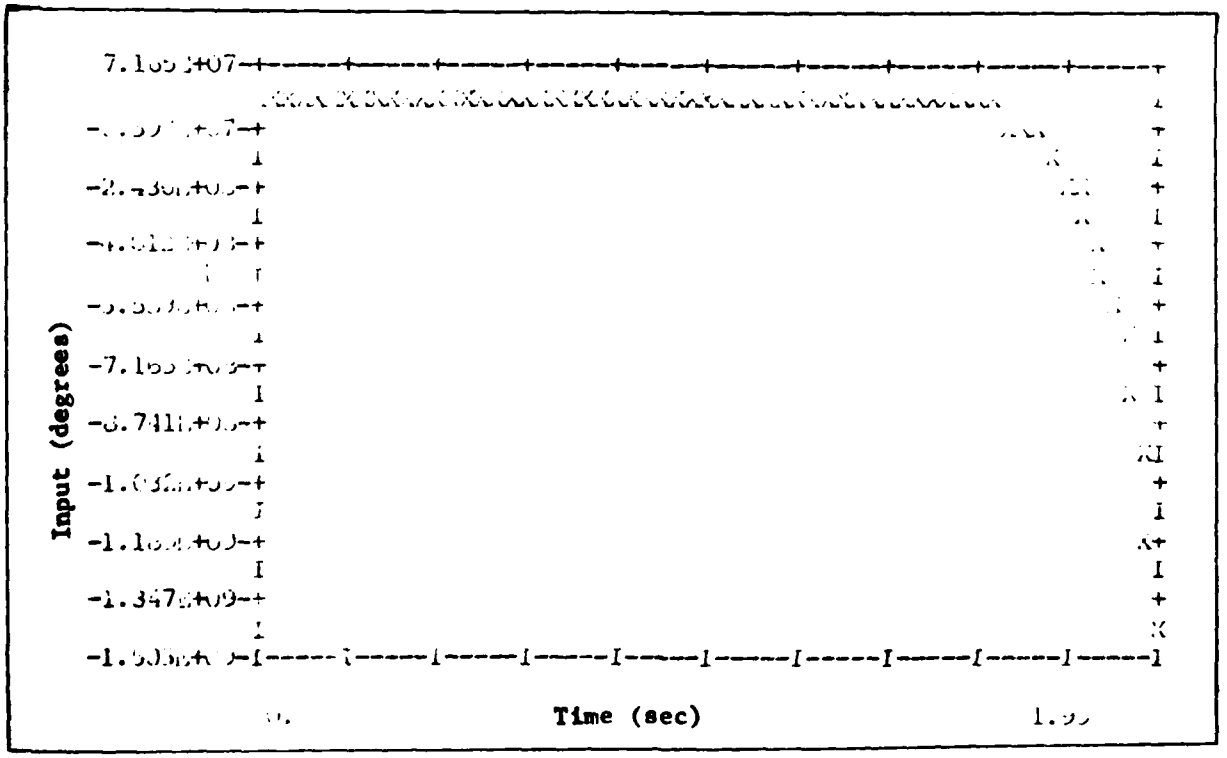

Figure B-95 δ_f **Input for** γ **Tracking Using Mach 0.6 Control Law at Mach 0.18**

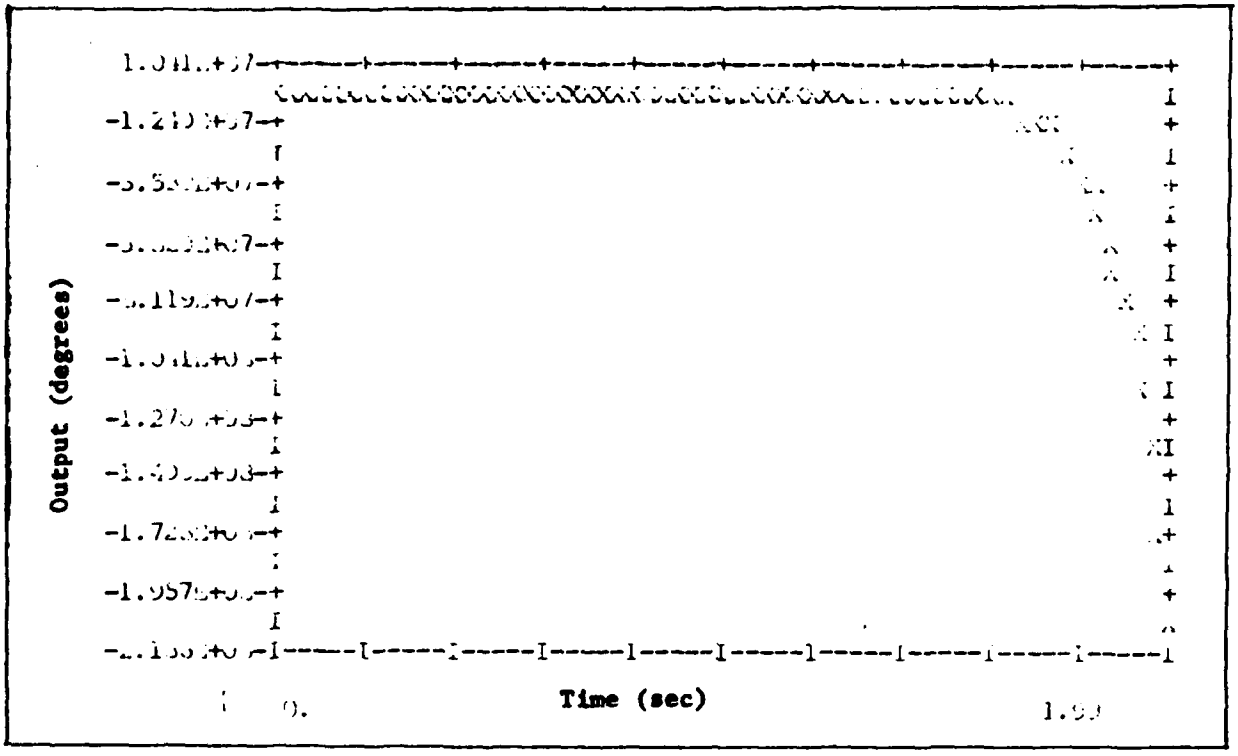

Figure B-96 γ Tracking Response Using Mach 0.6 Control Law at Mach 0.18

Vita

Randall N. Paschall was born in Memphis, Tennessee on June 23, 1958. He attended Oklahoma University under a Navy scholarship his freshman year in college. He resigned from the Navy program, and returned home to attend Christian Brothers College. During his sophmore year he was awarded a 2½ year AFROTC scholarship. He graduated magna cum laude with a B.S. degree in electrical engineering and a reserve commission in the U.S. Air Force on May 10, 1980. He reported to the Air Force Institute of Technology as a direct accession selectee on June 2, 1980. Upon completion of the guidance and control graduate program at AFIT, he is being assigned to the Armament Division at Eglin, AFB, Florida.

UNCLASSIFIED

SECURITY CLASSIFICATION OF THIS PAGE *(When Data Entered)*

REPORT DOCUMENTATION PAGE		READ INSTRUCTIONS BEFORE COMPLETING FORM
1. REPORT NUMBER AFIT/GE/EE/81D-47	2. GOVT ACCESSION NO. AD-A127443	3. RECIPIENT'S CATALOG NUMBER
4. TITLE *(and Subtitle)* Design of a Multivariable Tracker Control Law for the A-7D Digitac II Aircraft		5. TYPE OF REPORT & PERIOD COVERED MS Thesis 6. PERFORMING ORG. REPORT NUMBER
7. AUTHOR(s) Randall N. Paschall 2Lt USAF		8. CONTRACT OR GRANT NUMBER(s)
9. PERFORMING ORGANIZATION NAME AND ADDRESS Air Force Institute of Technology (AFIT/EN) Wright-Patterson AFB, Ohio 45433		10. PROGRAM ELEMENT, PROJECT, TASK AREA & WORK UNIT NUMBERS
11. CONTROLLING OFFICE NAME AND ADDRESS AFWAL/Flight Dynamics Laboratory (FDL) Wright-Patterson AFB, Ohio 45433		12. REPORT DATE Dec 1981 13. NUMBER OF PAGES 161
14. MONITORING AGENCY NAME & ADDRESS*(if different from Controlling Office)*		15. SECURITY CLASS. *(of this report)* UNCLASSIFIED 15a. DECLASSIFICATION/DOWNGRADING SCHEDULE

16. DISTRIBUTION STATEMENT *(of this Report)*

Approved for public release; distribution unlimited

17. DISTRIBUTION STATEMENT *(of the abstract entered in Block 20, if different from Report)*

18. SUPPLEMENTARY NOTES

Approved for public release; IAW AFR 190-17

7 APR 1983

Approved for public release: IAW AFR 190-17.
LYNN E. WOLAVER
Dean for Research and Professional Development
Air Force Institute of Technology (AFIT)
Wright-Patterson AFB OH 45433

19. KEY WORDS *(Continue on reverse side if necessary and identify by block number)*

Unknown Plant, Regular Plant, Irregular Plant, Output Weighting Matrix, Longitudinal Modes, Lateral Modes, Tracking, Digital, High Gain, Low Gain, Transmission Zeros, Transducer Matrix, Rank

20. ABSTRACT *(Continue on reverse side if necessary and identify by block number)*

This thesis uses the design procedures developed by Professor Porter at the University of Salford, England in an attempt to design a multivariable tracker control law for the A-7D Digitac II Aircraft. Some of the limitations and problems associated with this design procedure are uncovered in this study.

A six degree-of-freedom aircraft model is developed and is then modified to a form that is required by the design procedure. The theory used for

DD FORM 1 JAN 73 1473 EDITION OF 1 NOV 65 IS OBSOLETE

UNCLASSIFIED

SECURITY CLASSIFICATION OF THIS PAGE *(When Data Entered)*

Block 20 (con't)

the design determines the necessary arrangement of the equations. A tracker control law is first designed for one flight condition. Then it is checked for robustness by applying the control law at a different flight condition and also by removing the rudder from the inputs. A design computer program called MULTI is developed to perform the computations and simulations.

It is found that the design techniques developed by Professor Porter are valid, but that they are not applicable to all systems. A problem occurs when the inputs, as with an aircraft, are bounded.

Problems may also be encountered when the sensor and actuator models are incorporated into the design. Therefore, for this study, the sensor and actuator models are removed and approximated as unity.

More work is needed in this research to expand knowledge about the selection of the adjustable parameters in order to develop a better design and to more effectively utilize the basic design. Further work is also needed to prefect the useability of the program MULTI. This thesis provides a good stepping stone to a better understanding of this design technique and its applicability.

END

DATE
FILMED

5 -83

DTIC